

UNIVERSITY OF TASMANIA
(PHYSICS DEPARTMENT)

LIMITED INTERPOLATIVE DESIGN

OF

LENS SYSTEMS

OF

THE TRIPLET TYPE

by

A.L.H. Aldersey

Thesis submitted for the
Degree of Doctor of Philosophy

November 1967

Theses
Physics

CONTENTS

| | Page |
|--|------|
| ABSTRACT | 1 |
| INTRODUCTION | 4 |
| HISTORICAL REVIEW | 7 |
| SECTION 1. A PRELIMINARY STUDY OF THE TYPE 121 TRIPLET. | |
| 1.1 THEORY OF THE BASIC TRIPLET OUTLINED. | 20 |
| 1.1.1 The Basic-Triplet and the Basic-Parameters Φ , χ , P, L, T. | |
| 1.1.2 The Replacement of a Single Thin Component with a Cemented Pair of Thin Lenses. | |
| 1.1.3 The Basic Parameter k' . | |
| 1.1.4 Fictitious Glass. | |
| 1.1.5 Optical Parameters and the Division of the Degrees of Freedom. | |
| 1.1.6 Notes on Classification of Design Parameters. | |
| 1.1.7 Summary. | |
| 1.2 THE SYSTEMATIC DESIGN OF A 3RD ORDER TYPE 121 TRIPLET. | 32 |
| 1.2.1 General Considerations. | |
| 1.2.2 The Systematic Design Process of the 3rd Order Type 121 Triplet Outlined. | |
| 1.2.3 Theory of the 3rd Order Type 121 Triplet. | |
| 1.2.3.1 Stage 1. Finding the Initial Arrangement of the 121. | |
| 1.2.3.2 Stage 2. Finding Initial Shapes of the Thin Solution. | |
| 1.2.3.3 Stage 3. Developing a Thick System from the Thin Solution. | |

- 1.2.3.3.1 Adjusting Powers.
- 1.2.3.3.2 Adjusting the Thick Lens Residuals.
- 1.2.4 Summary.
- 1.3 PROGRAMMING THE 3RD ORDER TRIPLET. 53
 - 1.3.1 Introduction.
 - 1.3.2 General Considerations.
 - 1.3.3 The Basic Programme as a Sub-Routine.
 - 1.3.4 The Initial Design Programme or Basic Programme.
 - 1.3.5 Main Types of Sub-Routine or Procedure Defined.
 - 1.3.6 Description of the Basic-Procedures and System-Procedures used in the Basic-Programme.
 - 1.3.7 Description of the Basic-Programme.
- 1.4 A PRELIMINARY STUDY OF SOME 3RD ORDER SOLUTIONS OF A TYPE 121 SYSTEM VERSUS k' USING FAMILIAR TECHNIQUES. 66
 - 1.4.1 Introduction.
 - 1.4.2 General Discussion of Triplet Properties and Design Methods.
 - 1.4.3 Initiating the Preliminary Study of the Type 121.
 - 1.4.4 Selecting the Initial Values of the Basic Parameters.
 - 1.4.5 The Spherical Aberration of the Type 121 versus and versus k' .
 - 1.4.5.1 The Basic-Programme for Spherical Aberration.
 - 1.4.5.2 The Effect of χ and k' on the Spherical Aberration.
 - 1.4.6 Right and Left Hand Solutions versus k' .

- 1.4.6.1 The R and L Programme.
- 1.4.6.2 Controlling Spherical with k' .
- 1.4.6.3 Discussion of Type 121 Solutions.
- 1.4.7 Discussion of the Design Process as a Result of work with the Type 121.
- 1.4.8 Methods of Design - Some General Considerations.

SECTION 2. MONOCHROMATIC DESIGN.

- 2.1 THE DESIGN PROCESS AND INTERPOLATIVE DESIGN. 86
 - 2.1.0 Introduction.
 - 2.1.1 The Design Process.
 - 2.1.2 Interpolative and Extrapolative Techniques in Optical Design.
 - 2.1.3 A Limited Interpolative Design Method Using Aberration Coefficients.
 - 2.1.4 Implementing a Limited Interpolative Study of the Type 121.
 - 2.1.5 Limited Interpolative Design Compared with Other Design Techniques.
- 2.2 A LIMITED INTERPOLATIVE STUDY OF THE MONOCHROMATIC TYPE 121. 103
 - 2.2.0 Introduction.
 - 2.2.1 Spherical Coefficients of the Monochromatic System versus χ , k' , P , $\frac{1}{L}$.
 - 2.2.1.1 Description of Results Obtained for the Spherical Aberration Coefficients.
 - 2.2.1.2 Discussion of the Properties of the Spherical Aberration Coefficients.
 - 2.2.2 The Petzval Coefficient and the Separations versus (χ , k' , P).
 - 2.2.2.0 Introduction.

- 2.2.2.1 The Petzval Coefficient versus (\mathcal{X} , k' , P).
- 2.2.2.2. The Separations versus (\mathcal{X} , k' , P).
- 2.2.3 The 5th and 7th Order Comatic and Astigmatic Coefficients versus (\mathcal{X} , k' , P).
- 2.2.3.0 Introduction.
- 2.2.3.1 The Comatic Coefficients versus (\mathcal{X} , k' , P).
- 2.2.3.2 The Astigmatic (S-Type) Coefficients versus (\mathcal{X} , k' , P).
- 2.2.3.3 Discussion and Comparison of the General Properties of the Aberration Coefficients of the Type 121 Triplet with those of other Types of Systems.
- 2.3 THE POTENTIAL OF THE MONOCHROMATIC TYPE 121. 130
 - 2.3.1 The Field of the Type 121 versus \mathcal{X} , k' , P .
 - 2.3.2 The Five Types of Aberration Plotted in Three Principal Sections of (\mathcal{X} , k' , P)-space.
 - 2.3.3 The Type 121 versus the Type 111.
 - 2.3.4 The Uniqueness of Type 121.
 - 2.3.5 Discussion of Design Principles Emerging from Section 2.
- 2.4 OPTIMIZING THE COEFFICIENTS OF THE MONOCHROMATIC TYPE 121. 139
 - 2.4.0 Introduction.
 - 2.4.1 Equivalence of P and R_4 .
 - 2.4.2 The Programme for Computing Solutions with Prescribed Petzval.
 - 2.4.3. The Range of R_4 .
 - 2.4.4 The Spherical Coefficients of the R and L Solutions versus (k' , R_4).
 - 2.4.5 Zonal Spherical Aberration and the Sign Pattern of the Coefficients.

- 2.4.6 Coincident R and L Solutions and Tangential Solutions.
- 2.4.7 Symmetrical-Tangential Solutions and the Symmetry Parameter R_8 .
- 2.4.8 The Parameter R_8 and the Turning Point Solutions versus (\mathcal{X}, k', P) and (\mathcal{X}, k', R_4) .
- 2.4.9 Conclusions.
- 2.5 SYMMETRICAL SOLUTIONS AND CORRECTION OF ZONAL SPHERICAL AT TWO ZONES. 153
 - 2.5.0 Introduction.
 - 2.5.1 The SS Programme.
 - 2.5.2 The Spherical Aberration Coefficients of the Symmetrical Solutions versus R_4 .
 - 2.5.3 Predicted Zonal Spherical of Symmetrical Solutions versus R_4 .
 - 2.5.4 Failure of Zonal Predictions at Apertures $> f/3.5$.
 - 2.5.5 Balancing Higher Order Zonal Spherical mainly with R_1 .
 - 2.5.6 The Effect of R_4 on the Marginal Zones.
 - 2.5.7 The Combined Effects of R_1 and R_4 on the Marginal Zones and the Intermediate Zones.
 - 2.5.8 Optimizing LA' with R_1 and R_4 .
 - 2.5.9 The Final Adjustment of the Monochromatic System.
 - 2.5.9.1 Selecting the Optimum System (The minimum effective interval of R_4).
 - 2.5.9.2 Adjusting the Off-Axial Image of the Monochromatic System.

2.6 THE BASIC GLASS PARAMETERS AND THE OPTIMUM MONOCHROMATIC REGION.

173

2.6.0 Introduction.

2.6.1 The Effect of Different Combinations of Basic Glasses.

2.6.1.1 Technique.

2.6.1.2 Discussion of Type 121 versus Basic Glasses.

2.6.2 Proposing a Fictitious Glass for Lens Group c.

2.6.3 Selecting the Fictitious Glass.

SECTION 3. CHROMATIC DESIGN.

3.1 DEVELOPING THE CHROMATIC TYPE 121.

179

3.1.0 Introduction.

3.1.1 The Chromatic Aberration of the Optimum Monochromatic System SS(4).

3.1.2 The Effect of Changing L.

3.1.3 Zonal Achromatism and Reduced Petzval. (The effects on the zonal aberration of combining R_4 and L).

3.1.4 Adjusting the Transverse Chromatic Aberration with T and its Effect on the Longitudinal Chromatic Aberration and the Petzval Curvature.

3.1.4.1 Final Adjustment of L and R_4 .

3.1.4.2 The Effects of T on the Axial and Off-Axial Pencils of the Type 121.

3.1.5 Discussion of some Important Properties Observed during Adjustment of the Chromatic Aberrations.

- 3.2 THE SIMULTANEOUS CONVERGENCE OF ALL AVAILABLE ORDERS OF SPHERICAL ABERRATION COEFFICIENTS WITH RESPECT TO THE BASIC PARAMETERS (\mathcal{X} , k' , P , L , T): 200
- 3.2.0 Introduction.
 - 3.2.1 Review of Indirect Evidence of the Convergence of Coefficients with respect to all the Basic Parameters (\mathcal{X} , k' , P , L , T).
 - 3.2.2 Direct Evidence Confirming the Simultaneous Convergence of the Spherical Coefficients of all available Orders versus (\mathcal{X} , k' , P , L , T).
 - 3.2.2.0 Discussion.
 - 3.2.2.1 Convergence of 3rd, 5th and 7th Order Spherical Coefficients versus (\mathcal{X} , k' , P , L , T) Demonstrated.
 - 3.2.3 The Study of the Spherical Coefficients Extended to the 9th and 11th Order.
 - 3.2.3.0 Introduction.
 - 3.2.3.1 Computing Techniques Using 9th and 11th Order Spherical Coefficients.
 - 3.2.3.2 Behaviour of 9th and 11th Order Buchdahl Coefficients in the Optimum-Monochromatic-Region.
 - 3.2.3.3 Behaviour of the 9th and 11th Order Spherical Coefficients in the Optimum-Chromatic-Region.
 - 3.2.3.4 The Convergence of the 9th and 11th Order Spherical Coefficients versus (\mathcal{X} , R_4 , L , T) Demonstrated.
- 3.3 THE OPTIMUM TYPE 121 WITH THE STOP IN AIR. 218
- 3.3.0 Introduction.
 - 3.3.1 Computing Technique for Shifting the Stop.
 - 3.3.2 Optimizing the System after Shifting the Stop.

| | | |
|-------|--|-----|
| 3.3.3 | Comparing the Hektor with the Pentac. | |
| 3.3.4 | Comparing the Parameters of the Type 121 with the Pentac at Various Design Stages. | |
| 3.4 | THE DEVELOPMENT OF A TYPE 122 TRIPLET WITH TWO-ZONE CORRECTION. | 228 |
| 3.4.0 | Introduction. | |
| 3.4.1 | A Limited Interpolative Study of the Type 122. | |
| 3.4.2 | Optimizing the Chromatic Type 122 Triplet. | |
| 3.4.3 | The Parameters of the Type 122 Compared with those of the Type 121 and the Pentac. | |
| 3.5 | CONCLUDING REMARKS. | 238 |
| 3.5.1 | General. | |
| 3.5.2 | New Work. | |
| | ACKNOWLEDGEMENTS | 241 |
| | REFERENCES | 242 |

ABSTRACT

An extensive study of the Leitz Hektor or type 121 triplet lens has revealed fairly simple relationships between the aberrations and the design parameters at large apertures. These relationships, although more complicated than the direct well known relationships for small apertures of triplet systems, nevertheless, are simple enough to allow the designer to systematically correct the zonal spherical between $f/3.5$ and $f/2.5$ in both the monochromatic and chromatic stages of design. The design principles developed for the type 121 triplet have been applied successfully to the type 122 triplet: they have been found by interpolative rather than extrapolative design techniques. Interpolative design is a feature of this work.

Initially the 3rd, 5th and 7th order Buchdahl aberration coefficients of the "3rd order type 121 triplets" have been mapped with respect to all the monochromatic design parameters. This "limited interpolative study" has revealed that most of these coefficients approach zero in a small region. In particular, in this "optimum region" the first three orders of spherical aberration are near zero or pass through zero. This property enables the "optimum region" to be located accurately and rapidly with a comparatively small amount of calculation.

The spherical aberration (to 7th order) of some systems in the "optimum region" is predicted to be zero at two zones (the 0.707 and the marginal zone). This two-zone correction, however, fails to hold at apertures between $f/3.5$ and $f/2.5$ due to the presence of 9th order and higher order spherical aberration. However, it has been found that these outer zones of the monochromatic system are controlled by the Petzval sum and the spherical aberration residual; thus allowing two zone correction for an aperture of $f/2.5$ in the presence of higher order aberrations.

When correcting the chromatic aberrations of the type 121 a similar situation has been found with the large apertures ($> f/3.5$). The longitudinal chromatic aberration residual, in particular, is linked to the Petzval sum's influence on the spherical aberration of the zones beyond $f/3.5$ and, the transverse chromatic aberration residual has a smaller but still significant effect also. Thus it has been found that adjustment of the chromatic aberration leads to a system with a smaller Petzval sum.

On the basis of this property, it was predicted that the 3rd, 5th and 7th order spherical coefficients must converge to a minimum with a small Petzval sum when the chromatic aberration is optimized for all zones. This has been confirmed by repeating the maps of the 3rd, 5th and 7th order spherical aberration coefficients with

respect to the monochromatic and chromatic design parameters. The aberration coefficients are found to converge to an optimum set in a single region of the entire design space. This model of the system's behaviour explains many published properties of triplets.

It has also been predicted from the study of the spherical aberration that the 9th and higher orders of spherical aberration must converge to a minimum in step with the 3rd, 5th and 7th orders. This has been confirmed by mapping the 9th and 11th order Buchdahl spherical aberration coefficients with respect to the design parameters. Thus in the "optimum region" the 3rd, 5th, 7th, 9th and 11th order spherical aberration coefficients are near to, or pass through, zero.

The type 121 with optimum zonal spherical aberration for $f/2.5$ has been developed and compared with published Pentac $f/2.5$ designs.

Finally the principles developed for correcting the zonal aberrations beyond $f/3.5$ have been applied to the systematic development of the type 122 triplet. This has resulted in the easy location of two zone correction.

INTRODUCTION

The original aim of this work was to investigate the potential of the Hektor or the type 121 triplet with a view to producing a four-component-system with good zonal correction for an aperture of $f/2.5$ whilst, at the same time, achieving a moderate semi-field of at least 10° . It was hoped that it would be possible to develop the design systematically from a given set of glasses with the aid of the existing analysis and techniques of workers such as Cruickshank^(2.1), R.E. Hopkins^(4.3), Kingslake^(5.1) and others. However, a preliminary study of this triplet which is described in Section 1, showed that the effectiveness of existing systematic optical design techniques ceases at $f/3.5$. This is so because beyond this point designers seem to rely largely on experience or some automatic correction process that uses a merit function or the like in order to improve a triplet design. Consequently, in the course of this work the aim has become essentially the more general one of finding how to design systematically beyond an aperture of $f/3.5$.

The work is divided into three sections:

(1) In Section 1, the theory is discussed, the programmes described and a preliminary study is made of some type 121 triplets which are generated from a given set of glasses.

A discussion of this work leads to the development of an interpolative method of design for triplets.

(2) In Section 2, a practical method of interpolative design is created and applied to the optimization of a "monochromatic type 121 triplet". In particular, the design principles are discovered for controlling the aberrations of monochromatic triplets with apertures beyond $f/3.5$.

(3) In Section 3, the technique is discovered for the "interpolative design" of the "chromatic system" and the control of its aberrations at apertures beyond $f/3.5$. Then the optimum "chromatic type" 121 is developed for $f/2.5$ and compared with other $f/2.5$ systems. Finally, in Section 3, the type 122 triplet is developed using the design principles which were discovered for the type 121.

From another point of view this thesis may be considered to be divided into two main parts only, Section 1 and the sections following it, because these divisions deal with the design process in two essentially different ways: "interpolative and extrapolative". Section 1 deals with the principle of "extrapolation" whereas Sections 2 and 3 deal with the principle of interpolation.

The familiar extrapolative method of design used in Section 1 begins a design from a promising set of

thin-lens parameters and then the design is developed by searching around this starting point. On the other hand the interpolative method does not start with a promising region but begins by making a complete map of the optical system's potential with respect to its design parameters.

Although this appears to be a formidable task when carried to the limit, it is shown in Section 2, that it can be approximated sufficiently by using the Buchdahl aberration coefficients. This approach allows a "limited-interpolative technique" which yields good results in the design of a system such as the type 121.

HISTORICAL REVIEW

Early Work.

In 1893 H. Dennis Taylor^(22.1) patented a photographic objective with a flat field that was substantially free from astigmatism; besides being rectilinear and achromatic. This anastigmat was achieved with three simple lenses (the minimum number of lenses possible) two outer positive lenses and an inner negative lens which were separated in air. The system in general has since become known as the Cooke Triplet Objective or the Taylor Triplet.

Later Taylor (1904)^(22.2) described the design and construction of the "Franklin-Adams astrographic triplet; a Cooke photographic lens modified for "celestial purposes". In particular in this paper he outlined his reasons for creating a triplet: showing how by varying the distribution of power between a pair of separated positive lenses he could balance the spherical aberration of any "desired negative lens". Thus he was led to the triplet arrangement.

The elegance and power of his invention is evident from the way he develops it to an advanced initial design by simple reasoning. He shows for example that the power of the back lens should be stronger than the front in order to reduce zonal aberration.* He sees that a high refractive

* Practical designs have the power of the back lens $1\frac{1}{2}$ times the power of the front lens.

index for the inner lens will produce low Petzval.

Also he finds that if the front air space is smaller than the back one then coma, transverse colour and distortion are improved.

The final paper of Taylor's^(22.3) concerning triplets was published in 1923. This paper was invited so that Taylor could express his views on optical design in a belated attempt to make up for his absence from a conference held two years before at Cambridge, to discuss "The Future of Geometrical Optics". Consequently his remarks are closely linked to the material presented at Cambridge. Indeed, looking back on this meeting of 45 years ago, one gains considerable insight into the development of triplets and the optical design process since that time. Thus we digress for a moment to consider some aspects of this occasion.

After the 1914-18 war a considerable controversy arose concerning the most effective method of lens design: whether it should be by analytical algebraic methods (British) or by precision ray-tracing (German). This had been induced largely by Taylor's claims that he designed lenses without ray-tracing using instead only analytical solutions and workshop models. Indeed his outstanding success with triplets had influenced men such as Professor Filon and Professor Cheshire to seek the interest of

Cambridge mathematicians in developing higher order aberration theory with the aim of getting accurate analytical solutions without using time consuming precision ray-traces. Their endeavours culminated in this Cambridge conference⁽²³⁾ in 1921.

At the conference two types of people were present: the optical analyst like Commander T.Y. Baker and practical designers like A. Warmisham and Conrad Beck.

Baker opened the conference by putting the case for development of algebraic aberration theory. He said that if a ray is incident on a system with coordinates α and β then its transverse aberration may be written in a power series of the form

$$PP' = A\alpha^3 + B\alpha^2\beta + C\alpha\beta^2 + D\beta^3 + \text{5th degree terms} \\ + \text{7th degree terms} + \dots\dots\dots$$

where the coefficients are functions of the systems construction parameters. He said the cubic terms are what the optician calls the "first order" ^{*}aberrations.

He pointed out that in certain senses it may be said that algebraic formulae are available, by means of which, first order aberrations can be written down for a system of lenses and to a certain extent optical designers make use of such formulae. He continued saying "But an

* The terms first order, second order and third order are used indiscriminately throughout the literature to denote the lowest order of aberration.

instrument cannot be wholly designed by an elimination of first order coefficients because the "higher order" coefficients cannot be neglected. He said that the expressions for higher order aberrations lead to hopeless difficulties adding that even the second order expressions are far more complicated than the first.

Thus in order to overcome the outstanding difficulties of analytical design Baker proposed the pursuit of new approximate forms of the aberration function instead of finding general coefficients in the higher order terms of the aberration power series. The forms he hoped for were expected to allow the calculation of the most correct form of a lens. Also he wanted the parameters to be such that those of one system could be compounded with another. These new forms were to be simpler than the few known 5th order expressions and were to converge more rapidly. Indeed complexity of existing expressions and their slow convergence were the main worries of the analyst of that time.

Conrad Beck in reply to Professor Cheshire's question, (What are the methods adopted in optical factories for designing optical instruments?) pointed out that successful designing on paper depended on the invention that lay behind it. Furthermore he said "No one can make a new instrument by computation. There are no mathematical formulae capable of solution that will give the data for

an optical system of 20 to 60 variables. Computing is no more than a clumsy trial and error method of testing the design and improving it by trial." In his concluding remarks Beck says "A mathematical formula may be of no practical use for direct application but may be of the utmost value in revealing tendencies, and pointing out unproductive directions of research".

Warmisham however outlined his "practice in designing photographic lenses". This we find to be essentially the optical design process used by designers to this day especially with regard to a triplet. It is evident that he finds analytically an initial arrangement of powers and separations with prescribed primary spherical, Petzval sum, transverse and longitudinal chromatic aberration and focal length. The remaining degrees of freedom represented by the shapes he uses to control the first order coma, astigmatism and distortion analytically. This thin system is thickened and the first order aberrations of the thick system computed.

At this stage the system is modified to reduce the "first" order aberrations to "likely" amounts usually by changing the shapes. This is done with finite difference equations connecting the aberrations with the change in shape. Thus he obtains a triplet system of known focal length that has known amounts of the seven primary aberrations.

Finally he submits the system to trigonometrical computation and determines the aberrations accurately. Then he says: "If the likely amounts of first order aberrations left in the system were well chosen, they are more or less accurately balanced over the required aperture and field by higher order aberrations. It is generally sound to assume that the usually small outstanding aberrations revealed by trigonometrical work can be eliminated by altering the first order terms an equal amount, the higher order aberrations remaining substantially unchanged. It may, however, be necessary to go further back and make radical alterations in powers and separations if large higher order aberrations are revealed.

I believe most designers of photographic lenses economise in trigonometrical work where possible. For all ordinary work the calculation of coma is confined to three skeleton rays in the meridian plane. If this gives a good result, other things being good, it is time to make a model rather than compute a pencil of skew rays.

Taylor (1923)^(22.3), outlined again the development of his triplet objective. He described how initially he tried to correct the curvature of field and linear astigmatism of a positive lens, by means of a negative lens of the same glass and power, using the separation to give sufficient positive power. However he found rectilinear images could only be formed by splitting the positive lens and placing

the negative component between them.

At this point Taylor has only referred to his 3rd order analysis in very broad terms, however, it seems that his initial design method is the same as that of say Warmisham. It appears that Taylor obtained an initial thin lens arrangement of powers and separations by solving five equations for an assumed set of four 3rd order residuals for spherical, Petzval sum, longitudinal chromatic and transverse chromatic aberrations and a fifth condition for the total power. He says nothing about solving for the shapes and thickening of the thin system but we assume he must have done this. Instead of assessing his rough analytical design with ray-traces Taylor constructed the design and measured its aberrations. On the basis of this assessment he chose new 3rd order residuals for the thin lens analysis and repeated the whole design process if necessary. Thus Taylor used a method in which he mapped design parameters against the actual optical performance. This method worked for Taylor because, he had the skill and experience for assessing actual aberrations of a finished system and correlating them with the "initial design". Thus in view of this gift of Taylor's his choice of title "Optical Designing as an Art" is appropriate.

It appears in the 1920's that the geometrical design process had gone as far as it could with existing

knowledge and computing facilities. Indeed the designers of that time expected that the main hope for improved design techniques lay in the development of aberration theory rather than computing equipment.

Modern Work.

After Taylor (1923) the triplet design process seems to have remained dormant until R.E. Stephens (1948)⁽¹⁾ examined the design process of triplet anastigmats of the Taylor Type. He developed the thin lens analysis of triplets on a more systematic basis than before, taking into account both near and infinitely distant object planes, discrete values of dispersion and triplets with cemented components.

His work enables the designer to generate a thin lens system from a given set of thin lens parameters which consists of the total power A , the Petzval sum P , the longitudinal chromatic aberration $\Delta S_3'$, the transverse chromatic aberration $\Delta M/M$ and the height h_3 which is the intersection height at lens 3.

He then describes how this solution is thickened and assessed on the basis of 3rd order aberration theory (Seidel sums). After assessment he assumes that the Seidel sums may be reduced to desired values by computing the system again with a new set of values of P , $\Delta S_3'$, $\Delta M/M$, $S-1$, $S-11$, $S-111$, $S-V$ which differ from the original values by negative changes expected on the introduction of thickness.

In the final adjustment he says that the 3rd order thick system is examined trigonometrically and using these residuals a different set of $P, \Delta S_3', \Delta M/M, S-1, S-11, S-111,$ and $S-V$ are chosen for the calculation of the final system. Several trials may be required at this stage. However if the final system is not satisfactory then he says "start again with a new glass selection!"

Although Stephens suggests that his methods "should facilitate the production of good designs without extensive experience on the part of the designer", he gives little guidance with regard to starting a design and finishing it. Basically his design process is that of designers from the time of Warmisham at least.

Lessing (1958) ^(3.2) pointed out that no one had shown how to select the glass for a triplet. Designers like Stephens for example made their glass selection on the basis of a sequence of trials or from published designs. Thus he finds that although much has been written about the preliminary calculation of triplets in most cases the glasses are assumed selected.

Lessing (1958) ^(3.2) sets out to overcome this by assuming two conditions in addition to the usual five conditions of the preliminary design stage. The conditions he uses are two properties concerning the distribution of power in a triplet which were mentioned by Taylor:

(1) that the power of the back lens is one and a half times the first lens. (2) that the powers of the lenses are small. In other words Lessing's method reduces to finding the glass combinations that give thin lens arrangements which satisfy additional power conditions that are supposed to ensure small zonal spherical aberration and Petzval sum. In the final paper of this work Lessing^(3.3)(1959) also discusses the selection of glass that will give a thin lens solution with specified longitudinal chromatic aberration and diaphragm position.

Cruickshank (1956, 58, 60)^(2.1,2.2,2.3) emphasized that all triplets with cemented components can be generated from the simple Cooke-triplet or as he called it a type 111 triplet (see Figure 1.1.1). Thus in view of the fundamental importance of the simple triplet he has examined its properties in a systematic way.

He proposed that the triplet could be better thought of as a positive lens with a corrector system in front of it, especially, as the power contributed by the front two lenses is zero in many triplets. Thus he replaced the parameter h_2 of Stephens' analysis by the new thin lens parameter \mathcal{X} , the power of the corrector. This gives a very simple set of five equations for the initial arrangement. With this modification the designer can generate a triplet from a given set of parameters $(\Phi, \mathcal{X}, P, L, T)$ where.

Φ = total power,

P = Petzval sum,

L = longitudinal chromatic aberration,

T = transverse chromatic aberration,

Cruickshank^(2.1) showed, firstly, that most triplets occur in the range $-2 < \mathcal{X} < 0.4$ and, secondly, that the primary spherical aberration of a triplet is approximated by a quadratic function of \mathcal{X} thus:

$$\mathcal{T}_1 = a_0 + a_1\mathcal{X} + a_2\mathcal{X}^2$$

where \mathcal{T}_1 is the 3rd order Buchdahl spherical coefficient of the Seidel form. Consequently he showed that if the parameters P, L, T and the glasses are correctly selected then there are two solutions. Also he pointed out that most published triplets appeared to be developed from the smaller negative value of \mathcal{X} , whereas, the larger negative value had more potential. However, apart from examining the properties of the thin lens solution, Cruickshank (1958) also applied the 5th order Buchdahl coefficients to the correction of the final thick system. Thus after 30 years the wishes of Commander Baker were partly satisfied by the publication of Buchdahl's aberration coefficients (1954) and their use by Cruickshank in obtaining "a good balance between the primary and higher order aberrations."

Cruickshank (1960)^(2.2) discussed in detail the general principles of generation of triplets with cemented

components. This he illustrated with an example of a Pentac (212) objective which he developed from a "typical set of aberration residuals" (\mathcal{X} , P, L, T) and fictitious glasses. The final adjustment of the system was made with 5th order aberration coefficients. He shows a plot of the 5th order coefficients of the Pentac versus \mathcal{X} which indicates the optimum \mathcal{X} very clearly. This example illustrates the use of fictitious glasses in finding the initial solution of a triplet system with cemented components and also the use of the Buchdahl coefficients as a measure of the correction state of the design. It shows clearly the benefit of being able to see the trend of the design with 5th order coefficients.

Cruickshank and Hills (1960)^(2.4) followed up Cruickshank's earlier application of 5th order Buchdahl aberration coefficients to triplets with a discussion of their use in "Optical Design". In particular they showed the total aberration of the point image may be analysed into symmetrical and asymmetrical types which may be broken down into surface contributions; a property belonging to the Buchdahl coefficients. They illustrated their discussion with the final stages of design of a telephoto system.

R.E. Hopkins (1962)^(4.3) recognised that the out-standing problem with triplet design is not how to develop a solution from a given set of parameters but how to select

the best lens from an infinite number of 3rd order solutions.

In view of this he made a systematic study of a region of triplet solutions. He corrected the solutions to the same 3rd order values and then analysed them by calculating the 5th order Buchdahl aberration coefficients.

Thus he has obtained some very interesting maps of functions of 5th order coefficients versus various thin lens parameters. In particular he introduces a parameter ΔV as a measure of the glass variations and he finds that the 5th order coefficients tend to become smaller near $\Delta V = 25$. Thus he has examined nine degrees of freedom whereas other workers have only examined the eight geometrical degrees of freedom.

This work of Hopkins seems to be the first serious attempt to map thoroughly the trends in design potential with Buchdahl coefficients and a computer.

SECTION 1.

A PRELIMINARY STUDY
OF
THE TYPE 121 TRIPLET.

CHAPTER 1.1 THEORY OF THE BASIC TRIPLET OUTLINED.

1.1.1 The Basic-Triplet and the Basic-Parameters ϕ, χ .P, L, T.

It has been shown^(2.1) that any system of the triplet type has an EQUIVALENT TRIPLET or as we shall call it a BASIC TRIPLET (see top diagram of Figure 1.1.2). Thus in this work all the triplets with cemented components in place of simple components are treated as being generated from the basic triplet.

It is defined to be a system of positive power consisting of three thin lenses in air separated by real spaces and whose powers are arranged in a characteristic pattern of (+ - +). The components are of glasses (Na, Va), (Nb, Vb), (Nc, Vc), their powers are denoted by ϕ_a, ϕ_b, ϕ_c and the front air space by t_a and the back by t_b . The aperture stop coincides with the middle lens b.

The "basic triplet" satisfies five paraxial conditions; two of them are power conditions the other three are aberration conditions. It is defined to have the following for an object plane at infinity: a total power ϕ , a Petzval sum R_4 , residual longitudinal chromatic aberration R_6 , residual transverse chromatic aberration R_7 and its two leading components with an effective power χ . These conditions are represented analytically by the thin lens equations in which three of the "construction parameters⁽¹⁾"

(ϕ_a, ϕ_b, ϕ_c) are obtained as implicit functions of "performance parameters⁽¹⁾" $(\Phi, \chi, R_4, R_6, R_7)$ as follows: (2.1)

$$1/y_{oa} \sum_{j=a}^c \phi_j y_{oj} = \Phi \quad 1.1$$

$$1/y_{oa} \sum_{j=a}^c \phi_j y_{oj} = \chi \quad 1.2$$

$$\sum_{j=a}^c \phi_j / N_j = R_4 \quad 1.3$$

$$1/u'_{oj} \sum_{j=a}^c \phi_j y_{oj}^2 / V_j = R_6 \quad 1.4$$

$$1/u'_{oj} \sum_{j=a}^c \phi_j y_{oj} \cdot y_{jj} / V_j = R_7 \quad 1.5$$

where y_j is the height of the principal paraxial ray (y_a, u_a) at the j^{th} component and y_{oj} is the height of axial paraxial ray (y_{oa}, u_{oa}) at the j^{th} component. The angle u'_{oj} is the inclination of axial paraxial ray after refraction at the j^{th} component.

When considering the paths of the pair of paraxial rays defined above, it is convenient to introduce other construction parameters, the separations, into the analysis. Thus, since the diaphragm is at the middle lens the path of the principal paraxial ray is such that

$$y_b = 0, y_a/y_c = -t_a/t_b \quad 1.6$$

$$y_{ob} = y_{oa}(1 - t_a \phi_a) \quad 1.7$$

$$y_{oc} = y_{ob} - t_2 \cdot y_{oa} \cdot \chi \quad 1.8$$

In proceeding to explicit expressions for the powers and separations it is convenient to define the glass constants, intersection heights and the residuals R_4 , R_6 and R_7 in terms of new parameters. Thus the glass constants are expressed as ratios giving the relative distributions of the refractive indices and V-numbers by: (2.1)

$$V_a/V_b = \alpha, \quad V_a/V_c = \xi \quad 1.9$$

$$N_a/N_b = \beta, \quad N_a/N_c = \gamma \quad 1.10$$

while for the remainder we also write

$$y_{ob}/y_{oa} = \eta_{ob}, \quad y_{oc}/y_{oa} = \eta_{oc} \quad 1.11$$

$$P = R_4 \cdot N_a^*, \quad L = R_6 \cdot V_a/y_{oa}, \quad T = R_7 \cdot V_a/u_a \quad 1.12$$

Using equations 1.9 to 1.12 and putting the total power $\Phi = 1$ and also remembering that the paraxial rays are chosen such that $(y_{oa} = 1, u_{oa} = 0)$ and $(y_b = 0, u'_a = 1)$ then equations 1.1 to 1.8 become

$$\phi_a + \eta_{ob}\phi_b + \eta_{oc}\phi_c = 1 \quad 1.13$$

$$\phi_a + \eta_{ob}\phi_b = \chi \quad 1.14$$

$$\phi_a + \beta\phi_b + \gamma\phi_c = P \quad 1.15$$

$$\phi_a + \alpha\eta_{ob}^2\phi_b + \xi\eta_{oc}^2\phi_c = L \quad 1.16$$

$$(1 + T)t_a\phi_a - t_b\xi\eta_{oc}\phi_c = T \quad 1.17$$

$$(1 - t_a\phi_a) = \eta_{ob} \quad 1.18$$

$$(\eta_{ob} - t_b\chi) = \eta_{ob} \quad 1.19$$

From these we obtain the following explicit expressions for

* This residual of the Basic Triplet is related to the Buchdahl coefficient of the Seidel form as follows $R_4 = 2 \cdot \sigma_4$

the powers and separations of the initial arrangement of the basic triplet:

$$\phi_b = (\mathcal{H}\eta_{ob} - L) / (1 - \alpha\eta_{ob})\eta_{ob} \quad 1.20$$

$$\phi_c = \xi(1 - \chi)^2 / (\mathcal{H}\eta_{ob} - \chi) \quad 1.21$$

$$\phi_a = \chi - \eta_{ob} \cdot \phi_b \quad 1.22$$

$$t_a = (1 - \eta_{ob}) / \phi_a \quad 1.23$$

$$t_b = 1 - (1 + T)\eta_{ob} / \xi(1 - \chi) \quad 1.24$$

$$\text{where } \mathcal{H} = \xi + \chi(1 - \xi + T) \quad 1.25$$

and η_{ob} is given by

$$G_3 \eta_{ob}^3 + G_2 \eta_{ob}^2 + G_1 \eta_{ob} + G_0 = 0 \quad 1.26$$

where

$$G_3 = \mathcal{H}^2 + \alpha\mathcal{H}(\chi - P) \quad 1.27$$

$$G_2 = \mathcal{H}(P - L - 2\chi - \beta\mathcal{H}) + \alpha[\xi(1 - \chi)^2 - \chi(\chi - P)] \quad 1.28$$

$$G_1 = \beta\mathcal{H}(\chi + L) - [\delta\xi(1 - \chi)^2 - \chi(\chi - P)] + L\chi \quad 1.29$$

$$G_0 = -L/\beta\chi. \quad 1.30$$

Therefore three initial arrangements are possible; one for each of the roots of the cubic equation (1.26).

In general, there is only one root of this equation that yields an initial arrangement satisfying the conditions

$(\phi_1 > 0, \phi_2 > 0, \phi_3 > 0, \phi_4 > 0, t_a > 0, t_b > 0)$. The system generated from this arrangement is usually a real triplet. This root, in general, is not far away from $\eta_{ob} = 0.7$.

There are some special triplet solutions that, although they have initial arrangements with at least one

separation negative, yield acceptable systems on thickening; these unusual solutions will not be studied here. In this work only the solutions in the region of $\eta_{ob} = 0.7$ are examined.

1.1.2 The Replacement of a Single Thin Component with a Cemented Pair of Thin Lenses.

Now consider replacing one of the components of the basic triplet by a cemented pair of thin lenses. The values of the residuals $\bar{\phi}_1, \chi_1, P_1, L_1, T_1$ of a particular initial arrangement will remain unchanged by the replacement if the powers (ϕ_1, ϕ_2) of the components $(N_1, V_1, \phi_1), (N_2, V_2, \phi_2)$ replacing the j^{th} lens of the basic triplet satisfy the following

$$\phi_1 + \phi_2 = \bar{\phi}_j \quad 1.31$$

$$\phi_1/N_1 + \phi_2/N_2 = \bar{\phi}_j/N_j \quad 1.32$$

$$\phi_1/V_1 + \phi_2/V_2 = \bar{\phi}_j/V_j \quad 1.33$$

where $j = a, b, c$. Thus thin lenses may be replaced by pairs of thin lenses which have the same power, Petzval and longitudinal and transverse chromatic aberration.

(This can be extended to replace groups by other groups^(2.1) which consist of greater or lesser numbers of components).

TYPICAL TRIPLET CONSTRUCTIONS

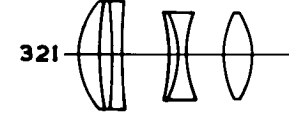
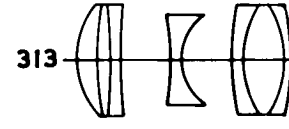
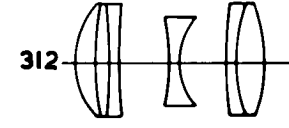
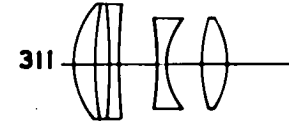
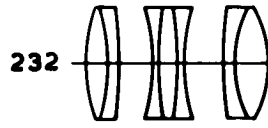
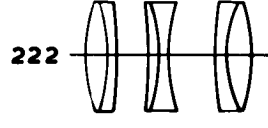
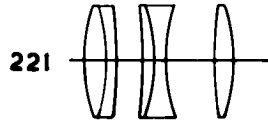
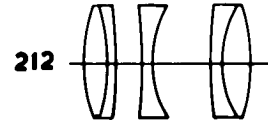
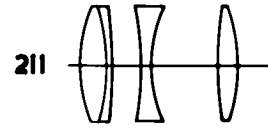
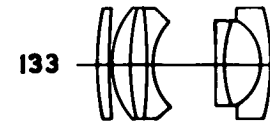
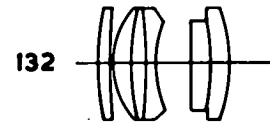
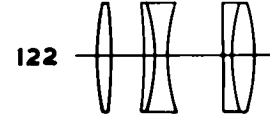
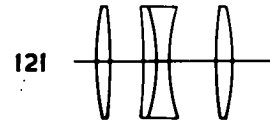
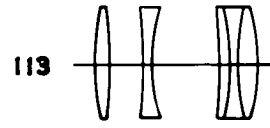
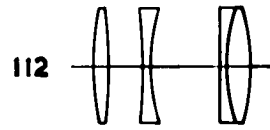
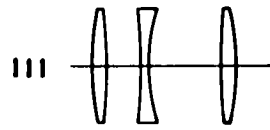


Fig. 1.1.1

1.1.3 The Basic Parameter k' .

A convenient way of representing this replacement is to use a parameter k' ^(2.2) that denotes the distribution of power in the doublet. However, in this work it has been noticed that care must be taken in defining k' because it must account for the order of the components as well as the magnitude of their powers in order to avoid ambiguities or at least awkward steps in the logic.

Just as he has had to specify the order of the signs of the powers of the components a, b, c in the basic triplet, the designer now has to make a similar decision when a single component is replaced by a compound one. A doublet for example, may be inserted with either its positive or negative component leading and thus, the type 121 triplet (a triplet with a cemented doublet in place of lens b, see Figure 1.1.1)* may have either the power pattern $+(+ -)+$ or $+(- +)+$. These possibilities are accounted for if the parameter k' is defined as follows:

$$k'_j \stackrel{\text{defn.}}{=} \phi_2 / \phi_1 \quad 1.34$$

where ϕ_2 is the power of the back component and ϕ_1 the power of the front component of the j^{th} doublet.

It is convenient to name the two ways a doublet may be inserted. Thus when the main power of the doublet leads, for example, if we have a positive doublet with the

* (Figure 1.1.1 reproduced from Cruickshank's paper,^(2.1))

positive power in the front, then we will call it a positive normal doublet replacement (denoted by PND).

If the negative component is allowed to lead then we will call it a positive reversed doublet replacement (PRD).

Similarly, the negative doublet replacement is either an NND (negative normal doublet) or an NRD (negative reversed doublet). So for example, a power pattern $+(+ -)+$ is a "type 121 NRD".

Each replacement of a component of the basic triplet by a doublet introduces a new degree of freedom in the form of a parameter k' which takes two ranges of values. For the normal form we find $-1.0 < k'_{ND} < 0$ and for the reversed form $-\infty < k'_{RD} < -1.0$. Although we are formally distinguishing between the k primes with the subscripts ND and RD these will be omitted when the numerical value is quoted, because the magnitude of k' is sufficient to signify the type of replacement.

1.1.4 Fictitious Glass.

So far we have assumed that a triplet with compound components is generated from a basic triplet of real glasses. However this need not be so, because, it is only required that the glasses of the compound arrangement be real, that is, (N_1, V_1) , (N_2, V_2) of equations 1.32 and 1.33 be real, in order to generate a real system. It is of no consequence when generating a real system whether the glass (N_j, V_j) of

the basic triplet, as given by these equations, is real or not; if the glass is imaginary it is called a "fictitious glass".

In this way the limitations imposed ^{by the set of real glasses} Λ is relieved to some extent. It is now possible to think of the basic triplet as a continuous function of the "basic glasses" ($N_j, V_j, j = a, b, c$) which comprise both real and fictitious glasses. Using this concept it is possible to penetrate regions of the design not available to the simple triplet ^(2.2). Also in thinking of the basic glasses as continuous variables, even if their ranges are limited, is also equivalent to saying $\alpha, \beta, \xi, \gamma$ are continuous in certain regions.

The fictitious glass constants expressed as functions of k^i are:

$$N_F = (1 + k^i)N_1 / (1 + k^i \cdot N_1/N_2) \quad 1.35$$

$$V_F = (1 + k^i)V_1 / (1 + k^i \cdot V_1/V_2) \quad 1.36$$

where (N_1, V_1) and (N_2, V_2) are given glasses.

For each fictitious glass (N_F, V_F) arising from a doublet, there are two possible arrangements, which are distinguished by having different parameters k_{ND}^i and k_{RD}^i each being the reciprocal of the other thus:

$$k_{ND}^i = 1/k_{RD}^i \quad 1.37$$

1.1.5 Optical Parameters and the Division of the Degrees of Freedom.

In this work we consider that the fundamental degrees of freedom available in the optical system are of two types, geometrical (curvatures, thicknesses and separations) and physical (refractive indices and V-numbers). In general, these fundamental variables are used in the final* stages of design when balancing or optimising the various aberrations. On the other hand the parametric degrees of freedom of the "basic triplet" that are used in the initial stages of design, cannot be classified as either simple geometrical or physical parameters since each is a function of both types of the fundamental degrees of freedom.

However, a broad distinction may be made. The parameters Φ, χ, k', P, L, T may be classified as either degrees of freedom depending on V or not depending on V. This is the distinction made in this work. We begin with a study of the monochromatic parameters (χ, k', P) and leave the chromatic parameters L and T until the monochromatic design principles are established. In this way the thin lens parameters are separated into those that are dependent on V and those that are not.

* (References 2.4, 4.2, 6.2, 8. 13.2)

1.1.6 Notes on Classification of Design Parameters.

The use of the terms Construction Parameters⁽¹⁾ and Performance Parameters is in keeping with the philosophy of design that is followed in this work. We will use the term construction parameter to mean any of those parameters which are used to define the structure of the optical system at each stage of development, eg. $\Phi, \lambda, k', P, L, T, N_a, V_a$ etc. in the thin stage or curvatures and separations in the thick stage.

Also we will use the term performance parameter to mean parameters that are chosen to define the properties of the system at the various stages of the design, eg., aberration residuals of all kinds⁽⁸⁾. For convenience the construction parameters can be subdivided further into "basic construction parameters and fundamental construction parameters". Also each of these classes may be divided into chromatic and monochromatic parameters. Thus we may speak of chromatic-basic-construction-parameters, monochromatic-basic-construction-parameters, chromatic-fundamental-construction-parameters and monochromatic-fundamental-construction-parameters. These construction parameters are associated with either chromatic or monochromatic performance parameters. (See application of these Chapter 2.1)

1.1.7 Summary.

In this chapter the basic theory has been developed for finding the initial arrangement of triplets, with constructions involving compound components, so that they have certain 3rd order residuals specified. We began with the thin lens analysis of a simple triplet and showed how its initial arrangement can be converted into the initial arrangement of a more complex triplet type. Also we showed how this conversion, which consists of the replacement of a single thin lens by a group of thin lenses, is equivalent to a change in the glass parameters of the initial thin lens arrangement of the simple triplet. Treating the thin lens analysis of the triplets in this way allows the replacement of a single component by a doublet to be represented by a single parameter k^1 that defines the distribution of power within the doublet.

Thus in this chapter a general triplet system has been defined "The basic triplet" and in keeping with our approach to design we think of it as being the set of powers and separations $\phi_a, \phi_b, \phi_c, t_a, t_b$ that are generated from the set of parameters $\bar{\phi}, \gamma, P, L, T, N_a, N_b, N_c, V_a, V_b, V_c$. We call these "basic parameters" and in particular we call $(N_a, V_a), (N_b, V_b), (N_c, V_c)$ the "basic glasses" that may be either real or fictitious. When the basic glasses are all real glasses we have the simple Taylor Triplet which we call the type 111. When

the basic glasses are fictitious the basic triplet is generated from a set of basic parameters that now contain a k' for each doublet.

In this preliminary study of triplet objectives the systems are restricted to an infinitely distant object plane and a centrally placed stop.

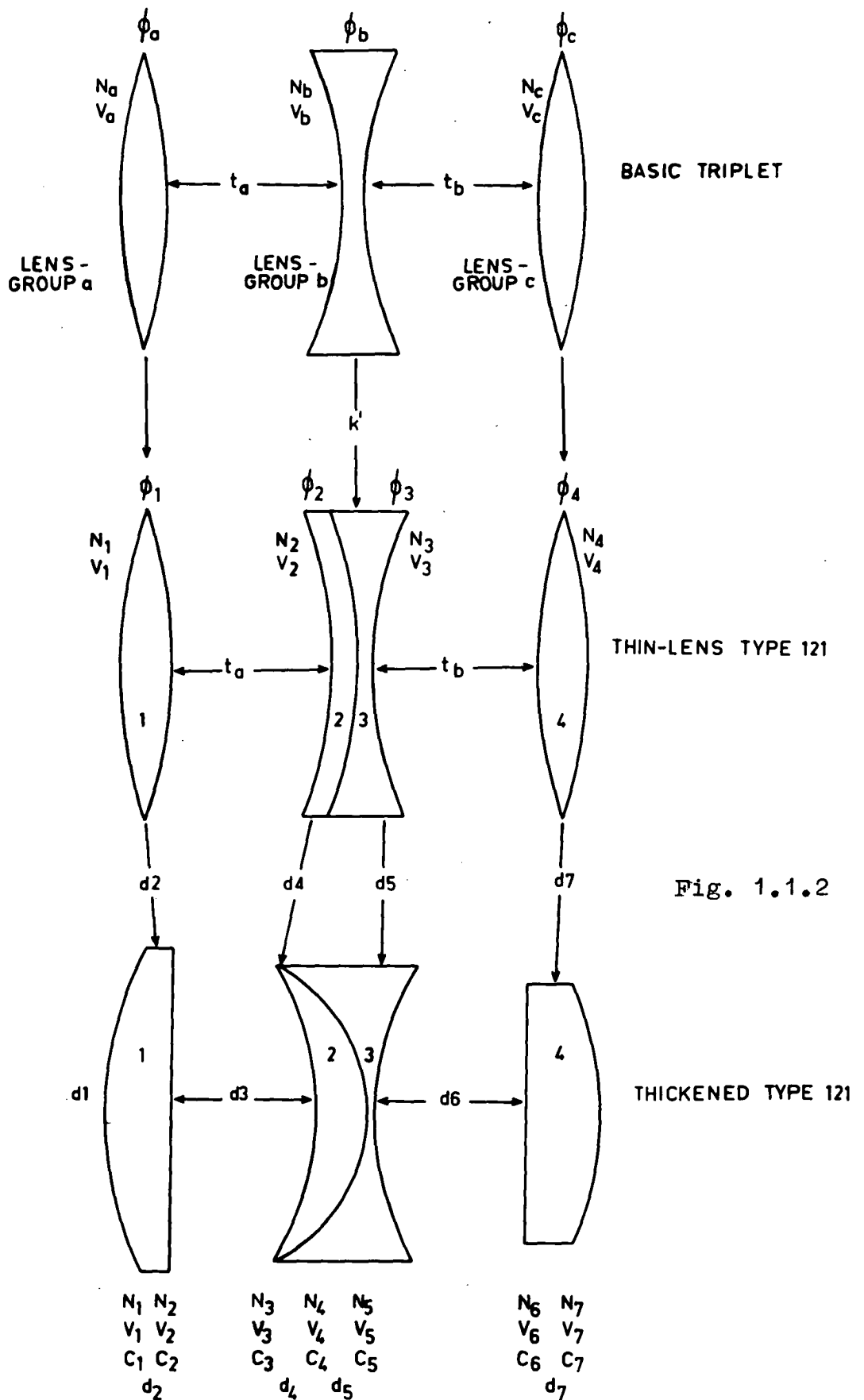
CHAPTER 1.2 THE SYSTEMATIC DESIGN OF A 3rd ORDER TYPE 121 TRIPLET.

1.2.1 General Considerations.

A type 121 triplet (the middle lens is a cemented doublet, see Figure 1.1.1) has the following construction parameters available for controlling the optical characteristics of the system: four glass types, seven curvatures, four axial thicknesses, two separation distances and the location of the aperture stop. These fundamental parameters are shown in the bottom diagram of Figure 1.1.2 where they are as follows:

- (1) The four glasses are (N_1, V_1) , (N_2, V_2) , (N_3, V_3) , (N_4, V_4) .
- (2) The curvatures are c_1 to c_7 .
- (3) The axial thicknesses are d_2, d_4, d_5, d_7 .
- (4) The separations are d_3, d_6 .
- (5) The stop position is not shown but it will be given as the distance p^* from the back surface of lens 1 whenever it is required.

The glass parameters (index of refraction N and the dispersion V) are not considered to be continuous variables in this primitive design. Indeed the choice of glass in the initial example that is described in Chapter 1.4 is made on the basis of the experience of other designers (2.1, 4.2).



The position of the aperture stop is also not considered to be a continuous variable^(1, 2.1, 4.2) in the preliminary design of the type 121. It is kept at the front principal point of the cemented lens group in the Thickened-Type 121 and at the thin lens b in the Thin-Lens Type 121.

The four axial thicknesses are not considered to be continuous variables; they are given fixed values that allow sufficient aperture for a large variation in the design parameters.

The nine remaining fundamental parameters ($C_1, C_2 \dots C_7, d_3, d_6$) may be considered to be continuously variable over large ranges. Thus there are nine variables available for controlling nine design quantities; This number exceeds by one the minimum number which is required for the design of a fully corrected system of moderate aperture and field. These minimum requirements^(1, 2.1, 4.2) are as follows:

- (1) Scale of the system (equivalent focal length).
- (2) Petzval sum.
- (3) Longitudinal Chromatic Aberration.
- (4) Lateral Chromatic Aberration.
- (5) Third Order Spherical Aberration Residual R_1 .
- (6) Third Order Coma Residual R_2 .
- (7) Third Order Astigmatism Residual R_3 .
- (8) Third Order Distortion Residual R_5 .

In this work the attack on the design of the type 121 triplet is concerned in the initial stages with the behaviour of a primitive stage of the design, the 3rd Order Triplet which is defined below. This initial design is generated systematically by a well known process^(1, 2.1, 4.2) which is outlined in the following section.

1.2.2 The Systematic Design Process of the 3rd Order Type 121 Triplet Outlined.

If the designer sets out to construct a "3rd order type 121 triplet" from a given set of glasses he can do it systematically in three stages starting from the "basic triplet" and going via the thin lens arrangement of the type 121 to the "Thick Type 121" as shown schematically in Figure 1.1.2. Using this method in this chapter the design theory is started from a given set of glasses and "basic parameters" and developed to the stage where the thick system has the following features determined:

- (1) The scale of the system (equivalent focal length)

$$f^* = R_9.$$

- (2) Axial thicknesses d_2, d_4, d_5, d_7 .

- (3) The 3rd order coma residual $R_2 = 0$.

- (4) The 3rd order condition for a flat tangential field

$$R_3 = 0.$$

- (5) The 3rd order distortion residual $R_5 = 0$.

In this approach to designing a type 121 it is assumed to have the following continuous independent variables:

- (1) The "basic parameters" $\bar{\phi}, \bar{\chi}, P, L, T, k$ in the first stage.
- (2) The shapes S_1, S_2, S_4 in the second stage.

These parameters account for the nine degrees of freedom available with the type 121 for controlling nine features of the design. However we decided above to only use five of them in the initial stage. The triplet with these features we will call the "3rd order type 121 triplet".

The nine features to be controlled in the finished design of the type 121 will be denoted by R_1 to R_9 of which only R_2, R_3, R_5 and R_9 have been defined for the 3rd order triplet; the remaining ones will be defined as they occur in more advanced stages which are dealt with in later chapters. So from the beginning we know that the designer is free to choose any nine features but he has only selected five initially.

In order to compute the 3rd order type 121 triplet the designer supplies the following:

- (1) Four glasses $(N_1, V_1), (N_2, V_2), (N_3, V_3)$ and (N_4, V_4) .
- (2) Basic parameters $\bar{\phi}_1, \bar{\chi}_1, P_1, L_1, T_1, k_1$.
- (3) The axial thicknesses d_2, d_4, d_5, d_7 and he is given the following:
- (4) The stop position p' which for the 3rd order triplet is kept at the first principal point of lens group b.

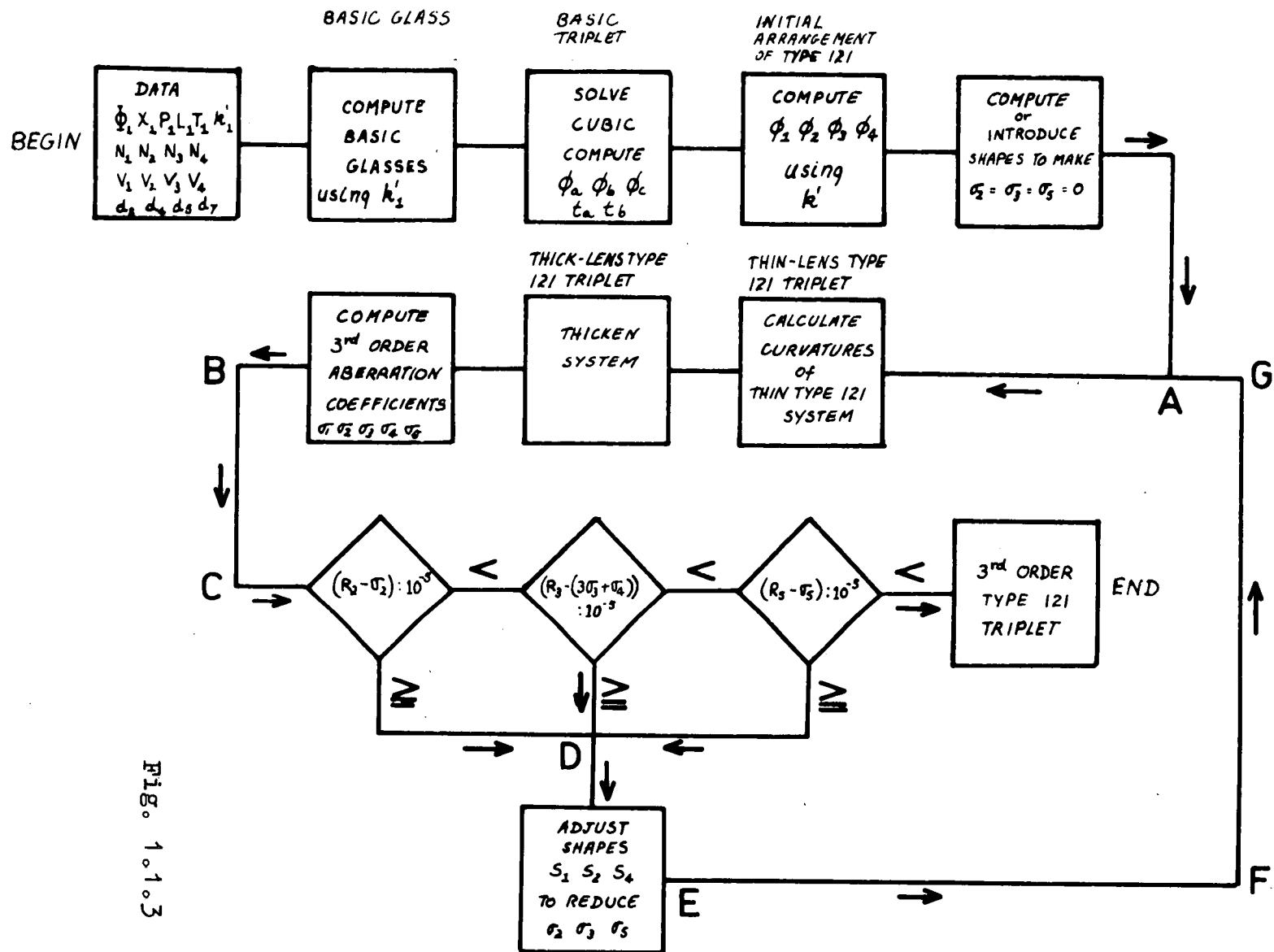


Fig. 1.0.1.3

(5) $R_2 = R_3 = R_5 = 0$ (R_3 is the 3rd order condition for a flat tangential field).

(6) $R_9 = 1$.

The main steps in the systematic design of a 3rd order type 121 triplet are shown schematically in the flow diagram* Figure 1.1.3; the ensuing description refers to this diagram.

The design is started by selecting the data and computing the fictitious glass constants (N_b , V_b). This enables the cubic equation (1.26) of the basic triplet to be set up and solved iteratively, starting with $\eta_{ob} = 0.7$. Then the basic-triplet is converted into the initial arrangement (powers and separations) of the type 121^{by} using k' to convert ϕ_b to ϕ_2 and ϕ_3 .

The Thin-Lens Type 121 is obtained by analytically** (2.1) finding the shapes which make the 3rd order Seidel coefficients σ_2 , σ_3 and σ_5 zero^(13.1), 13.2). Thus the Thin-Lens Type 121 (stage 2, Figure 1.1.2) has unit power and zero 3rd order coma, astigmatism and distortion.

In the third stage the system is thickened using Berek's Method which produces the Thick-Type 121 with its powers ϕ_1 , ϕ_2 , ϕ_3 , ϕ_4 and total power unchanged from those

* This flow diagram is only intended to illustrate the design process of a 3rd order system in a compact form that will assist the reader to grasp the essential steps in this design process.

** Experience has shown that this design process may be started from a given set of approximate shapes there being

of the Thin-Type 121. However, the thickening process causes changes in the aberration coefficients σ_2 , σ_3 and σ_5 so that they differ from R_2 , R_3 and R_5 .

In the fourth stage the coefficients σ_2 , σ_3 and σ_5 of the Thick-Type 121 are reduced to the prescribed values R_2 , R_3 and R_5 by adjusting the shapes iteratively in the cycle A B C D E F G (Figure 1.1.3) using Newton's method^(4.1). This well known method finds difference quotients $(\Delta\sigma_k/S_j)$ *** for given finite shape changes dS_j in each cycle. These difference quotients are used in place of differentials in estimating the required shape changes. The cyclic process is continued until the three conditions are met.

On completion of this design process the designer has a thick type 121 triplet of unit focal length, zero 3rd order coma, distortion and a flat tangential field. Its stop is located at the front principal point of the cemented doublet which is usually between surfaces 3 and 4.

The remaining sections of this chapter briefly describe all the theory of this systematic design process

** (cont.)

no need to find the 3rd order thin triplet exactly for this iterative process. This dispenses with the shape analysis after the first solution or if approximate shapes are available from other similar designs the analysis is not required.

*** $k = 2, 3, 5$ $j = 1, 2, 3, 4$ for the type 121.

necessary for programming the 3rd order triplet. However at this point the reader at first reading may prefer to go directly to Chapter 4 where a preliminary study of some 3rd order type 121 triplets is discussed. This study may be understood without absorbing background theory from the rest of this chapter or the discussion of programming from Chapter 3. The reader only needs to know for this purpose the contents discussed so far and also that a programme called the basic programme (denoted sometimes by BP121), which computes the 3rd order type 121 triplet from the data described above, has been written.

Moreover, any programming details that have been discussed as the need has arisen in later chapters, have been treated under separate headings so that the reader may by-pass them if he wishes without serious loss of continuity in the discussion of the systems properties.

However, the writer believes that a better appreciation of the optical design process is gained from a discussion of the basic programme and therefore he prefers the logical development of the design theory and programming of it prior to becoming involved in the numerical details of the study of the actual systems. This of course is not the way he approached the problem which was via a desk calculator and existing design techniques created for this facility. However, this was before a computer was available.

Now after some experience with both phases he believes that an understanding of the known theory and flexible programming of it, before looking at numerical results of examples, is preferable. In view of existing knowledge this seems to be the most objective approach.

1.2.3 Theory of the 3rd Order Type 121 Triplet.

1.2.3.1 Stage 1:- Finding the initial arrangement of the 121.

In this stage the powers and separations are computed from the given initial conditions. To begin, the fictitious glass constants (N_F , V_F) are computed as follows:

$$N_F = (1 + k^t)n_1 / (1 + k^t \cdot n_1/n_2) \quad 2.1$$

$$V_F = (1 + k^t)v_1 / (1 + k^t \cdot v_1/v_2) \quad 2.2$$

where $n_1 = N_2$, $n_2 = N_3$ 2.3

$$v_1 = V_2$$

$$v_2 = V_3 \quad 2.4$$

and $k^t = k_1^t$ 2.6

Now we can proceed with finding the initial arrangement of the "basic triplet" that is constructed from the following "basic glasses":

$$N_a = n_1, N_b = N_F, N_c = N_4 \quad 2.7$$

and $V_a = v_1, V_b = V_F, V_c = V_4$ 2.8

Briefly, the ratios α , β , ξ and γ are obtained and these, together with the given basic parameters ϕ_1, χ_1 ,

P_1, L_1, T_1, k_1^i are used in equations 1.27 to 1.30 to calculate the coefficients G_0, G_1, G_2, G_3 . Then equation 1.26 is solved iteratively, starting with $\eta_{lob} = 0.7$, and then, the powers and separations ($\phi_a, \phi_b, \phi_c, t_a, t_b$) of the "basic triplet" are computed using equations 1.20 to 1.25.

In concluding this stage the basic triplet is converted into the initial arrangement of the type 121. Although this conversion only requires the replacement of ϕ_b by ϕ_2 and ϕ_3 , it is preferable to keep all three operations formally detailed, even if they seem trivial, in order to establish, if possible, a general design procedure.

So that in this case we have:

$$\phi_1 = \phi_a \quad 2.9$$

$$\phi_2 = k_1^i \cdot \phi_b \quad 2.10$$

$$\phi_3 = k_2^i \cdot \phi_b \quad 2.11$$

$$\phi_4 = \phi_c \quad 2.12$$

$$d_3 = t_a \quad 2.13$$

$$d_6 = t_b \quad 2.14$$

At this point the triplet system has a focal length $f^i = 1$, a Petzval residual of $R_4 = P/N_a$, a longitudinal chromatic residual of $R_6 = L \cdot y_{oa}/V_a$, a transverse chromatic residual of $R_7 = T \cdot \bar{u}_a/V_a$, $\mathcal{X} = \mathcal{X}_1$ and $k^i = k_1^i$. The value of $k^i = k_1^i$ also implies that we have given \mathcal{Q} and β the values

$$\mathcal{Q} = N_F/N_a, \quad \beta = V_F/V_a \quad 2.15$$

1.2.3.2 Stage 2:- Finding initial shapes of the thin solution.

The three remaining degrees of freedom of the thin system are used to control its 3rd order coma, astigmatism and distortion. For this purpose the shapes of the first, second and fourth components, S_1 , S_2 and S_4 are used. The shape of the third component is given by putting $S_j = S_2$ in the cementing condition:

$$S_{j+1} = Z(S_j + 1) - 1$$

where
$$Z = [(N_{j+1} - 1) / (N_j - 1)] / k^2 \quad 2.16$$

(In this work the shape of the leading component of a doublet is selected to be the independent one.)

The shapes are defined by

$$S_j = [(C_1 + C_2) / (C_1 - C_2)]_j \quad 2.17$$

after Coddington.

The 3rd order correction is defined in terms of the 3rd order Buchdahl coefficients^(13.1, 13.3, 2.6) of the Seidel form. These are represented by $\overline{\sigma}_1, \overline{\sigma}_2, \overline{\sigma}_3, \overline{\sigma}_4$ and $\overline{\sigma}_5$ being the coefficients of primary spherical, coma, astigmatism, Petzval curvature and distortion respectively.

At this stage of the design we want the system to have shapes that make the primary residuals zero, that is we want $\overline{\sigma}_2 = R_2 = 0, \overline{\sigma}_3 = R_3 = 0, \overline{\sigma}_5 = R_5 = 0$ 2.18
As we are looking at this design for the first time, we must find an initial solution for the shapes by solving the following three thin lens equations^(2.1, 2.5, 2.6, 2.7) for the

thin lens type 121.

$$\sigma_2 = \sum_{j=1}^1 (a_{21}S^2 + a_{22}S + a_{23})_j \quad 2.19$$

$$\sigma_3 = \sum_{j=1}^1 (a_{31}S^2 + a_{32}S + a_{33})_j \quad 2.20$$

$$\sigma_5 = \sum_{j=1}^1 (a_{51}S^2 + a_{52}S + a_{55})_j \quad 2.21$$

where 1 = number of components of system which for the type 121 is four. The placing of the stop at the middle thin lens reduces 2.20 and 2.21 to equations of two variables, S_1 and S_4 , that are solved by a simple iterative method. The equation 2.16 is used to convert S_3 to S_2 in equation 2.19.

Thus at the end of Stage 2 we have a thin-lens type 121 with the following specifications

| | | | | | |
|------------------|----------|----------|----------|----------|------|
| Refractive index | N_1 | N_2 | N_3 | N_4 | |
| V-numbers | V_1 | V_2 | V_3 | V_4 | |
| Powers | ϕ_1 | ϕ_2 | ϕ_3 | ϕ_4 | |
| Shapes | S_1 | S_2 | S_3 | S_4 | 2.22 |

$$d_1 = d_2 = d_4 = d_5 = d_7 = 0$$

$$d_3 = t_a, \quad d_6 = t_b$$

$$\phi_1 = 1, \quad \chi = \chi_1, \quad k' = k_1'$$

$$P = P_1, \quad L = L_1, \quad T = T_1$$

1.2.3.3 Stage 3:- Developing a thick system from the thin solution.

1.2.3.3.1 Adjusting Powers.

In this step the lenses are assigned axial thicknesses that are sufficient to provide for an adequate aperture. (Indeed in this study of the type 121 triplet system the values of d_2 , d_4 , d_5 and d_6 are chosen, if possible, to allow for the variation in the aperture for a large range of the parameters \mathcal{N} , k' and P .) After thickening, the powers of the system are kept the same as those of the thin solution. This is achieved in two steps^(2.7):

(1) The curvatures and intersection heights of each lens are recomputed, following the general method of Berek, so as to adjust their powers to those of the thin lens. A paraxial-ray (p-ray) with initial co-ordinates ($y_{01} = 1$, $v_{01} = 0$) is traced. The thick curvature of the leading surface of each of the basic groups of components that we have denoted by a , b and c is given by

$$^*c_1 = c_1 / (1 + l_{p1}^* / l_{01}) \quad 2.23$$

where $*$ denotes the thick quantity.

This requires l_{p1}^* which is not known, therefore, the process is started with l_{p1} and then the remaining curvatures and intersection heights are determined by:

$$^*c_j \cdot y_j = c_j \cdot y_j \quad 2.24.1$$

$$y_{j+1}^* = y_1^* - d_{j+1}^* \cdot v_{oj+1}^* \quad 2.24.2$$

The values obtained for c_j^* and y_j^* , of course, will only be approximations to the required values, because of l_{p1}^* . However, these approximate values of c_j^* and y_j^* allow us to calculate a better estimate of l_{p1}^* with which to recalculate c_1^* of the lens group. In general, three repetitions are sufficient to adjust the curvatures and intersection heights.

(2) The separations are altered so as to keep the total power of the thick system the same as that of the thin system. The object and image planes are not shifted. Thus the separations after thickening are given by:

$$d_3 = t_a + l_{pa}^* - l_{pb}^* \quad 2.25.1$$

$$d_6 = t_b + l_{pb}^* - l_{pc}^* \quad 2.25.2$$

1.2.3.3.2 Adjusting the Thick Lens Residuals.

The stop is placed at the first principal point of the middle lens group (b), so that its distance from the pole of the rear surface of lens group (a) is

$$p' = t_a = l_{pa}^* \quad 2.26$$

and the distance of the entrance pupil from the pole of the front surface of the system is therefore

$$p = (D_a \cdot p' - B_a) / (A_a - C_a \cdot p') \quad 2.27$$

where A_a , B_a , C_a and D_a are paraxial coefficients^(2.5).

Now the 3rd order coefficients^(2.6) are obtained from the results of two paraxial ray traces,

the p-ray $(y_{01} = 1, v_{01} = 0)$ 2.28

and the q-ray $(y_1 = p, v_1 = 1)$ 2.29

As a result of thickening, the aberration residuals σ_2, σ_3 and σ_5 are, in general, significantly different from those of the thin system and therefore must be reduced to the target values by making appropriate changes in shape. (This involves finding the partial differential coefficients of the primary aberration coefficients with respect to the shapes. This is normally a lengthy computation. However, in this work, it has been found that a simple approximation to the partial differential coefficients is sufficient for, at least, systems of the triplet type. The computation using the simple approximation is shorter and allows more efficient programming. It is described and discussed along with other methods in appendix 2.1.)

On the basis of computational experience with several types of triplet it has been found that an empirical relationship may be assumed between the residuals R_2, R_3 and R_5 of the thick system and the independent shapes of its basic thin system, so that we may formally write:

$$\begin{aligned} R_2 &= \sigma_2 = f_1(S_a, S_b, S_c) \\ R_3 &= \sigma_3 = f_2(S_a, S_b, S_c) \\ R_5 &= \sigma_5 = f_3(S_a, S_b, S_c) \end{aligned} \quad 2.30$$

where S_a, S_b, S_c signify the independent shapes of the lens groups associated with the initial arrangement. For the

type 121 then, $S_a = S_1$, $S_b = S_2$, $S_c = S_4$.

The approximate changes^(17.1, 18) in S_a , S_b , S_c necessary to correct the residuals of the thick system therefore are given by the solution of three simultaneous "small error"^(17.1) equations:

$$\begin{aligned} \text{(i)} \quad & a_1 dS_a + b_1 dS_b + c_1 dS_c = -dR_2 \\ \text{(ii)} \quad & a_2 dS_a + b_2 dS_b + c_2 dS_c = -dR_3 \\ \text{(iii)} \quad & a_3 dS_a + b_3 dS_b + c_3 dS_c = -dR_5 \end{aligned} \quad 2.31$$

where for $X = a, b, c$ we have

$$\begin{aligned} \text{(i)} \quad & X_1 = \partial \sigma_2 / \partial (S_X)_1 \\ \text{(ii)} \quad & X_2 = \partial \sigma_3 / \partial (S_X)_2 \\ \text{(iii)} \quad & X_3 = \partial \sigma_5 / \partial (S_X)_5 \end{aligned} \quad 2.32$$

(Several methods for estimating X by Newton's Method are discussed in the appendix 2.1).

After the new shapes have been computed the calculation is restarted at the end of stage 2. This cycle is repeated until $\sigma_2 = R_2$, $(3\sigma_3 + \sigma_4) = R_3$ and $\sigma_5 = R_5$. The "3rd order triplet" has, by definition, $R_2 = R_3 = R_5 = 0$.

1.2.4 Summary.

We have seen that the design process consists of four stages:

- (1) The initial solution to get Powers and Separations.
- (2) The selection or calculation of shapes to control 3rd order residuals, coma, astigmatism and distortion.
- (3) Thickening of the thin solution and computing of the 3rd order residuals of the thick system.
- (4) The bending of the system to adjust R_2 , R_3 and R_5 .
This involves repetition of stages 2 and 3 until target values are reached. We have found that the adjustment of the shapes can be accomplished by a simple iterative process when the contributions of each lens are used to compute the partial differential coefficients of the residuals with respect to the shapes. (See appendix 2.1)

On completion of this design process the triplet has 3rd order residuals of coma = R_2 , distortion = R_5 and a flat tangential field.

APPENDIX 2.1 METHODS FOR CALCULATING THE DIFFERENTIAL COEFFICIENTS OF THE ABERRATION RESIDUALS VERSUS THE SHAPES.

A.2.1.0 Introduction.

A simple iterative method* which is based on the additive property of the surface contributions of the Buchdahl coefficients has been devised in this work for optimizing the residuals. It is convenient for us to approach the description of this method through a description of earlier techniques used in this laboratory.

Prior to this work, the partial differential coefficients were estimated in either of the following two ways:

A.2.1.1 Method 1. Using Thin Lens Differential Coefficients.

Expressions for the thin lens partial differential coefficients were obtained by differentiating equations 2.19, 2.20, 2.21 and these were used in place of the thick differential coefficients. However, the differential coefficients given by these expressions need to be recomputed frequently if the initial residuals are relatively large in comparison with the target values.

* First discovered with the type 121 later used in 111, 112, 122, 212 and 222.

A.2.1.2 Method 2. Using Thick Lens Differential coefficients.

This method involves the direct computation of the partial differential coefficient using finite differences in the shapes. From the equation 2.32 we see that there are nine of these partial differential coefficients and that they are divided into three equal sets, one for each of the lens groups a, b and c. A separate computation must be made for each group and this involves recomputing the thick system starting from the initial arrangement each time a shape is altered.

For example, consider finding the differential coefficient of the lens group (a) of the type 121 triplet.

Let the independent shapes of the initial thick system be S_{11} , S_{21} and S_{41} where the first subscript denotes the order of the lens component and, the second subscript denotes the order of the triplet system; in this case the initial system obtained during the calculation of the differential coefficients. The residuals of the initial system are R_2 , R_3 and R_5 . In order to estimate the partial differential coefficients of group (a) the 121 system is computed with the independent shape of group (a) ^{changed} by a small amount S_1 , resulting in residuals $(R_2)_a$, $(R_3)_a$ and $(R_5)_a$. This analysis for the differential coefficients of group (a) is set out in the following table together with that of the differential coefficients of the other lens groups (b) and (c).

| | Shape Change | | | Input (Shapes) | | | Output Residuals | | |
|------------------|--------------|--------------|--------------|-----------------------|-----------------------|-----------------------|------------------|-----------|-----------|
| | ΔS_a | ΔS_b | ΔS_c | S_a | S_b | S_c | R_2 | R_3 | R_5 |
| Initial Solution | 0 | 0 | 0 | S_{11} | S_{21} | S_{41} | $(R_2)_1$ | $(R_3)_1$ | $(R_5)_1$ |
| changing a | ΔS_1 | | | $S_{11} + \Delta S_1$ | | | $(R_2)_a$ | $(R_3)_a$ | $(R_5)_a$ |
| changing b | | ΔS_2 | | | $S_{21} + \Delta S_2$ | | $(R_2)_b$ | $(R_3)_b$ | $(R_5)_b$ |
| changing c | | | ΔS_3 | | | $S_{41} + \Delta S_3$ | $(R_2)_c$ | $(R_3)_c$ | $(R_5)_c$ |

thus the differential coefficients of group (a) are

$$\begin{aligned}
 \partial \sigma_2 / \partial S_a &\approx \Delta R_2 / \Delta S_1 = [(R_2)_a - (R_2)_1] / \Delta S_1 \\
 \partial \sigma_3 / \partial S_a &\approx \Delta R_3 / \Delta S_1 = [(R_3)_a - (R_3)_1] / \Delta S_1 \\
 \partial \sigma_5 / \partial S_a &\approx \Delta R_5 / \Delta S_1 = [(R_5)_a - (R_5)_1] / \Delta S_1
 \end{aligned} \tag{2.33}$$

and a similar set of expressions is required for lens group (b) and lens group (c).

A.2.1.3 Approximate Differential Coefficients.

Each of the 3rd order coefficients may be expressed as the sum of the contributions from the surfaces since $R_j = \sigma_j = \sum_{k=1}^n \sigma_k$ where $j = 1, 2, 3, 4, 5$ and $n =$ number of surfaces of the system. Therefore we may expand the residuals of the triplet into the contributions from each of the basic lens groups a, b, c, for example,

$$(R_2)_1 = (R_2)_{1a} + (R_2)_{1b} + (R_2)_{1c} \tag{2.34}$$

$$(R_2)_a = (R_2)_{aa} + (R_2)_{ab} + (R_2)_{ac} \tag{2.35}$$

where for example $(R_2)_1$ = residual of the initial system

$(R_2)_{aa}$ = residual due to lens group a

for a change in shape of $\Delta S_a = \Delta S_1$.

If ΔS_1 is small then $(R_2)_{ab} = (R_2)_{1b} + \epsilon$ 2.36

and $(R_2)_{ac} = (R_2)_{1c} + \epsilon$ 2.37

where ϵ = infinitesimal.

Therefore if ΔS_1 is chosen properly it is sufficient in the practical design of triplets to ignore the contributions from lens groups other than the one in which the change in shape is made.

Thus for example,

$$\partial \sigma_2 / \partial S_a \approx [(R_2)_{aa} - (R_2)_{1a}] / \Delta S_a$$

where $(R_2)_{aa}$ is the contribution of group (a) due to ΔS_a and $(R_2)_{1a}$ is the corresponding contributions in the preceding system. This property of the residual that its significant change is confined, in general, to the lens group in which the shape change occurs, suggests that the differential coefficients of all the lens groups may be computed simultaneously from only one calculation of the system instead of three. Thus we come to the short method that was developed in this work for computing the approximate partial differential coefficients.

A.2.1.4 Method 3. Using Simultaneous Shape Changes.

If instead of a single shape change we calculate the system with shapes $(S_a)_2 = (S_a)_1 + \Delta S_a$, $(S_b)_2 = (S_b)_1 + \Delta S_b$ and $(S_c)_2 = (S_c)_1 + \Delta S_c$ and if these changes ΔS_a , ΔS_b and ΔS_c are small given values then we may write:

$$\left(\partial \sigma_j / \partial S_x\right)_m \approx \left(\Delta \sigma_{jx} / \Delta S_x\right)_m = \left[(R_j)_{(m+1)x} - (R_j)_{mx} \right] / \Delta S_x \quad 2.38$$

where now $j = 2, 3, 5$ and $X = a, b, c$ and $m =$ the order of the system in the iterative process.

In practice we found that $(\Delta \sigma_j / S_X)_m$ is a sufficiently good estimate of the partial differential coefficient of the m^{th} stage of the iteration. Therefore we have been able to develop a very simple iterative process for the adjustment of the 3rd order coma, astigmatism and distortion because the differential coefficient can be estimated simultaneously from the results of each stage of aberration adjustment without doing any auxiliary calculations.

In order that the notation of this method is clear we write the expression for one of the partial differential coefficients. Thus for example, the differential coefficient of coma relative to a change in the shape of lens (a) in the first iterative stage of the type 121 is

$$\left(\partial \sigma_2 / \partial S_a\right)_1 \approx \left(\Delta \sigma_{2a} / \Delta S_1\right)_1 = \left[(R_2)_{2a} - (R_2)_{1a} \right] / \Delta S_1$$

where the ΔS_a of the type 121 has the small value ΔS_1 throughout the iteration.

CHAPTER 1.3 PROGRAMMING THE 3RD ORDER TRIPLET.

1.3.1 Introduction.

In this chapter the construction of the basic-programme is described with the aid of flow diagrams. The basic-programme generates from a given set of thin lens parameters the 3rd order type 121 triplet. However, apart from this immediate objective of computing the 3rd order type 121 system the programming of all triplet types has been kept in mind also. Thus the design process has been programmed in a form that is intended to be both general and flexible.

1.3.2 General Considerations.

Considered as a whole the computation of the 3rd order triplet is complicated, however, it is found that it can be reduced to simple units which may be treated with comparative ease. This becomes clear when one compares the flow diagrams of this chapter with the flow diagram and the analysis of Chapter 2. The programmes of this work are seen to be made up of a number of "building blocks" or sub-routines. (A similar approach has been described by R.E. Hopkins and G. Spencer^(4.2).)

Although the immediate objective in this work has been the 3rd order design stage of the type 121 it has been found from experience that it is best in this sort of problem

to programme the smallest step with the general application in mind. If this approach is adopted then instead of finishing with a programme of limited use the designer will have a research facility that will not only enable him to handle the variations in the development of his immediate system but also will allow him to adapt it to other triplet types and possibly even to other systems, with little alteration.

The programme that satisfies these general concepts we will call the basic-programme. For convenience we denote it by the symbol BP121 that stands for the basic-programme of the type 121 triplet, the programme that generates the 3rd order type 121 triplet.

1.3.3 The Basic Programme as a Sub-Routine.

Programming with the general application in mind it soon becomes obvious to the designer that although the basic programme is constructed of many sub-routines it is also itself a sub-routine when considered in the context of the complete design process. This point must be grasped at the beginning if effective flexible programmes are to be written. Thus the material has been presented in Chapter 1 and 2 with the general application in mind. Indeed, this general approach has been essential for the successful treatment of the later parts of this work which are described in sections 2 and 3.

It is a straight forward matter to programme the type 121 directly from the equations of Chapter 2 and the flow diagram Figure 1.1.3. However, this approach yields, in general, a lengthy inflexible programme suitable for the immediate calculation but almost beyond comprehension of anyone except the actual programmer. This sort of thing occurs all too readily when using a modern pneumatic programming language such as Algol that allows the beginner and, for that matter, even the experienced worker who sacrifices flexibility for expediency, to make lengthy translations of the computing schemes similar to those of Chapter 2.

If we are to proceed efficiently with this type of optical design problem, we need a high speed computer and a flexible and reasonably efficient programme. From experience gained in this work, it is apparent that flexibility is the important property in all cases, a conclusion shared with other workers^(4.2).

Flexibility is achieved by programming in units of logic or sub-routines whenever possible. Indeed we find that Algol⁽¹¹⁾ is eminently suitable for flexible programming because it is endowed with many special features for constructing a great variety of sub-routines or, to use the Algol term, procedures.

Effort spent in creating these sub-routines for general application gives the designer great power.

1.3.4 The initial Design Programme or Basic Programme.

The initial design programme developed here, in general, possibly only differs from initial design programmes of other designers in the arrangement of the logic and not in the main concepts. Although, of course, there are also minor differences in the selection of design parameters because they have been defined for general application to the triplet family in this programme. However, in the search for generality, it has been found that the well known initial design process of the triplet^(2.1, 4.2, 4.3) which was described in Chapter 1.2 can be constructed almost entirely from sub-routines thus facilitating the programming of the more advanced stages of design which are dealt with later in this thesis as they arise.

Although many designers have written programmes employing sub-routines similar to many of those used here, it is believed that this is one of the few attempts^(4.2) to write each main unit of the logic of the design process in the form of a sub-routine. Thus the design process has been reduced to a set of basic sub-routines that may be assembled in almost any form required to meet the changes in the research problem. Consequently the final programme in each phase of the research consists of an executive-control routine that operates on a basic set of sub-routines. The simplest form of this initial design programme is the

"basic programme" if, and only if, it is written so that it can be incorporated in the more advanced stages of research without major changes.

1.3.5 Main Types of Sub-Routine or Procedure Defined.

In this "building block"^(4.2) approach to programming the design process, it is evident that the procedures can be conveniently divided into two main classes, those depending on the structure of the optical system and those that are not. We will call those that depend on the structure of the system or, in other words, those depending on the design concepts, the "system procedures", and those that perform fundamental optical, arithmetical and algebraical operations, "basic procedures". So for example, a sub-routine which calculates the position of the front principal point of an arbitrary lens group or solves three simultaneous equations is a "basic procedure or basic sub-routine". Whereas one that carries out a design stage such as computing a thin system from a given set of shapes and powers is a system procedure or system sub-routine.

1.3.6 Description of the Basic-Procedures and System Procedures used in the Basic Programme.

In the following list the procedures are arranged in the two main groups as defined above. The first contains the basic-procedures and the second the system-

procedures. In each group the procedures are arranged according to the order in which they occur in the basic programme. Each one is accompanied by a brief description of its function. The group of procedures for flexible triplet programming is as follows:

Basic Procedures.

1. Procedure Sum.

This adds n consecutive numbers between specified limits.

2. Procedure S.E.

This procedure finds the solution of three simultaneous equations whose coefficients and parameters are given.

3. Procedure Fictitious Glass.

This computes the fictitious refractive index and V-number of a cemented doublet that is specified in the procedure call by its position in the triplet.

4. Procedure Initial Solution.

This finds the basic triplet from the given set of thin lens parameters

$N_j, V_j, \alpha, \beta, \xi, \gamma, P, L, T$ where $j = a, b, c$.

5. Procedure Ray Trace (x, y)

Traces a paraxial ray through from $n = x$ to $n = y$. The initial ray coordinates y and v are specified in the procedure call.

6. Procedure Paraco (x, y).

Computes the paraxial coefficients^(4.4) of the part of an optical system between given surfaces $n = x$ to $n = y$.

7. Procedure lp (x, y, z).

Computes either the front or back principal point distance of any system defined to be between given surfaces $n = x$ and $n = y$. The interger z determines which principal point is calculated.

8. Procedure Thick (x, y).

This procedure thickens the thin lens group between surfaces $n = x$ and $n = y$.

9. Procedure ac(y).

Computes the Buchdahl 3rd order aberration coefficients^(2.6) of the optical system of 1 to n surfaces. The y is used to differentiate between systems.

Procedures 1 to 9 are the set of "basic-procedures" required for computing the 3rd order triplet. The point to be observed here is that the structure of the "basic-procedures" is independent of structural changes in the triplet optical system. So the details of the computation of the 3rd order triplet that depend on the system's structure are reduced by this means to a few procedure calls. This enables the designer to write a greatly simplified programme.

In order to complete the 3rd order triplet programme we require the system procedures that deal with the structure of the triplet; they are as follows:

System Procedures.

1. Procedure Ac(x).

This procedure which is shown in Figure 1.5 assembles the necessary basic procedures to carry out the task of obtaining the thick triplet from a given set of shapes and powers. It also computes the 3rd order aberration coefficients of the thick system. The parameter X differentiates between systems at successive stages of iteration (see changing shapes, Chapter 1.2).

2. Procedure Bending.

This procedure which is shown in Figure 1.4 carries out the shape changes required to adjust R_2 , R_3 and R_5 . The final system of this procedure is the "3RD ORDER TRIPLET".

3. Procedure Compound Parameters.

This converts the basic triplet into the initial arrangement of the complex triplet which is the type 121 in this example (see Figure 1.3).

4. Basic Glass.

This allots the basic glass constants (N_a , V_a), (N_b , V_b), (N_c , V_c) of the basic triplet. The procedure is similar in form to the procedure Compound Parameters being mainly the computation of the fictitious glass

constants of lens group b.

At this point all the procedures necessary for assembling the programme of the 3rd order type 121 triplet are available.

This list of procedures forms the basis of the programming technique used here and clearly it enables the designer to comprehend easily the processes involved in the design problem. Thus the main advantage of this approach is the flexibility it affords the designer in advanced stages of design. In the first place he can confidently carry the main features of his problem in his mind more easily because he can think of the steps in the problem as a set of operations; he is not overwhelmed by details. Secondly, any change in the design process can, in general, be reduced to a rearrangement of the procedures or to the construction of a new procedure that does not disturb the existing basic procedures. In general, alterations are confined to the executive control routines and they are usually of a minor nature. For example a typical change in the design process is when the designer changes from finding a triplet with $R_2 = R_3 = R_5 = 0 + 0(5)$ to finding one that, in addition to these residuals, has its spherical residual specified to 7th order (i.e. $R_1 = 0 + (9)$). This, as we shall see (Chapter 1.4), is handled by the inclusion of a procedure to compute the spherical coefficients of 3rd, 5th and 7th order and an additional executive control routine.

1.3.7 Description of the Basic-Programme.

The basic-programme computes the triplet with $R_2 = R_3 = R_5 = 0$ to 3rd order from a given set of basic-construction-parameters $\phi, \chi, k', P, L, T, S_1, S_2, S_4$ and glasses $(N_1, V_1), (N_2, V_2), (N_3, V_3)$ and (N_4, V_4) . The power is automatically adjusted to unity.

Following the programming principles discussed above we have found that the basic-programme reduces to the simple linear assembly of five sub-routines shown in Figure 1.2. The sub-routines are represented by blocks which are numbered 1.1 to 1.5 in this figure. The blocks 1.1, 1.3, 1.4 and 1.5 stand for four system-procedures and block 1.2 for a basic-procedure^{*}. The main details of all these sub-routines, with the exception of procedure "basic glasses" (block 1.1), are shown in auxiliary flow diagrams (Figures 1.3 to 1.6). The procedure basic-glasses is trivial merely being mainly the computation of the fictitious glass constants for the lens group b.

Experience has shown that the set of sub-routines which have been constructed in this work endow the basic-programme with great flexibility. The main reason for this flexibility is that the system-procedures keep all

* This is only a basic procedure with respect to triplet systems. In the general design process for all lens types this would be a system procedure also.

the systems construction-parameters in a compact and readily accessible form. In the interests of clarity and conciseness we have confined the flow diagrams to depicting the essential steps only, details of the triplet theory are described fully in Chapters 1.1 and 1.2. The computing of the Buchdahl coefficients is available in the literature where it has been described by several workers apart from the originator^(13.1, 2.4, 2.6).

The procedure Bending (Figure 1.4) is perhaps the most significant sub-routine because it embodies the design stages 2 and 3 of Chapter 1.2 in which the design progresses from the initial arrangement through the thin system to the thick system of prescribed R_2 , R_3 and R_5 (the 3rd order triplet). This procedure employs the remaining control-routine of this programme, procedure $Ac(x)$ (Figure 1.5) which is a complex system-procedure that controls several basic-procedures. It generates the thick system and its 3rd order aberration coefficients from a given set of shapes and thin lens parameters.

Although bending and $Ac(x)$ are the largest control-routines it is clear from the flow chart of Figure 1.2 that the procedures basic-glasses and compound-parameters Figure 1.3 also play significant roles. They allow a smooth progression from the data through the initial solution to the 3rd order triplet. Also they make the business of altering the programme for the

generation of a triplet of a different structure a trivial affair. If, say, we want to construct a Tessar programme from our type 121 programmes, then only simple changes are required in the control-routines. For example, when constructing the control-routine compound-parameters (Figure 1.3) for the Tessar, ϕ_2 is equated to ϕ_b , ϕ_3 and ϕ_4 become functions of the k' of the lens group c of the Tessar and the separation d_5 replaces d_6 . Of course, d_6 is retained elsewhere as the thickness of lens 4.

Thus in general the changes required in the basic programme for a change in triplet structure consist of the following:

- (1) change of a few subscripts.
- (2) alterations in a few procedure calls - simple numerical or parametric changes.
- (3) replacement of a single command by a double command or the reverse, as in procedure compound-parameters of the Tessar programme.

However, what is most important is that these alterations are confined to a small number of instructions in the five control-routines.

The schematic form of the programme's flow chart (Figure 1.2) shows very clearly the cybernetic-nature of the optical design process. It is evident that the process is one in which the observable quantities are a set of

input-parameters and a corresponding set of output-parameters. In this work with the type 121 "input-parameters" are the thin lens parameters $\bar{\phi}, \chi, k', P, L, T, S_1, S_2, S_4, N_1 \dots N_4, V_1 \dots V_4$, and the output-parameters are the thick lens "performance-parameters" $R_1, R_2 \dots R_8, R_9$ ($R_9 = \text{focal length}$).

BASIC PROGRAMME (BP121)

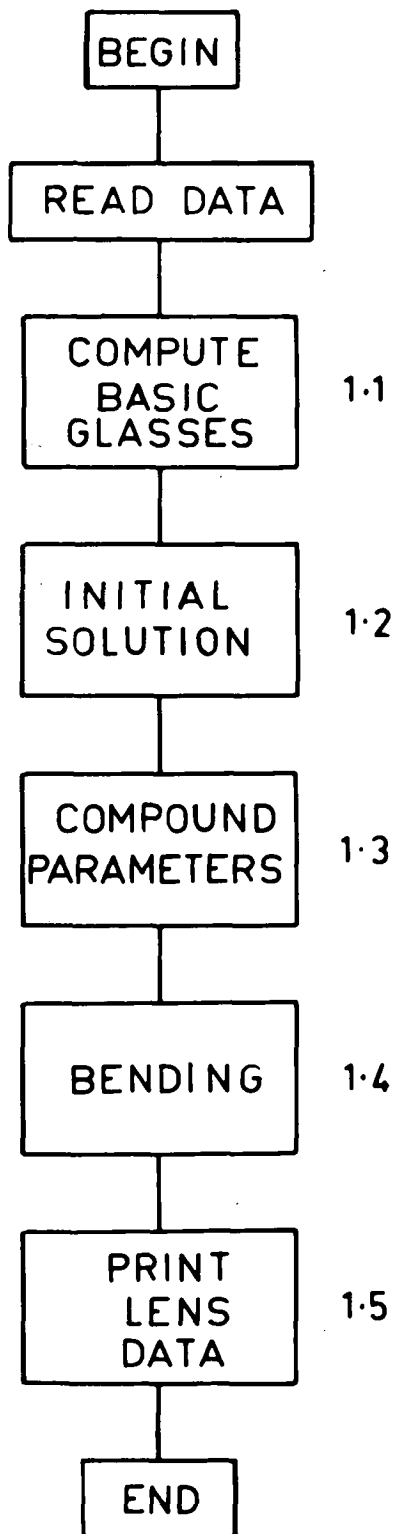


Fig. 1.2

SUB-ROUTINE (1.3) COMPOUND PARAMETERS

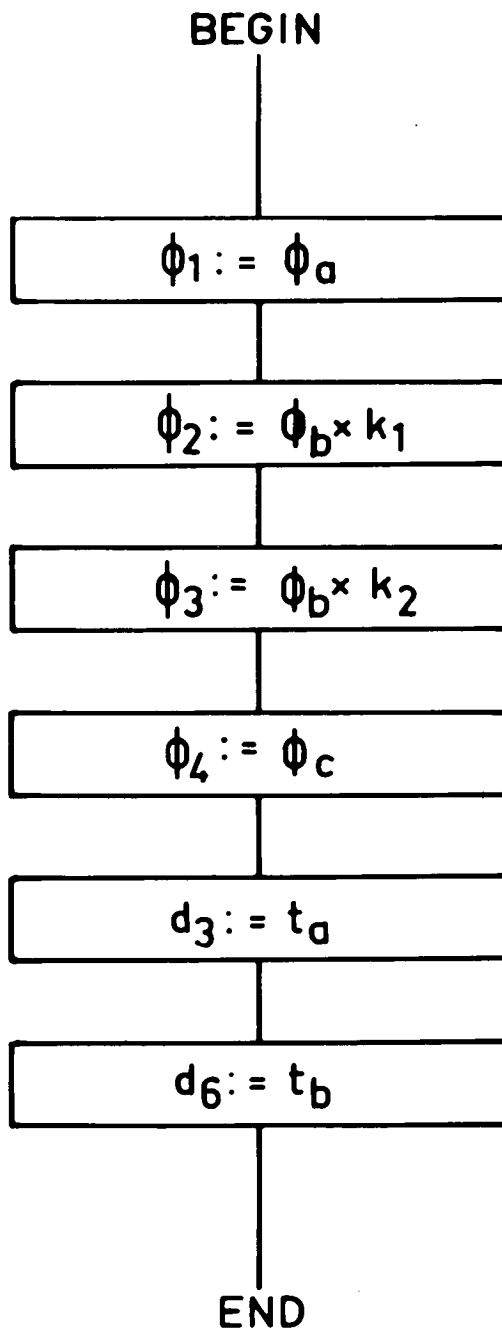


Fig. 1.3

SUB-ROUTINE. BENDING

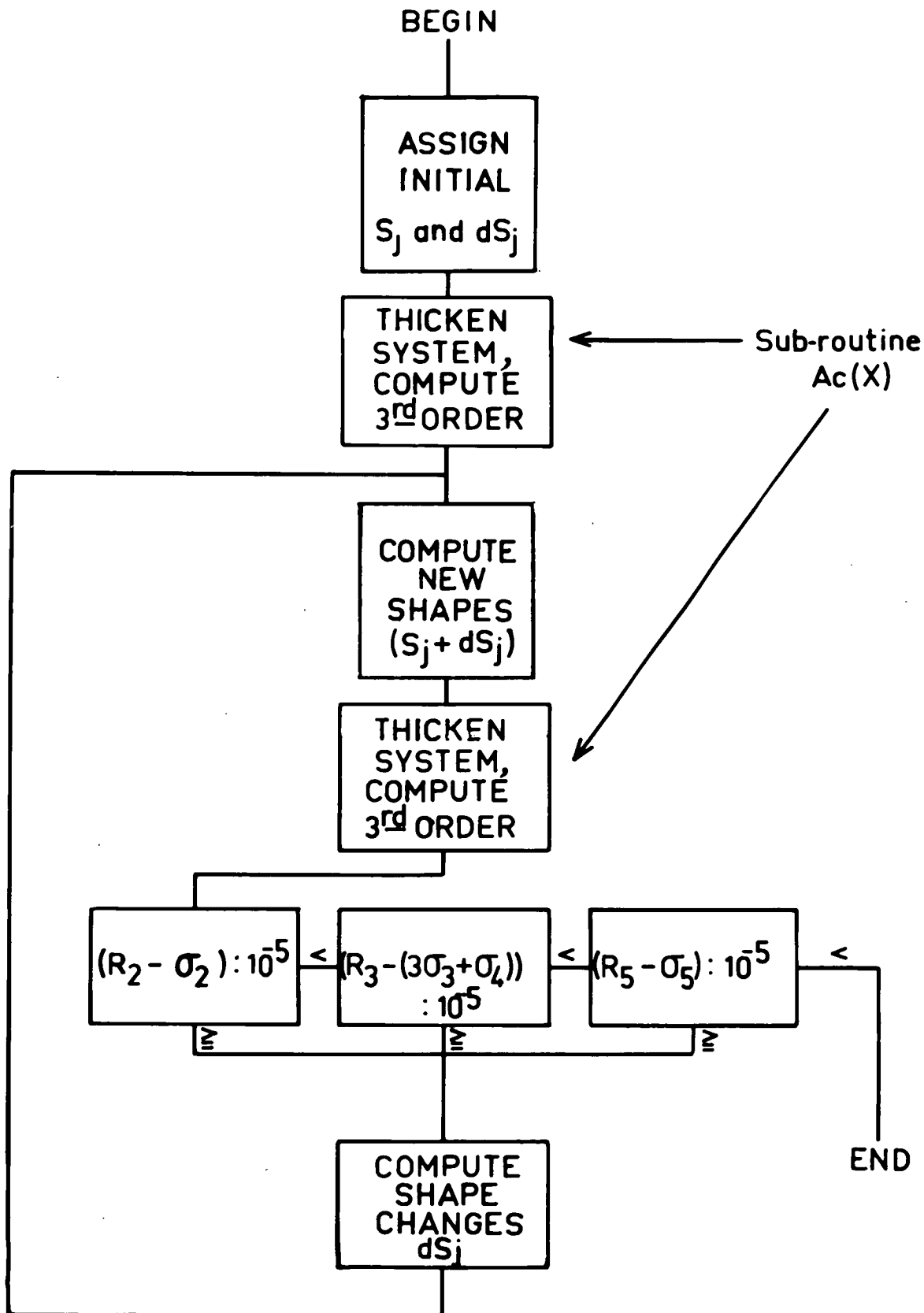


Fig. 1.4

SUB-ROUTINE $Ac(X)$

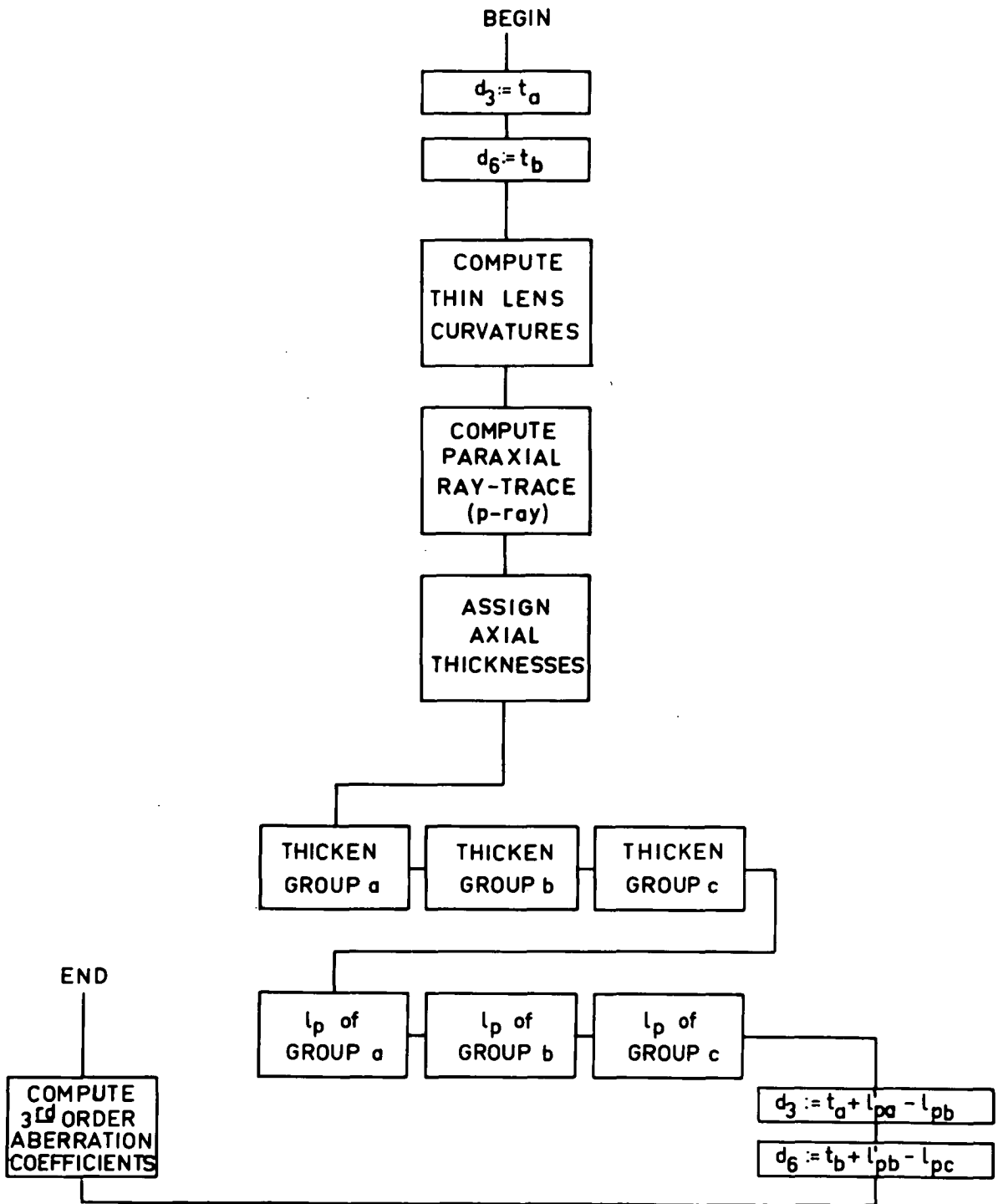


Fig. 1.5

SUB-ROUTINE INITIAL SOLUTION

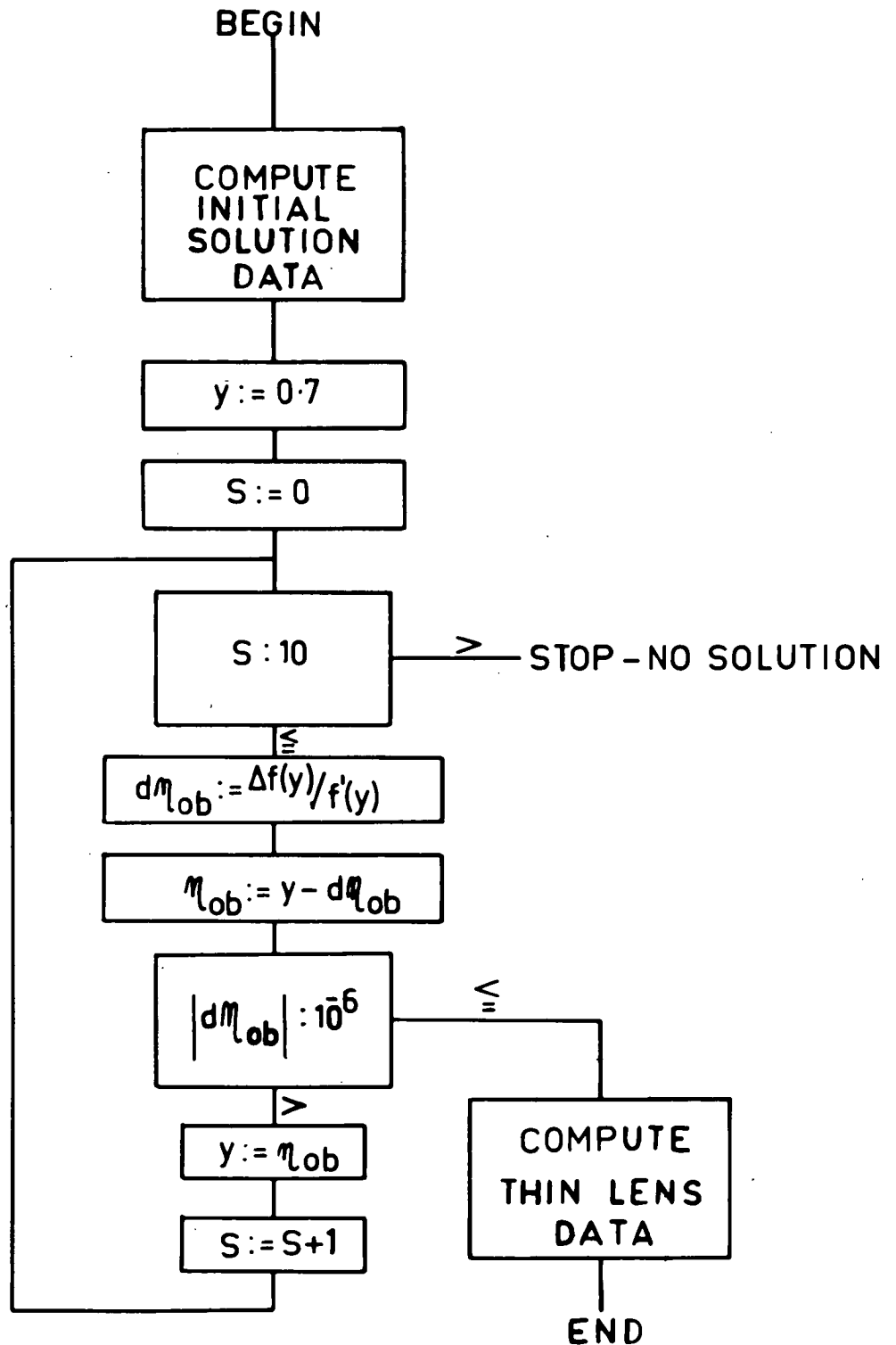


Fig. 1.6

CHAPTER 1.4 A PRELIMINARY STUDY OF SOME 3RD ORDER SOLUTIONS OF A TYPE 121 SYSTEM VERSUS k^* USING FAMILIAR TECHNIQUES.

1.4.1 Introduction.

In this chapter a preliminary study of some 3rd order type 121 triplets that are generated from a given set of glasses and thin lens residuals is described. From this work, we are able to elucidate some of the properties that the parameter k^* brings to the triplet family in the early stage of the design. By the early stage, we mean, the stage at which the system has specified 3rd order coma, astigmatism and distortion and also has its spherical aberration corrected to 7th order.

1.4.2 General Discussion of Triplet Properties and Design. Methods.

The initial design methods for triplets of Cruickshank^(2.1, 2.2), Hopkins^(4.3), Kingslake^(5.1) and others, are very similar. Cruickshank's method differs from other methods in two particular instances, initially in the choice of one of the thin lens parameters and in the final stages of design, possibly, in the order to which he adjusts the aberration residuals before resorting to ray-traces. (However, since the publication of Cruickshank^(2.4) and Hills in 1960 it is expected that the 7th order correct-

-ion of spherical aberration using Buchdahl coefficients is now commonplace.)

The systematic design methods used by Cruickshank form the basis of this preliminary study. In his approach to the initial design of the type 111 triplets he introduces the thin lens parameter \mathcal{X} and uses it to control spherical aberration. Thus for a given set of glasses and thin lens parameters P , L and T he finds that the 3rd order spherical aberration is an approximately quadratic^(2.1) function of \mathcal{X} (for $-1 < \mathcal{X} < 0$).

He also shows that the spherical aberration curve may be raised or lowered by changing glass values. Furthermore, it is mentioned by R.E. Hopkins that changing the Petzval sum^(4.3) also shifts the spherical curve vertically. Therefore for a given set of glasses it is possible to find many 3rd order triplet solutions with specified marginal spherical by adjusting \mathcal{X} and P . Of course, generally, the designer intuitively aims at a small Petzval (thus restricting P), so that in the case of a simple triplet he would most likely look first to \mathcal{X} and then to the glass constants in order to optimize spherical^(2.1).

As for the basic chromatic parameters L and T it is generally accepted that they affect only the chromatic residuals significantly and so after \mathcal{X} and P are determined little can be done with the design, apart from small changes in residuals R_2 , R_3 and R_5 . The point coming out of this

is that, with an ordinary type 111 triplet, once the glass is fixed then $\chi^{(2.1)}$ is the only significant parameter left for adjusting the spherical aberration. Consequently once χ is used to control the marginal spherical of the type 111 triplet then the triplet is determined, there are no further geometrical degrees of freedom available for controlling its zonal spherical. (As a result of more recent work Cruickshank uses χ to control coma and R_4 to control spherical of the type 111 triplet^(2.8)).

Consequently if a Cooke triplet design has large zonal spherical nothing can be done except to start again with either a modified or a completely new set of glasses. This is the point made by Cruickshank that any improvement in triplets lies with glass selection and therefore the design is limited because the real glasses from a set of parameters taking discrete values. He suggests that this might be overcome by using fictitious glass values or their equivalent, the parameter k^t . This brings us to the reason for tackling the type 121; it is expected to offer some control over zonal spherical and thus give a triplet of wider aperture than the $f/3.5$ of ordinary triplets.

Of course it is well known that cemented^(15, 16) surfaces provide control over higher order zonal spherical but it seems that little systematic knowledge has been acquired about them. The fictitious glass concept, however, is suitable for the systematic study of systems with cemented

surfaces and the type 121 appears to be a suitable type to start with.

1.4.3 Initiating the Preliminary Study of the Type 121.

We have shown theoretically in Chapter 1.2 that for a given set of glasses the 3rd order triplet of the type 121 can be computed from the set of basic-parameters $\bar{\Phi}, \chi, P, L, T$ and k' . This is one more parameter than in the set for generating the 3rd order type 111 triplet.

It has been shown^(2.8) that the 3rd, 5th and 7th order spherical aberration coefficients of the type 111 triplet are quadratic functions of χ for a given set of glasses, basic parameters ($\bar{\Phi}, P, L, T$) and 3rd order residuals (R_2, R_3, R_5). Thus we may write:

$$\sigma_1 = a_0 + a_1\chi + a_2\chi^2 \quad 4.1$$

$$\mu_1 = b_0 + b_1\chi + b_2\chi^2 \quad 4.2$$

$$\tau_1 = c_0 + c_1\chi + c_2\chi^2 \quad 4.3$$

Now since the transverse spherical aberration residual to 7th order is given by^(13.2, 2.4):

$$\epsilon'_{\text{Sph}} = \sigma_1\rho^3 + \mu_1\rho^5 + \tau_1\rho^7 + o(9) \quad 4.4$$

Then it follows because of equations 4.1, 4.2 and 4.3 that ϵ'_{Sph} of the type 111 triplet is also a quadratic function of χ and we may write:

$$\epsilon'_{\text{Sph}} = d_0 + d_1\chi + d_2\chi^2 \quad 4.5$$

Fig. 1.7.1

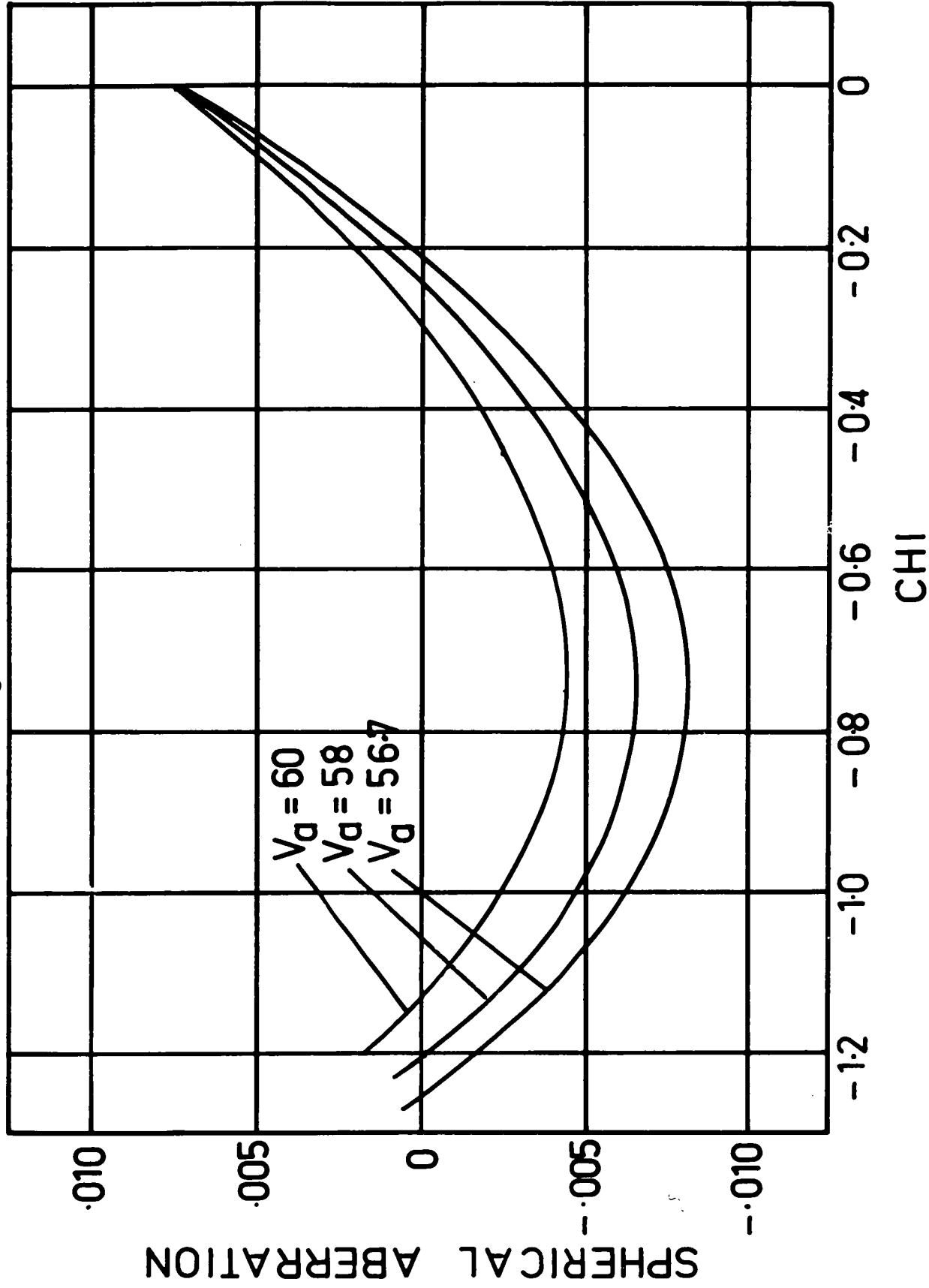
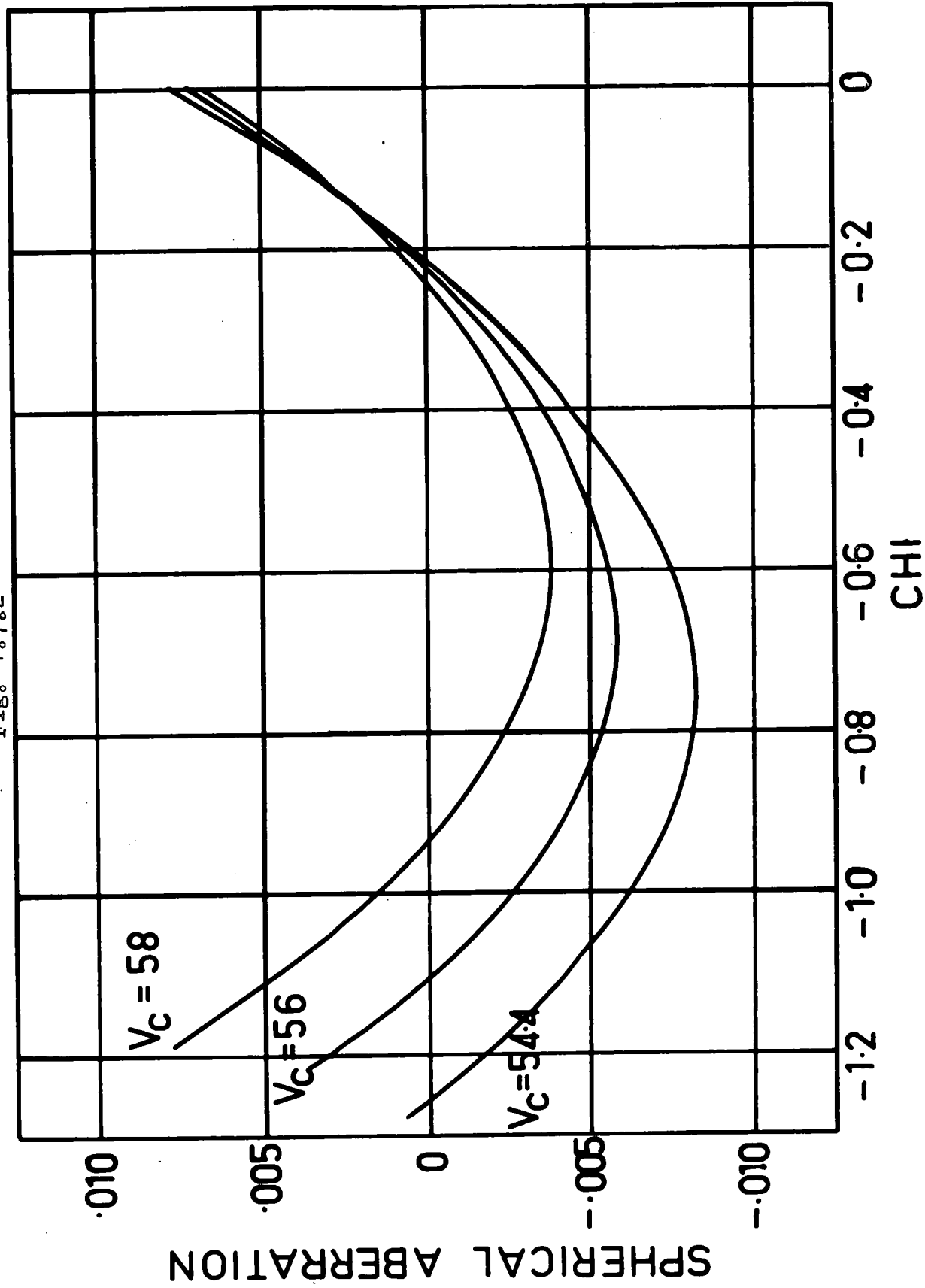


Fig. 1.7.2



SPHERICAL ABERRATION TO SEVENTH ORDER

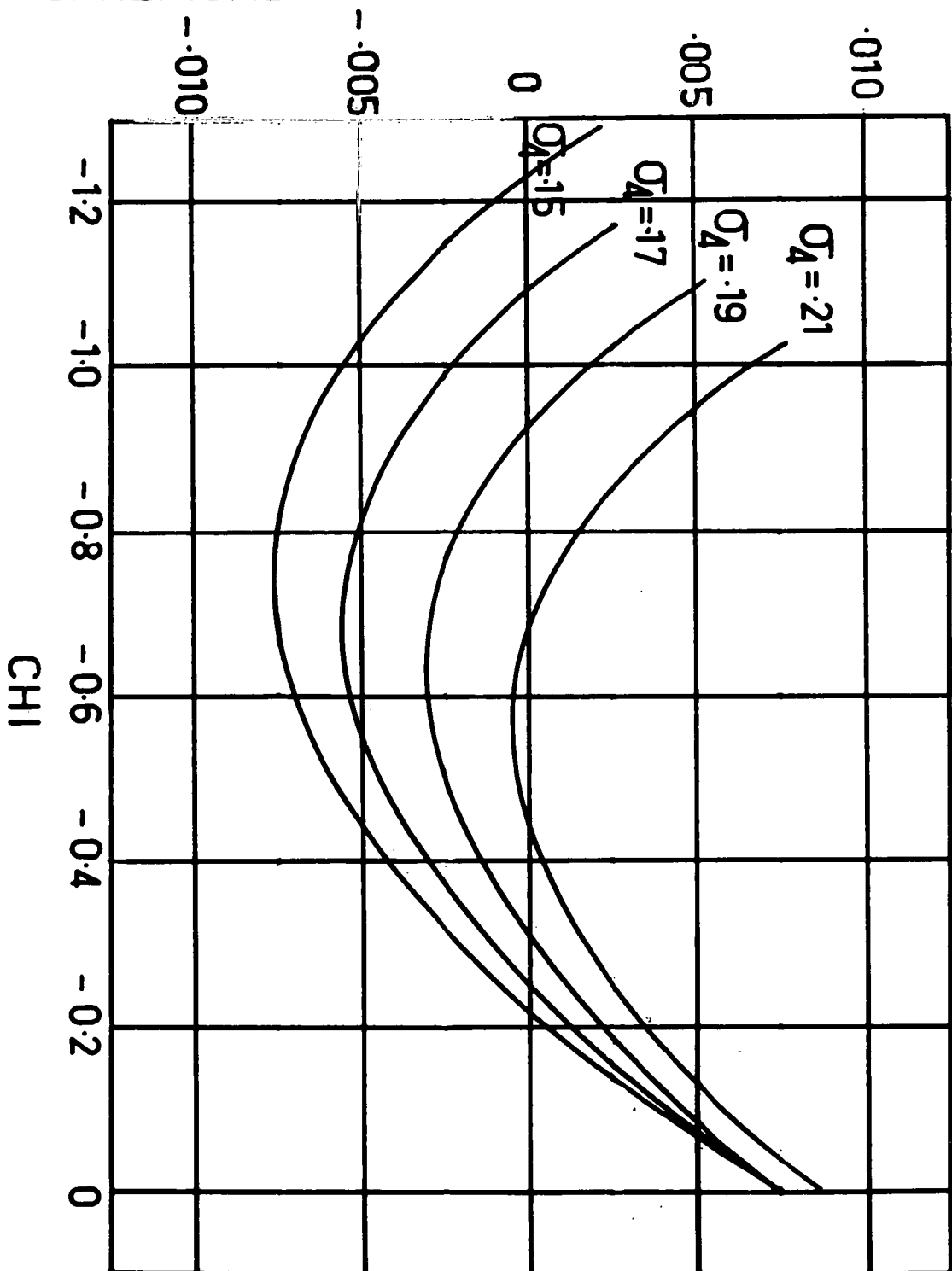


Fig. 1.7.3

where $d_0 = a_0 \ell^3 + b_0 \ell^5 + c_0 \ell^7$

$$d_1 = a_1 \ell^3 + b_1 \ell^5 + c_1 \ell^7$$

$$d_2 = a_2 \ell^3 + b_2 \ell^5 + c_2 \ell^7$$

(Note: ϵ'_{Sph} will be taken to mean the predicted spherical aberration to 7th order unless stated otherwise.)

Thus with the 3rd order type 111 triplet the predicted spherical aberration curve of ϵ'_{Sph} varies as in Figures 1.7.1, 1.7.2, 1.7.3^(2.8). These figures show how the spherical aberration curve ϵ'_{Sph} versus \mathcal{X} varies with the basic-glass parameters V_a and V_c and also, with changes in the Petzval aberration coefficient σ_4 .

The curves show that for any given set of basic-glasses and basic-parameters there are two values of \mathcal{X} at which the spherical aberration of the 3rd order triplet is zero. The solution on the left is called the left-hand solution^(2.1) or left solution^(4.3) and the solution on the right is called the right-hand solution or right solution.

The spherical curve may be moved vertically by changing $P^{(2.1, 4.3)}$ (or σ_4)^(2.8), the glass in the first element or in either one of the crown elements and the thickness of the elements^(4.3). Indeed the curve may be moved so far vertically that there are no solutions with $\epsilon'_{\text{Sph}} = R_1 = 0$ or it may be moved just far enough to make the solutions coincide when the curve is tangential to the \mathcal{X} -axis.

In view of the above properties of the spherical curve of the type 111 triplet the preliminary study of the type 121 has been devised to find how k' affects this spherical curve. Thus the questions examined in this study are as follows:

- (1) Are the spherical aberration coefficients ($\tau_1, \mu_1, \bar{\tau}_1$) and the marginal spherical (ϵ'_{Sph}) reasonably approximated by quadratic functions of \mathcal{X} when k' is constant?
- (2) What happens to the spherical curve when k' is changed?

1.4.4 Selecting the Initial Values of the Basic-Parameters.

In order to start this preliminary study of the type 121 triplet we have first to make a glass selection. To simplify this selection the well known practice of making simple triplets from two ^(1, 2.1, 3.2) glasses such that $(N_a, V_a) = (N_c, V_c)$. This makes $\xi = \gamma = 1$ and leaves only α and β as effective "basic-glass parameters".

In the selection of α and β we have been guided by the wish which was expressed earlier, to construct a large aperture system. This, it has been shown, requires a high α and a high β ^(2.2). Also we note that it has been found that large α values give long systems and therefore this must be considered when excessive length is undesirable. It is also a general rule to make the front and back components of a triplet of high N, High V glass and the middle lens of low N, low V glass.

Thus the glasses and the initial value of k^t chosen for the preliminary study of the 3rd order type 121 triplets have been chosen so that the basic-glasses comply with the selection principles outlined above so that they give $\alpha = 1.6975$ and $\beta = 1.0429$.

These real glasses are the following Jena Types:

| Type | N_d | V_d |
|-------------------|---------|-------|
| lens 1 Jena SK16 | 1.62101 | 60.18 |
| lens 2 Jena BaF10 | 1.67038 | 47.31 |
| lens 3 Jena F8 | 1.5959 | 39.13 |
| lens 4 Jena SK16 | 1.62101 | 60.18 |

and the initial $k^t = -2.50$ which gives $N_b = N_F = 1.5498$
 $V_b = V_F = 35.086$. Finally the values used for P, L and T are of the same order as values obtained for well known triplet systems being $P = 0.35$, $L = 0.20$ and $T = 0.05$. This leaves \mathcal{X} as the only independent parameter since R_2 , R_3 , R_5 and R_9 are implied in the definition of the 3rd order triplet.

1.4.5 The Spherical Aberration of the Type 121 versus \mathcal{X} and versus k^t .

1.4.5.1 The Basic-Programme for Spherical Aberration.

In order to study the dependence of spherical aberration on the independent parameter \mathcal{X} we have used a

modified form of the basic-programme called BP/S/121.

This programme computes the 3rd order type 121 triplets for either a range of \mathcal{X} values between \mathcal{X}_1 and \mathcal{X}_2 in steps of $\Delta\mathcal{X}$, or a single value of \mathcal{X} for a given set of Φ , P, L, T, k' , R_2 , R_3 , R_5 . This programme contains a new basic-procedure called Sph357 that generates the 3rd, 5th and 7th order Buchdahl spherical aberration coefficients (σ_1 , μ_1 , τ_1) of each triplet and from these also computes the predicted transverse spherical aberration ϵ'_{Sph} (equation 4.4).

The construction of this modified programme BP/S/121 is the first example of the technique used throughout this work to simplify the writing of these design programmes. The flow diagram Figure 1.8 shows that the new programme consists essentially of the linear assembly of one control-routine called T121 and a basic-routine called Sph357. The control-routine reduces the body of the basic-programme (BP121) to a single instruction (see Figure 1.8). Thus all the complexity associated with generating a 3rd order triplet is reduced to a single instruction or operation in this and in all future programmes.

Thus for example, from the set of data which consists of the values selected above and also suitable values for the other parameters as follows:

BASIC PROGRAMME BP/S/121

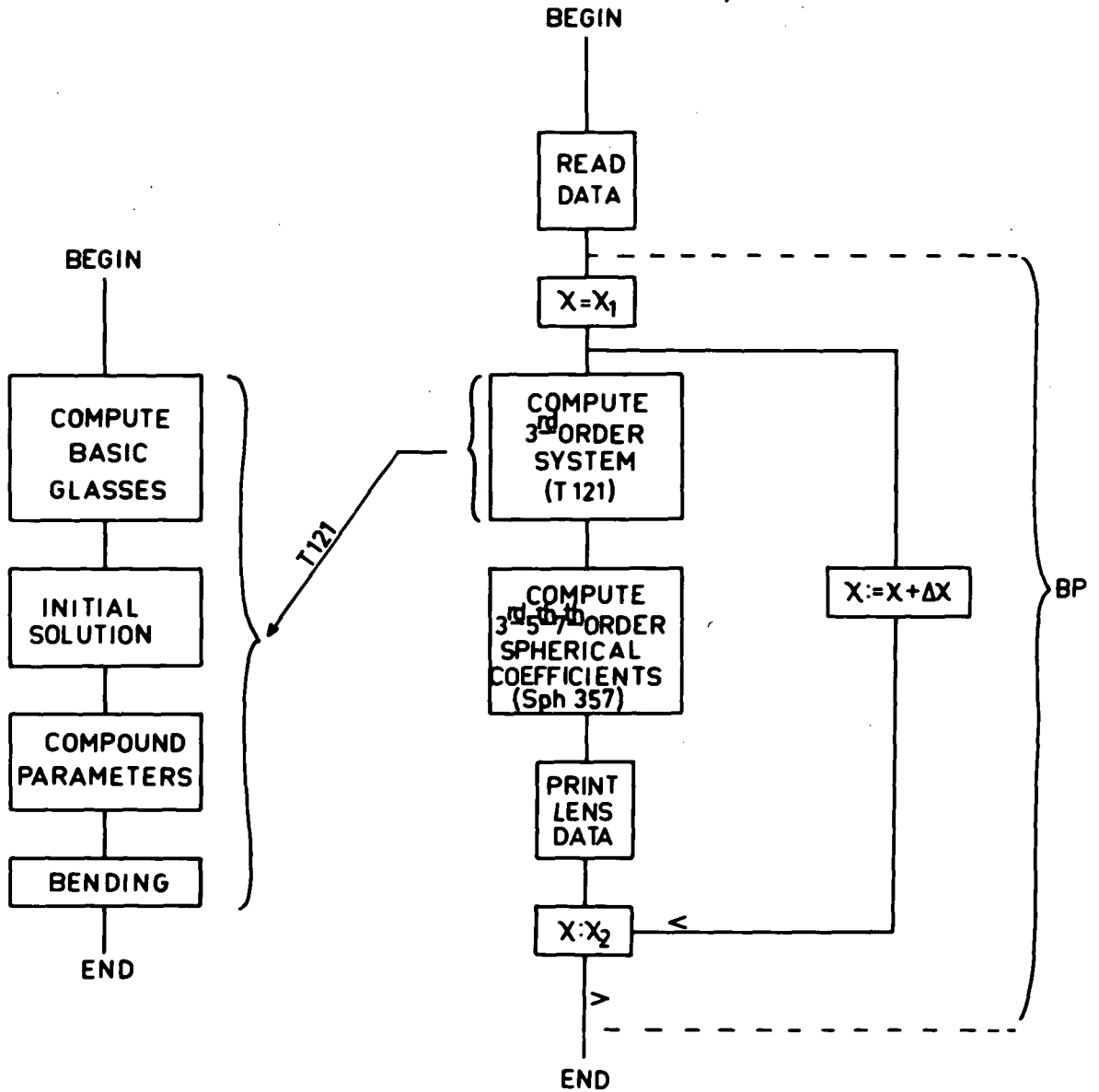


Fig. 1.8

$$\begin{array}{lll}
N_1 = 1.62101 & V_1 = 60.18 & d_2 = 0.1 \\
N_2 = 1.67038 & V_2 = 47.31 & d_4 = 0.07 \\
N_3 = 1.5959 & V_3 = 39.13 & d_5 = 0.02 \\
N_4 = 1.62101 & V_4 = 60.18 & d_7 = 0.07 \\
\phi = 1 & R_2 = 0 & S_1 = 0.7 \\
P = 0.35 & R_3 = 0 & S_2 = -2.0 \\
LL = 0.2 & R_5 = 0 & S_4 = -0.4 \\
T = 0.05 & \rho = 0.2 & \\
k' = -2.5 & &
\end{array}
\left. \begin{array}{l} \\ \\ \\ \end{array} \right\} \text{approximate shapes}$$

and $\chi = -0.5$

the programme BP/S/121 has generated a 3rd order type 121 triplet. In doing so it has supplied the essential details of the system at the various stages which are shown in Figures 1.1.2 and 1.8. Thus after reading in the data it has computed the following:

(1) The Basic Triplet.

$$\begin{array}{llll}
\phi_a = 1.7146 & & N_a = 1.62101 & V_a = 60.18 \\
& t_a = 0.16709 & & \\
\phi_b = -3.1038 & & N_b = 1.54983 & V_b = 35.085 \\
& t_b = 0.16722 & & \\
\phi_c = 1.8818 & & N_c = 1.62101 & V_c = 60.18
\end{array}$$

(2) The Initial Arrangement (Thin-Lens Type 121)

$$\begin{array}{llll}
\phi_1 = 1.7146 & & S_1 = 0.61190 & \\
\phi_2 = 2.0692 & t_a = 0.16709 & S_2 = -2.7336 & \\
\phi_3 = -5.1731 & t_b = 0.16722 & S_3 = 0.32753 & \\
\phi_4 = 1.8818 & & S_4 = -0.35334 &
\end{array}$$

(3) 3rd Order Triplet (Thick-Lens Type 121).

| | | |
|-------------------|------------------|--|
| $c_1 = 2.22522$ | $d_1 = 0$ | 3rd Order Residuals $\sigma_1 = 0.1137$ |
| $c_2 = -0.585687$ | $d_2 = 0.1$ | $\sigma_2 = 0$ |
| $c_3 = -2.52857$ | $d_3 = 0.093184$ | $\sigma_3 = -0.055215$ |
| $c_4 = -5.58035$ | $d_4 = 0.07$ | $\sigma_4 = 0.165644$ |
| $c_5 = 2.862875$ | $d_5 = 0.02$ | $\sigma_5 = 0$ |
| $c_6 = 0.998400$ | $d_6 = 0.1095$ | |
| $c_7 = -2.087722$ | $d_7 = 0.07$ | |

Finally it has computed the spherical aberration coefficients and then from them computed the marginal spherical for the given $\ell = 0.2$ which is equivalent to an $f/2.5$ system since $f' = 1$. Thus we have

$$\sigma_1 = 0.11370$$

$$\mu_1 = 7.3268$$

$$\tau_1 = 557.06$$

$$\text{and } \epsilon_{\text{Sph}}' = 0.010384$$

1.4.5.2 The Effect of \mathcal{X} and k' on the Spherical Aberration.

The above example has been repeated for the range of \mathcal{X} from $\mathcal{X}_1 = 0$ to $\mathcal{X}_2 = -1.0$ in uniform steps of $\Delta\mathcal{X} = 0.1$ and for $k' = -2.22, -2.50$ and -2.857 . The values of σ_1, μ_1, τ_1 and ϵ_{Sph}' obtained are shown plotted against \mathcal{X} for the different values of k' in Figures 1.9, 1.10, 1.11, and 1.12. These curves are closely approximated by quadratics in \mathcal{X} . Thus the behaviour of ϵ_{Sph}' of the type 121 when k'

is constant, is similar to that of the type 111 when, for example, V_a is constant (Figure 1.7.1). However, it is evident from the figure that increasing k' raises the spherical coefficient and spherical aberration curves and decreasing k' lowers them. This is a very useful property because simply by varying k' a range of triplet right and left hand solutions may be obtained with their marginal spherical specified to 7th order. (We will call them R solutions and L solutions.)

Thus with the parameter k' the designer can accomplish what he normally has to do with real glasses or the Petzval sum in the design of the type 111 triplet. (See Figures 1.7.1, 1.7.2). Therefore, fictitious glasses seem to be as effective as real glasses in shifting the spherical curves.

With the data of the above example R and L solutions are available from near $k' = -2.66$ to at least $k' = -2.857$. The next stage of this preliminary study, which is discussed in the following section, deals with the selection and development of solutions in this region.

$P=0.35 \quad L=0.2 \quad T=0.05$

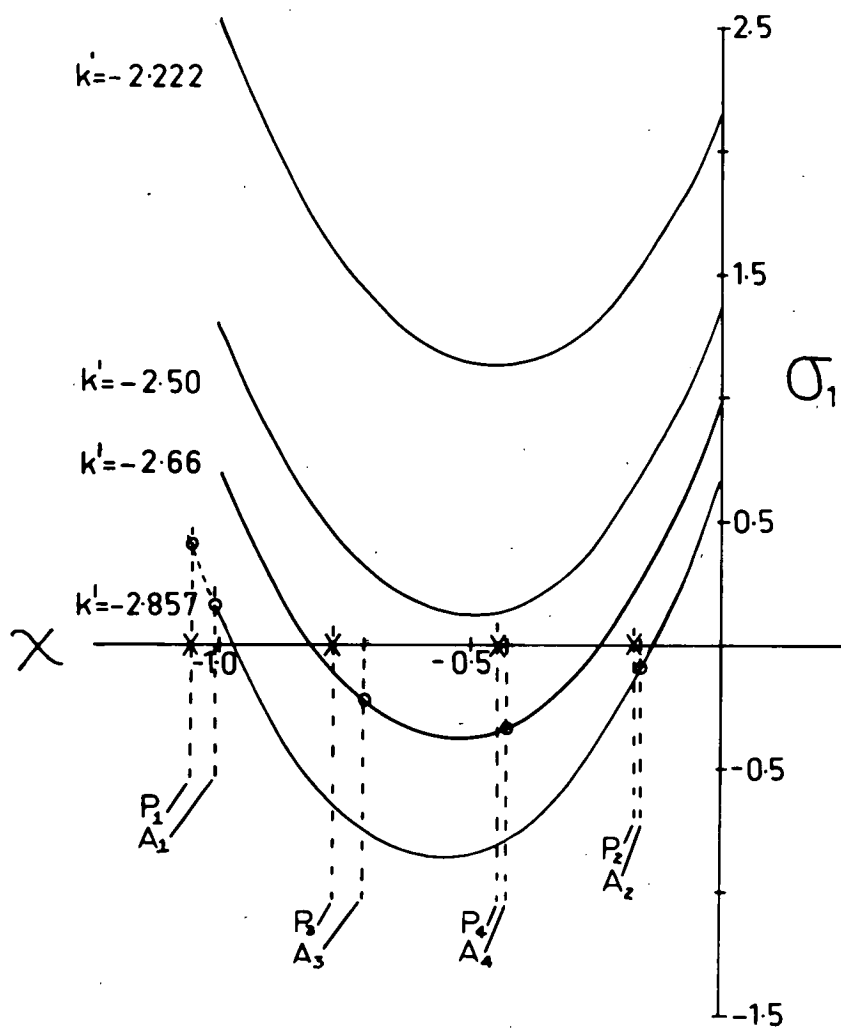


Fig. 1.9

$P=0.35 \quad L=0.2 \quad T=0.05$

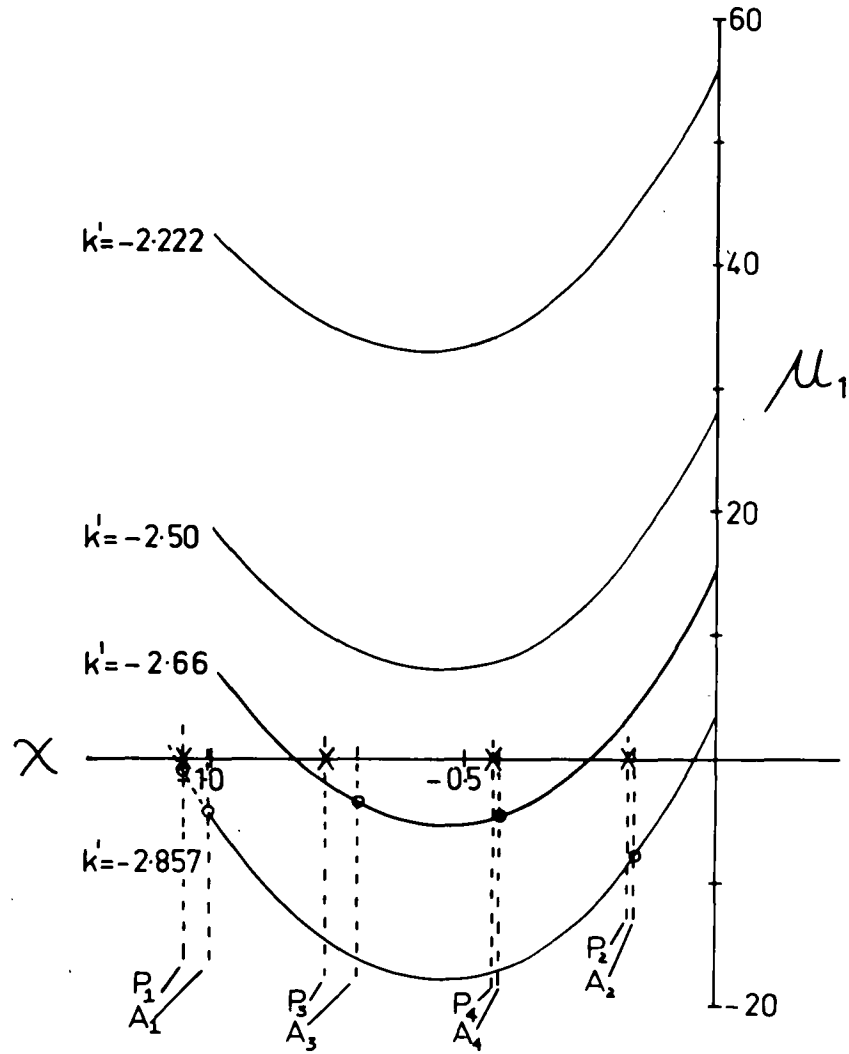


Fig. 1.10

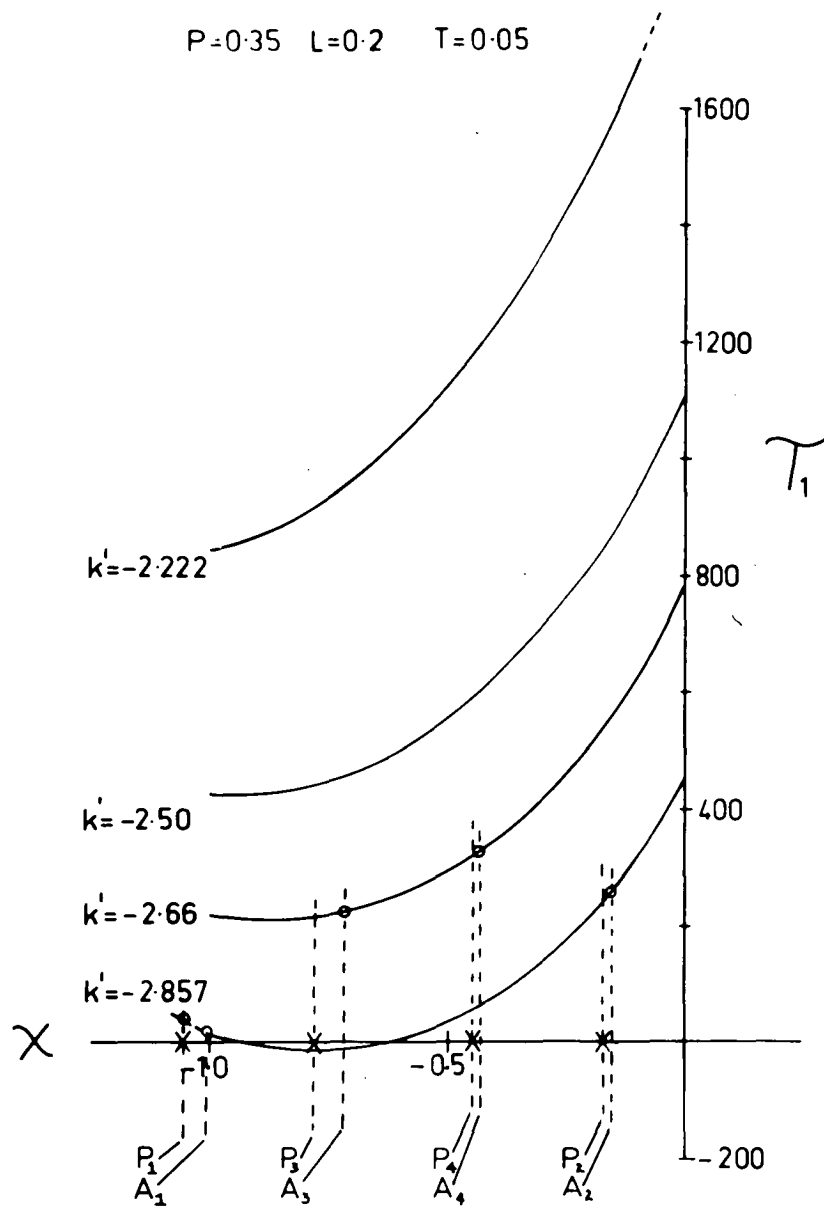


Fig. 1.11

$P=0.35 \quad L=0.2 \quad T=0.05$

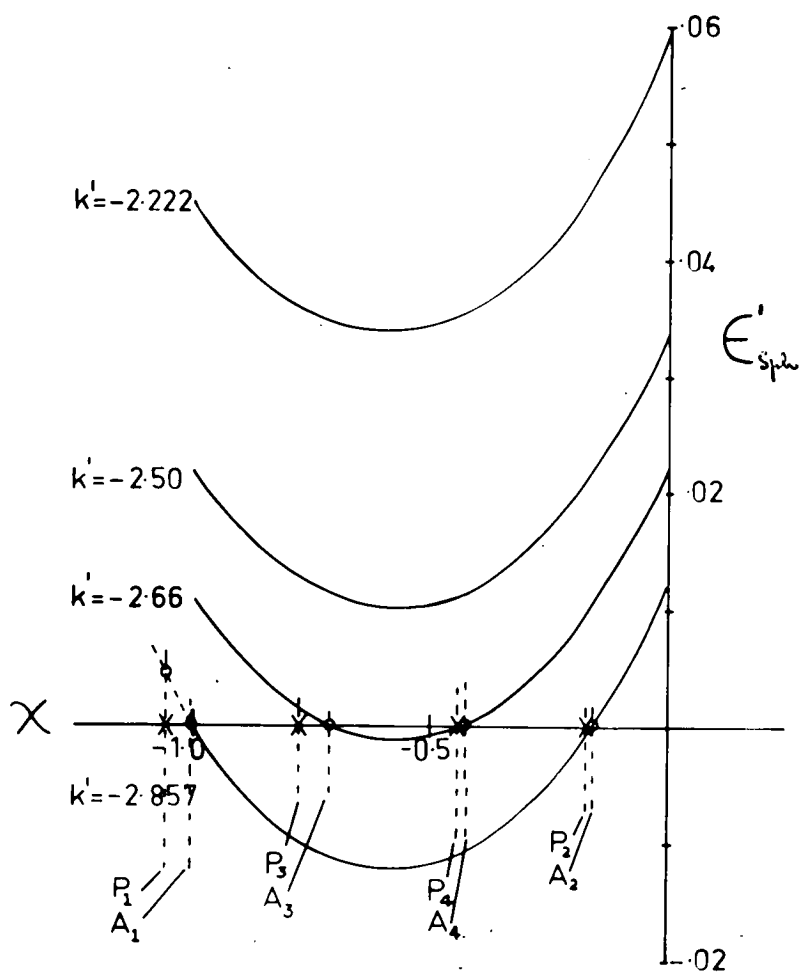


Fig. 1.12

1.4.6 Right and Left Hand Solutions versus k' .

1.4.6.1 The R and L Programme.

For each k' chosen in the region of the triplet solutions there are two solutions, the well known right and left hand solutions of a triplet system. These are computed with a programme LR/BP/S/121 that is derived very simply from the programme BP/S/121; its flow chart is Figure 1.13. For convenience we will call it the R and L programme.

There are two parts to this programme. The first part is merely BP (see Figure 1.8) which is arranged so as to produce three separated points* on the ϵ'_{Sph} -curve for the purpose of fitting it with the quadratic in χ (equation 4.5). The second part computes the approximate solutions χ_L and χ_R that make $\epsilon'_{\text{Sph}} = R_1$ by solving the quadratic equation. (R_1 is supplied in the data). The remainder of the programme iterates the sub-routine T121 (see Figure 1.14) about the region of either χ_L or χ_R until $\epsilon'_{\text{Sph}} = R_1 \pm 10^{-5}$. In the early stage of the design which we are studying now, R_1 is set to zero, but it may be given a value other than zero by the designer in order to balance the higher aberrations in the final stages of the design.

1.4.6.2 Controlling Spherical with k' .

The first solutions of the type 121 with $R_1 = 0$ are at A_1 and A_2 on the ϵ'_{Sph} -curve at $k' = -2.857$ (Figure 1.12); the points P_1 and P_2 appearing near A_1 and A_2 are

* For convenience we have used $\chi = 0, -0.5, -1.0$.

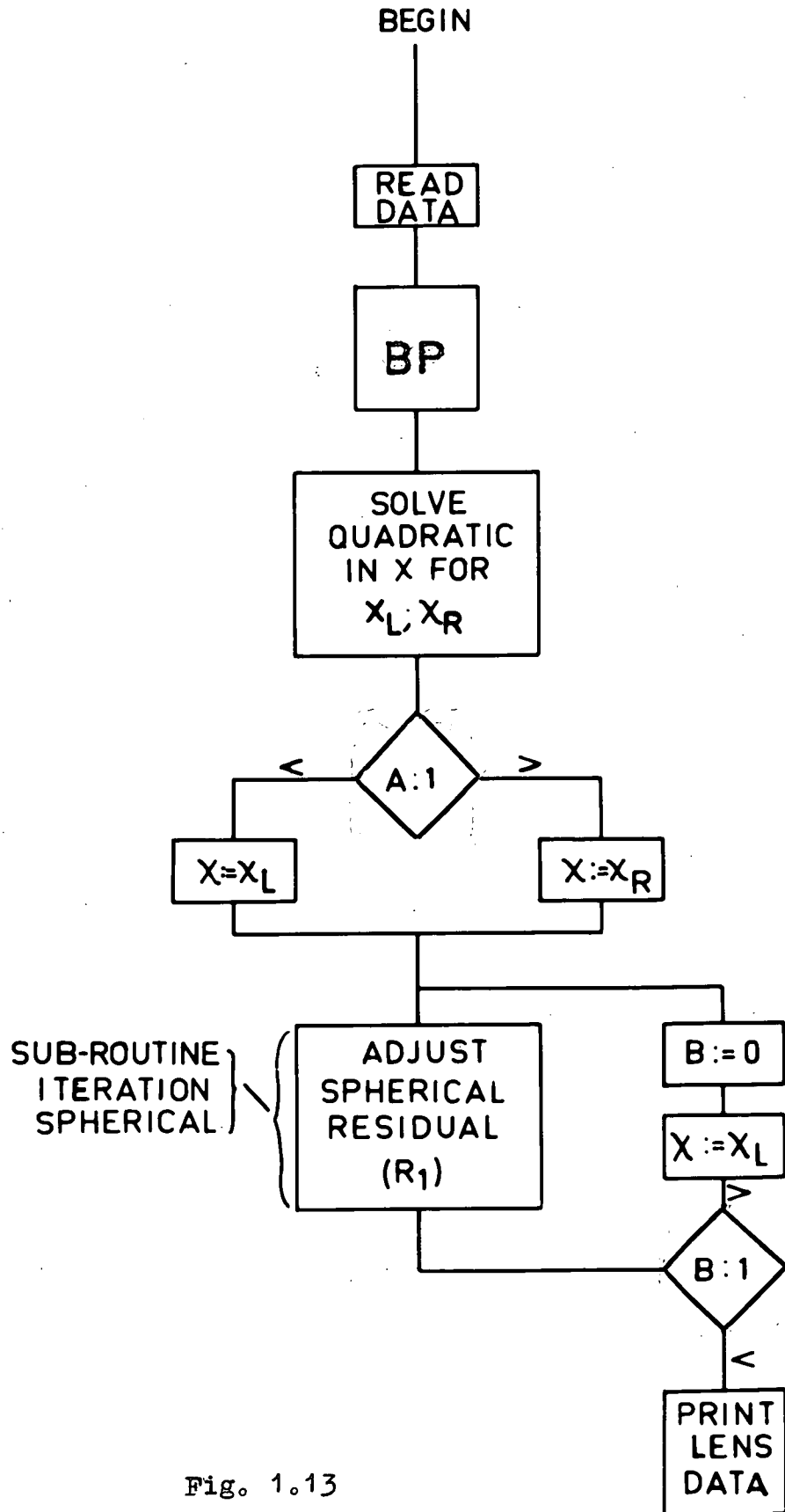


Fig. 1.13

SUB-ROUTINE ITERATION SPHERICAL

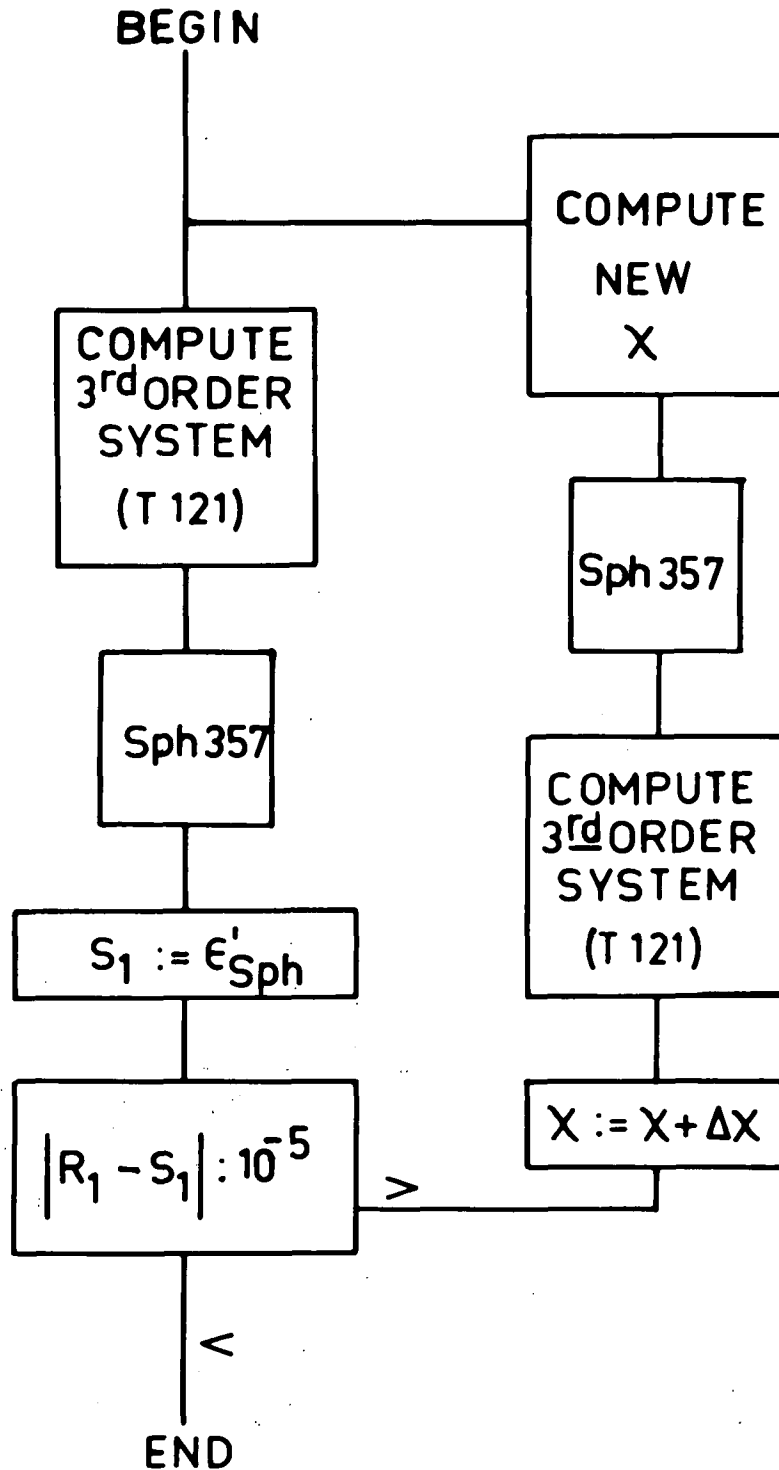


Fig. 1.14

the solutions predicted by the quadratic approximation whereas A_1, A_2 are the actual solutions arrived at by the iteration.

As we are aiming initially at well corrected zonal spherical another pair of solutions (A_3, A_4), with smaller spherical coefficients, were chosen at $k' = -2.66$. This new k' was selected by interpolating between $k' = -2.857$ and -2.5 . Let us now examine the potential of both pairs of solutions to see if one of the four is significantly better than the others.

1.4.6.3 Discussion of Type 121 Solutions.

TABLE 5.1

Spherical Coefficients 3rd, 5th, 7th Order.

| | Left hand Solutions | | Right Hand Solutions | |
|------------|---------------------|---------|----------------------|---------|
| | A_1 | A_2 | A_3 | A_4 |
| k' | -2.857 | -2.66 | -2.857 | -2.666 |
| σ_1 | 0.1536 | -0.2060 | -0.0890 | -0.3365 |
| μ_1 | -4.4078 | -3.636 | -7.9309 | -4.710 |
| τ_1 | 14.2029 | 220.0 | 253.94 | 328.0 |

At first sight (see Table 5.1) the solutions A_1 appears to have significantly better zonal correction than the others because of its very small set of spherical coefficients. However, this prediction is not supported by the LA' -curves which have been obtained from actual ray-traces and which are compared with the predicted LA' -

curves* in Figure 1.15. These curves show that there is little to choose between the four solutions below $f/3.5$, while beyond $f/3.5$ there is also not much difference between them, because, they all suffer from massive under-correction. Even so, any of these solutions may be considered as being sufficiently well corrected on axis for a system working at a maximum aperture of $f/3.5$. (In passing we note that the prediction is better when the higher order coefficients μ_1 and τ_1 are small. (See Figure 1.15 where the solution A_1 has best agreement between the predicted and ray-trace LA^* -curves.)

In order to further assess the potential of these solutions we turn to the coefficients that describe the off-axial aberrations. It is well known^(2.8) that we need only look at a few coefficients that are characteristic of the 5th and 7th order comatic and astigmatic aberrations in order to select the most promising solution at this early stage. Previous workers in this laboratory have found it is sufficient in the early stages of design to plot the following coefficients in order to assess the off-axial correction:

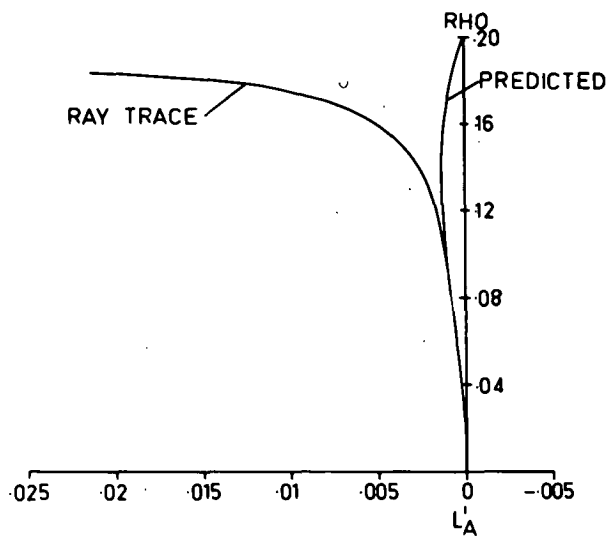
- (1) for coma, the 5th order coefficients μ_2 and μ_7 and for the 7th order τ_2 and τ_{15} .
- (2) for astigmatism, the 5th order coefficients μ_4 and μ_{10} and for the 7th order τ_4 and τ_{11} .

* Predicted $LA^* = \epsilon'_{Sph}/\rho$

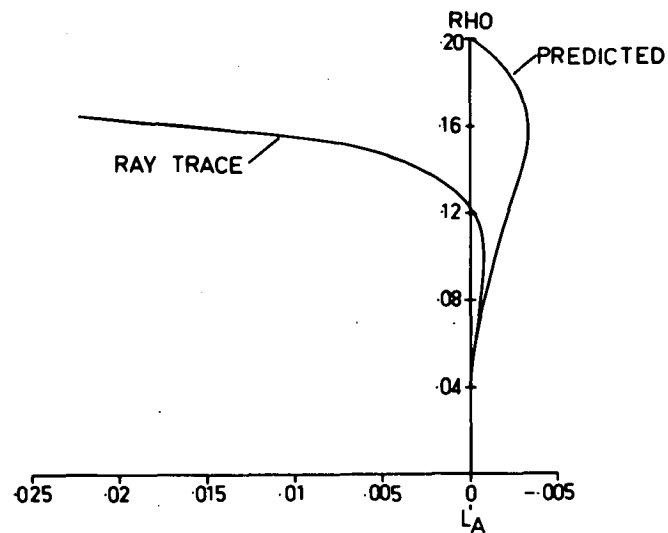
Fig. 1.15

LEFT SOLUTION (A_1)

$k' = -2.857$

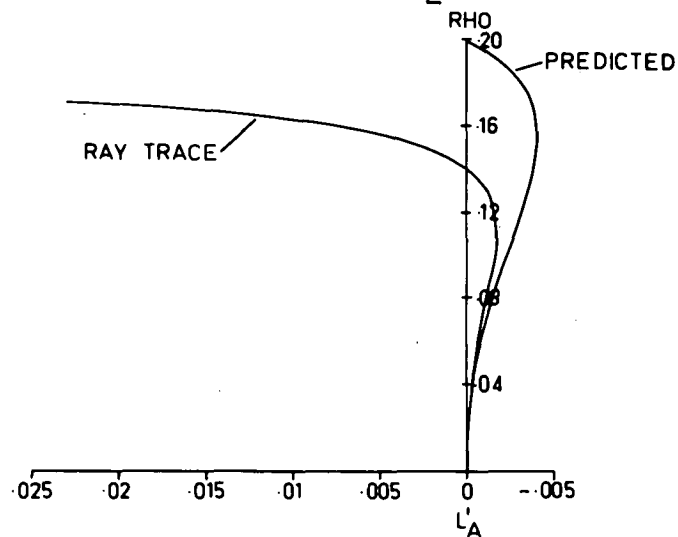


RIGHT SOLUTION (A_3)

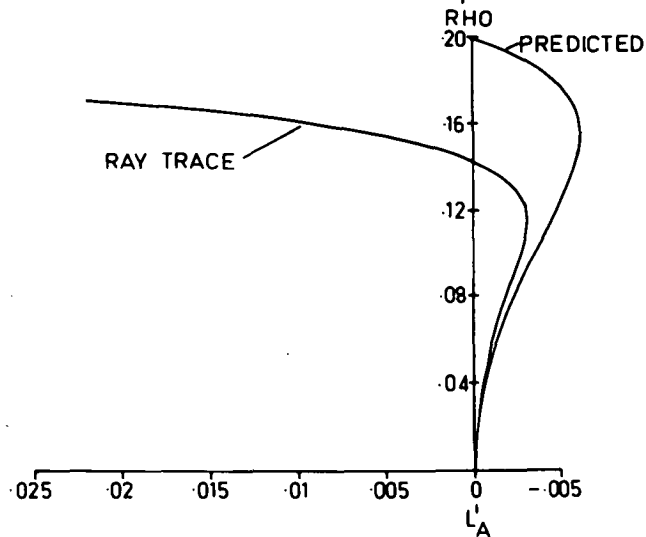


LEFT SOLUTION (A_2)

$k' = -2.666$



RIGHT SOLUTION (A_4)



These coefficients have been computed for the systems at $k' = -2.857$ and -2.66 for the usual range of $\mathcal{X} = 0$ to -1.0 in steps of $\Delta\mathcal{X} = -0.1$. The results of this work are plotted in four diagrams, Figures 1.16 to 1.19. In Figure 1.16 we have these characteristic astigmatic coefficients for $k' = -2.857$ and in Figure 1.17 we have plotted the comatic coefficients for the same systems. Similarly we have plotted the same pairs of astigmatic and comatic coefficients of the systems at $k' = -2.66$ in Figures 1.18 and 1.19. It is seen that k' has the same general effect on these comatic and astigmatic curves as it has on the spherical curves. An increase in k' raises them and vice versa.

It is evident from the figures that solutions near $\mathcal{X} = -0.5$ are the most promising because their 5th and 7th order comatic coefficients are a minimum and also their astigmatic coefficients are not excessive at this minimum. Consequently if we proceed with the development of a solution in the region of $(\mathcal{X} = -0.5, k' = -2.66)$ we are confident that a reasonable $f/3.5$ system may result. However, there is no justification at this stage for anticipating the existence of a type 121 system that will perform well at or near $f/2.5$. Indeed, in view of these results we are inclined to believe that $f/3.5$ cannot be exceeded with the type 121.

ASTIGMATIC COEFFICIENTS
 $k' = -2.857$ $P = 35, L = 2, T = 05$

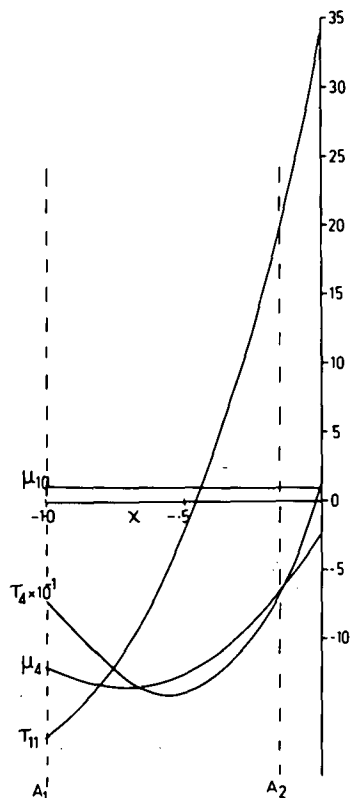


Fig. 1.16

COMATIC COEFFICIENTS
 $k' = -2.857$ $P = 35, L = 2, T = 05$

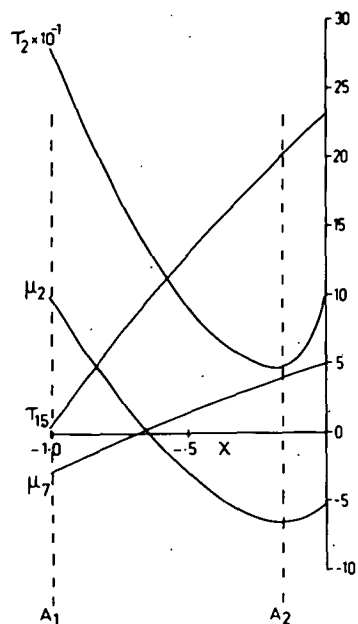


Fig. 1.17

ASTIGMATIC COEFFICIENTS
 $k' = -2.666$ $P = .35, L = .2, T = .05$

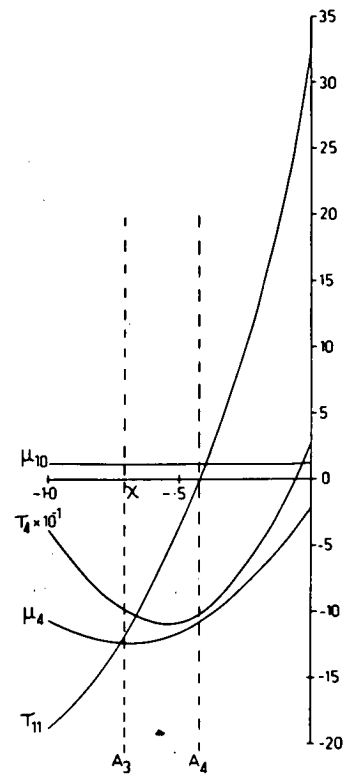


Fig. 1.18

COMATIC COEFFICIENTS
 $k' = -2.666$ $P = .35, L = .2, T = .05$

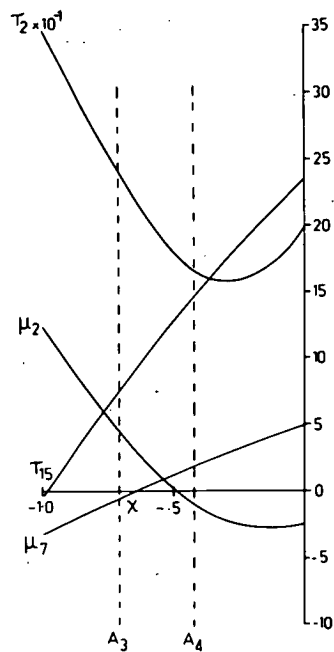


Fig. 1.19

1.4.7 Discussion of the Design Process as a Result of Work with the Type 121.

It is clear that when the familiar systematic design process outlined in Chapter 1.2 is combined with 5th and 7th order coefficients the development of a system of moderate field (less than 20°) and aperture (less than $f/3.5$) becomes a simple matter; especially with a flexible programme like the one developed in this work.

So using the well known systematic design process we have arrived at the point beyond which systematic design ceases to be straight forward, largely it seems, because there are no aberration coefficients readily available for orders higher than the 7th (except for the 9th and 11th order spherical coefficients).^{*} The need for coefficients of higher order than the 7th is obvious if accurate predictions are to be made at apertures in excess of $f/3.5$. This is demonstrated by the divergence of the predicted LA' -curves from those of the ray-trace LA' -curves in Figure 1.14.

* (a) 9th and 11th order coefficients, Buchdahl (13.4, 13.8)
During this part of this work the Elliott 503 computer could only handle the simultaneous computation of a 3rd order solution and its spherical coefficients of 3rd, 5th and 7th order. However, in a later part of this investigation more storage became available which enabled the 9th and 11th order spherical coefficients to be computed as well. This is discussed in Chapter 3.2.

There are only a few design principles available for the design of modern photographic objectives (that is, systems with fields 20° and apertures $f/3.5$). Of the few empirical principles that have emerged from design experience it is generally accepted that the higher order aberrations are fairly stable; it appears that they are not significantly altered by small changes in the final design stage. So, it is said, that they can be off-set or balanced, to some extent, by an equivalent lower-order aberration residual of opposite sign. It is said that this makes geometrical optical design possible. This stability of the higher order spherical aberration is supported obviously by the pattern of the LA' -curves of the four solutions of Figure 1.15. Here, although the zonal spherical below $f/3.5$ varies within small limits from one solution to the other, that above $f/3.5$ remains almost unchanged, being highly asymptotic. (The solutions are equally good below $f/3.5$ and equally bad above.) So this conclusion about stability seems to be trivial in this case. Moreover we shall see that if we take stability at face value as with LA' -curves, then we are likely to miss subtle behaviour beyond $f/3.5$.

We are now faced with the dilemma of what to do next. The present solutions predict at the best an $f/3.5$ system, therefore, we are left with the old adage "change the glass" and start again in an attempt to control the

higher orders.

To have to start again with another glass selection seems inevitable since the experiences of other designers leads us to believe that the higher orders cannot be reduced effectively by changes in the geometrical design parameters. They seem to assert that the higher orders can only be offset by balancing them with the lower order residuals.

However, balancing is a compromise that only gives good results at a particular zone of the aperture or a particular point in the field.

1.4.8 Methods of Design - Some General Considerations.

There are two types of optical design methods in use today. The first is in the manner of the work described in this preliminary study of the type 121. This method* assumes some knowledge of the whereabouts of the optimum region of the design parameters as well as the basic behaviour of the aberrations with respect to the design parameters. This method enables the designer to produce workable systems of moderate aperture and field with a minimum amount of computing effort. Such an optical design method is fashioned primarily by the need to conserve computing effort.

* Method is used to mean something more than process. We have a design process but this can be used in several methods.

On the other hand, the opposite of this method has come into being with the advent of digital computers; it is "automatic lens design". With this, the emphasis is on the complete removal of the designer from decisions in the optimizing of the design and almost no limit is placed on computing effort with this technique. Although this "method" of automatic design has enabled improvements to be made in known systems^(6.2) the designer is never sure whether the programme has attained the best solution for the type of design being studied. Doubt has been expressed as to whether there are "other valleys"^(8, 6.2) in the multi-variable space of the design.

The method used in the rest of this thesis lies between the two extremes of design technique mentioned above. It is a semi-automatic method. In this new approach semi-automatic design programmes which embody the systematic design process of Chapter 1.2 are used to map the 3rd, 5th and 7th order residuals of the 3rd order triplets which are generated in a regular pattern throughout a range of the thin lens parameters corresponding to all real systems of, say, the type 121. From this mapping a set of design principles which incorporate the thin lens parameters emerge for controlling the thick lens residuals, especially at large apertures. (We note, of course, that the pendulum of fashion is moving away from

automatic design in some schools of research. In particular R.E. Hopkins^(4.2) is one of the first to make clear statements about the relative merits of the automatic or semi-automatic approach to design. It seems that he has also anticipated much of what has been said and done in the programming of the design process in this thesis.)

SECTION 2.

MONOCHROMATIC DESIGN

CHAPTER 2.1 THE DESIGN PROCESS AND INTERPOLATIVE DESIGN.

2.1.0 Introduction.

In Section 1 we have discussed the familiar analysis of optical systems of the triplet type and showed how they may be generated from the "basic triplet". From this we have seen that it is possible to design a "basic programme" that simplifies the study of the triplet systems of different constructions. Following this, a preliminary study of the construction of a triplet of the type 121 from a given set of glasses and thin lens parameters has led to many possible 3rd order solutions that arise from different values of k' . All these solutions are almost equally suitable up to $f/3.5$ on axis, but they differ in their off-axial correction.

However, our aim with the type 121 is to design for an aperture of $f/2.5$ and so we have to decide which of the solutions above^(4.3) will develop into the best wide aperture system on balancing the higher order aberrations with the aid of ray-traces. Thus conventional design methods have led us to a more general problem. It becomes not just a question, in this work, of the design of the type 121, but the procedure that should be adopted in order to design a modern photographic objective systematically at large apertures.

A study of the literature shows that there is no method at present for designing wide-aperture systems systematically. So if we are to do more than just find a useful solution of the type 121 then our problem is first to discover if possible how to control the higher order aberrations at large apertures in a systematic way and, secondly, locate the best solution for our requirements.

If we look at the optical design process in a very general way we learn that all intelligent optical design is a cybernetic process^(4.3, 20, 21): being the achievement of a goal through the monitoring of the input to a controlled process by feed back from its output. An effective feed back control can only be constructed with certainty, when the relationship between the input and output is fully understood. In optical design this reduces to mapping or charting^(4.3) performance parameters versus initial design parameters before attempting to satisfy some performance criteria. Thus the effectiveness of a design process must rest inevitably on the accuracy, scope and significance of the maps it constructs and uses.

This leads us on occasion to ask if the designer has sufficient information for making predictions at various stages of design or if he is guessing the behaviour of output versus input. The designer may deny guesswork, saying

that he has adjusted parameters or chosen his solution as a result of his experience⁽²¹⁾ or the experience of others, having no need to pursue anything other than the solution of his immediate design problem with the utmost economy of effort. However, in saying or implying this, he is indirectly referring to a mental picture that has been put together through years of design experience. The weakness here, of course, is that the controlled process may be constructed from insufficient and therefore possibly misleading information. Such design is not really systematic.

It would appear that systematic design ceases when the designer has to conjecture about the behaviour of the performance parameters with respect to the design parameters.

Throughout the literature we are regaled with comments about designer's tastes, referring no doubt to their different preferences in the selection of parameters at various stages or levels of the design process. This widespread variation in the selection of design parameters and, consequently, in design technique is to be expected with the computing facilities and state of the theoretical knowledge of the past. However, with the recent growth of computers and computer languages, coupled with the advances in theoretical optics of the last 20 years, it is to be expected that the design process is being better organized

by optical designers. In this work a serious attempt has been made to do so. Finally we note that although this research deals only with triplet types it can be argued, however, that the principles may have wider application.

2.1.1 The Design Process.

Let us consider the essential features of the design methods that are possible with today's knowledge and, in so doing, try to find the preferred sequence for the design process.

Although the various theoretical techniques available to the designer may be employed in whatever order he desires, nevertheless it seems that they should occupy particular positions in the design process. This is apparent when the design process is represented by a flow diagram that is constructed with the design procedures arranged in a logical sequence as in Figure 2.1.

The design process as it applies to the triplet system is depicted in Figure 2.1. It starts from the "basic parameters" ($\phi, \chi, P, L, T, N_a, N_b, N_c, V_a, V_b, V_c$) passes through the thin lens solution to a set of "performance-parameters" ($\phi_1, \phi_2, \phi_3, t_a, t_b$) which are converted with the aid of the shape-parameters into the thin lens "fundamental parameters", the curvatures and separations.

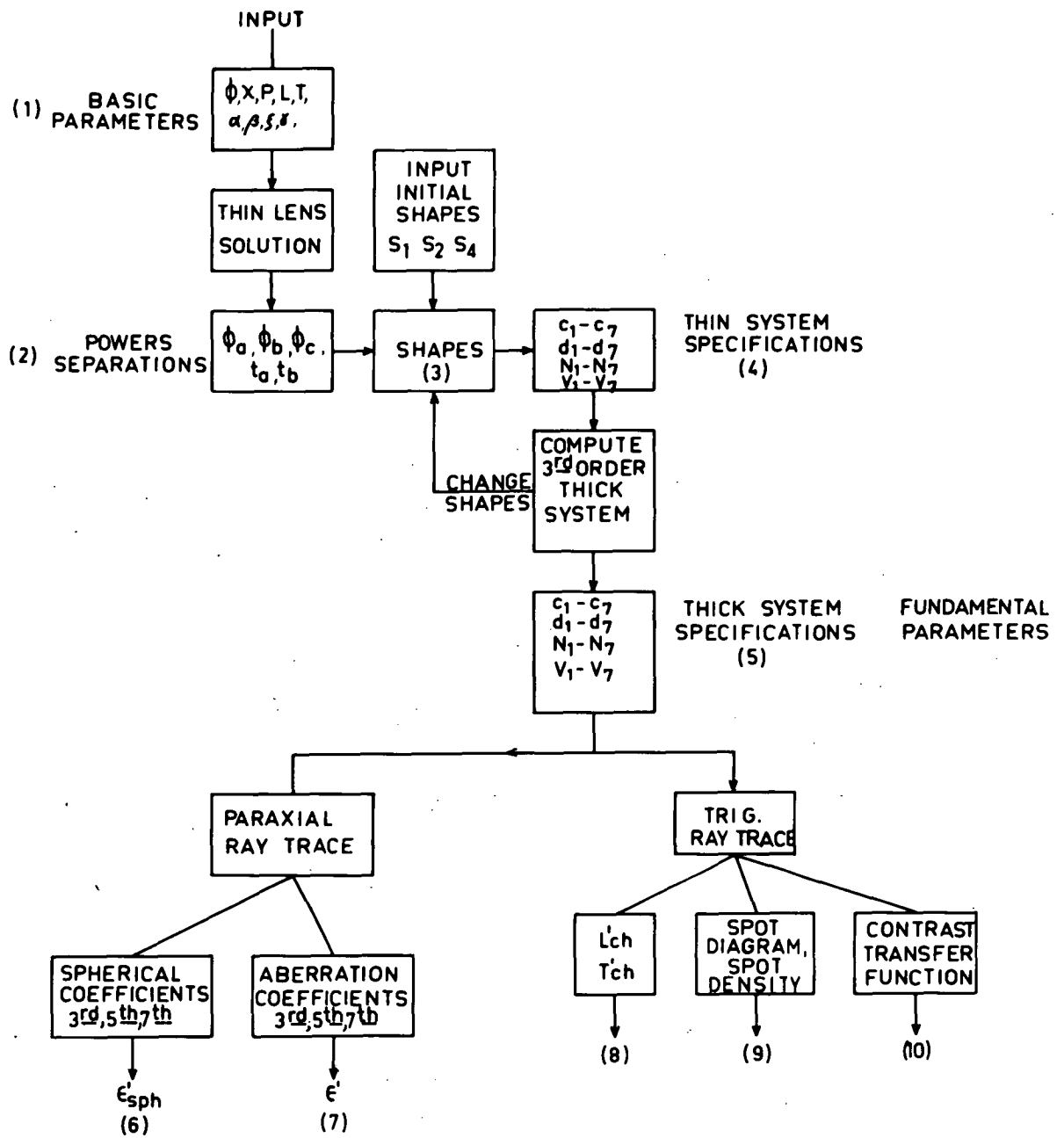


Fig. 2.1

(These sets of different parameters are numbered (1) to (4) in the diagram.) Then starting with the thin solution "the 3rd order analysis" generates the thick system with prescribed 3rd order coma, astigmatism and distortion by adjusting the shapes. Having computed a 3rd order system the designer is at position (5) in the flow diagram at which he must decide how to assess the system, whether to use aberration coefficients that are computed from paraxial quantities or whether to use exact quantities that are computed from trig-ray-traces, for example, spot diagrams, O.T.F., etc.. In this final stage of the design process these quantities which we have called "performance parameters" are compared with a set of target values or tolerances.

Although this discussion has so far been concerned with the design process of the triplet it is evident, however, that it can be easily converted to the general design process. For example, the sub-routine thin solution of Figure 2.1 could be replaced by the thin solution of, say, a telescope doublet and so on for all the parameters and all the other stages. Clearly the design process consists of a sequence of levels or degrees of approximation to the final system. It seems to the author that the "preferred process" is the natural sequence of these degrees or levels of design.

In order to adjust the residuals to the target values many designers seem to prefer to use the thick system's

"fundamental parameters", (the curvatures and thicknesses etc.) that occur in position (5) of Figure 2.1. So, in keeping with this design technique, Buchdahl^(13.1) has created an analysis that gives the surface contributions of the aberration coefficients and, also, has developed differential coefficients of his aberration coefficients with respect to the "fundamental parameters"(curvatures, thicknesses etc.)

Cruickshank and Hills (1960)^(2.4) have used both the Buchdahl surface contributions and the Buchdahl differential coefficients to improve a long focal length telephoto design of small aperture and field that was generated initially from a set of thin lens parameters. Other designers⁽⁸⁾, in later work than theirs, have used large computers to automatically optimize some thick systems with respect to their "fundamental parameters". Thus all of these designers in the final stage of their designs start at position (5) and confine their cybernetic process to a loop between positions (5) and one of the assessment sub-routines (LA', spot diagram, O.T.F., etc.).

2.1.2 Interpolative and Extrapolative Techniques in Optical Design.

As far as the author can discover all familiar design methods appear to be based on "extrapolation" techniques rather than "interpolation" techniques. Indeed, "extrapolation" seems inevitable when the designer bases

his design process on the "fundamental parameters"
(curvatures, thicknesses etc.) Also, since these parameters do not embody the characteristics of the particular type of system being designed, then the designer must explore cautiously around the starting point in order to avoid unrealistic systems. Moreover, even if he proceeds cautiously and achieves a useful system, he will not be sure that it is the best possible one of its type.

Under a heading "Problems for the Future", which he says have not been solved, Feder⁽⁸⁾ sums up extrapolation techniques when he says: "I am unhappy about the rate of convergence of any of the methods with which we are familiar." All these methods have in common one thing, they are all extrapolative methods. They collect information about the behaviour of a function in the neighbourhood of a point.... This is similar to a blind man trying to predict the shape of a mountain by feeling the ground around him with a cane."

So if a designer begins by assuming a set of thin lens parameters or even if he starts with a real system, then he is committing himself to an extrapolation technique. Consequently he must proceed blindly, relying either on his intuition or the decisions of his programme.

On the other hand, there is the ideal design principle of interpolation. This means he removes supposition by mapping the entire design with respect to all the design parameters; at first sight a formidable task. Feder

comments on this saying "It must have occurred to many people that it would be better to evaluate a merit function Φ over a network of points distributed over the region of the independent variables and to interpolate between these computed systems, a solution. However, when one calculates the number of points necessary, one is overcome by hopelessness. If we suppose that 10 points are computed for each variable, then it is necessary to compute for an eight-surface lens 10^{25} times in order to make a workable network."

Clearly Feder proposes working between the thick lens parameters of position (5) of Figure 2.1 and a merit function Φ that is made up of several performance parameters. This approach does not look promising with regard to either the choice of the design parameters or the starting point in the design process*. How can the designer have a realistic interpolative method when he has chosen a set of fundamental parameters (curvatures, thicknesses etc.) as the independent variables? This means that he is going to let the programme enter a multi-dimensional-space of unknown structure in which it is allowed to follow any path that shows improvement in the design. The generality of this approach would appear to be its downfall. For example, the

* R.E. Hopkins, London (1961) (4.1) Optical Design on Large Computers says: "Experience with these programmes has convinced us that it is not feasible to blindly explore in a multi-dimensional space and reduce a Merit Function to its lowest possible value etc.."

eight surfaces of Feder's example are indistinguishable - they can be varied in any order and, for that matter, so can the other fundamental variables, such as, thickness, refractive index etc.. Consequently this process may become either an aimless or an infinitely slow* journey through a multi-variable space that is fraught with impractical systems which appear without the designer knowing how.

In addition to an unfortunate choice of independent variables (fundamental parameters), the choice of a merit function Φ as the dependent variable is unfortunate, because its construction is such that it must be calculated for all field angles and aperture-zones^(4.1). This requires a huge amount of computation for each assessment. Consequently, although Feder and others who pursue a purely automatic approach do propose interpolation they have not, it seems, as yet, constructed or proposed a realistic cybernetic-process.

The question now, as far as we are concerned, is can we construct a workable "interpolative design process" using established "theoretical tools" of optical design. We attempt to answer this question in the next section.

* Reference Kingslake, pp39-42, Vol.3, Applied Optics and Optical Engineering.

2.1.3 A Limited Interpolative Design Method Using Aberration Coefficients.

If we are to make satisfactory progress with the interpolative method of design we must choose design parameters that can be treated in a particular order. This will allow us the practical advantage of dividing the design process systematically into manageable steps.

The "basic parameters" are eminently suitable because they have the necessary properties; they are both distinguishable and separable. We saw in Chapter 1, Section 1, that they can be separated according to their dependence on V and so we can divide the design process into a monochromatic-stage and a chromatic-stage. Also, they are individually distinguishable and, furthermore, each one can be associated with a dependent variable of a similar type until a fairly advanced stage of design is reached.

While workers, such as Feder, seek to go from a real system to an exact measure of its performance in one step in order to assess and improve it, we, on the other hand, propose to study the behaviour of the system in detail at an earlier stage of the design process. Thus we will be content initially with a complete assessment of the system's potential to 7th order made with respect to its basic parameters.

The Buchdahl coefficients of 3rd, 5th and 7th order represent indirectly the behaviour of all the rays of all

the pencils of the symmetrical optical system for a prescribed colour; this fact, it seems, is often overlooked. In contrast with this, the exact assessment quantities like O.T.F. or the radius of gyration of a spot diagram only contain information about a particular pencil of rays and so an enormous amount of computation is required to gain the same results as a single computation of the coefficients (except in the final stages of the design of systems with large apertures and fields when coefficients to 7th order are not enough.).

It has been established that the set of 3rd, 5th and 7th order coefficients enable us to estimate most geometrical optical quantities with reasonable accuracy up to a maximum aperture of $f/3.5$ and a maximum field of between $20^\circ - 30^\circ$, Buchdahl (1958)^(13.5), Cruickshank and Hills (1960)^(2.4). This accuracy is sufficient for our initial purpose since it is not our aim to measure the design potential with the precise performance parameters (O.T.F., LA' , etc.) at this early stage. All we are aiming to do now is to understand how the main features of the design vary with respect to its basic parameters. Obviously, we must discover, initially, whether there are several regions of equal promise or, whether is only a single optimum region for a particular lens type that is constructed from a given set of glasses. For this purpose, merely seeing how the relative magnitude of the coefficients varies with respect to the design parameters should be sufficient

This question has not been treated comprehensively by past workers because of the enormous amount of computation involved. No one knows conclusively how any system depends on its design parameters to 5th order, let alone 7th order.

The only comprehensive results in the literature stem from extrapolative surveys of triplets. Cruickshank, (as we saw earlier), has done a lot of pioneering work with coefficients and triplets but in all cases his coefficient surveys are restricted to small ranges of the basic parameters; broadly speaking, his work is extrapolative^(2.1, 2.2, 2.8). Hopkins also has surveyed some triplet solutions but this work is confined to the 5th order and it appears that his surveys are extrapolative also.

From this discussion we conclude that a "limited-interpolative-study" of a design with the aberration coefficients and thin lens parameters (basic-parameters) seems to be the most logical and practical first stage in the design process. Not just a study of a small region of one or two thin lens parameters but a systematic map of the coefficients of 3rd, 5th and 7th order for a range of the "basic parameters" that will exhaust the design potential to 7th order. This will, of course, only map the design's potential with sufficient accuracy up to an aperture of about $f/3.5$ and up to a field of about 20° ^(13.1, 13.5, 2.4). Beyond these values,

* Limited is used here to mean limited to a finite range of the parameters. However, the range, although finite, is chosen to exhaust the potential of the design.

we will have to resort to other means for mapping what are, in effect, coefficients of order greater than the 7th. However, we will leave this till later. All we want to know now is where the best system is most likely to occur when our approximation does not go beyond the 7th order.

2.1.4 Implementing a Limited Interpolative Study of the Type 121.

Although by choosing the basic parameters as design or construction parameters and the aberration coefficients as performance parameters, we make a limited interpolative study possible, we need, however, to think about how we are going to break the problem down. In view of our earlier discussion we will think of the system as being designed for monochromatic work in d-light only and, thus, we will have no practical need to be concerned with the chromatic residuals R_6 and R_7 of the thick system. Consequently we will fix L and T and think of the final design as being one of the family of triplets with construction constants $\bar{\Phi}$, L , T , R_2 , R_3 and R_5 . So all we have left as independent variables in this the monochromatic stage are (\mathcal{X}, k', P) .

If we vary the design parameters (\mathcal{X}, k', P) we can generate a set of triplets with the same $(\bar{\Phi}, L, T, R_2, R_3, R_5)$ and these triplet systems will have different aberration coefficients or residuals. By doing this we will be mapping aberration coefficient-space against (\mathcal{X}, k', P) -space

for a constant set of values of $(\Phi, L, T, R_2, R_3, R_5)$. Consequently the process of systematic design will be initially an interpolative-monochromatic-study in (\mathcal{X}, k', P) -space, whereas the earlier work in Section 1 is only an extrapolative-study in (\mathcal{X}, k', P) -space about the point $P = 0.35$ with $L = 0.2$ and $T = 0.05$. Thus by mapping all the independent variables of the "monochromatic system" versus the dependent variables as completely as possible to 7th order, we will be working interpolatively in our attack on the type 121. This approach is supported by Buchdahl's remarks when he says: "If one proceeds up to and including the 7th order terms one then has the convenient set of "28 performance" numbers describing the "monochromatic" behaviour of the system as a whole."(13.5)

2.1.5 Limited Interpolative Design Compared with Other Design Techniques.

The design process we will use does not allow the designers' taste or intuition to select alternative paths or loops in the flow diagram. We assert that each selected level or stage of the cybernetic design process should be used in its turn to study systematically its performance parameters versus the basic parameters before advancing to the next more sophisticated stage. Thus in each new stage new performance parameters will be surveyed with respect to

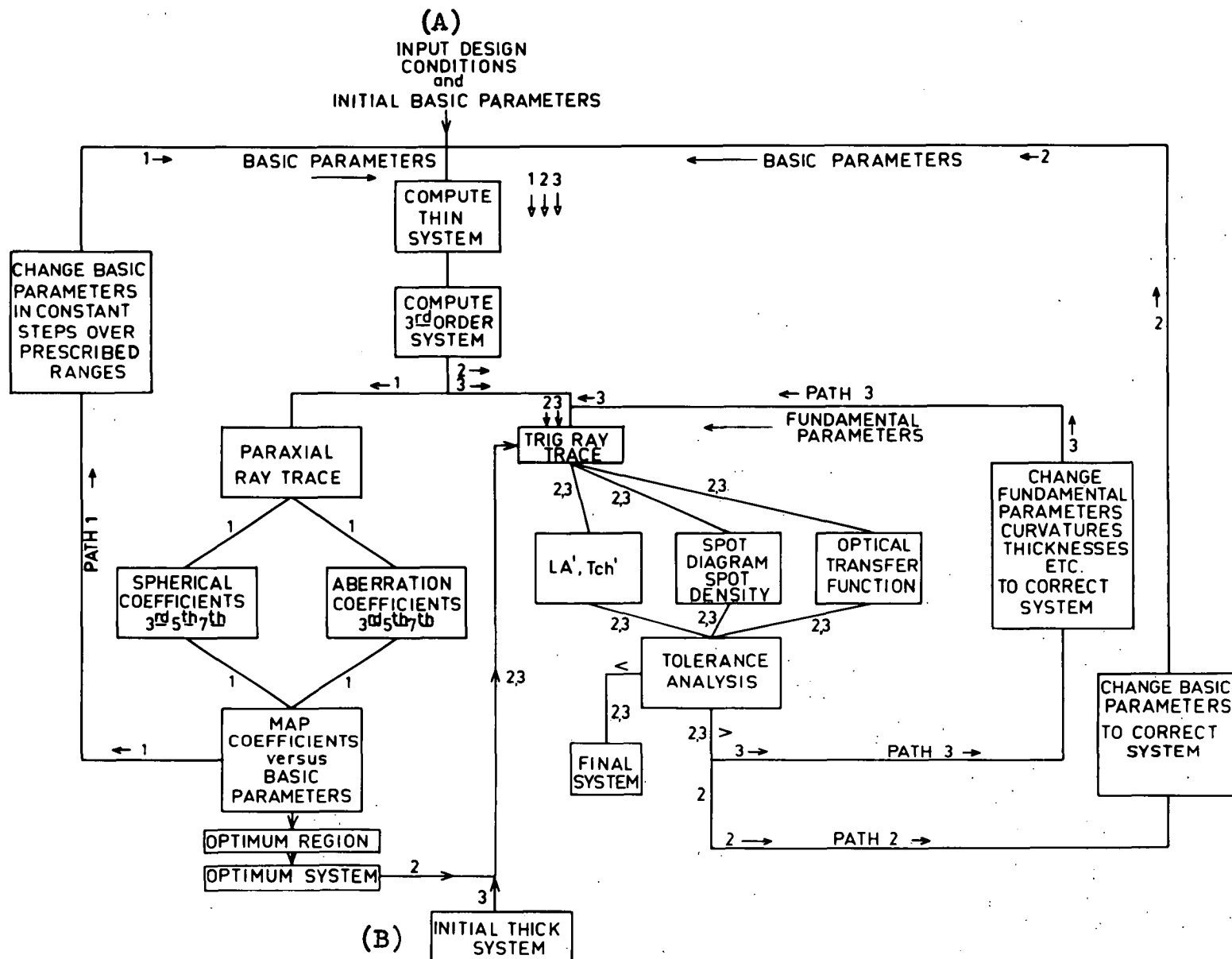
the original design-parameters which are the "Basic Parameters" of this work.

The different paths possible in the optical design process are shown in Figure 2.2. The process can be started at either position (A) or position (B). Automatic design is started in general at (B) with the specifications of a real system and passes directly into the loop which is denoted by path (3). The process continues in path (3) until the performance parameters chosen by the designer satisfy the tolerance conditions.

Designers in the past have mainly worked from position (a). After generating a 3rd order system from thin lens residuals they pass into the loop denoted either by path (2) or path (3). Mostly designers have favoured path (3), that is changing fundamental parameters as soon as their initial process has produced a crude real system.

The techniques for adjusting the fundamental parameters in path (3) are of two types, being based on either trigonometrical ray-traces or paraxial ray-traces. The trig ray-trace methods usually involve direct calculation of differential coefficients from finite changes in fundamental-parameters. This seems to be a naive approach to optical design; it relies too much on where the designer starts his process. Also, it does not seem possible for the designer to get a very clear picture of "design trends" because of the large number of parameters involved except,

FIG. 2.2



perhaps, when dealing with very simple systems. This direct approach to optical design would seem to be defeated by the overwhelming amount of computation required for the complete assessment of an optical system.

The drawback of large amounts of computation has been alleviated, to some extent, with the advent of Buchdahl-coefficients. Thus, workers using path (3) have been provided with the means for computing differential coefficients with respect to fundamental-parameters analytically to 5th order at least. (Cruickshank and Hills pioneered this technique, 1960.)^(2.4) We have not shown details of the path followed by this type of calculation, however it would be included in the block "change of fundamental parameters etc." in path (3).

Cruickshank and R.E. Hopkins have made some use of path (1) when they mapped 5th order coefficients of simple triplets with respect to some thin lens construction-parameters. They have selected likely systems from these simple maps and used some differential method, usually path (3), to correct them. It is evident that all three paths of the design process have been used by designers at some time. Indeed, probably most combinations of these paths may have been used. However, it does not appear that any have proposed the thorough mapping that we have asserted is necessary for systematic design.

The "limited interpolative method" that we have used starts at position (A) and continues in path (1) until a complete map of the coefficients of 3rd, 5th and 7th order versus the basic parameters is produced. Then the most interesting region is selected and mapped in detail so as to predict the optimum system accurately. This optimum system initiates loop (2) in which the design process continues until tolerances are satisfied.

The method we have used seems to follow the basic rules of research. We appear to have used the optical tools in the most suitable way. Initially we map the phenomena with our coarsest instrument, the aberration coefficients, in order to observe the whole potential of the design. We follow this with detailed maps of promising regions, using more sophisticated optical tools that approximate the real system more closely than the coefficients.

It is anticipated that by studying the type 121 triplet system in this general way, that useful design principles will emerge which will help us to design other triplets.

CHAPTER 2.2 A LIMITED INTERPOLATIVE STUDY OF THE MONOCHROMATIC TYPE 121.

2.2.0 Introduction.

Ideally, given a large high speed computer, all that needs to be done for our interpolative survey is to include, in the final stage of the basic programme, a sub-routine that computes the Buchdahl coefficients and then arrange for this programme to generate 3rd order systems at regular intervals of χ , k' and P . However, the Elliott 503 computer used in this work is only large enough to handle the basic programme and, therefore, we have had to compromise and do this sort of mapping in two stages; the first with the basic programme or some equivalent programme, and the second with a programme that was written by P.W. Ford (1959)^(12.1) for computing the Buchdahl coefficients of a given system.

The first stage does not require much data preparation but the second involves punching up the specifications of each system individually. So just to map a monochromatic design is a large task, but the results seem to have justified this extensive piece of preliminary work.

Instead of insisting on equal intervals for each of the basic parameters we gain an advantage by relaxing this for χ . This enables us to employ the left and right

hand solutions programme (LR/BP/121) which for each set of values of the parameters (k' , P , L , T , R_2 , R_3 , R_5) automatically generates type 121 triplet systems that are corrected for 3rd order coma, astigmatism and distortion at $\mathcal{X} = 0, -0.5, -1.0$ and in addition it generates the 3rd order left and right hand solutions at $\mathcal{X} = \mathcal{X}_L$ and $\mathcal{X} = \mathcal{X}_R$ and the turning point solution at $\mathcal{X} = \mathcal{X}_{TP}$. Also, the solutions are corrected for 7th order spherical. So now the problem of making a network in (\mathcal{X}, k', P) -space is no more than arranging sets of curves like those of σ_1, μ_1, τ_1 and ϵ'_{Sph} of Chapter 1.4 in a rectangular array. As for k' and P it has been found that by taking k' in steps of -1 and P in steps of 0.1 a sufficiently dense network is formed.

Thus the network used here is

$$\mathcal{X} = 0, -0.5, -1.0$$

$$\text{by } k' = -2, -3, -4, -5$$

$$\text{by } P = 0.1, 0.2, \dots 0.6$$

$$\text{at } L = 0.2, T = 0.05, R_2 = R_3 = R_5 = 0.$$

2.2.1 The Spherical Coefficients of the Monochromatic Type 121 System versus \mathcal{X}, k', P .

2.2.1.1 Description of Results Obtained for the Spherical Aberration Coefficients.

Although of necessity the spherical aberration coefficients of 3rd, 5th and 7th order are computed before the rest of the coefficients it is, for all that, the logical

sequence in designing a system. In optimizing the spherical aberration we are achieving the optimum axial image and at the same time improving all the off-axial images.

In Figure 2.3 the Spherical coefficients of 3rd, 5th and 7th order and the predicted marginal spherical ϵ'_{Sph} in transverse measure are plotted with respect to χ , k' and P . This figure can be interpreted as a map of the zonal and marginal spherical to 7th order of the type 121 triplets that can be constructed from a given set of glasses. Or, in other words, we are saying that in our cybernetic process, if we hold Φ , L , T and the basic glasses (N_a, V_a) and (N_c, V_c) constant for the 3rd order 121 systems generated from the four real glasses, then the spherical aberration parameters σ_1, μ_1, τ_1 and ϵ'_{Sph} depend on (χ, k', P) as in Figure 2.3. Here, then, we are observing the potential of the "axial-monochromatic" type 121 system to 7th order in a single rectangular array.

The essential quantitative features of this figure are:

1. The horizontal scale of each set of rectangular axes is $\chi = +1$ to -3 in units of $\Delta\chi = 1$.
2. The quantities plotted on the vertical axes are shown in the left hand margin being σ_1, μ_1, τ_1 and ϵ'_{Sph} . Their scales are shown on their corresponding vertical axes.

3. The sets of rectangular axes from left to right occur at intervals of $\Delta P = 0.1$ from $P = 0.1$ to $P = 0.6$; the value of P is above each set of axes.
 4. The curves plotted on each set of axes range vertically from $k' = -5$ to $k' = -2$.
 5. All the systems have $\Phi = 1$, $L = 0.2$, $T = 0.05$,
 $R_2 = R_3 = R_5 = 0$, $N_a = N_c = 1.62101$, $V_a = V_c = 60.18$.
- This diagram is an array of two dimensional (\mathcal{X}, k') sections of (\mathcal{X}, k', P) -space.

2.2.1.2 Discussion of the Properties of the Spherical Aberration Coefficients.

The behaviour of the spherical coefficients and the marginal spherical with respect to the basic parameters (\mathcal{X}, k', P) is very interesting. The graphs of this limited interpolative survey of Figure 2.3 present an unexpectedly clear and simple picture of the design potential of the "axial-monochromatic system". For each of the quantities σ_1, μ_1, τ_1 and $\mathcal{E}'_{\text{Sph}}$ the groups of k' -curves converge towards the \mathcal{X} -axis from above and below as P increases. The rate of convergence is greater for the curves lying beneath the \mathcal{X} -axis than for those above it.

In the region close to $k' = -3$ the magnitudes of μ_1, τ_1 , and $\mathcal{E}'_{\text{Sph}}$ are less dependent on P than σ_1 . Nevertheless, the turning points of the $(k' = -3)$ -curves of all these quantities $(\sigma_1, \mu_1, \tau_1)$ and $\mathcal{E}'_{\text{Sph}}$ approach zero as P increases from $P = 0.1$. This suggests that there is a region

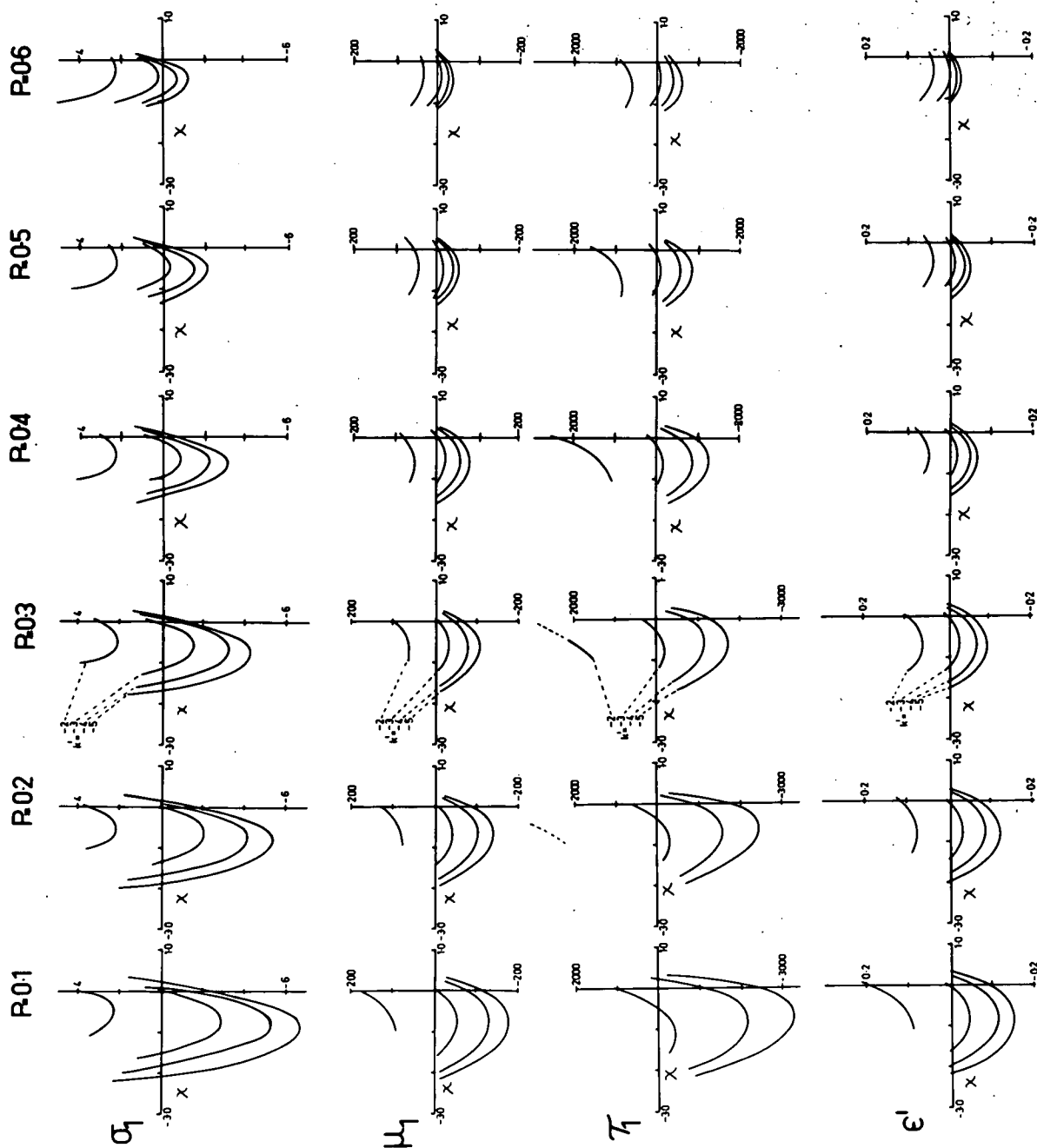


Fig. 2.3

of (\mathcal{X}, k', P) that gives zero marginal spherical as well as nearly zero zonal spherical. This "optimum region" is close to $\mathcal{X} = -0.5$, $k' = -3.0$, $P = 0.55$ and in this region we expect to be able to design a system with a nearly perfect monochromatic image on axis for all apertures up to about $f/3.5$, because, σ_1, μ_1, τ_1 and ϵ_{Sph}' approach zero almost simultaneously.

This result supports the idea now proposed by the author that this simultaneous convergence of the spherical aberration coefficients versus the monochromatic basic parameters is a characteristic property of triplets.

(If this is so then a significant principle can be established.)

In varying k' we are changing the magnitudes of the basic glass parameters (N_b, V_b) of the middle lens group. However, with the glasses chosen in this example of the type 121, we are, in effect, only changing one basic parameter significantly, the parameter V_b . This is shown clearly in Table 2.1 where for $N_a = N_c = 1.6210$ and $V_a = V_c = 60.18$ we have:

Table 2.1

| k' | N_b | V_b | $\Delta V = V_a - V_b$ |
|------|-------|-------|------------------------|
| -2.0 | 1.528 | 33.36 | 26.8 |
| -2.5 | 1.550 | 35.08 | 25.1 |
| -3.0 | 1.561 | 36.02 | 24.2 |
| -4.0 | 1.573 | 37.00 | 23.2 |
| -5.0 | 1.578 | 37.51 | 22.7 |

By close inspection of Figure 2.3 we estimate that the optimum k' lies about midway between -2.0 and -3.0 and this corresponds to a basic glass with $V_b = 35.08$ (at $k' = -2.5$). Consequently the difference between the basic V -values of lens groups a and b is $\Delta V = (V_a - V_b) = 25.1$ (at $k' = -2.5$).

The parameter ΔV is used by R.E. Hopkins as a basic parameter in his study of a set of Cooke triplets or type 111 triplets with $N_a = N_c = 1.6200$, $V_a = V_c = 60.28$, which are almost equal to those of the type 121.

In this study he, in effect, varies V_b systematically whilst keeping the other basic glass parameter N_b nearly constant by careful glass selection. Therefore, in this respect his study of the initial design principles of the type 111 is analogous to our study of the type 121 except that, as we shall see, it is extrapolative rather than interpolative.

He shows that the 5th order Buchdahl coefficient of spherical aberration (μ_1) and also the comatic coefficients of the 5th order (μ_2, μ_3, μ_7 and μ_8) "all tend to become smaller for the solutions close to $\Delta V = 25$ ". This is significant in the light of our more detailed study of a more complex triplet type. However, for the present we will confine our comparison between Hopkins' work and the type 121 to the spherical coefficients τ_1, μ_1, τ_1 and come back to the other coefficients of the off-axial aberrations (μ_2, μ_3, μ_7 and μ_8) when we look at the off-axial image.

The property that μ_1 becomes smaller near $\Delta V = 25$ (observed by Hopkins) is also a feature of the set of converging parabolas of μ_1 versus (\mathcal{X}, k', P) in Figure 2.3. However, in order to be equivalent to Hopkins' work it is necessary to replace (\mathcal{X}, k', P) by the Hopkins' parameters $(K, \Delta V, P)$. It can be shown that these sets of parameters are equivalent "basic-parameters" as far as the broad features of the spherical aberration coefficients of 3rd, 5th and 7th order of both this work and that of Hopkins are concerned. Firstly, in both studies the P-parameters are measures of the Petzval blur and, therefore, they are equivalent. Also, we have already shown that k' can be replaced by ΔV and, so, we are only left with Hopkins' K and our \mathcal{X} . However, K can be shown to be the simple function of \mathcal{X} ; it is $K = (\phi_a \cdot y_{oa}) / (1 - \mathcal{X})$ where $y_{oa} = 10$. Thus the main effect of replacing \mathcal{X} by K will be to produce the mirror image of the parabolas of the type 121. They will be modified only slightly in shape by the factor ϕ_a because the power ϕ_a is shown by Cruickshank to be a linear function of \mathcal{X} . Furthermore, the comparison of these two studies of the type 111 and the type 121 is credible because the "basic glasses" are almost identical.

Hopkins has only computed the 5th order coefficients of specific solutions of type 111 triplets and, consequently, he has not observed that the 5th order spherical aberration has a parabolic form; nevertheless, this has been observed

for the type 111 by Cruickshank^(2.8). However, Hopkins notices that the 3rd order spherical parabolas are raised or lowered by changing either P or ΔV . These facts, when considered in conjunction with his observation that he finds μ_1 smaller near $\Delta V = 25$ with P a maximum, supports our conclusion that he is observing some of the facets of convergent behaviour similar to that of Figure 2.3.

Perhaps the most interesting feature of the results of the "limited interpolative survey" is that the parabolas of the three orders of spherical aberration behave in such a regular way converging, it seems, to a single optimum solution for the monochromatic "axial-system" of the type 121. Also, in the light of Hopkins' work this seems to occur with type 111 triplets and, we conjecture, possibly with more complex triplets. However, although we have found evidence indicating that the simple type 111 triplet has similar behaviour to the type 121, this "optimum region" is probably not accessible to it, because ΔV can only assume a finite number of discrete values (the type 111 basic triplet is constructed from real basic-glasses). But we avoid this glass-restriction when we create a basic glass from a cemented pair of lenses, hence the type 121 has exciting potential.

Thus it appears at this early stage that the "basic-triplet" and its parameters the "basic-parameters"

are fundamental quantities in the design-process. So much so, that as a result of this work the author feels that design principles based on the basic-parameters such as (\mathcal{X}, k', P) or $(K, \Delta V, P)$ apply to triplet systems in general. Further evidence to support this idea will be produced in appropriate places as they arise in this thesis.

2.2.2 The Petzval Coefficient and the Separations versus (\mathcal{X}, k', P) .

2.2.2.0 Introduction.

Before looking at the other higher order coefficients there are two types of quantities that we will consider now because their general behaviour bears on the later work. The first is the remaining 3rd order coefficient that is not controlled during the present design process, namely, the Petzval coefficient \mathcal{T}_4 . Secondly, we want to consider the behaviour of the separations of the lens groups of the triplet which are the quantities d_3 and d_6 of the type 121 (ref. Figure 1.1.2). It is also appropriate that we choose to discuss these quantities immediately after the spherical coefficients because like the spherical coefficients $(\sigma_1, \mu_1, \tau_1)$ the quantities \mathcal{T}_4 , d_3 and d_6 are part of the output of the programme LR/BP/121, whereas the remaining higher order coefficients that are discussed after this section are obtained using the coefficient programme of P.W. Ford^(12.1).

We look upon these quantities σ_4 , d_3 and d_6 as another set of performance parameters generated from the "basic-parameters" (\mathcal{X} , k' , P) and so we plot them in the same (\mathcal{X} , k' , P)-network as before (see Figure 2.4 and 2.5).

2.2.2.1 The Petzval Coefficient versus (\mathcal{X} , k' , P).

The Petzval coefficient versus \mathcal{X} -curve (Figure 2.4) may be approximated by a quadratic function of \mathcal{X} and so once more we find that we have groups of parabolas converging towards each other as P increases. Only this time the order of the curves is inverted, the bottom curve is at $k' = -2$ and the top at $k' = -5$. However, although the parabolas are converging they are, at the same time, rising to higher values, and so, as is to be expected, the net effect of increasing P is to increase σ_4 . But balancing the apparent ill-effect of large σ_4 we see that as P approaches the region of optimum spherical aberration of the monochromatic system, between $P = 0.5$ and $P = 0.6$, σ_4 becomes almost independent of changes in \mathcal{X} and k' . Indeed, it is clear that little is to be gained by attempting to improve the Petzval sum with the design parameters (\mathcal{X} , k' , P). So, at this stage, we will accept the σ_4 associated with the optimum spherical region and make no attempt to improve it at the expense of the zonal correction.

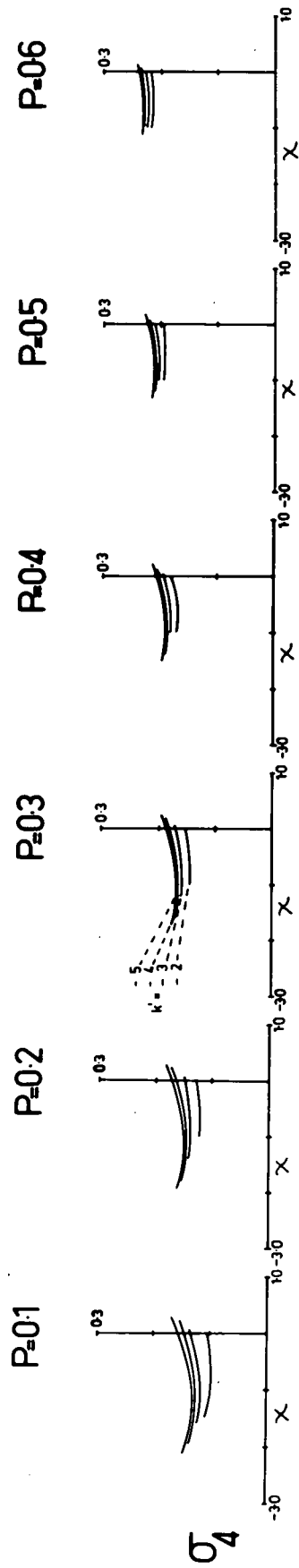


Fig. 2.4

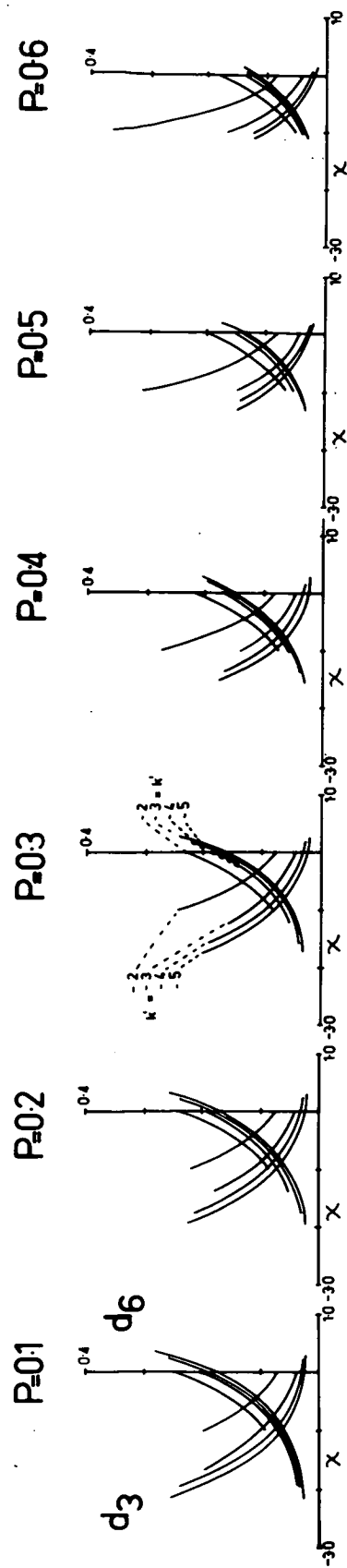


Fig. 2.5

2.2.2.2. The Separations versus (χ , k' , P).

In Figure 2.5 the separations d_3 and d_6 are plotted on the same axes. On any pair of rectangular axes in Figure 2.5 the left hand group of curves shows the variation of d_3 versus χ and k' and the right hand group is that of d_6 versus χ and k' . The outermost curves of the two groups are $k' = -5$ and the innermost curves are $k' = -2$.

As P increases there is only a slight tendency for the groups of (d_3, d_6) -curves to converge towards each other, but they do shift as a whole towards $\chi = 0$. Thus the sum of the separations is almost unchanged for all values of χ and P . This is equivalent to saying that the length of the system is independent of χ and P . However, both d_3 and d_6 increase as k' increases and, therefore, it follows that the length of the system increases as k' (or ΔV) increases.

We note for future reference that the intersection points of the corresponding pairs of (d_3, d_6) -curves shift towards $\chi = 0$ as P increases from $P = 0.1$. In particular, the intersection point of the pair of (d_3, d_6) -curves at $k' = -3$ approaches $\chi = -0.5$ as P approaches $P = 0.6$. So the intersection point of the $k' = -3$ curves possibly passes through the region of "optimum spherical aberration" which we estimate to be near the point $(\chi = -0.5, k' = -3, P = 0.55)$. Thus these systems may have equal

air spaces, $d_3 = d_6$.

Cruickshank^(2.1) observes for the type 111 triplets that "an increase in P enlarges the front air space, particularly for large negative values of \mathcal{X} , and diminishes the back air space." This observation is consistent with the behaviour of groups of curves shifting towards $\mathcal{X} = 0$ as P increases, just as we have in Figure 2.5 for the separations d_3 and d_6 of the type 121.

R.E. Hopkins^(4.3) says in his discussion of the type 111 triplet: "This simple triplet objective helps us to understand more complicated objectives. For example, if a wide angle objective is needed in a triplet, one can see that it is necessary to use a small ΔV . This keeps the lens short and \bar{H}_n becomes larger for any given value of P ."

\bar{H}_n is the estimated image height to 5th order relative to the Gaussian image height, at which the sagittal and tangential fields cross. This image height \bar{H}_n is obtained from the Buchdahl coefficients σ_3 , μ_{11} and μ_{10} being given by the equation

$$\bar{H}_n = \left[2\sigma_3 / (\mu_{11} - \mu_{10}) \right]^{\frac{1}{2}} / 0.364$$

(The equation quoted in R.E. Hopkins' paper^(4.3) contains two misprints.)

It is not possible to form good images beyond the intersection point of the tangential and sagittal fields.

However, we also have observed that the length of the type 121 triplet ($d_3 + d_6 + \text{constant}$) decreases as k' (or ΔV) decreases, and so the concept of the equivalence of the basic parameters k' and ΔV and the fundamental nature of these basic parameters receives further support.

Nevertheless, for the moment, we will not discuss whether a short system or small ΔV will improve the field until we study the astigmatic aberration coefficients.

2.2.3 The 5th and 7th Order Comatic and Astigmatic Coefficients versus (χ, k', P).

2.2.3.0 Introduction.

The first part of the "limited interpolative study" of the type 121 has been concerned mainly with the behaviour of the marginal spherical aberration and the spherical aberration coefficients, and, consequently, is a study of the system's axial potential. The point to be dealt with now in the second part of the interpolative study is concerned with mapping all the remaining aberration coefficients of the 5th and 7th order and, therefore, is a study of the system's "off-axial" potential.

These remaining aberration coefficients of the 5th and 7th order of the system are shown in Figures 2.6 to 2.17 in which they are arranged according to their aberration type (after Buchdahl) and therefore neither the order of the aberrations nor their numerical sequence is adhered to.

They are arranged in three principal groups: Figures 2.6 to 2.10 are the combined 5th and 7th order comatic or c-type coefficients, Figures 2.11 and 2.15 are the combined 5th and 7th order or S-type coefficients and Figures 2.16 to 2.17 are the 5th and 7th order coefficients of distortion.

The nomenclature for the aberration types has been proposed by Buchdahl^(13.3). He defines two aberration types that are based on the earlier work of Steward and calls them the c and S types. This nomenclature in effect classifies the coefficients according to the type of deformation they produce in the point image, denoting whether it is either symmetrical (S-type) or asymmetrical (c-type). (Some of the practical aspects of this nomenclature are discussed and illustrated very clearly in an example by Cruickshank and Hills^(2.4). In particular, they show graphically how the different aberration types of 3rd, 5th and 7th order contribute to the blur patch of the point image.)

Although the spherical aberration and Petzval sum may also be classified^(2.4) as S-type aberrations, and the distortion as a c-type aberration, we prefer, however, in this work, to call them by their usual names and treat them as separate quantities from the c and S types as we have in Figures 2.3 and 2.4. Thus with this

Table 2.1

| | | SPHERICAL | ASYMMETRIC ABERRATIONS | | | ASTIGMATIC ABERRATIONS | | | DISTORTION |
|-------------------|--------------------|-------------------------------|---|--|---|---|--|--|-----------------------|
| | | S - TYPE | C - TYPE | | | S - TYPE | | | C - TYPE |
| ORDER | $\Delta \epsilon'$ | | Linear Coma | Cubic Coma | Quintic Coma | Linear Astigmatism | Cubic Astigmatism | Quintic Astigmatism | |
| 3 rd . | ϵ'_y | $\sigma_1 \cos \theta \rho^3$ | $\sigma_2 (2 + \cos 2\theta) \rho^2 \bar{H}$ | | | $(3\sigma_3 + \sigma_4) \cos \theta \rho \bar{H}^2$ | | | $\sigma_5 \bar{H}^3$ |
| | ϵ'_z | $\sigma_1 \sin \theta \rho^3$ | $\sigma_2 (\sin 2\theta) \rho^2 \bar{H}$ | | | $(\sigma_3 + \sigma_4) \sin \theta \rho \bar{H}^2$ | | | |
| 5 th . | ϵ'_y | $\mu_1 \cos \theta \rho^5$ | $(\mu_2 + \mu_3 \cos 2\theta) \rho^4 \bar{H}$ | $(\mu_7 + \mu_8 \cos 2\theta) \rho^2 \bar{H}^3$ | | $\mu_{10} \cos \theta \rho \bar{H}^4$ | $(\mu_4 + \mu_6 \cos^2 \theta) \cdot \cos \theta \rho^3 \bar{H}^2$ | | $\mu_{12} \bar{H}^5$ |
| | ϵ'_z | $\mu_1 \sin \theta \rho^5$ | $\mu_3 \sin 2\theta \rho^4 \bar{H}$ | $\mu_9 \sin 2\theta \rho^2 \bar{H}^3$ | | $\mu_{11} \sin \theta \rho \bar{H}^4$ | $(\mu_5 + \mu_6 \cos^2 \theta) \cdot \sin \theta \rho^3 \bar{H}^2$ | | |
| 7 th . | ϵ'_y | $\tau_1 \cos \theta \rho^7$ | $(\tau_2 + \tau_3 \cos 2\theta) \rho^6 \bar{H}$ | $(\tau_7 + \tau_8 \cos 2\theta + \tau_{10} \cos 4\theta) \rho^4 \bar{H}^3$ | $(\tau_{15} + \tau_{16} \cos 2\theta) \cdot \rho^2 \bar{H}^5$ | $\tau_{18} \cos \theta \rho \bar{H}^6$ | $(\tau_{11} + \tau_{12} \cos^2 \theta) \cos \theta \rho^3 \bar{H}^4$ | $(\tau_4 + \tau_6 \cos^2 \theta) \cdot \cos \theta \cdot \rho^5 \bar{H}^2$ | $\tau_{20} \bar{H}^7$ |
| | ϵ'_z | $\tau_1 \sin \theta \rho^7$ | $\tau_3 \sin 2\theta \rho^6 \bar{H}$ | $(\tau_9 \sin 2\theta + \tau_{10} \sin 4\theta) \rho^4 \bar{H}^3$ | $\tau_{17} \sin 2\theta \rho^2 \bar{H}^5$ | $\tau_{19} \sin \theta \rho \bar{H}^6$ | $(\tau_{13} + \tau_{14} \cos^2 \theta) \sin \theta \rho^3 \bar{H}^4$ | $(\tau_5 + \tau_6 \cos^2 \theta) \cdot \sin \theta \rho^5 \bar{H}^2$ | |

nomenclature, the five familiar aberration types of spherical, coma, astigmatism, Petzval and distortion are retained when we study aberrations beyond the 3rd order. This simplifies the cybernetic process of design, because, each "basic parameter" can still be associated with a single type of aberration when we include the higher orders. Thus each coefficient is associated with one of the familiar defects of the point image of the aberrated system.

However, not only can the comatic and astigmatic coefficients be divided into 3rd, 5th and 7th orders, but also each order can be separated into linear, cubic and quintic forms. This is illustrated in Table 2.1.1 where the components $^{(2,4)}\zeta'_y$ and ζ'_z of the total aberration of a monochromatic ray $(\rho, \theta, \bar{H}_n)$ are shown resolved into these "minor forms". Thus the comatic types are associated with odd powers of \bar{H} and even powers of ρ ; the reverse occurs with the astigmatic types.

It is evident that the linear forms of coma are functions of \bar{H} , the cubic forms are functions of \bar{H}^3 and the quintic forms are functions of \bar{H}^5 . On the other hand, with the astigmatic types, the linear, cubic and quintic forms are associated with ρ , ρ^3 and ρ^5 respectively.

We have used the grouping of the coefficients of the Table 2.1 when plotting them in the (\mathcal{X}, k', P) -network.

Thus each of the Figures 2.6 to 2.15 depicts the coefficients of a particular "minor form" of the astigmatic and comatic aberrations. For example, in Figure 2.6 the coefficients that contribute the linear 5th order coma are plotted in the (\mathcal{X}, k', P) -network. Similarly, in subsequent figures, are the coefficients of cubic 5th order coma (Figure 2.7), the coefficients of linear 7th order coma (Figure 2.8) and so on.

The remaining Figures, 2.16 and 2.17, show the 5th order distortion coefficient (μ_{12}) and the 7th order distortion coefficient (τ_{20}) versus (\mathcal{X}, k', P) .

2.2.3.1 The Comatic Coefficients versus \mathcal{X}, k', P .

The pattern exhibited by the spherical coefficients, the spherical aberration, the Petzval coefficient and the separations of the type 121, persists with remaining aberration coefficients. In all cases the curves of each group converge towards each other as P increases (see Figures 2.6 to 2.17). However, the most interesting feature is that all the comatic coefficients, Figures 2.6 to 2.10, approach zero simultaneously near $\mathcal{X} = -0.5$, $k' = 3$, $P = 0.55$. Therefore, the "optimum^{*} region" is expected to give a system with almost equal air spaces (see section 2.2.2.2) that has both the zonal spherical and the coma nearly zero for all orders up to and including the 7th order. Of course, this is only so if the system is used

* The contributions of σ_1 , μ_1 and τ_1 almost zero.

in monochromatic light of the wavelength in which it is designed in this case λ_d .

2.2.3.2 The Astigmatic (S-type) Coefficients versus

$\chi, k', P.$

The behaviour of the astigmatic coefficients is different from that of the comatic coefficients, because, although all the curves of each group of each astigmatic-coefficient converge towards each other, they do not necessarily converge to zero. For example, in Figure 2.11, the μ_{10} -group slowly approaches zero as P increases so that near the "optimum region" ($\chi = -0.5, k' = -3.0, P = 0.55$), μ_{10} tends to zero, but, the μ_{11} -curves, although converging, approach a value between $\mu_{11} = -0.4$ and -0.5 . (It has been shown that a value of $\mu_{11} = -0.5$ occurs with type 111 triplets, Cruickshank^(2.8). Thus in the optimum region we may expect a negative residual of linear 5th order astigmatism which from the point of view of balancing aberrations, is useful in offsetting the positive $(\sigma_3 + \sigma_4) \bar{H}^2$ sagittal curvature of field.)

Further inspection and comparison of the other astigmatic coefficients shows that the optimum region of the spherical and the comatic coefficients is also the optimum region of the astigmatic coefficients. Clearly in the "optimum region" the astigmatic coefficients are minimized since all except μ_{11} approach zero simultaneously in

P=01

P=02

P=03

P=04

P=05

P=06

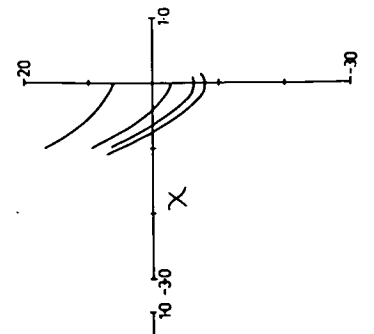
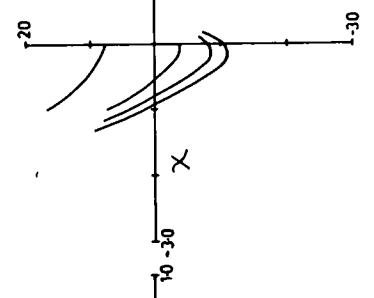
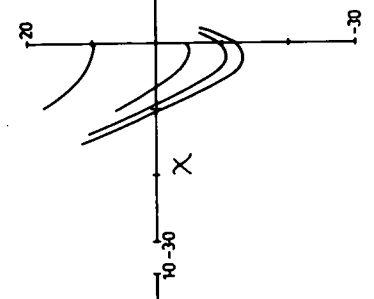
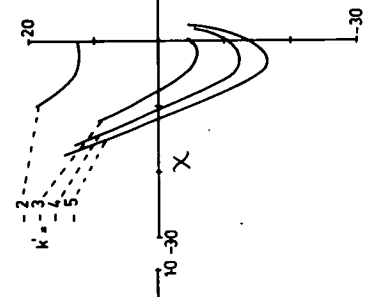
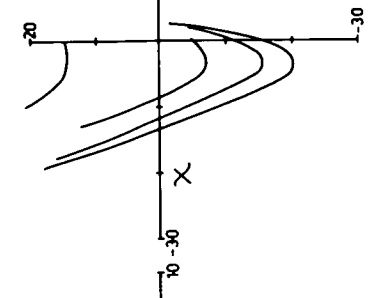
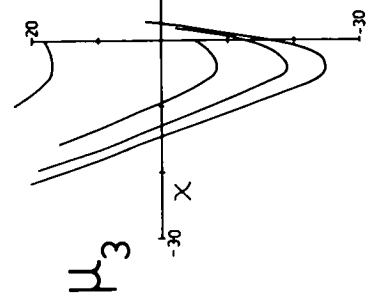
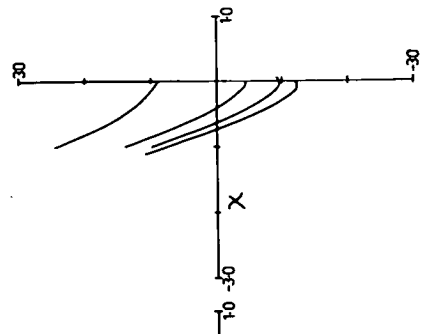
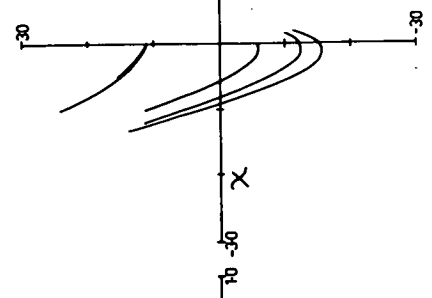
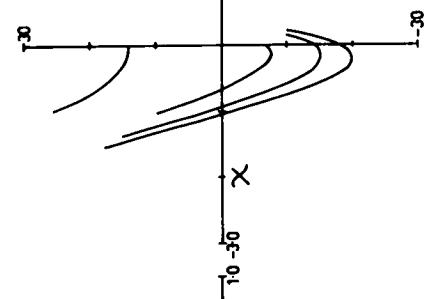
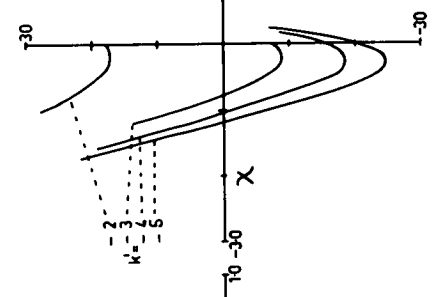
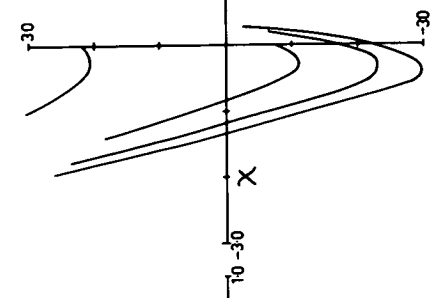
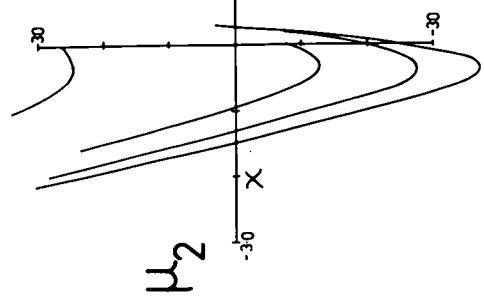


Fig. 2.6

P-01

P-02

P-03

P-04

P-05

P-06

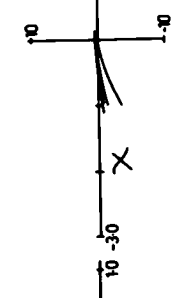
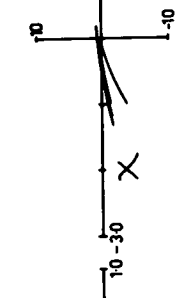
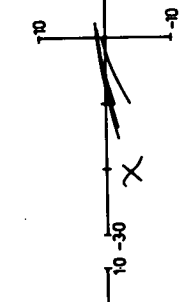
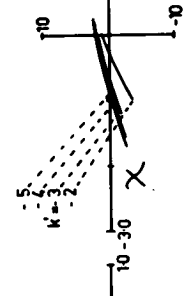
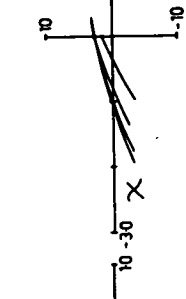
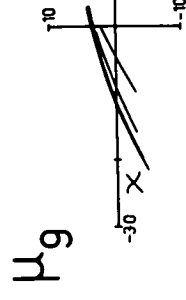
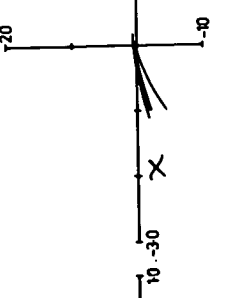
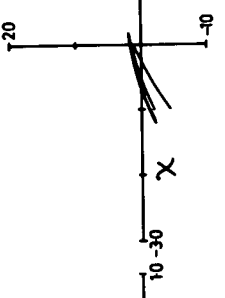
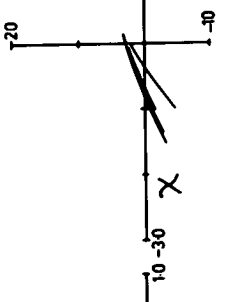
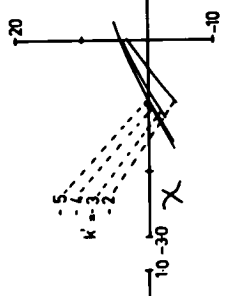
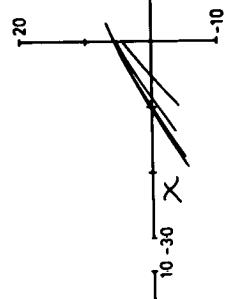
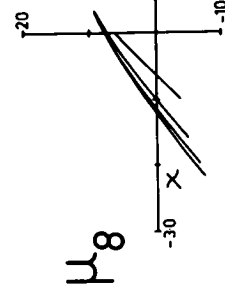
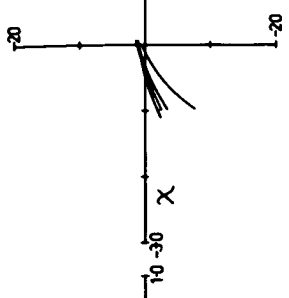
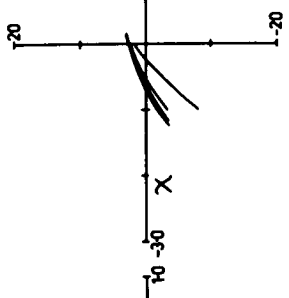
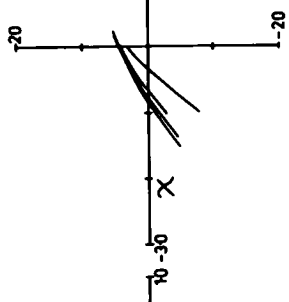
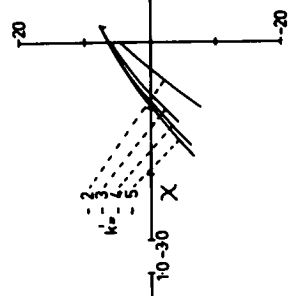
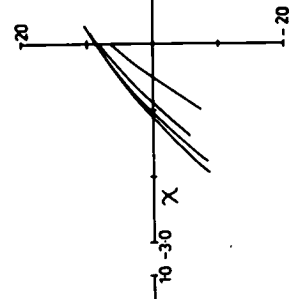
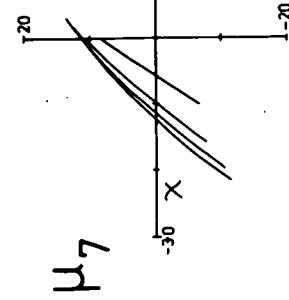


Fig. 2.7

$P=0.1$

$P=0.2$

$P=0.3$

$P=0.4$

$P=0.5$

$P=0.6$

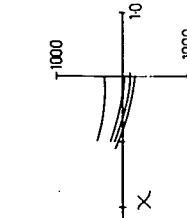
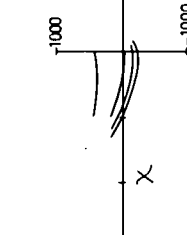
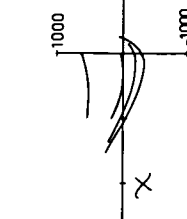
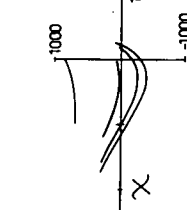
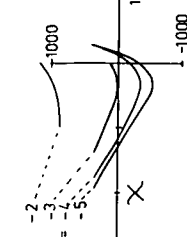
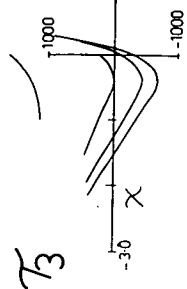
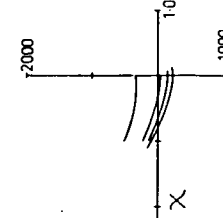
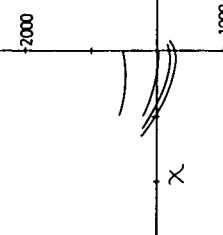
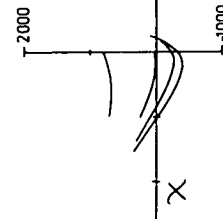
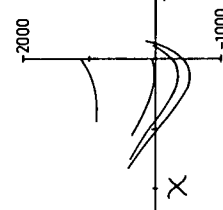
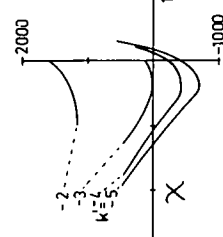
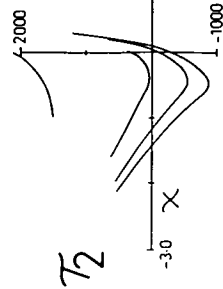


Fig. 2.8

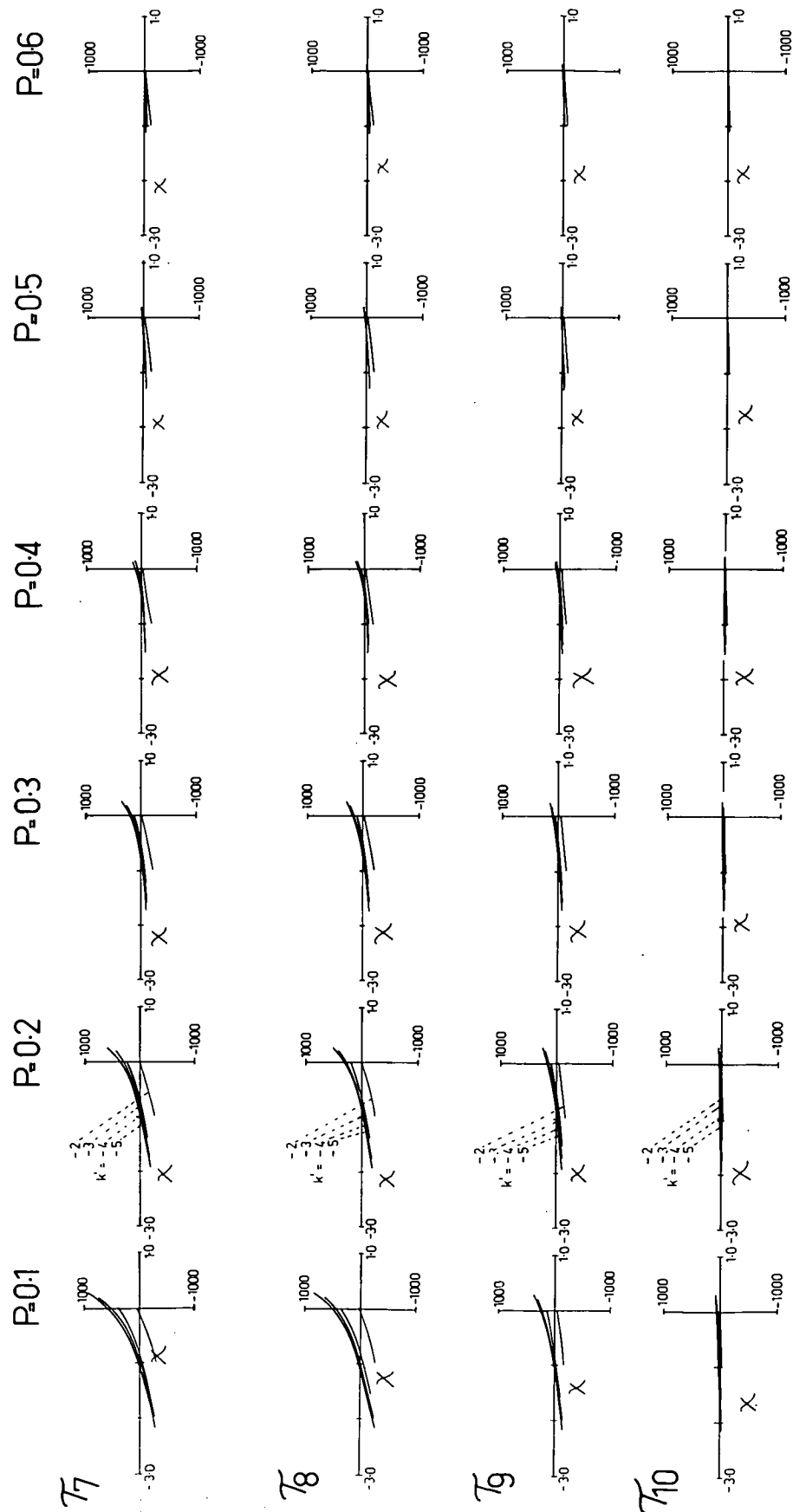


Fig. 2.9

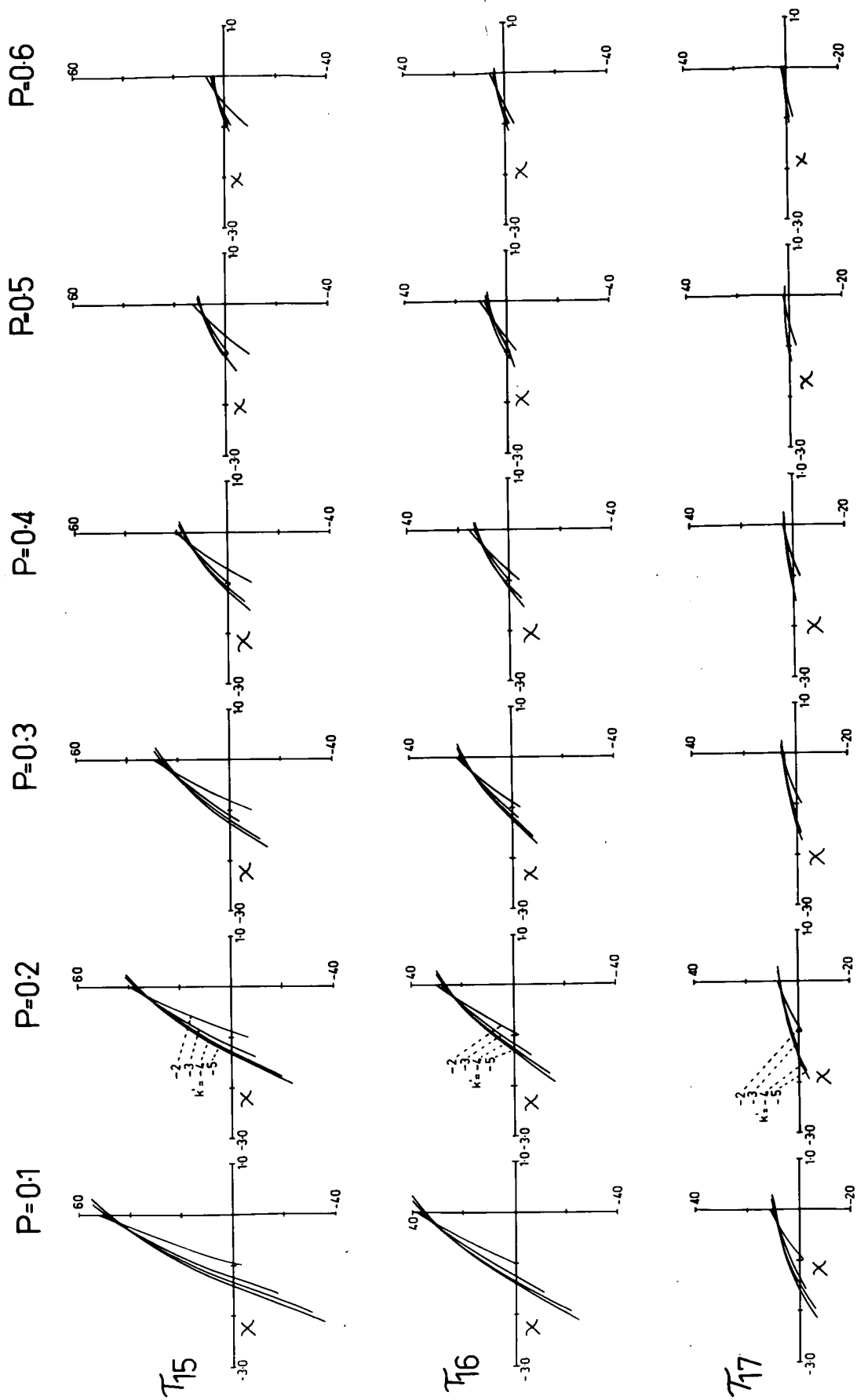


Fig. 2.10

7

P=0.1 P=0.2 P=0.3 P=0.4 P=0.5 P=0.6

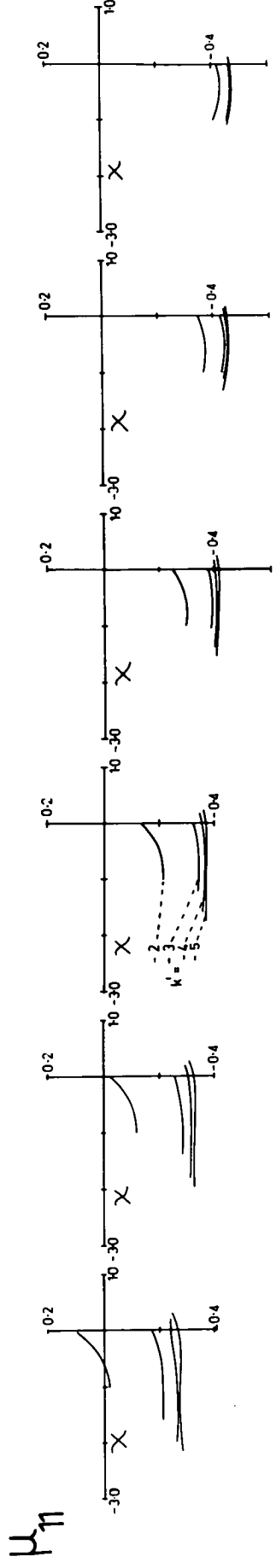
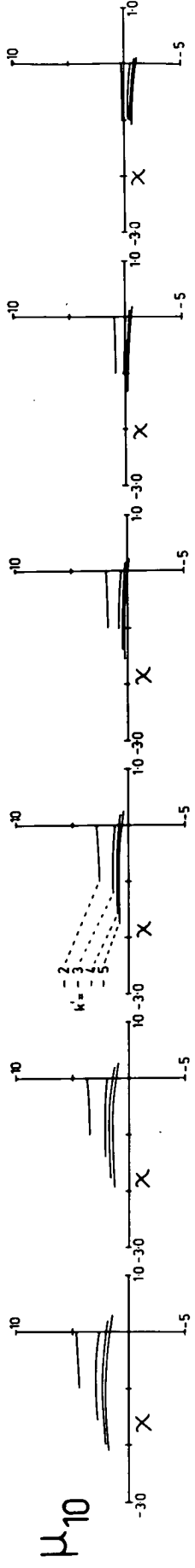


Fig. 2.11

$P=0.1$

$P=0.2$

$P=0.3$

$P=0.4$

$P=0.5$

$P=0.6$

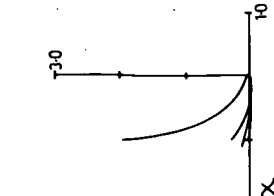
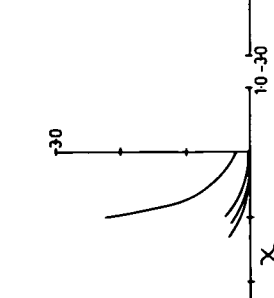
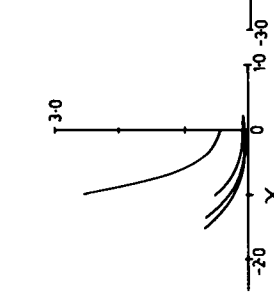
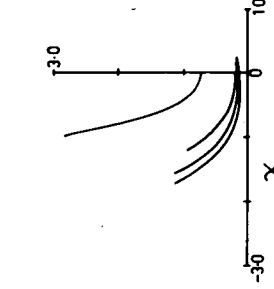
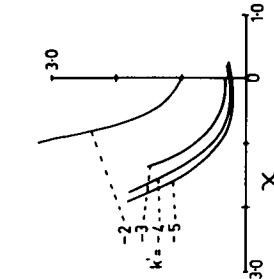
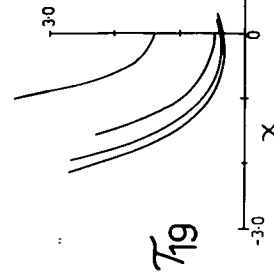
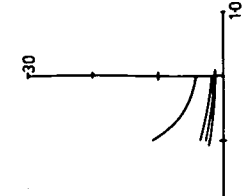
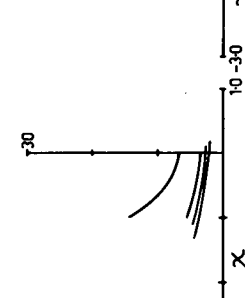
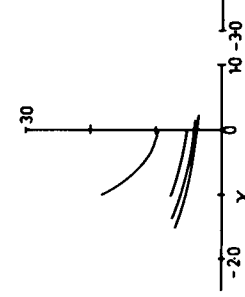
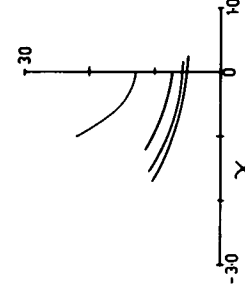
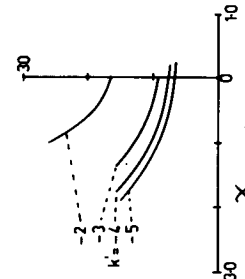
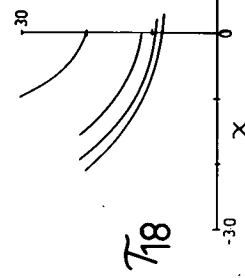


Fig. 2.12

P=0.1

P=0.2

P=0.3

P=0.4

P=0.5

P=0.6

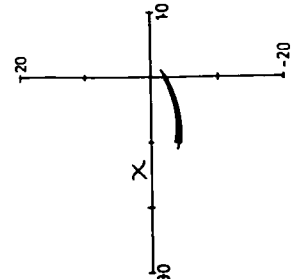
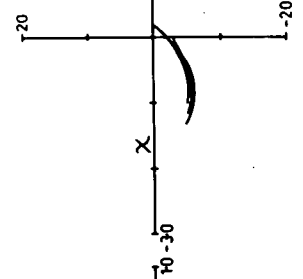
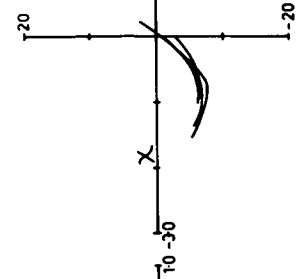
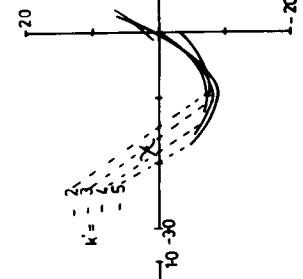
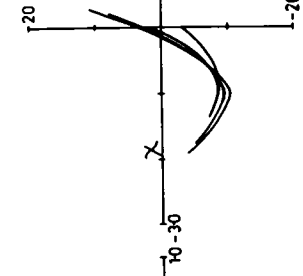
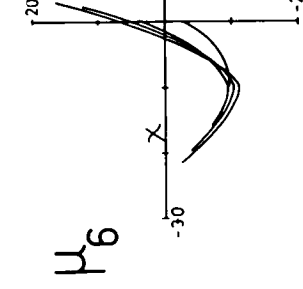
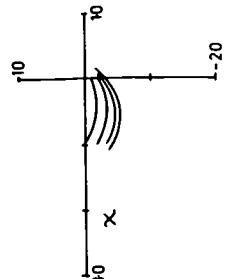
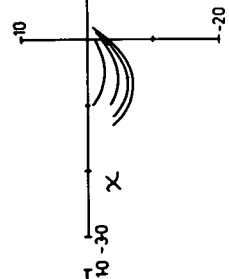
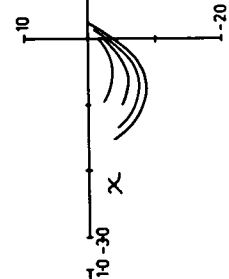
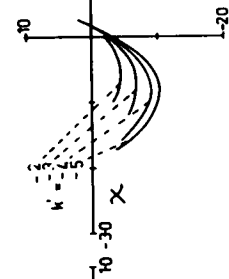
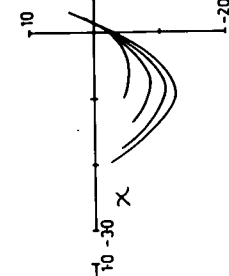
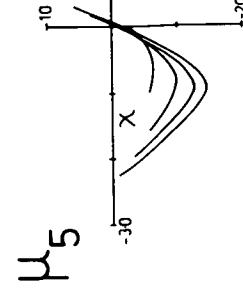
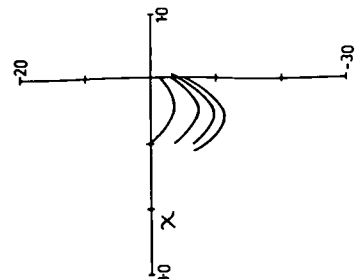
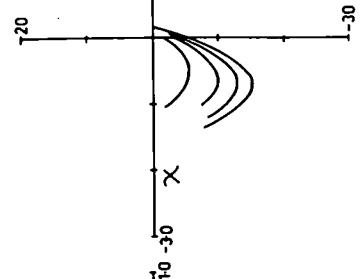
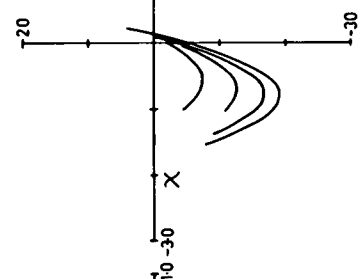
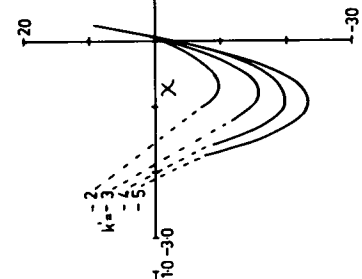
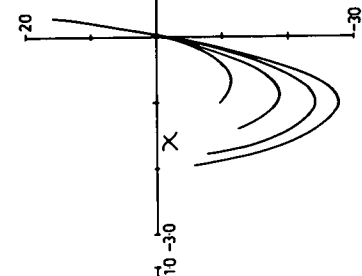
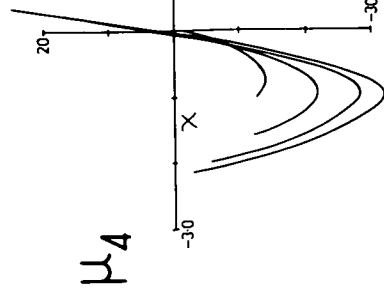


Fig. 2.13

P-01 P-02 P-03 P-04 P-05 P-06

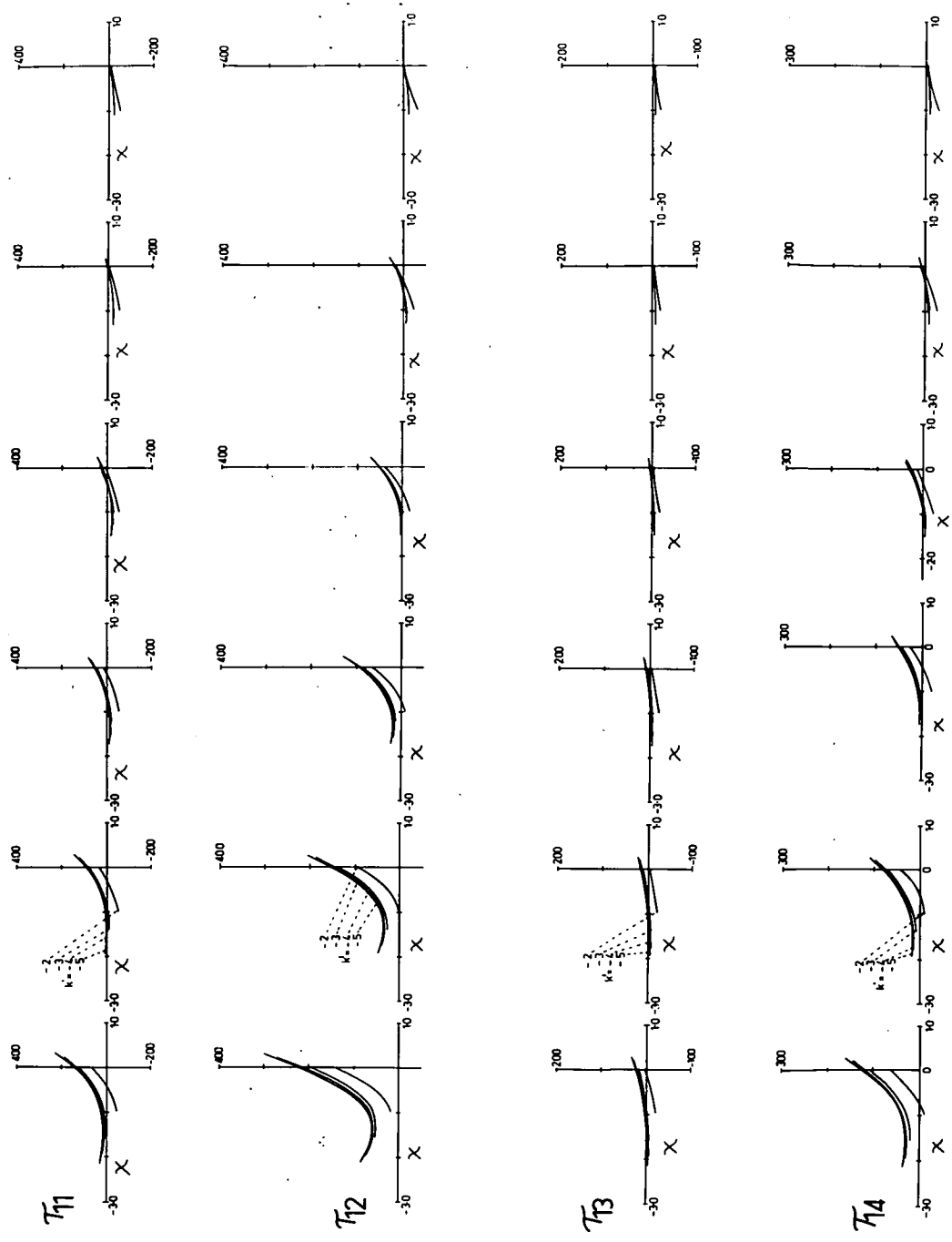


Fig. 2.14

P-06

P-05

P-04

P-03

P-02

P-01

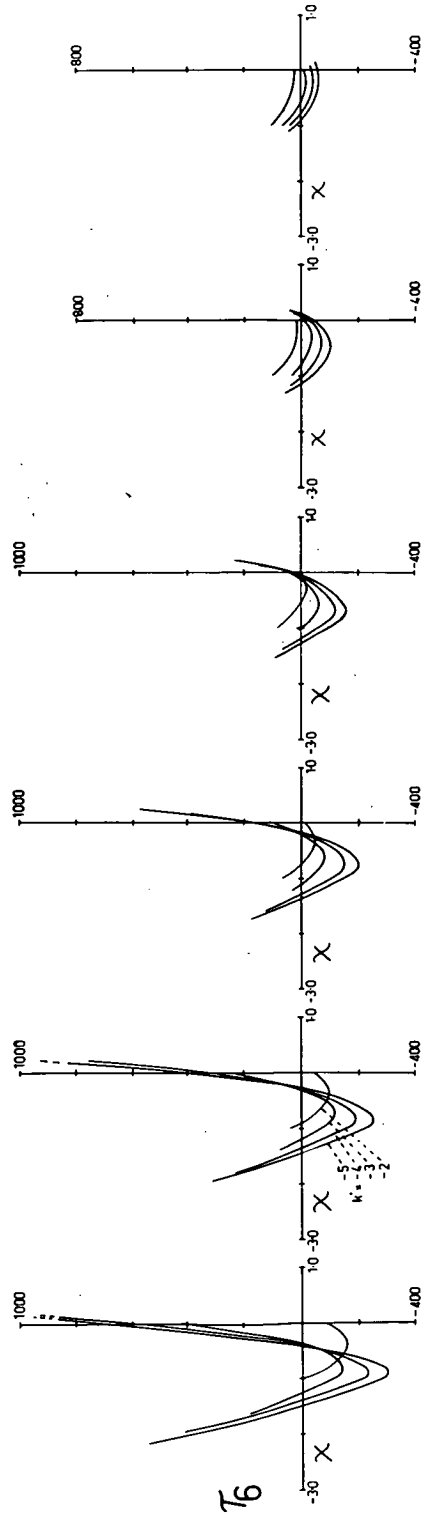
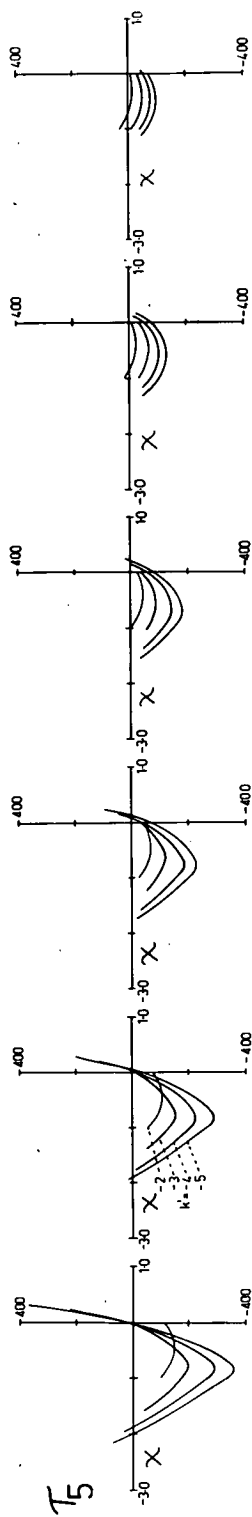
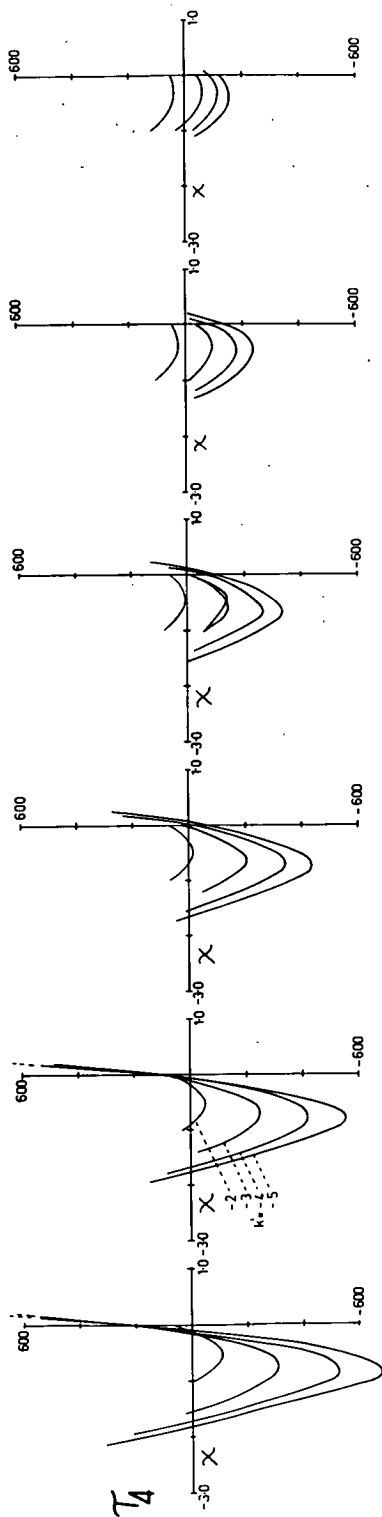


Fig. 2.15

P=0.6

P=0.5

P=0.4

P=0.3

P=0.2

P=0.1

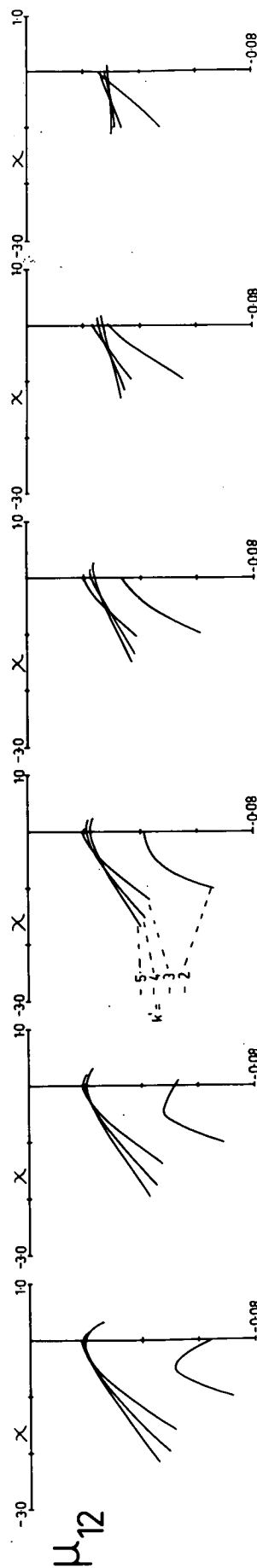


Fig. 2.16

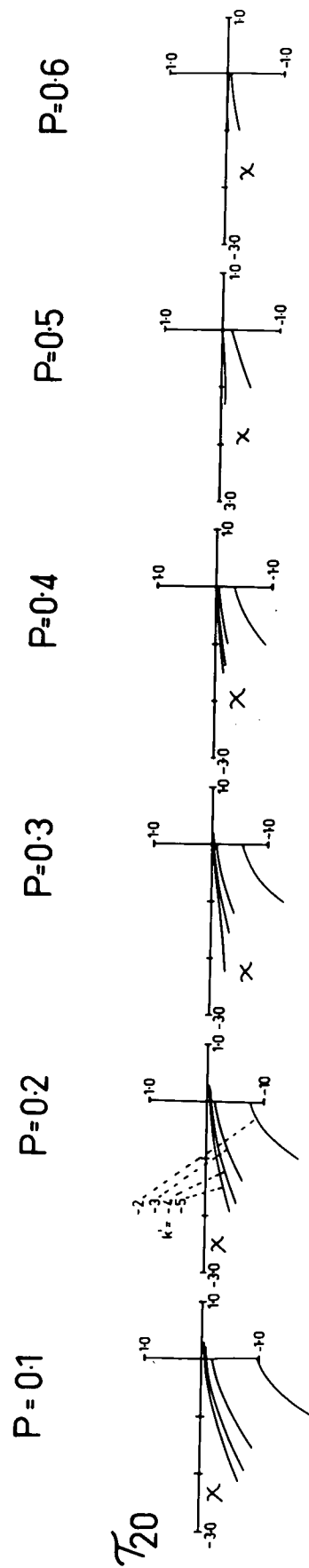


Fig. 2.17

this region; nowhere else it seems can this be improved on in (χ, k', P) -space.

2.2.3.3 Discussion and Comparison of the General Properties of the Aberration Coefficients of the Type 121 Triplet with those of other types of Systems.

R.E. Hopkins^(4.3) observed that the comatic coefficients μ_2, μ_3, μ_7 and μ_8 of the type 111 triplet, which has $N_a = N_c$ and $V_a = V_c$, "become smaller close to $\Delta V = 25$ at large P ." Clearly this also applies to the behaviour of the equivalent type 121 triplet (see Figures 2.6, 2.7) where $k' = -3$ is equivalent to $\Delta V = 24.2$, see section 2.2.1.2.

However, it seems that he has only observed part of the complete picture that we see now with the type 121 triplet. For it is evident from the complete set of comatic coefficients (Figures 2.6 to 2.10) that not only are the 5th order comatic coefficients μ_2, μ_3, μ_7 and μ_8 near zero but, indeed, all the comatic coefficients of both 5th and 7th order converge nearly to zero in the "optimum region". In view of this, and, the agreement shown to exist between some of the spherical coefficients (σ_1, μ_1) and the comatic coefficients $(\mu_2, \mu_3, \mu_7, \mu_8)$ of these systems, we can suspect, therefore, that all the higher order comatic coefficients of the type 111 converge in a

similar way to those of the type 121.

The 5th order estimation of

$$\bar{H}_n = \left[2 \sigma_3 / (\mu_{11} - \mu_{10}) \right]^{\frac{1}{2}} / 0.364$$

(see section 2.2.2.2), used as a measure of the off-axial potential of a triplet, seems interesting when we examine all the astigmatic coefficients of 5th and 7th order of the type 121. We see by inspection of Figures 2.11 to 2.15 that most of the astigmatic coefficients of the type 121, like its comatic coefficients, tend to a minimum that is near zero in the "optimum region". The exceptions are μ_{11} , possibly μ_{10}^* and of course the 3rd order coefficient which is prescribed to be $-\sigma_4/3$ (recall that σ_4 increases with P). So in the "optimum region" the 5th order \bar{H}_n measures the only astigmatic quantities that become numerically larger as the basic parameter P is increased. They are the coefficients of linear 3rd order astigmatism (σ_3) and linear 5th order astigmatism (μ_{10} and μ_{11}). Therefore 5th order \bar{H}_n would appear, in view of this, to be a valid quantity for estimating the potential field of a type 121 system in the preliminary design stage. However, considering the quality of predictions of 5th order coefficients (4.2, 13.5) the 5th order \bar{H}_n may be expected to give reasonable accuracy only if the design is for moderate fields which are smaller

* μ_{10} passes through zero near $P = 0.5$. Beyond $P = 0.5$, μ_{10} becomes increasingly negative like μ_{11} .

than, at most, 20° semifield.

Indeed, Cruickshank^(2.8) has shown that the 5th order prediction of \bar{H}_n limits the accurate estimation of the field of a type 111 triplet to a maximum semi-field angle of about 10° . Actually \bar{H}_n to 7th order is given by the quartic equation

$$(\tau_{18} - \tau_{19})\bar{H}^4 + (\mu_{10} - \mu_{11})\bar{H}^2 - 2\sigma_3 = 0$$

where $\bar{H} = \tan V_k^*$ and $\bar{H}_n = \bar{H}/0.364$.

This equation is reduced to the 5th order expression of \bar{H}_n by neglecting the \bar{H}^4 term.

Cruickshank has shown for the type 111 triplet that when near $V_k = 10^\circ$ the neglect of τ_{18} and τ_{19} causes \bar{H}_n to be overestimated by only 10% but this can increase to between 50 and 100% near $V_k = 20^\circ$; at this angle the \bar{H}^4 term equals the \bar{H}^2 term. Consequently, the 5th order \bar{H}_n must be used with care being evidently applicable only to systems of moderate field.

However, if \bar{H}_n is found to be sufficient for predicting the maximum useful field of a triplet in the "optimum region" then, it seems to imply that σ_3 , μ_{10} and μ_{11} are the only significant astigmatic coefficients in the "optimum region". Therefore, it seems reasonable to assume since R.E. Hopkins finds that \bar{H}_n is satisfactory for predicting the field of his type 111 triplets (with $N_a = N_c, V_a = V_c$), that the astigmatic coefficients of these

* $V_k^* =$ the semi field angle which for convenience

triplets converge with respect to $(K, \Delta V, P)$ in the same way that those of the type 121 (with $N_a = N_c$, $V_a = V_c$) converge with respect to (χ, k', P) .

Although μ_{11} increases while the other astigmatic coefficients decrease, it is clear that some of these other astigmatic coefficients have significant values in the "optimum region". Of course μ_4, μ_5 and μ_6 , the coefficients of cubic astigmatism, and τ_4, τ_5 and τ_6 , the coefficients of quintic astigmatism, have the largest values and therefore seem to rival and, perhaps, even surpass the significance of, say, μ_{11} . However, for example, with apertures near $f/2.5$ and semi-fields of about $V = 45^\circ$ this is not so, because, the relative significance of these coefficients can only be judged by taking other factors into account. These factors are, in particular, the aperture, field and either the focal length or the overall magnification of the system, (i.e. scale of the system).

For example, with the type 121, typical values of μ_{11}, μ_4, μ_5 and μ_6 in the "optimum region" are $\mu_{11} = 0.4$, $\mu_4 = 8$, $\mu_5 = 4$ and $\mu_6 = 5$. For the purpose of demonstrating that $\mu_{11} = 0.4$ is the most significant quantity in this example it is sufficient to compare the maximum contributions that μ_{11} and (μ_5, μ_6) make to the Z-component of the aberration residual ϵ'_z . Taking $\bar{H} = 1$, ($V = 45^\circ$) and $\rho = 0.2$ ($f/2.5$) we have the values shown in Table 2.2.1

TABLE 2.2.1

$$\rho = 0.2, \quad \bar{H} = 1.0, \quad f' = 1.0$$

| Maximum contribution due to | $\Delta \epsilon'_z$ |
|--------------------------------|---|
| $\mu_{11} = -0.4$ | $\mu_{11} \rho \bar{H}^4 = -0.4 \times 0.2 = -0.8$ |
| $\mu_4 = 8, \mu_6 = 5$ | $(\mu_4 + \mu_6) \rho^3 \bar{H}^2 = 13 \times 8 \times 10^{-3} = 0.104$ |

Clearly the μ_{11} coefficient is eight times more significant in this case where $\rho = 0.2, \bar{H} = 1$. (We are not interested in whether a good image will actually be formed at $\bar{H} = 1$ in this example. From this it seems that μ_{11} is the quantity that limits the field of a triplet of moderate focal length at large field angles (45° semi-field).

It is obvious that with a monochromatic type 121 triplet design, nothing much can be done about the magnitude of μ_{11} with the degrees of freedom available because it only varies slowly with either the basic parameters (χ, k', P) or their equivalent the basic parameters ($K, \Delta V, P$) (see Figure 2.11). We also notice that nothing much can be done about the magnitudes of μ_4, μ_5 and μ_6 .

Of course the dominance of μ_{11} (assuming τ_{18} and τ_{19} are small) only applies to short focal length systems of fairly large aperture and field that have great disparity between ρ and \bar{H} as we have shown with $\rho = 0.2$ and $\bar{H} = 1.0$.

Whereas, if we want a system with ρ and \bar{H} nearly equal, say $\rho = 0.1$ ($f/5$) and $\bar{H} = 0.1$ ($V = 5.8^\circ$) then μ_{11} loses its significance (Table 2.2.2).

TABLE 2.2.2

$$\begin{aligned} \bar{H} = \rho = 0.1, \quad f' = 1.0 \\ \text{and} \quad \bar{H} = 0.1, \quad \rho = 0.2, \quad f' = 1.0 \\ \Delta \epsilon_z \end{aligned}$$

| Maximum contribution due to | $\rho = 0.1$ | $\rho = 0.2$ |
|-----------------------------|---|-----------------------|
| $\mu_{11} = -0.4$ | $\mu_{11}\bar{H}^4 = 4 \times 10^{-6}$ | 8×10^{-6} |
| $\mu_4 = 8, \mu_6 = 5$ | $(\mu_4 + \mu_6)\bar{H}^2 = 1.3 \times 10^{-4}$ | 1.04×10^{-3} |

However, this change in significance is of no practical importance until the image is magnified either through auxiliary optics or by increasing the focal length of the system. So if the system has $\bar{H} = \rho = 0.1$ and $f' = 100\text{mm}$ then μ_{11} contributes $\epsilon_z = 4 \times 10^{-4}\text{mm}$ and (μ_4, μ_6) contribute $\epsilon_z' = 1 \times 10^{-2}$. Therefore, the significance of the astigmatic coefficients is reversed with monochromatic triplet systems of moderate aperture and field that have long focal lengths (100mm or more). In this example μ_4 , μ_5 and μ_6 contribute the significant part of the astigmatism. Thus systems limited by μ_4 , μ_5 and μ_6 are for example projection lenses, telephoto lenses and telescope objectives.

Although the dominant astigmatic coefficients of systems with small fields, moderate apertures and either long focal lengths or short focal lengths and auxiliary magnification are μ_4 , μ_5 and μ_6 , nevertheless it seems that

the maximum possible field is predicted by \bar{H}_n and therefore is always determined by σ_3, μ_{11} and μ_{10} . So we have the general rule: σ_3, μ_{11} and μ_{10} predict the limit of the field and μ_4, μ_5 and μ_6 determine the quality of the image at high magnification. We can look upon this as a general rule because this sort of situation appears to have been encountered by Cruickshank and Hills (1960) when they designed a "telephoto system of very long focal length" (1500mm) and with a small ρ and \bar{H} ,

$$(\rho = 0.071 (f/7), \bar{H} = 0.1314 (V = 7.5^\circ)).$$

The pertinent coefficients of their final design stage IV are examined in Table 2.3.

TABLE 2.3

Stage IV Coefficients of Telephoto Design.

$$\mu_4 = -23.03$$

$$\mu_5 = -8.38$$

$$\mu_6 = -15.11$$

$$\mu_{10} = -13.30$$

$$\mu_{11} = -3.64$$

$$\rho = 0.071 \quad \bar{H} = 0.1314$$

| Maximum contribution due to | $\epsilon_z' (f' = 1.0)$ | $\epsilon_z' (f' = 1500\text{mm})$ |
|-----------------------------|---|------------------------------------|
| μ_{11} | $\mu_{11} \bar{H}^4 = -8 \times 10^{-5}$ | -12×10^{-2} |
| μ_5, μ_6 | $(\mu_5 + \mu_6) \rho^3 \bar{H}^2 = 5 \times 10^{-5}$ | 7.5×10^{-3} |

Thus $\bar{H} = \left[2\sigma_3 / (\mu_{11} - \mu_{10}) \right]^{\frac{1}{2}} = 0.148$ and therefore the predicted maximum semi-field angle $V = \arctan \bar{H} = 8.5^\circ$.

In this final stage of the telephoto design the contributions of μ_{11} and of (μ_5, μ_6) are balanced. However, the interesting point here is that the predicted semi-field given by the 5th order \bar{H} is 8.5° which compares fairly well with the value of 7.5° given by the designers. However, when \bar{H} is computed to 7th order the predicted semi-field is $7^\circ 40'$, a remarkable agreement.

When we examine the coefficients of this telephoto of Cruickshank and Hills, in the light of our experience with the limited interpolative study of the type 121, we observe a most interesting result which has apparently gone unnoticed. We find great similarity in the broad behaviour of the convergence of the coefficients of the four final stages quoted by the designers and that of triplets. (We have re-computed the 3rd, 5th and 7th order coefficients of the telephoto in unit focal length for the four design stages, see Table 2.4. In the published results^(2.4), the focal length varies slightly between stages and also only the 3rd and 5th orders are given.)

In particular we note that in going from stage 1 to stage 4 they have reduced μ_4, μ_5 and μ_6 , but they have not been able to alter μ_{10} and μ_{11} appreciably. Also, in going from stage 1 to stage 4 the coefficients of both the linear astigmatism (σ_3) and the Petzval sum (σ_4) increase, whereas, all the other 3rd order and 5th order coefficients decrease.

| Stage 1. | Stage 2. | Stage 3 | Stage 4 |
|-----------|-----------|-----------|-----------|
| -0.20767 | 0.13030 | 0.26212 | 0.086191 |
| -0.019716 | 0.11597 | -0.021919 | 0.055843 |
| 0.013924 | 0.058489 | 0.080015 | 0.10128 |
| -0.040672 | -0.040665 | -0.055664 | -0.010400 |
| 2.1024 | 2.1166 | 1.8192 | 1.7101 |
| -33.163 | -27.180 | -12.444 | -13.153 |
| -27.439 | -21.287 | -16.594 | -12.889 |
| -18.288 | -14.190 | -11.081 | - 8.5970 |
| -53.558 | -46.619 | -19.444 | -18.894 |
| -19.502 | -17.098 | - 7.0100 | - 6.8728 |
| -32.973 | -30.208 | -13.648 | -12.393 |
| -10.020 | - 6.4995 | - 5.0588 | - 4.5813 |
| - 8.0446 | - 6.0664 | - 4.5227 | - 4.2517 |
| - 1.8727 | - 1.0386 | -43.192 | - 0.55896 |
| -12.223 | -10.821 | -13.288 | -12.448 |
| - 4.0766 | - 3.8827 | - 3.7467 | - 3.4047 |
| 10.261 | 10.398 | 8.4776 | 7.3967 |
| -556.76 | -457.78 | -55.994 | -102.68 |
| -682.84 | -576.75 | -256.78 | -194.27 |
| -512.61 | -431.46 | -190.41 | -144.57 |
| -1239.9 | -1097.4 | -448.20 | -388.69 |
| -454.07 | -399.56 | -137.38 | -125.05 |
| -1227.1 | -1121.7 | -493.99 | -410.60 |
| -979.94 | -870.19 | -477.24 | -412.08 |
| -848.44 | -761.59 | -411.72 | -360.50 |
| -362.39 | -323.65 | -171.05 | -151.28 |
| -48.885 | -45.245 | - 23.347 | - 21.394 |
| -596.32 | -526.58 | -268.54 | -263.82 |
| -403.86 | -363.60 | -237.59 | -236.08 |
| -103.59 | -92.944 | - 50.351 | - 50.074 |
| -211.31 | -192.38 | -130.80 | -131.94 |
| -126.47 | -95.062 | - 44.638 | - 47.804 |
| -103.53 | -85.920 | - 44.533 | - 47.311 |
| -12.201 | -8.9326 | 1.2868 | - 1.9156 |
| -119.29 | -107.40 | -124.36 | -113.28 |
| -24.041 | -23.352 | - 21.920 | - 19.371 |
| 61.747 | 62.925 | 51.422 | 43.179 |

Table 2.4

Therefore, since σ_4 increases while most of the other coefficients approach a minimum, the designers are, in effect, optimizing the system by increasing a basic parameter (P), which is like the basic parameter (P) of a triplet. Clearly when we look at their results from this point of view, the pattern of convergence of the coefficients of 3rd and 5th order, quoted by the designers of this telephoto system, is very like the convergence that we have found with the type 121 and type 111 triplets. Thus, if we consider their stages 1 and 4 to be the monochromatic systems occurring at two values of a "basic-parameter" P, then the lines joining the stages in coefficient-space, approximate the contours of the coefficients versus P. This is so because the other basic-parameters are constant, or nearly so in these final stages of the telephoto. We see by inspection of Table 2.4 that the contours so formed will have the same trend as those of the monochromatic type 121, that is, most of the 3rd and 5th order coefficients approach zero as P increases.

The similarity between the convergence of the 5th order coefficients of the telephoto and the triplets, is found to extend also to the telephoto's 7th order coefficients (see Table 2.4). Therefore, even with this telephoto-system, we find that the spherical coefficients of the first three orders tend to a minimum in the "optimum region".

Cruickshank and Hills have used an "extrapolative technique" that is based on the differential coefficients of the Buchdahl-aberration-coefficients formed with respect to the "fundamental-parameters" (curvatures, thicknesses, etc.). However, in spite of it being an extrapolative technique, and, even though we only have the results of four design changes, the simultaneous convergence of most of the aberration coefficients with respect to the "basic parameter" P is evident. Therefore, the property of convergence of the spherical aberration coefficients would appear to offer a very simple way of finding the optimum system.

In view of the evidence presented above, the author believes that a design process based on finding the simultaneous minima of the spherical aberration coefficients, of 3rd, 5th and 7th order, offers the most systematic way of locating the optimum system. (It may well be the only way of doing this systematically.) Indeed, this would appear to offer a new approach from which, it seems, a simple design process for optimizing optical systems automatically could be developed.

CHAPTER 2.3 THE POTENTIAL OF THE MONOCHROMATIC TYPE 121.

2.3.1 The Field of the Type 121 versus (χ , k' , P).

We assume that 5th order \bar{H}_n is sufficiently accurate for estimating the potential of small fields and use it now to examine the potential field of the type 121.

In Figure 2.18.1 the 5th order \bar{H}_n and the corresponding semi-field angle $V = \Theta^\circ$ are plotted against P , k' and ΔV at $L = 0.2$, $T = 0.05$ for $\chi = 0$, -0.5 and -1.0 . The full lines show \bar{H}_n at $\chi = -0.5$, the broken lines \bar{H}_n at $\chi = 0$ and the dotted lines \bar{H}_n at $\chi = -1.0$. This diagram depicts, in two dimensions, the variation of the field of the monochromatic type 121 triplet throughout the region of (χ, k', P) -space or $(\chi, \Delta V, P)$ -space that is expected to produce any real system worthy of consideration. However, Figure 2.18.1 is of interest only because it shows the trend in \bar{H}_n ; values of \bar{H}_n greater than 1 are extremely inaccurate. (2.8)

As P increases the field is augmented whereas when either k' or ΔV increases the field is diminished. Furthermore, since promising systems, in general, occur in the range $\chi = 0$ to -1.0 then it is clear from Figure 2.18.1 that χ can have little effect on the field. For example, at $(k' = -3, P = 0.5)$ in going from $\chi = 0$ to -1.0 the semi-field decreases from 30° to 25.7° , a variation of only 4.3° . This is typical of the effect of χ on the field in the

MONOCHROMATIC TYPE 121

Predicted Field

----- $X = 0$
 ——— $X = -0.5$ at $L = 0.2$
 $X = -1.0$ $T = 0.05$

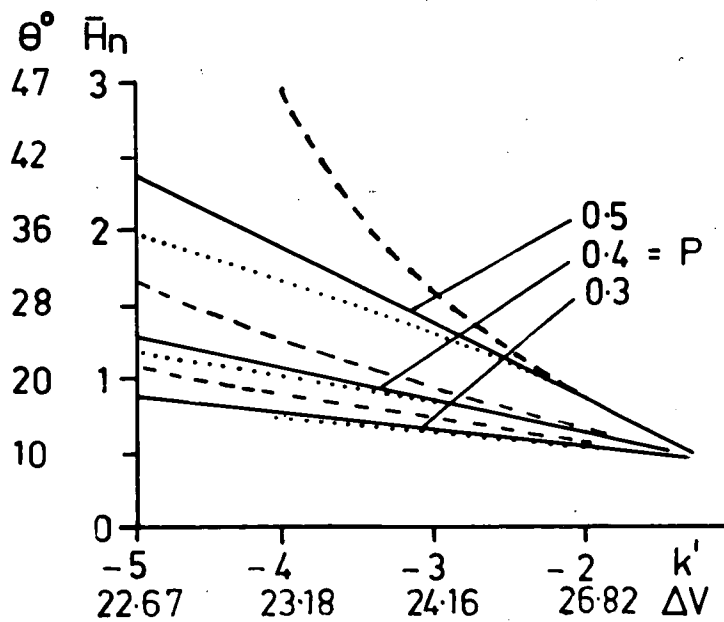


Fig. 2.18.1

optimum region; it is, at most, only of the order of a few degrees.

The greatest value of \bar{H}_n in Figure 2.18.1 is about 3.0; it occurs near $k' = -4$, $P = 0.5$ and $\mathcal{X} = 0$. Just beyond this point \bar{H}_n has imaginary values only and therefore the semi-field of the type 121 cannot exceed 47° . Fields of this magnitude occur at some distance from the optimum region and so the aberrations must necessarily be very large and therefore such large fields cannot be considered feasible.

It is evident that the field is not critically dependent on any of the "monochromatic parameters" (\mathcal{X} , k' , P) and so we ^{may} choose systems anywhere in a small region centred on $k' = -3$, $P = 0.5$, $\mathcal{X} = -0.5$ without causing more than a few degrees variation. Thus there is sufficient freedom for optimizing the other aberrations in the optimum region.

In Figure 2.18.2 the "7th order \bar{H}_n " (see section 2.2.3.3) is plotted versus (\mathcal{X} , k' , P). This shows that 5th order \bar{H}_n overestimates the semi-field, for example, at $k' = -3$, $P = 0.5$ and $\mathcal{X} = -0.5$ by 50%: the range of values given by 7th order \bar{H}_n for V is more likely those obtained for practical triplet systems. Also, it is evident that in the "optimum region" the semi-field angle is still not critically dependent on the basic parameters (\mathcal{X} , k' , P) when we include the 7th order terms.

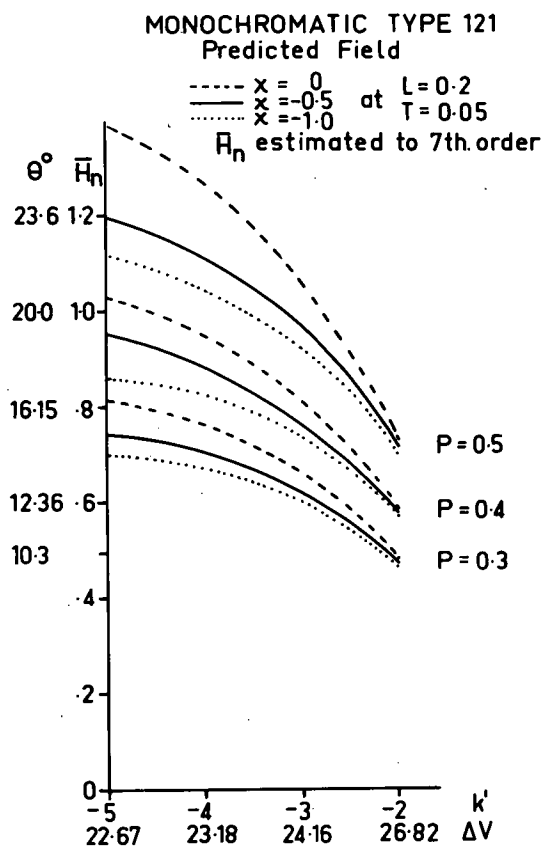


Fig. 2.18.2

2.3.2 The Five Types of Aberration Plotted in Three Principal Sections of (\mathcal{X} , k' , P)-Space.

Now let us compare the five types of aberrations and the field as \mathcal{X} , k' and P converge on the optimum region. In Figures 2.19, 2.20 and 2.21 several performance parameters of the monochromatic type 121 are plotted in the three principal sections of (\mathcal{X} , k' , P)-space which intersect the optimum region at the point with $\mathcal{X} = -0.5$, $k' = -3$ and $P = 0.5$, $L = 0.2$ and $T = 0.05$.

In these diagrams the behaviour of the aberrations to 7th order, the ^{tangent of the} maximum semi-field ^{angle} \bar{H}_n^* to 5th order and the symmetry of the separations ($R_8 = d_3 - d_6$) are compared. All these performance parameters have been reduced to the same order of magnitude, for the sake of clarity, by either multiplying or dividing by powers of ten as necessary. Also, in the interest of clarity, the scale of some quantities is varied from one diagram to another, for example the scales of R_8 in Figure 2.19 and 2.20 differ by a power of ten.

The limited interpolative study has shown that the coefficients of each type of aberration have a common behaviour. Consequently at this stage it is sufficient to plot one coefficient of each type in order to assess the potential of the type 121 triplet. Thus we have

and 1/2.

* 7th order \bar{H}_n will be 30% less than 5th order \bar{H}_n .

(μ_2, τ_2) for coma and (μ_4, τ_4) for astigmatism.

The scale factors of the performance parameters are as follows:

| | Fig. 2.19 | Fig. 2.20 | Fig. 2.21 |
|--------------------------|-----------|-----------|-----------|
| τ_4 | 10^{-1} | 10^{-1} | 10^{-1} |
| σ_1 | 1 | 1 | 1 |
| μ_1 | 10^{+1} | 10^{+1} | 10^{+1} |
| τ_1 | 10^{+3} | 10^{+3} | 10^{+3} |
| ϵ'_{Sph} | 10^{-1} | 10^{-2} | 10^{-2} |
| R_8 | 10^{-1} | 10^{-2} | 10^{-1} |
| μ_2 | 10^{+1} | 10^{+1} | 10^{+1} |
| τ_2 | 10^{+3} | 10^{+3} | 10^{+3} |
| μ_4 | 10 | 10 | 10 |
| τ_4 | 10^{+2} | 10^{+2} | 10^{+2} |
| μ_{12} | 1 | 1 | 1 |

The actual value of the performance parameter = graphical value x scale factor.

The Figure 2.19 shows that the following quantities,

1. the spherical aberration $\epsilon'_{\text{Sph}} = \sigma_1 \rho^3 + \mu_1 \rho^5 + \tau_1 \rho^7$,
($\rho = 0.2$),

2. the spherical coefficients σ_1, μ_1, τ_1 ,

3. the comatic coefficients μ_2, τ_2 ,

4. the parameter $R_8 = (d_3 - d_6)$ which is a measure of symmetry,

passes through zero in a small range of k ($-3 < k < -2.7$)

at ($\mathcal{X} = -0.5, P = 0.5, L = 0.02, T = 0.05$).

MONOCHROMATIC TYPE 121
Performance versus k' or ΔV
Parameters
at $\chi = -0.5, P = 0.5, L = 0.2, T = 0.05$

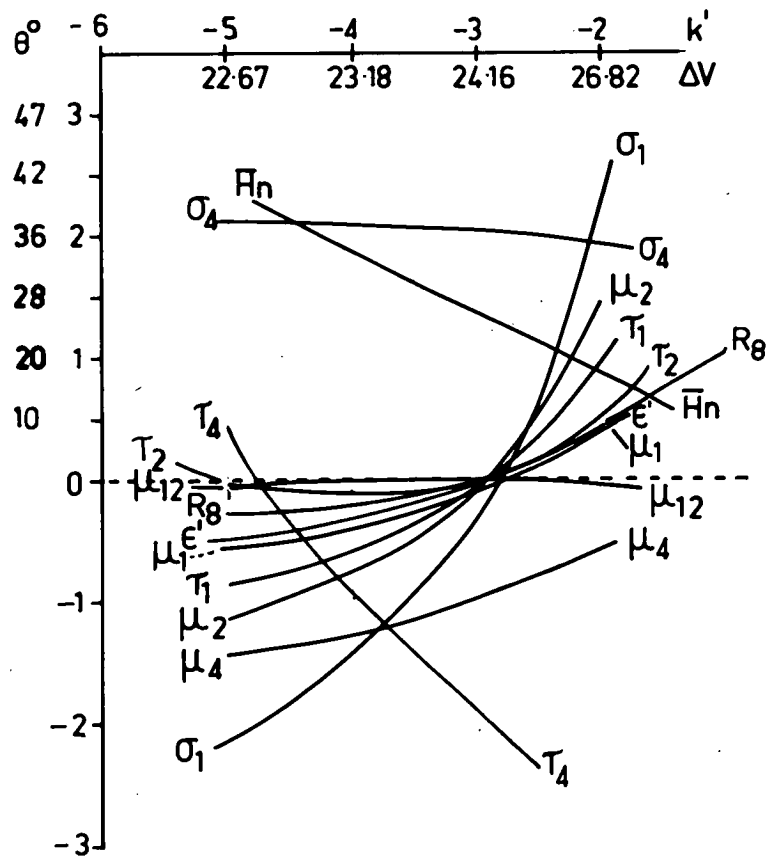


Fig. 2.19

MONOCHROMATIC TYPE 121
Performance versus P
Parameters
at $X=-0.5, k=-3.0, L=0.2, T=0.05$

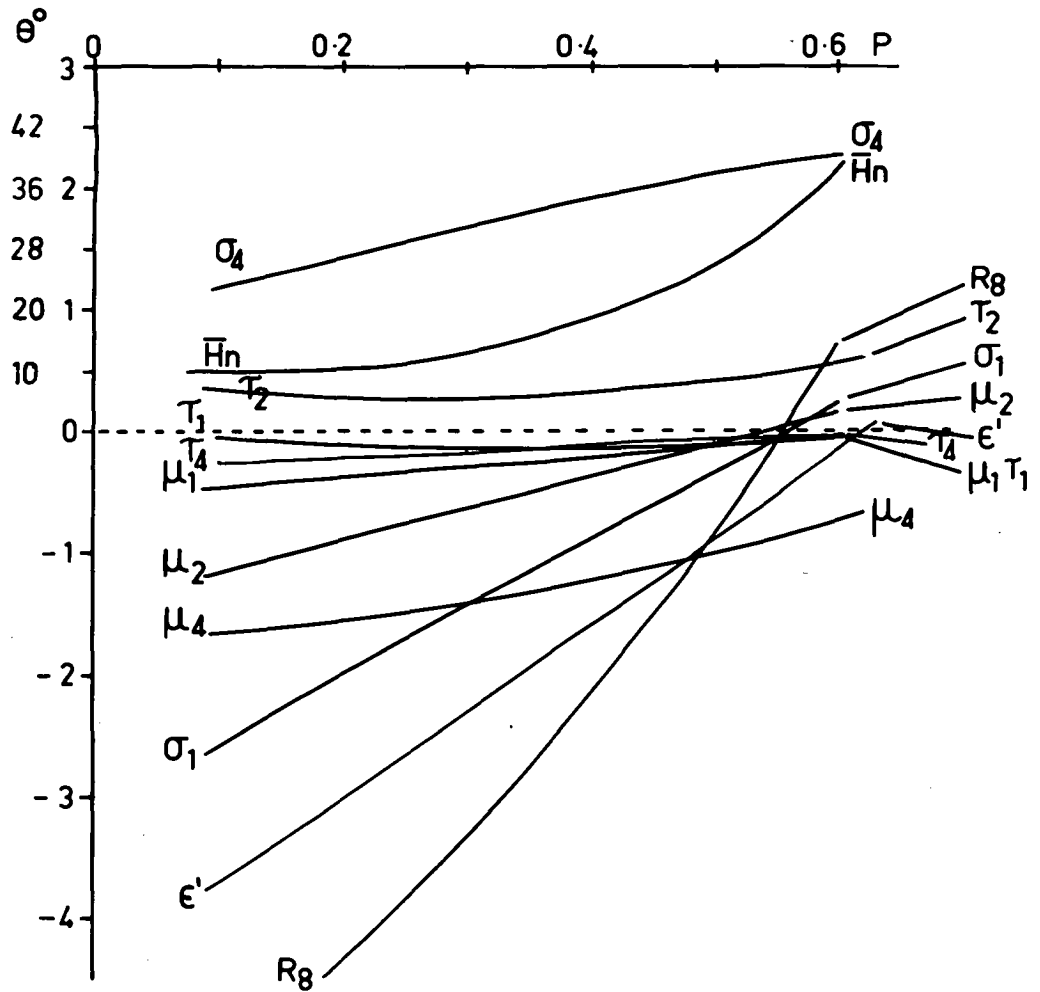


Fig. 2.20

MONOCHROMATIC TYPE 121
Performance versus X
Parameters
at $k=-3.0, P=0.5, L=0.2, T=0.05$

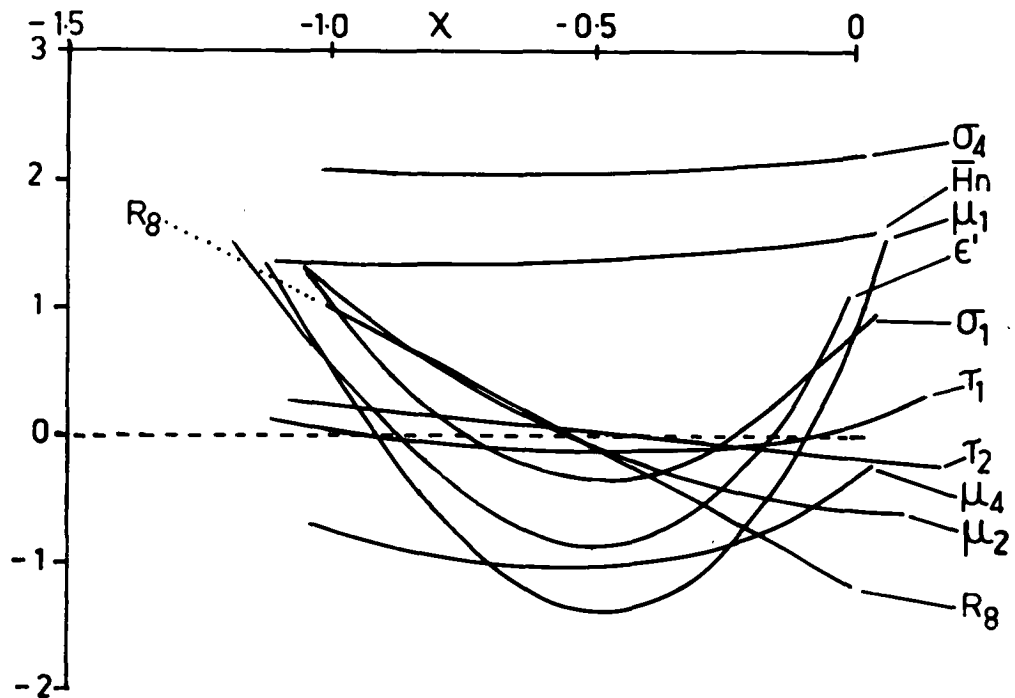


Fig. 2.21

In this region residuals of zonal spherical and coma of the 3rd, 5th and 7th orders are very small and therefore the type 121 made in this region can be expected to be well corrected for the zonal spherical and coma up to an aperture of $f/3.5$ at least.

2.3.3 The Type 121 Versus Type 111.

The best solution lies near $k' -2.7$. At this point we will expect its semi-field to be less than about^{*} 20° , its Petzval coefficient to be about 0.2 and its air-spaces to be symmetrical. If a larger field is required it can only be achieved by decreasing k' or ΔV (Figure 2.19), or by increasing P (Figure 2.20) but unfortunately both changes increase the Petzval sum. Since P has the most serious effect on the Petzval sum then decreasing k' appears to be the most attractive way of improving the field but this improvement can only be achieved by introducing large negative contributions from the spherical coefficients; σ_1 is the worst offender. This means that larger fields are only possible at very small apertures. For example, a semi-field of 20° (using 7th order \bar{H}_n) is associated with $\sigma_1 = -0.8$ (see Figure 2.19), and if we set the zonal tolerance LA'_{\max} at $\pm 0.005^{**}$ and as $LA' = \sigma_1 \rho^2$ then the system with a 20° semi-field can only be used at apertures

* Figure 2.19 gives 5th order values $V = \theta^\circ \begin{matrix} 24^\circ \\ 18^\circ \end{matrix}$
 Figure 2.18.2 gives 7th order value $V = \theta^\circ \begin{matrix} 24^\circ \\ 18^\circ \end{matrix}$.

** 0.005 for $f' = 1$ if $f' = 100\text{mm}$ then tolerance is $\pm 0.5\text{mm}$.

of less than $f/6$. This aperture at semi-fields of about 20° has been predicted for the type 111. Therefore it is not worthwhile to aim for a large field with the type 121 when the equivalent performance can be achieved with the simpler system.

2.3.4 The Uniqueness of Type 121.

The uniqueness of the type 121 is demonstrated by Figure 2.19. All the curves of this figure are continuous functions of the basic parameters k' or ΔV and therefore we are able to attain any point on them. On the other hand the equivalent graphs of the type 111 are discontinuous functions of ΔV and therefore consist of sets of points determined by the real glasses.

Figure 2.19 shows that the minimum of the spherical and the coma is very sharply defined, consequently it is very unlikely that this optimum region can be achieved with real glasses. It seems far more probable that the simple triplets of real glasses will take values of ΔV only somewhere near the "optimum region" at most. Thus the simple type 111 triplet systems may have slightly larger fields than the type 121 but their apertures will be limited by the primary spherical aberration (since σ_1 is the most sensitive to ΔV of σ_1, μ_1, τ_1).

Clearly if we accept the results of Figures 2.18 to 2.21 then there is no region of (χ, k', P) -space outside the "optimum region" that exhibits a real improvement

of the field of the type 121 over that of the type 111 triplet without a great loss of image quality. Thus if we seek a wide field at small apertures with a triplet system, then we will not look beyond the simple construction of the type 111. On the other hand it is now clear that if we want a high state of correction of zonal spherical and coma at a large aperture in conjunction with a moderate field then we will seek solutions in the optimum region of the type 121.

Figures 2.19, 2.20 and 2.21 confirm the uniqueness of the optimum region that was inferred from the interpolative study of the coefficients. Moreover, Figures 2.18.1, 2.18.2 and 2.19 also demonstrate the uniqueness of the type 121 in that the curves of these diagrams are continuous functions of the basic glass parameter ΔV .

The rest of this thesis is devoted mainly to developing the best type 121 from the optimum region with the emphasis on controlling the zonal spherical aberration between $f/3.5$ and $f/2.5$.

2.3.5 Discussion of Design Principles Emerging from Section 2.

The interpolative method of optical design that has been developed in this section has given us a clearer and simpler model of the design process. From this has arisen the concept of the 3rd, 5th and 7th order aberrat-

ions of the type 121, converging, with a few exceptions, towards zero points that are contained in a small "optimum region". This concept of simultaneous convergence also accounts for many results obtained by other workers for at least simple triplets and also it seems it may even apply to more complex systems such as the telephoto objective of Cruickshank and Hills. Thus we feel that the design principles established between the "performance parameters" and the basic parameters" of the type 121 triplet embody general design principles and, therefore, can assist us to understand other optical systems. We note that R.E. Hopkins^(4.3) says, "this simple triplet objective actually helps us to understand more complicated objectives."

As a result of the work of this section we postulate that this optimum region is uniquely and simply located by the minima of the first three orders of spherical aberration coefficients. Thus for a given type of system constructed from a given set of glasses it appears that most of the coefficients are minimized once the spherical coefficients are minimized. After this it seems that all that one can do is to make minor adjustments at the expense of the axial image.

With the type 121 we have the simplest arrangement for getting continuous variation of the monochromatic parameters. Moreover, with this arrangement we should be able to create a type 121 triplet of wider aperture than.

the less flexible type 111 triplet and its derivatives (triplets with a single lens for group b).

We are holding the "basic chromatic parameters" constant at this stage. However, we feel justified in ignoring their effects on the monochromatic system because other workers have found with simple triplets that they do not affect the monochromatic design significantly. But, of course, their observations mainly apply to apertures of $f/3.5$ or less and therefore our assumption may have to be modified later.

CHAPTER 2.4 OPTIMIZING THE COEFFICIENTS OF THE MONO- CHROMATIC TYPE 121.

2.4.0 Introduction.

In this chapter the techniques for locating the optimum monochromatic system precisely are developed and applied. Following this we discover how to control the zonal aberration of the monochromatic system at larger apertures, between $f/3.5$ and $f/2.5$.

The interpolative study of the type 121 has established the general properties of the system with respect to the basic parameters (\mathcal{X} , k' , P). As a result of this work we are confident that there is one optimum monochromatic system of large aperture. So now we are concerned with finding a way of locating this system which we expect to be the system with minimum zonal spherical and coma for at least an aperture of $f/3.5$ and possibly for an aperture of $f/2.5$. Since the coefficients of the type 121 converge in a very regular way we can seek the ideal system by studying the behaviour of particular types of solution (e.g. right hand, left hand etc.).

In the preceding work we have studied the 3rd order triplet that has $R_2 = R_3 = R_5 = 0$, $L = 0.2$ and $T = 0.05$ but from now on we will apply more restrictions to the correction state at each stage as we progress towards the final system. The first of these which we intro-

duce in the next sub-section will control the Petzval curvature of the thick system.

2.4.1 Equivalence of P and R_4 .

We have three monochromatic degrees of freedom, the basic parameters χ , k' , P which can be used to control any three residuals of the thick system. Already χ has been used to control the marginal spherical residual (R_1) to 7th order when finding the R and L solutions versus χ , k' , P but now let us, in addition to this, control the Petzval coefficient (σ_4) with the basic parameter P. Thus we will be generating type 121 systems with $R_1 = R_2 = R_3 = R_5 = 0$ and $\sigma_4 = R_4$ which, in other words, means we have monochromatic 3rd order triplets with prescribed Petzval sum and with their marginal spherical zero to 7th order.

By specifying systems with $\sigma_4 = R_4$ we are in effect constructing a map of the performance parameters versus χ , k' , R_4 . The question arises, therefore, as to whether or not this map will differ greatly from the (χ, k', P) -map, that is, will the coefficients still converge in the same simple way in this new grid of (χ, k', R_4) as they do in the (χ, k', P) -grid.

This is soon answered without recourse to extensive mapping of (χ, k', R_4) -space. Simply by inspection of Figure 2.4 it is clear that the variation

of σ_4 is very small over a large range of χ , k' , P and consequently the map of the performance parameters versus χ , k' , R_4 will be essentially the same as the map of χ , k' , P . Indeed, the only significant change will be a small change in the form of the curves; they will be slightly flatter in the (χ, k', R_4) -grid. (This can be seen by inspection of the (χ, k', P) -maps.)

Thus the general behaviour of the coefficients with respect to R_4 is inferred from the interpolative study of (χ, k', P) . Nevertheless although it is fairly obvious, this behaviour, however, has been confirmed by plotting some of the coefficients versus (χ, k', R_4) but it is not considered necessary to reproduce the graphs here.

To sum up: at this stage we are seeking the system that has:

1. Zero marginal spherical to 7th order

$$\epsilon'_{\text{Sph}} = R_1 = 0 + (09) \text{ at } \rho = 0.2$$

2. 3rd order coma zero, $\sigma_2 = R_2 = 0$.
3. 3rd order distortion zero, $\sigma_5 = R_5 = 0$.
4. A flat-tangential-field, $3\sigma_3 + \sigma_4 = 0$.
5. Minimum zonal aberration, i.e., an optimum set of spherical coefficients of 3rd, 5th and 7th order.
6. Specified Petzval, $\sigma_4 = R_4$.

We propose locating this optimum system by mapping the spherical coefficients of the right and left hand solutions in (k', R_4) -space.

2.4.2 The Programme for Computing Solutions with Prescribed Petzval.

The programme for computing the R and L solutions with prescribed Petzval is derived from the earlier programme that finds R and L solutions with prescribed P, the programme RL/BP/S121, (Chapter 1.4). In this new version of the RL-solution-programme the sub-routine T121 is iterated with respect to the basic parameter P until the target value of $\sigma_4 = R_4$ is reached. This step is performed by a new sub-routine TP121 (see Figure 2.22) that is called in place of the sub-routine T121 in the main executive control routine of the programme. This new programme is denoted by the code-number RL/BP/SP121.

2.4.3 The Range of R_4 .

If we plot R_4 against P for the R and L solutions and extrapolate the graphs we arrive at the upper and lower limits of the Petzval residual R_4 . In Figures 2.23.1 to 2.23.4 the range of the upper and lower limits of R_4 is examined as k' changes.

From the theory of the basic triplet it is clear that an initial arrangement cannot be found when $P < 0$. For example, at $k' = -5$ (Figure 2.23.1) P of the R-solution is zero at $R_4 = 0.16$ and therefore no R-solutions will be found by the RL-programme below this value of R_4 . This has been confirmed by the results shown in Figure 2.25.1.

SUB ROUTINE TP 121

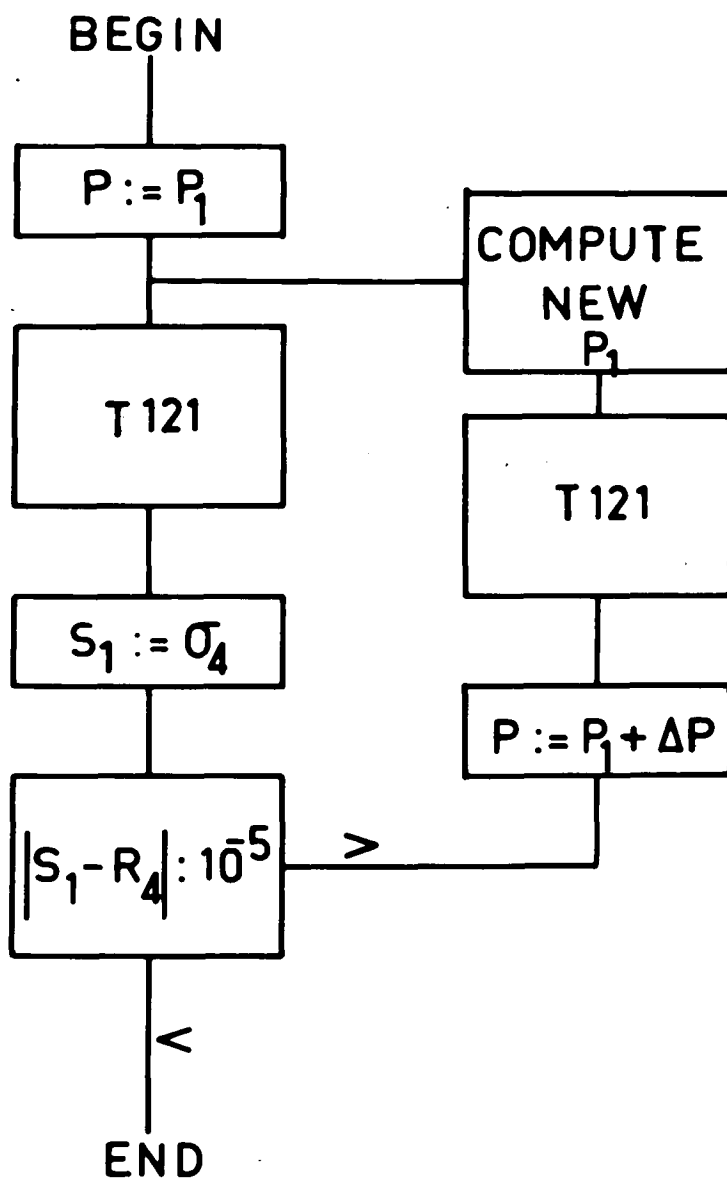


Fig. 2.22

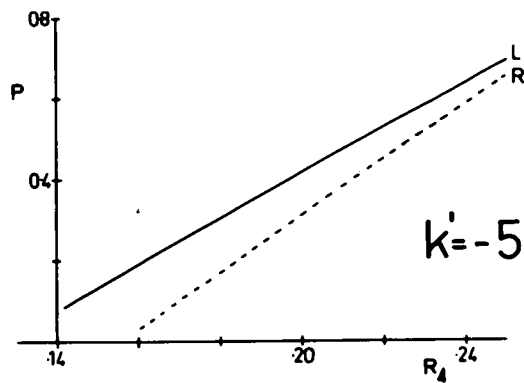


Fig. 2.23.1

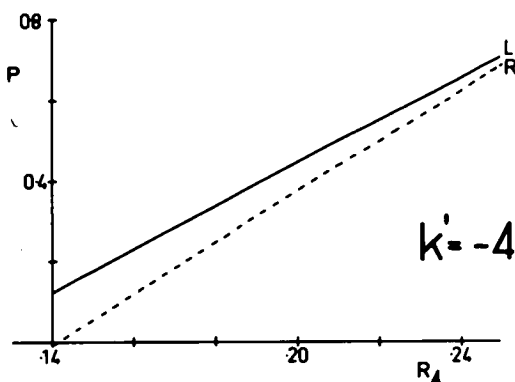


Fig. 2.23.2

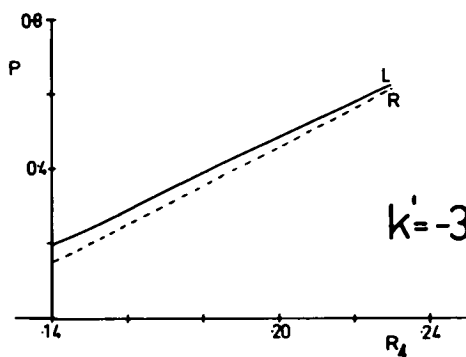


Fig. 2.23.3

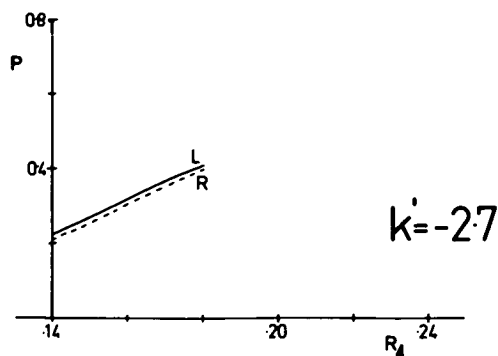


Fig. 2.23.4

It is clear that the lower limit of P must be known if we are to avoid costly programme failure when making a large survey of an unfamiliar system. Therefore it is advantageous to estimate the lower limit of P by linear extrapolation of a simple exploratory survey, before proceeding with a more comprehensive one.

2.4.4 The Spherical Coefficients of the R and L Solutions versus (k', R_4) .

In order to exhaust the potential of the monochromatic type 121 it has been found sufficient to compute solutions at $k' = -5, -4, -3, -2.7$ for $R_4 = 0.14$ to 0.22 in steps of $dR_4 = 0.01$. The results of this work are shown in Figure 2.24.

It is evident that the spherical coefficients σ_1 and τ_1 of the R and L solutions of the monochromatic type 121 approach zero in the region bounded by $-3 < k < -2.7$ and $0.2 < R_4 < 0.24$ at $L = 0.2, T = 0.05$. Here, however, μ_1 tends to a finite negative value as R_4 increases from 0.2 to 0.24 and so there is no possibility of making μ_1 zero although this can be done with σ_1 and τ_1 . But there is the possibility of balancing some of the negative residual due to μ_1 with some small positive residuals due to σ_1 and τ_1 . This means, of course, that the "optimum region" may give systems that not only have zero marginal spherical but ones that also have the spherical coefficients

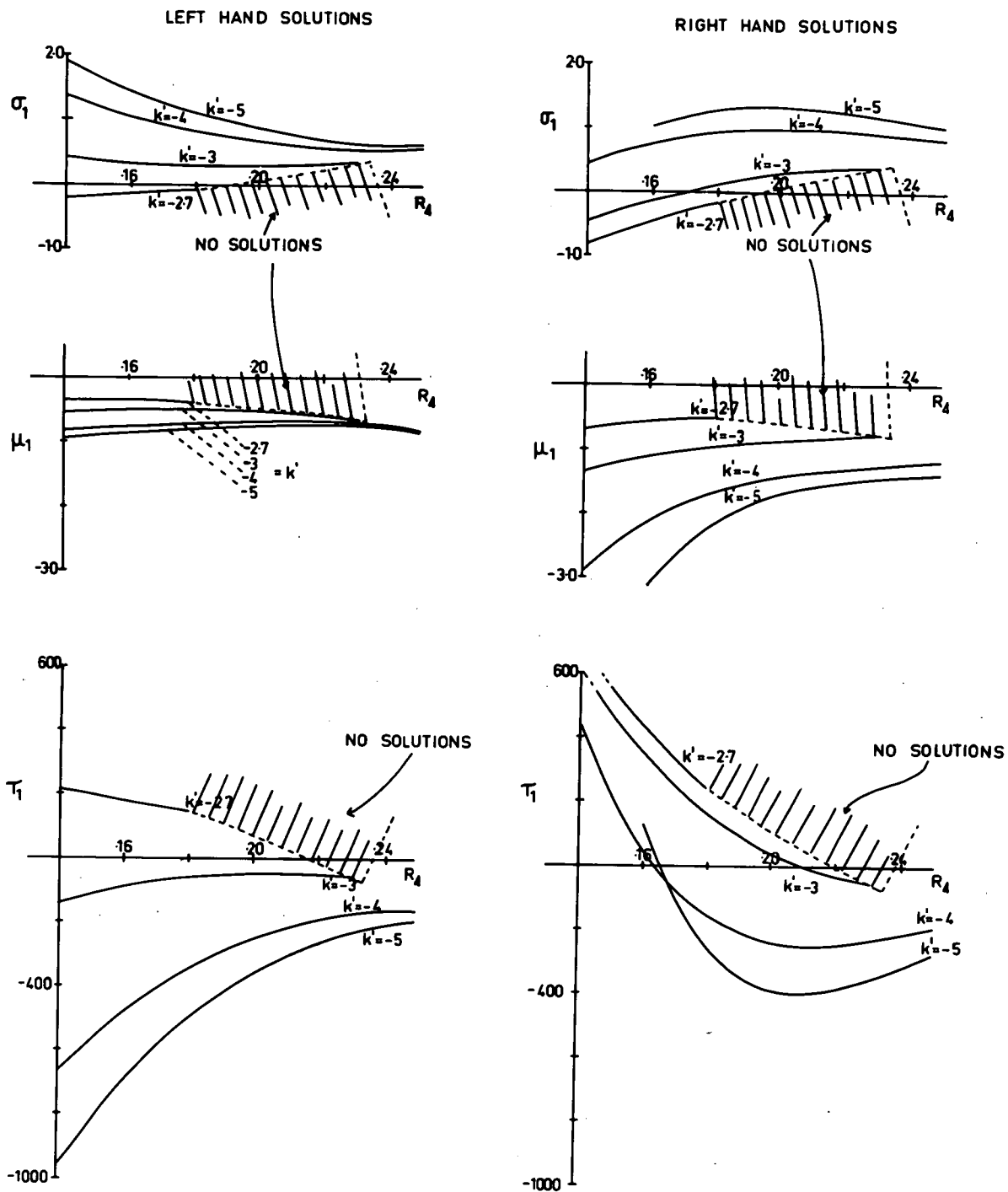


Fig. 2.24

of the first three orders alternating in sign as well.

A system having these properties can be shown to have two zones with zero spherical aberration, the marginal and the 0.707 zone.

2.4.5 Zonal Spherical Aberration and the Sign Pattern of the Coefficients.

The spherical aberration to 7th order of the zone of radius ρ is,

$$\epsilon'_{\text{Sph}} = \sigma_1 \rho^3 + \mu_1 \rho^5 + \tau_1 \rho^7$$

where $0 \leq \rho \leq \rho_{\text{max}}$

Now if the marginal zone is corrected then the roots or turning points of the zonal spherical equation (ϵ'_{Sph}), besides the root at ρ_{max} , are found by solving the three well known equations^(17.1, 18, 19).

Thus if we set:

$$(1) \epsilon'_{\text{Sph}} = 0, (2) d(\epsilon'_{\text{Sph}})/d\rho = 0 \quad (3) \quad d^2(\epsilon'_{\text{Sph}})/d\rho^2 = 0$$

then these equations have the following roots

$$(1) \rho^2 = 0, \rho = \sqrt{\frac{-\mu_1 \pm \sqrt{\mu_1^2 - 4\sigma_1\tau_1}}{2\tau_1}}$$

$$(2) \rho = 0, \rho = \sqrt{\frac{-\mu_1 \pm \sqrt{\mu_1^2 - 3\sigma_1\tau_1}}{3\tau_1}}$$

$$(3) \rho = \sqrt{\frac{-3\mu_1 \pm \sqrt{9\mu_1^2 - 15\sigma_1\tau_1}}{15\tau_1}}$$

The shape of the ϵ'_{Sph} curve depends on the order of the signs of the coefficients σ_1, μ_1, τ_1 , consequently there are two possible forms when $\epsilon'_{\text{Sph}} = 0$ at $\rho = \rho_{\text{max}}$.

They are:

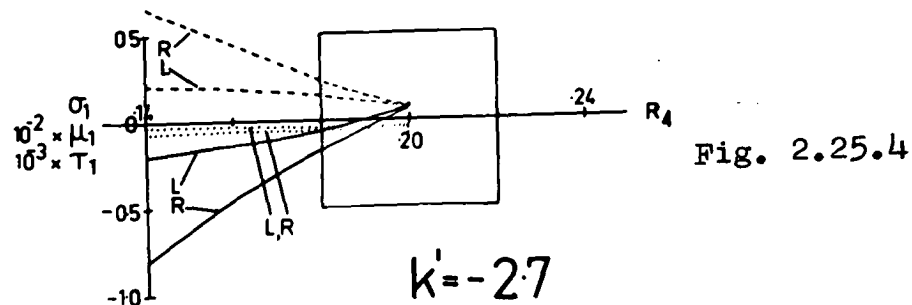
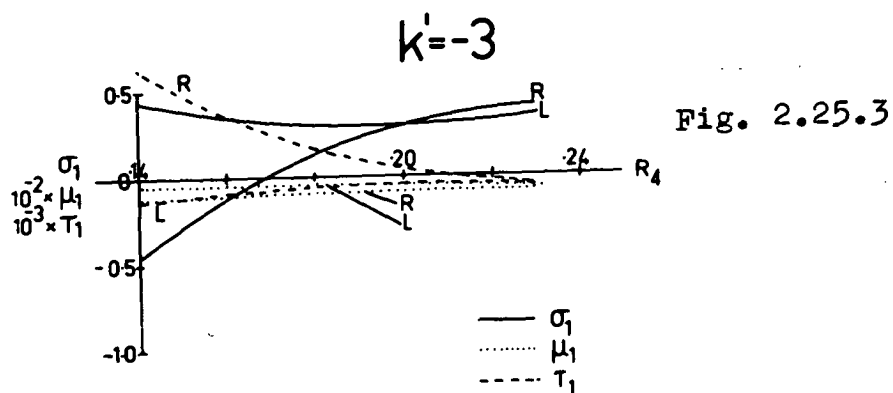
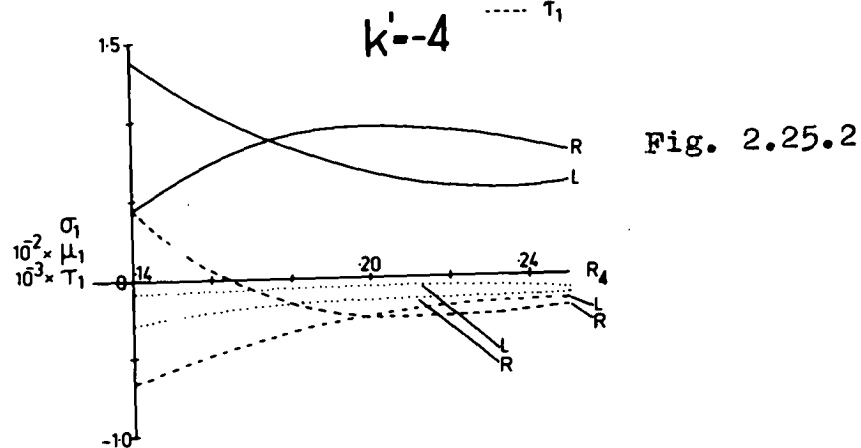
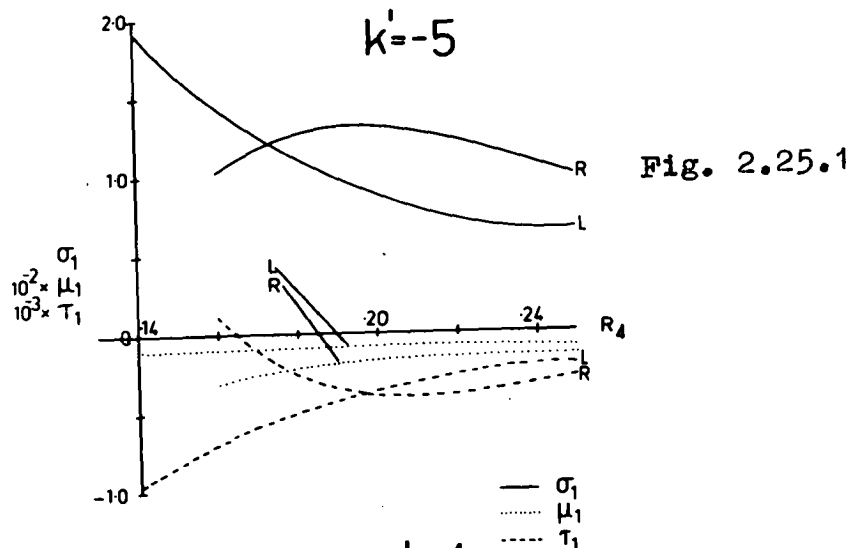
- (1) There is a maximum or a minimum at the $0.707 \times \rho_{\max}$ zone if two successive coefficients are alike.
- (2) There is a root at the $0.707 \times \rho_{\max}$ zone if the successive coefficients alternate in sign.

2.4.6 Coincident R and L Solutions and Tangential Solutions.

A better understanding of the way the spherical coefficients of the type 121 converge ^{is achieved} by plotting σ_1, μ_1 and τ_1 of both the R and L solutions on the same scale versus R_4 , see Figure 2.25.1 to 2.25.4. A different set of axes is used for each k' .

The set of diagrams emphasizes how the magnitudes of σ_1 and τ_1 of the R and L solutions change at a much greater rate than the corresponding values of μ_1 . Indeed, μ_1 remains almost constant while σ_1 changes from large positive to large negative values and while τ_1 changes in the opposite manner to σ_1 . Clearly the relative magnitudes of the spherical coefficients change most rapidly near the optimum region of (k', P) that is around $k' = -3$, $R_4 = 0.20$.

Now consider the behaviour of the intersection points of each pair of R-L curves of each coefficient. As k' increases from $k' = -5$ both the intersection point of the σ_1 -curves and the intersection point of the τ_1 -curves advance to the right while that of the μ_1 -curves retreats to the left. This trend is reversed on passing



through $k' = -3$, Figure 2.25.3. Consequently there is the possibility that the intersection points of the three orders of spherical coefficients will occur at the same value of R_4 at some point just beyond $k' = -3$. When this happens the ϵ'_{Sph} -parabola is tangential to the χ -axis in the (χ, k', R_4) -grid and σ_1 , μ_1 and τ_1 are a minimum for this particular value of k' .

Initial attempts to compute R and L solutions in the range $-3 \leq k' \leq -2.7$ with the programme RL/BP/SP121 failed as the intersection points approached each other. For example, at $k' = -2.7$ (Figure 2.25.4), the RL-programme failed to converge on solutions after $R_4 = 0.18$. However, the extrapolated curves of this graph of $k' = -2.7$ (enclosed by the square) intersect near $R_4 = 0.20$ and this solution, if it exists, satisfies the conditions that the coefficients shall be a minimum and that they shall alternate in sign. Since this optimum solution occurs when the ϵ'_{Sph} versus χ curve is tangential to the χ -axis then it is appropriate to call it the "tangential solution".

The RL-programme fails to converge on either an R-solution or an L-solution near the tangential solution because of the very small variation of ϵ'_{Sph} with χ near the turning point of the ϵ'_{Sph} -curve. This causes the programme to go into a loop of indefinite length when it iterates ϵ'_{Sph} with respect to χ . (The unsatisfactory nature of this type of programme was confirmed by later work in this region.

Although no RL-solutions were found beyond $R_4 = 0.18$ at $k' = -2.7$ with the RL-programme, it was found later by other means that the tangential solution existed at $R_4 = 0.22$ showing that R.H. and L.H. solutions exist beyond $R_4 = 0.18$.

Thus, provided solutions are not sought in close proximity to the tangential solutions then the RL-type of programme is satisfactory. However, it seems that with the type 121 triplet, at least, that the most interesting region is in the vicinity of a tangential solution. Therefore, in order to proceed with further development of the type 121 a method for computing systems in the tangential region of the ϵ'_{Sph} -curve is essential.

2.4.7 Symmetrical - Tangential Solutions and the Symmetry Parameter R_8 .

The preceding work has shown that certain of the tangential solutions are the ones with the best potential for correction of the zonal-spherical aberration to 7th order but these solutions cannot be investigated with a programme that controls ϵ'_{Sph} with χ . In the optimum region of σ_1, μ_1 and τ_1 of the type 121, ϵ'_{Sph} is nearly independent of χ so that iterations based on its dependence on χ converge very slowly in this region. Therefore, a performance parameter that is more sensitive to χ near the tangential solution than ϵ'_{Sph} and one that is also linked to the behaviour of ϵ'_{Sph} is required if we are to

compute the optimum solution. In the following the symmetry of the type 121 system is shown to have these properties.

The (χ, k', P) -interpolative study showed that as the ϵ'_{Sph} -curve at $k' = -3$ approached the tangential condition with increasing P , the separations of the components (d_3, d_6) of the R and L solutions tend to become equal (Figure 2.25). Later, the symmetry-performance parameter $(R_8)^*$ and the marginal spherical $(\epsilon'_{\text{Sph}})^{**} (= R_1)$ were plotted in each of the principal sections intersecting in the optimum region (Figures 2.19, 2.20, 2.21). This work showed R_8 passes through zero near either a minimum or a zero value of ϵ'_{Sph} in each of the principal sections. However, although this evidence suggests that the optimum tangential solution is symmetrical, it is not conclusive.

The connection between the symmetrical solutions and the tangential solutions is analysed in Figures 2.26 to 2.27. In Figure 2.26 the (χ, k', R_4) -coordinates of the R and L solutions are plotted for solutions computed from $k' = -2.9$ up to $k' = -2.7$ with the RL-programme (RL/BP/SP121). The graph beyond this point of $k' = -2.7$ has been obtained by fitting curves to these results. Clearly, coordinates of the turning-point of each R_4 -curve of Figure 2.26 are the coordinates of the tangential solution such that $\chi_{\text{Tg}} = \chi_{\text{L}} = \chi_{\text{R}}$; $k'_{\text{Tg}} = k'_{\text{L}} = k'_{\text{R}}$, $(R_4)_{\text{Tg}} = (R_4)_{\text{L}} = (R_4)_{\text{R}}$ (where Tg = tangential, L = Left-hand, R = Right-hand).

* $R_8 = d_3 - d_6$, introduced in section 2.3.2.

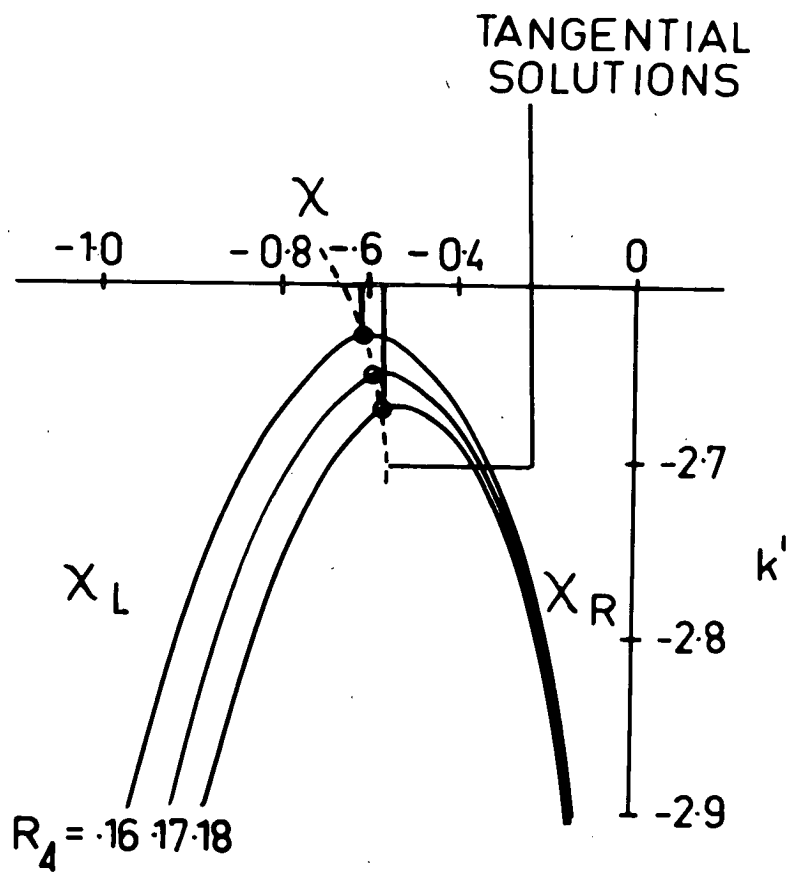


Fig. 2.26

LEFT HAND SOLUTIONS

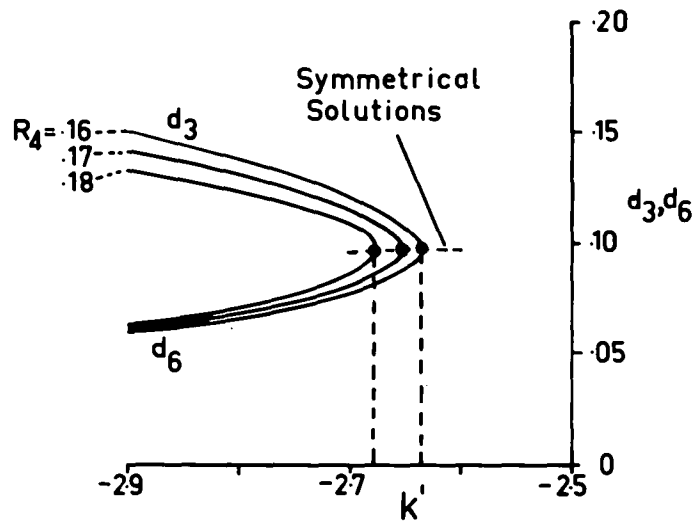


Fig. 2.27.1

RIGHT HAND SOLUTIONS

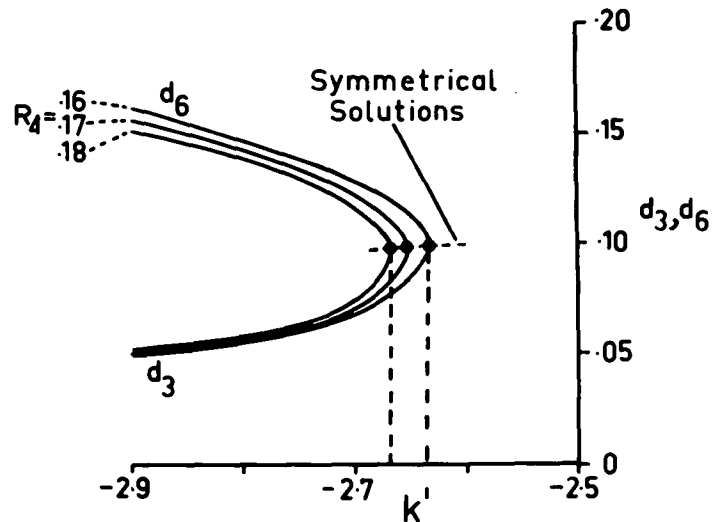


Fig. 2.27.2

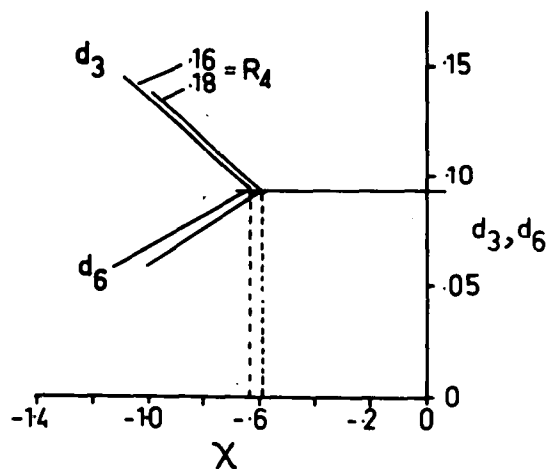


Fig. 2.27.3

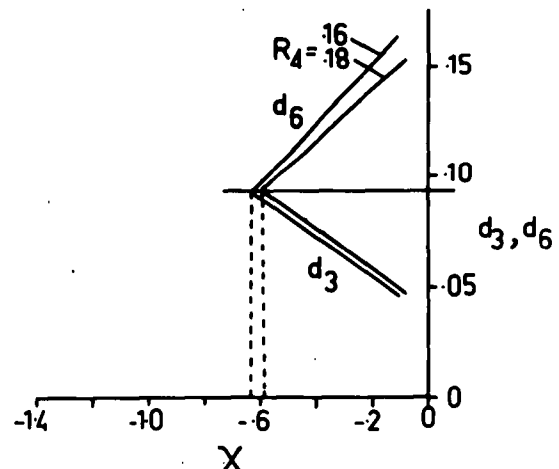


Fig. 2.27.4

In Figures 2.27.1 to 2.27.4 the dependence of the front and back air-spaces (d_3, d_6) of the R and L solutions of the type 121 on (χ, k', R_4) is established as follows. The separations of the L-solutions against k' are shown in Figure 2.27.1 where the intersection points have been found by extrapolating the curves beyond $k' = -2.7$, giving the (k', R_4) coordinates of the symmetrical-L-solutions. Similarly the χ -coordinates of these L-solutions have been determined in Figure 2.27.3. This analysis is repeated for the R-solutions in Figures 2.27.2 and 2.27.4. So from Figures 2.27.1 to 2.27.4 we see that the R and L solutions converge to identical symmetrical solutions such that $\chi_{SS} = \chi_L = \chi_R, k'_{SS} = k'_L = k'_R, (R_4)_{SS} = (R_4)_L = (R_4)_R$. Now on comparing the coordinates of the symmetrical solutions of figure 2.27 with the symmetrical solutions of Figure 2.26 we find that they are equivalent. Thus $\chi_{SS} = \chi_{Tg}; k'_{SS} = k'_{Tg}; (R_4)_{SS} = (R_4)_{Tg}$ and since $(\epsilon'_{Sph})_{max} = R_1 = 0$ at $(\chi_{Tg}, k'_{Tg}, (R_4)_{Tg})$ then $R_8 = R_1 = 0$ at $(\chi_{SS}, k'_{SS}, (R_4)_{SS})$. So the link between R_8 and R_1 is proved.

The other property we require in the performance parameter that replaces ϵ'_{Sph} is that its differential with respect to χ shall not approach too closely to zero as ϵ'_{Sph} approaches zero. The superiority of R_8 over ϵ'_{Sph} in this respect is obvious in Figure 2.21 and also it is demonstrated in the following numerical example. (The two solutions in this example have merely been chosen for the sake of showing how small the variation of ϵ'_{Sph} can be when k' approaches

its optimum region near $k' = -3$. Thus the first solution is a right hand one and the second is a symmetrical one.)

| Specifications of System | χ | k' | R_4 | R_8 | ϵ'_{Sph} |
|-----------------------------|--------|-------|-------|-------|--------------------------|
| R-solution | -0.500 | -2.70 | 0.19 | 0.012 | 0.0001 |
| S-solution | -0.541 | -2.70 | 0.19 | 0.000 | 0.0000 |

and $R_2 = R_3 = R_5 = 0$, $L = 0.02$, $T = 0.05$,
 where $\Delta R_8 / \Delta \chi \approx 100 \Delta \epsilon'_{\text{Sph}} / \Delta \chi$.

2.4.8 The Parameter R_8 and the Turning Point Solutions versus (χ, k', P) and (χ, k', R_4) .

We have found the connection between the parameter for the spherical aberration residual ($\epsilon'_{\text{Sph}} = R_1$) and the parameter for the symmetry (R_8) for the case when the spherical aberration parabola is tangential to the χ -axis. Now we ask "How does R_8 vary with χ , k' and P or χ , k' and R_4 in general?"

So far we have emphasized the tangential and symmetrical properties of the symmetrical solution and neglected the fact that it is primarily a turning point solution. This, of course, is the minimum of the spherical aberration parabola $\epsilon'_{\text{Sph}} = f(\chi)$ where $k' = k'_{\text{Tg}} = k'_{\text{SS}} = k'_{\text{TP}}$. (tg = tangential, SS = symmetrical solution, TP = turning point.)

There is only one $k' = k'_{\text{Tg}}$ for a given pair of the parameters either ($R_1 = 0$, $P = \text{constant}$) or ($R_1 = 0$, $R_4 =$

constant), whereas k'_{TP} is a continuous function of χ when R_1 is relaxed and either P or R_4 is controlled. The question therefore arises as to whether the property of symmetry is associated with all the turning-point solutions in general, or whether symmetry is only associated with the particular turning-point at $R_1 = 0$. (The Tangential or Symmetrical Solution as we know it now.) This question is examined in Figures 2.27.5 and 2.27.6.

In Figure 2.27.5 R_8 versus χ and ϵ'_{Sph} versus χ are plotted on the same axes for $k' = -3, -4$, and -5 and $P = 0.1, 0.3$ and 0.6 . This analysis is repeated in Figure 2.27.6 for R_4 instead of P where $R_4 = 0.16, 0.18, 0.20, 0.24$. These graphs show that the turning-point solutions are symmetrical for a large range of either χ, k' and P or χ, k' and R_4 . Thus by changing k' we can create a range of symmetrical systems which vary in marginal spherical R_1 . Consequently we can use R_8, R_1 and R_4 in place of χ, k', P . The set of monochromatic basic-parameters (χ, k', P) is thereby transformed into the set (R_8, R_1, R_4) and so we have now linked (χ, k', P) -space with the (R_8, R_1, R_4) -space.

In Figure 2.27.7 and 2.27.8 we have the same R_8 -graphs as above only now they are plotted with a typical coma coefficient μ_2 in place of the marginal spherical $\epsilon'_{Sph} = R_1$. From these graphs it is evident that the symmetry of the air space is not sufficient to ensure a system free of the higher orders of coma. The higher orders of coma are only minimized in the region of the optimum value of k' ,

($k' = -3$). If k' deviates from this then the higher order coma increases rapidly provided the Petzval coefficient is small. But if we approach the region of optimum P ($P = \text{about } 0.6$) or R_4 ($R_4 = \text{about } 0.24$) then the influence of k' and also \mathcal{X} on the coma is greatly reduced. This is in agreement with our earlier observation regarding the optimum region that the effectiveness of the "basic-parameters" is reduced at large P.

2.4.9 Conclusions.

At this stage we can predict several things about the wide aperture monochromatic type 121. We can expect it to have $R_8 = 0$, R_1 nearly zero and $R_4 = 0.2$ and therefore it will be symmetrical with small zonal spherical and fairly large Petzval sum. Its 3rd, 5th and 7th order coma contributions will be small but its 5th order astigmatic coefficients \mathcal{M}_4 , \mathcal{M}_5 and \mathcal{M}_6 will be large enough to contribute considerable oblique spherical aberration (13.3, 2.4). Therefore it appears that this higher order astigmatism will limit the field if the system is of reasonable focal length or if it is of short focal length and used with auxiliary magnification.

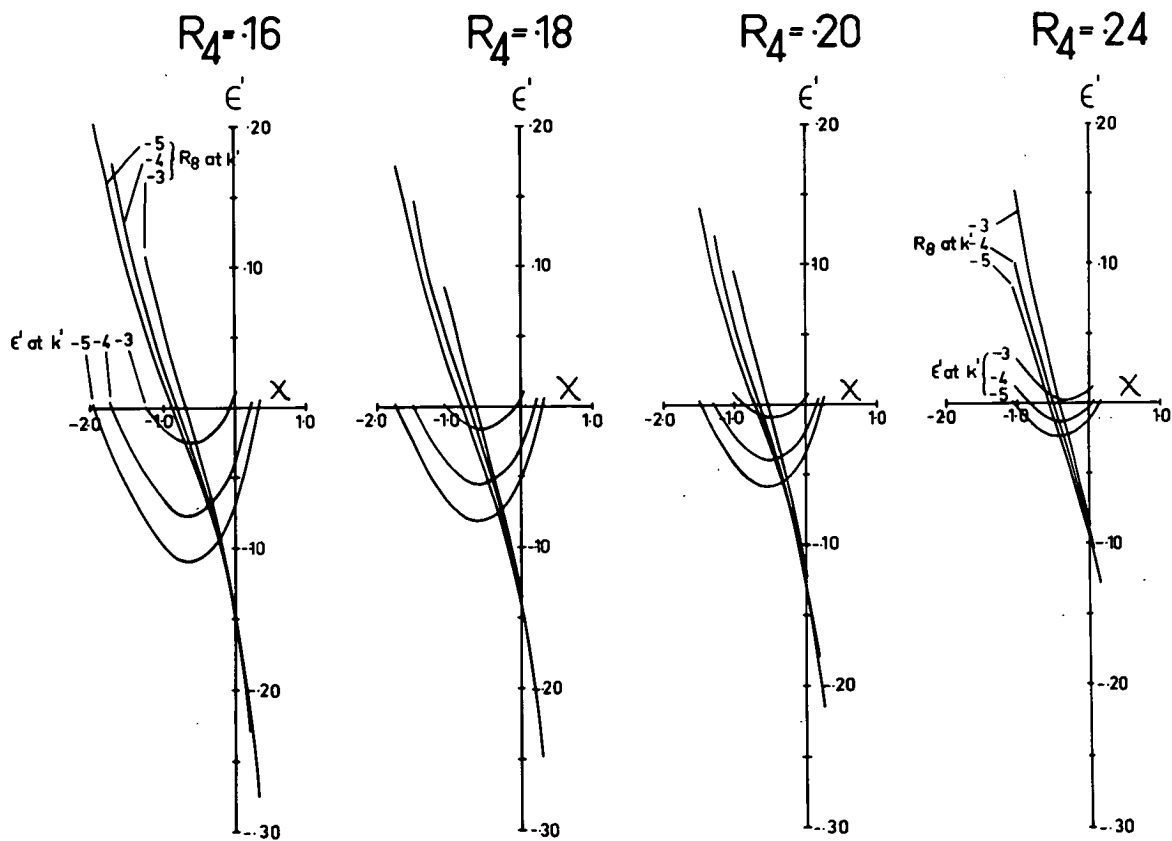
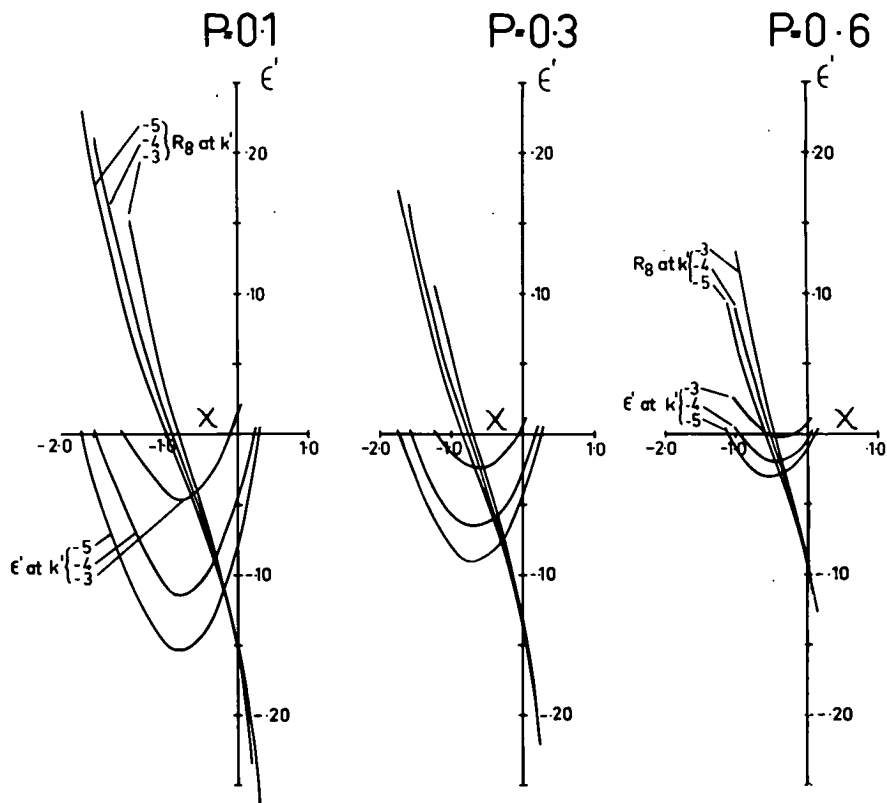


Fig. 2.27.6

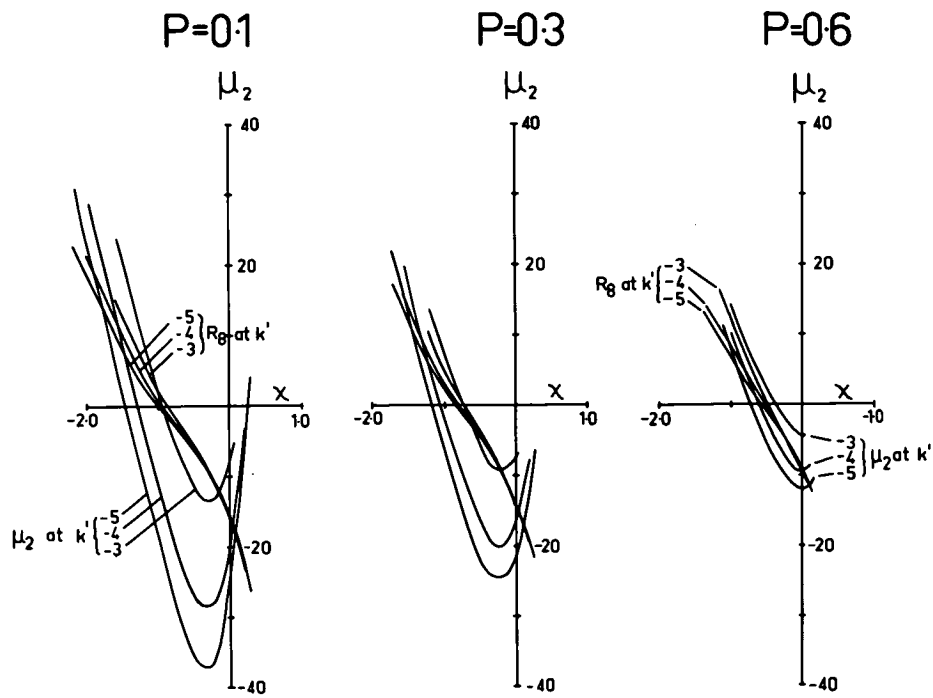


Fig. 2.27.7

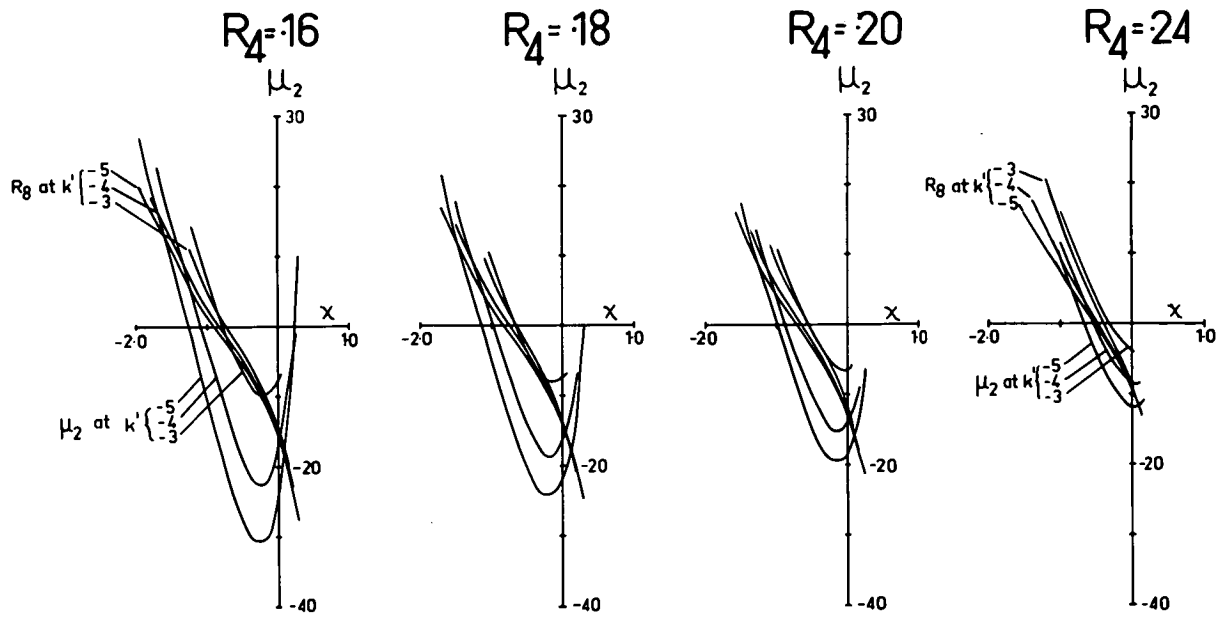


Fig. 2.27.8

CHAPTER 2.5 SYMMETRICAL SOLUTIONS AND CORRECTION OF ZONAL SPHERICAL AT TWO ZONES.

2.5.0 Introduction.

In the preceding work on the R and L solutions it was found that the RL-programme failed near the tangential solution, because ϵ'_{Sph} is nearly independent of χ in this region. However, the symmetry of the type 121, as measured by R_8 , was found to depend significantly on χ in the tangential region, and, in particular, a tangential solution of the type 121 has $R_8 = (d_3 - d_6) = 0$, and, $\epsilon'_{\text{Sph}} = R_1 = 0 + 9\text{th order terms etc..}$

The method devised for finding the tangential solution consists of two iterative processes. In the first one, χ is changed until $R_8 = 0$, and then in the second k' is changed until $\epsilon'_{\text{Sph}} = R_1 = 0 + 0(9)$. The iteration is started at $\chi = \chi_1$ and $k' = k'_1$ which are values known to be near the tangential solution. These initial values of χ and k' are estimated from the interpolative survey of the coefficients versus (χ, k', R_4) . In practice, it is necessary to repeat the compound cycle consisting of the adjustment of χ followed by the adjustment of k' several times before both R_8 and R_1 are less than 10^{-5} .

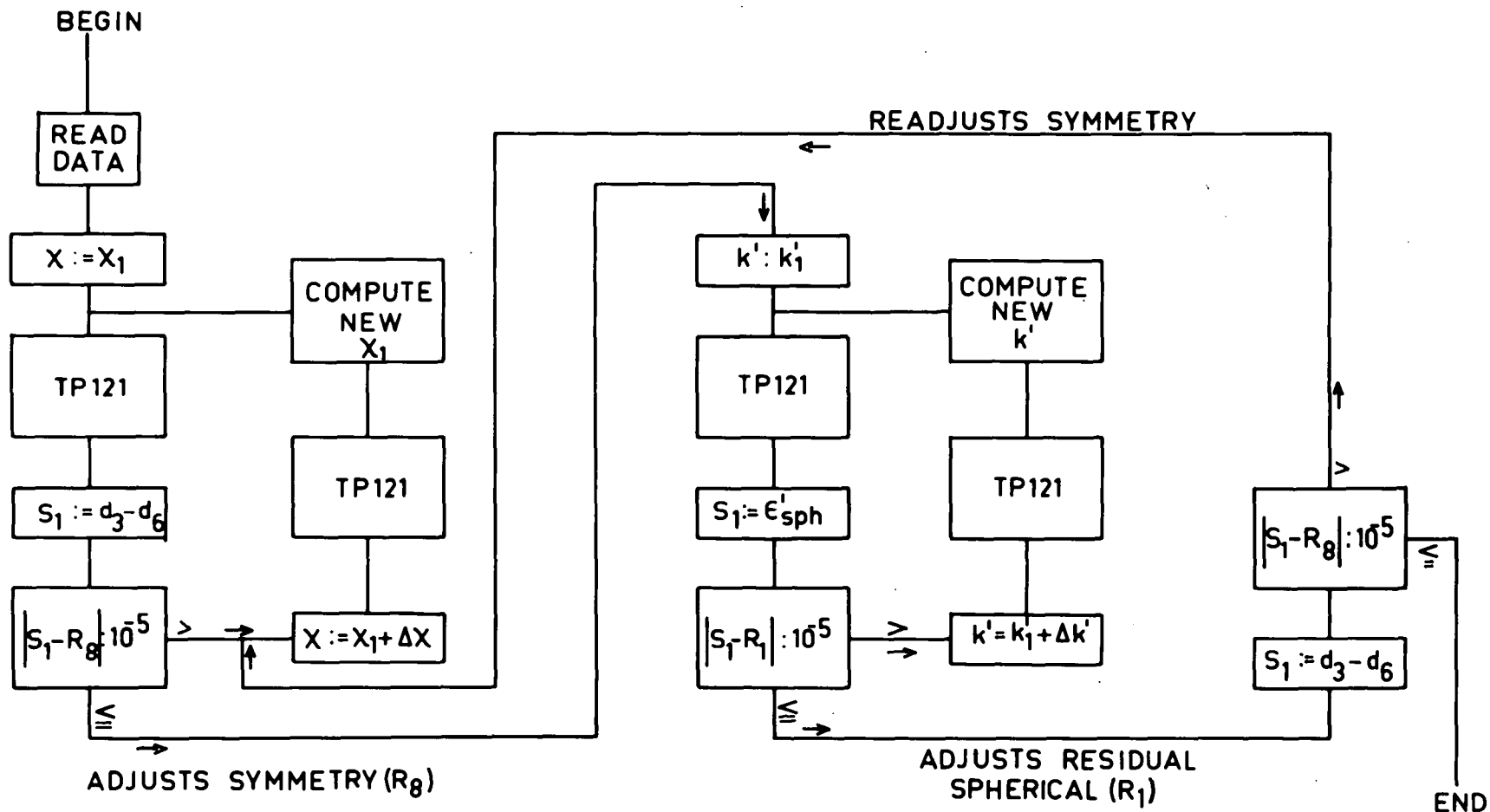
2.5.1 The SS Programme.

The programme for generating the tangential solutions is derived from the basic programme BP121 by

iterating the sub-routine TP121 first with respect to χ and then with respect to k' . The main features of this programme are shown in Figure 2.28. Basically it consists of three loops, the left hand loop, the right hand loop and a loop embracing both the left and right hand loops. The symmetry is adjusted to R_8 in the left hand loop and the spherical aberration residual ϵ'_{Sph} is adjusted to R_1 in the right hand loop. Both loops are repeated until R_8 and R_1 are simultaneously zero. When this occurs the programme prints out the lens data and goes to "END" where it receives further instructions which may, for example, restart it computing another system from fresh data.

The programme is called the symmetrical solution programme and it is denoted by the code number SS/BP/SP121 which, for convenience, we will usually call the SS programme. Moreover, although we are preoccupied with symmetry in this case, it is, in general, more useful to think of R_8 as measuring the asymmetry and the programme as the asymmetrical-solution programme. Consequently the symmetrical solution is the limiting case as the asymmetry is reduced.

In view of the equivalence of (χ, k', R_4) and (R_8, R_1, R_4) the SS programme can be used to find any solution in a (χ, k') plane of Figure 2.26, by giving R_8, R_1 and R_4 appropriate values. For example, if we set R_8 equal to zero then we will get turning point solutions only, or on the other hand if in addition we make $R_1 = 0$ then we will get tangential solutions only.



The SS programme is more flexible than the RL programme because it has direct control of k' through R_1 and R_8 . By way of contrast, we recall how the R and L programmes explored the R and L solutions. In that preparatory work, k' and R_4 were specified and then χ was used to control ϵ'_{Sph} whereas now, with the SS programme, χ and k' are associated directly with properties of the optical system. At this point we can see the two types of programme in their proper roles: the RL-programme is ideal for limited interpolative study and the SS-programme is best suited for examining a promising region of the interpolative study in detail.

2.5.2 Spherical Aberration Coefficients of the Symmetrical Solutions versus R_4 .

Now that χ and k' have specific tasks we are left with R_4 as the only independent parameter of the monochromatic system. Already as a result of our interpolative study of the coefficients we have tentatively proposed that R_4 will control the spherical coefficients σ_1, μ_1 and τ_1 . Therefore, in view of this, we now proceed to locate the systems with the optimum set of these spherical coefficients by varying R_4 .

The symmetrical solutions having $R_1 = R_2 = R_3 = R_5 = R_8 = 0$ were computed with the SS-programme over the range of $0.14 \leq R_4 \leq 0.22$ in steps of $\Delta R_4 = 0.01$. In

Figure 2.29, the spherical coefficients of these solutions are plotted on the same axes against R_4 . Here the 3rd and 7th order coefficients σ_1 and τ_1 pass through zero between $R_4 = 0.19$ and 0.22 but μ_1 , as we inferred from the earlier work of Section 1, remains almost unchanged, being negative throughout this range of R_4 . In the region bounded by $R_4 = 0.19$ and $R_4 = 0.22$ the successive coefficients alternate in sign and, as we already know, systems with this property are expected to have zero spherical at two zones of the aperture. (See section 2.4.5).

The values of σ_1, μ_1, τ_1 and χ, k', P of the symmetrical systems from $R_4 = 0.19$ to 0.22 are as follows:

TABLE 2.5

| R_4 | σ_1 | μ_1 | τ_1 | χ | k' | P |
|------------------|-----------------------|---------------------|-------------------------|--------------------|-------------------|------------------|
| 0.22 | .250 | -5.89 | -14.69 | -0.466 | -2.873 | 0.5789 |
| 0.21 | .171 | -5.34 | 26.74 | -0.490 | -2.799 | 0.5356 |
| 0.20 | .070 | -4.88 | 73.26 | -0.515 | -2.746 | 0.4925 |
| 0.19 | -.020 | -4.47 | 126.3 | -0.541 | -2.707 | 0.4493 |
| ΔR_4 .03 | $\Delta \sigma_1$.27 | $\Delta \mu_1$ 1.42 | $\Delta \tau_1$ -140.99 | $\Delta \chi$.075 | $\Delta k'$ -.166 | ΔP .1296 |

This table shows how very small the region of (χ, k', P) -space is in which the zonal spherical is optimized: it occupies only a very small region around the intersection point of the principal sections of (χ, k', P) -space which were shown in Figures 2.19, 2.20 and 2.21 of Chapter 2.4. The region is contained within $\chi = 0.075, k' = -0.166$

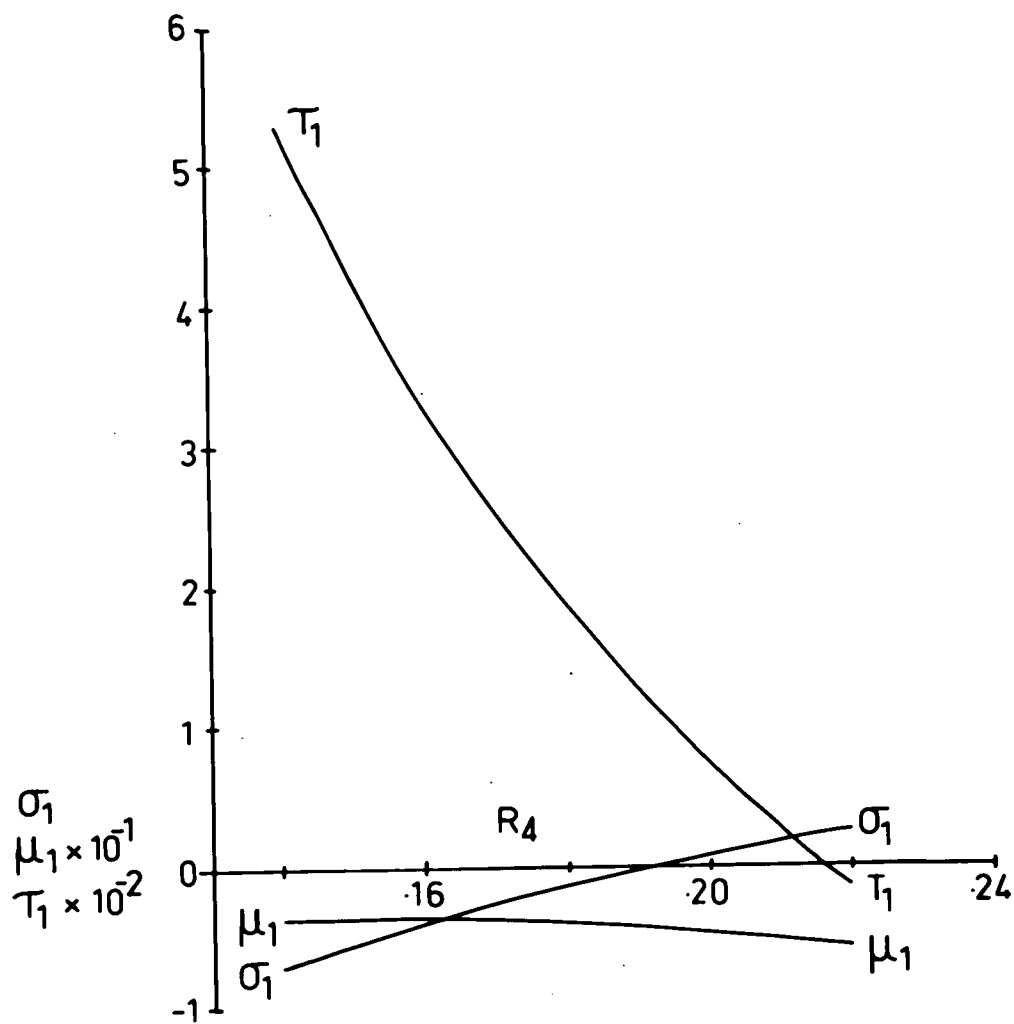


Fig. 2.29

and $\Delta P = 0.1296$ (or $\Delta R_4 = 0.03$). In this micro-region the greatest change in the spherical aberration is due to the change in σ_1 .

2.5.3 Predicted Zonal Spherical of Symmetrical Solutions versus R_4 .

After isolating the region of alternating signs, the SS-programme was modified to compute an additional quantity, the longitudinal spherical aberration, $LA' = \epsilon'_{Sph}/\ell$, for $0 \leq \ell \leq 0.20$ in steps of $d\ell = 0.02$. Thus with this modified programme both the predicted zonal spherical and the spherical aberration coefficients can be surveyed simultaneously with respect to R_4 . (After this the SS-programme will mean the modified SS-programme.)

With the SS-programme the predicted zonal-spherical aberration has been computed for a set of R_4 values (0.18, 0.19, 0.20, 0.21) that span the optimum region which was located in Figure 2.29. These results are plotted in Figure 2.30 in which the two-zone correction is seen to occur at $R_4 = 0.20$.

The region of two-zone correction is mapped in detail in Figure 2.31 where the predicted zonal aberration is plotted in steps of $dR_4 = 0.001$. From this graph the system at $R_4 = 0.198$ was selected for further development because it appeared to have the most even distribution of zonal aberration.

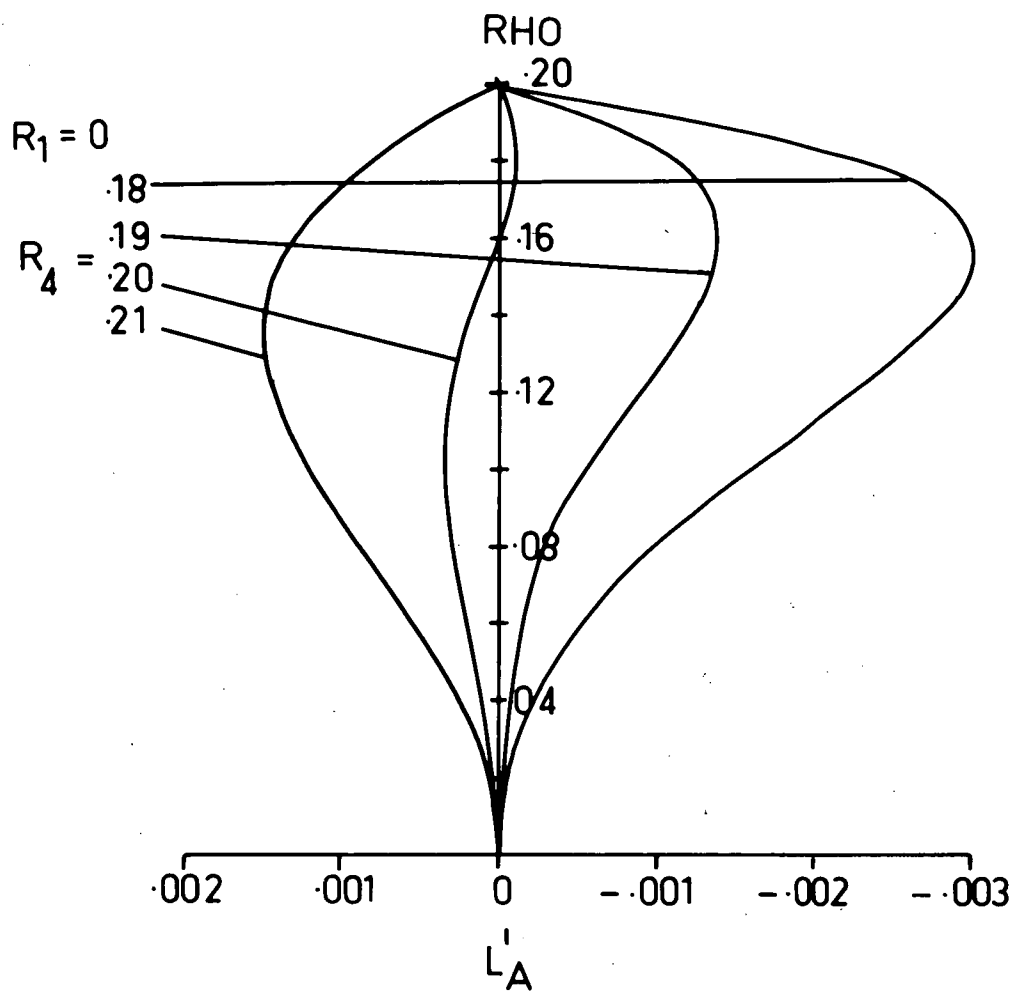


Fig. 2.30

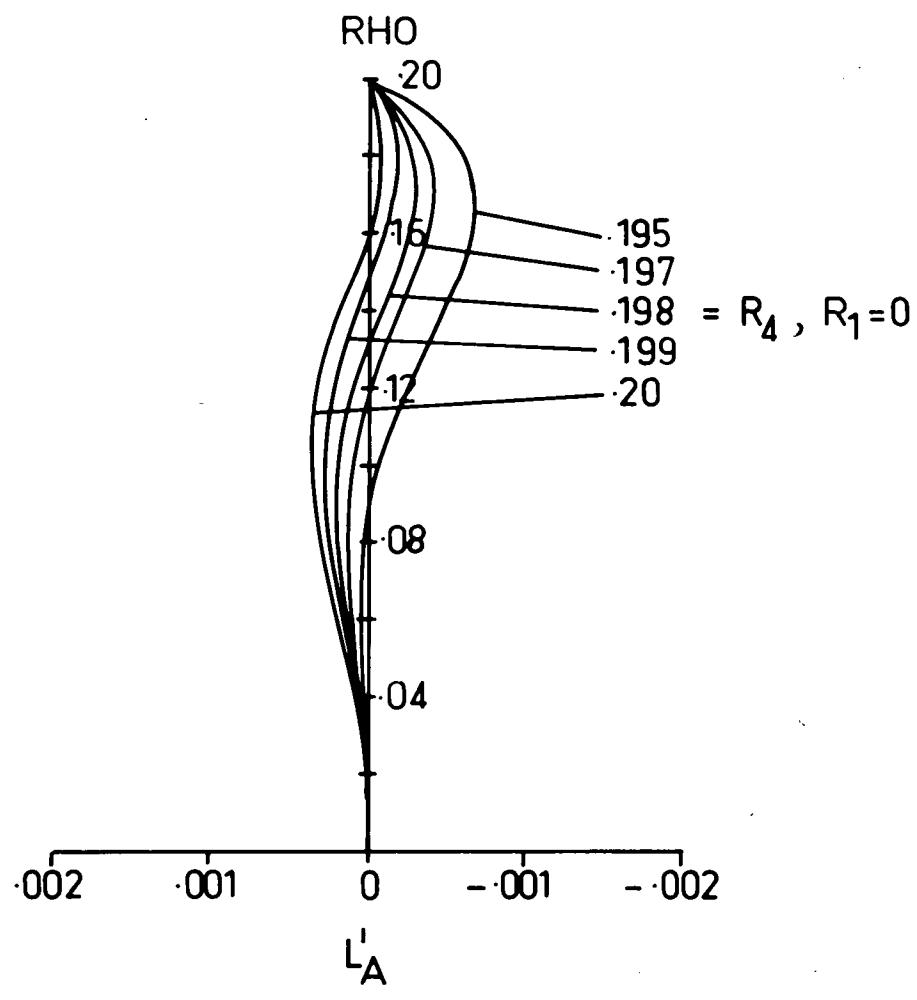


Fig. 2.31

Theoretically, The LA' -curves of Figure 2.31 should intersect the axis in the intermediate zone of $\rho = 0.1414$ but this is not so. This spreading of the intersection points along the vertical axis is due to rounding off the iterative sub-routine to six decimal places. Indeed, experience with later R_4 -surveys and spot diagrams have confirmed that $dR_4 = 0.005$ is the minimum effective interval of R_4 .

2.5.4 Failure of Zonal Predictions at Apertures $> f/3.5$.

The next thing to do is to compare the predicted zonal spherical aberration with the actual zonal spherical aberration computed from zonal ray-traces and show whether the two-zone correction is preserved in the presence of the higher order aberrations, that is, aberrations greater than the 7th order. This involves both the SS-programme and the Ray-Trace programme. The system must first be calculated with the SS-programme and then its specifications must be given to the Ray-Trace programme. Thus the SS-programme gives the "predicted- LA' " and the Ray-Trace programme the "actual- LA' ".

The Elliott 503 computer used in this work cannot store both the SS-programme and the Ray-Trace programme simultaneously, consequently the comparison of the predicted LA' and the actual LA' values is an unwieldy operation with it. Also, the SS-programme generates systems over a given

range in specified steps whereas the ray-trace programme requires the specifications of each system. So, in view of these disadvantages, the search for a system with two-
^{on locating it as accurately as possible with the coefficients,}
 zone correction has been conducted with the emphasis₂ in order to avoid a quite impractical amount of data preparation for the ray-trace; hence the detailed survey made in Figure 2.31. This, of course, raises the point that it would be desirable to link the coefficients accurately with the ray-trace anyway, because, apart from overcoming the lack of storage of this computer it would also make worthwhile savings in computer time even when storage is no problem. We are, at this point, echoing our earlier remarks about optimizing thoroughly at each level of the design-process before proceeding to the next. We are, in fact, now in this state of transition from one level of the design-process to another as we pass from coefficients to LA^1 -curves.

The predicted zonal aberration of the symmetrical solution at $R_4 = 0.198$ is compared, in Figure 2.32, with the actual zonal aberrations which have been computed by tracing rays at intervals of $d\rho = 0.02$. We see that there is a very large positive contribution not accounted for by predictions based on 3rd, 5th and 7th order coefficients. From $\rho = 0$ to $\rho = 0.08$ the ray-trace differs from the predictions by less than 1×10^{-4} , at $\rho = 0.10$ by less than 1×10^{-3} , at $\rho = 0.12$ by less than 3×10^{-3} , but, after $\rho = 0.12$, the ray-trace curve swings rapidly away

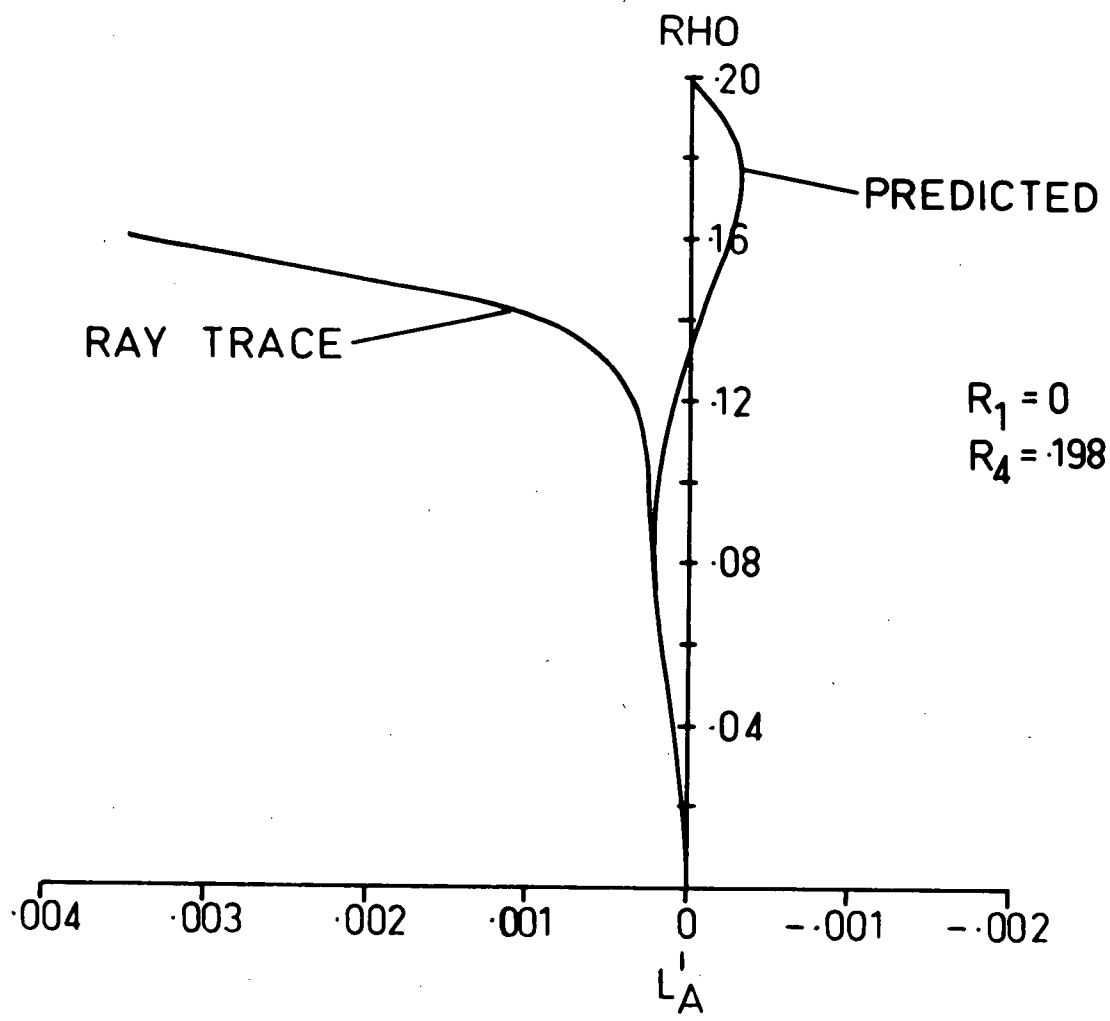


Fig. 2.32

from the predicted curve. From about $\rho = 0.14$ the ray-trace LA^s-curve becomes almost asymptotic. Therefore, it appears that even with the spherical coefficients of the first three orders it is not possible to predict the zonal-spherical aberration of the optimum system with a high degree of accuracy beyond $\rho = 0.10$ (f/4.5) and also it seems that the predictions are meaningless after

$\rho = 0.14$ (f/3.5). Moreover in this example, even the predictions between $\rho = 0.10$ and $\rho = 0.14$ are of doubtful value.

2.5.5 Balancing Higher Order Zonal Spherical Mainly with R_1 .

We are faced with two questions at this stage. Firstly does a system with two-zone correction exist in the vicinity of the predicted optimum system? Secondly, if one exists, we must also ask whether the familiar design technique of balancing higher order residuals with lower order residuals of the same type is sufficient for achieving two-zone correction?

When we approached this problem for the first time we had the above questions in mind so that we were prepared not to accept it as conclusive if R_1 failed to give two-zone correction.

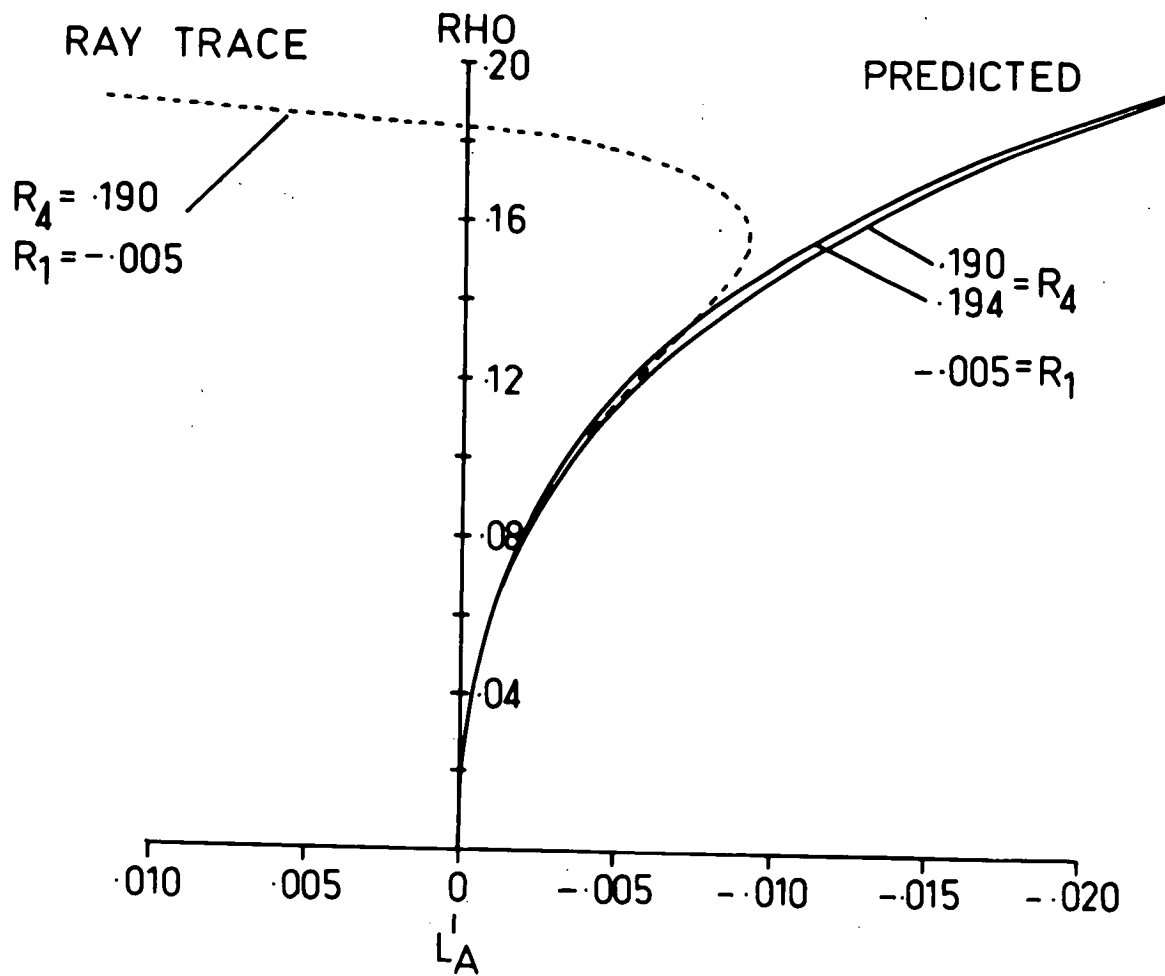
Adhering to the familiar design technique of balancing aberrations, an attempt was made to balance the positive residuals of the marginal zones mainly with a

negative spherical residual R_1 . At the same time it was decided to decrease the Petzval residual by a small amount ΔR_4 simultaneously with the change in R_1 . This change in R_4 was proposed because we had seen from Figures 2.30 and 2.31 that such a change would tend to reduce the lower zones whereas ΔR_1 was expected to reduce only the marginal zones significantly. Thus we expected that a proper combination of R_1 and R_4 would bring about an improvement of the zonal spherical aberration of the whole aperture.

Because we had gained no other experience of the system's response to R_1 and R_4 than that shown in Figures 2.30 to 2.32, we decided to proceed cautiously and to reduce the marginal aberration of Figure 2.32 in several moderate stages, starting with $R_1 = -0.005$ and $R_4 = 0.008$. The results of this first attempt with $R_1 = -0.005$ and $R_4 = 0.190$ are shown in Figure 2.33 where we have both the predicted LA'-curves at $R_4 = 0.190$ and $R_4 = 0.194$, for $R_1 = -0.005$, plotted with the ray-trace-LA'-curve for $R_4 = 0.190$.

It is evident from the Figure 2.33 that the zonal aberrations have been reduced in all zones so that the LA'-curve of the ray-trace is now negative from $\rho = 0.02$ to $\rho = 0.18$. However, the marginal zone ($\rho > 0.18$) still has a large positive residual but, it is very much less than that of the previous Figure 2.32. Nevertheless, this improvement in the marginal zones has been achieved at the

Fig. 2.33



expense of the zones below $\rho = 0.14$ which are now decidedly negative.

Attempts (not shown) were made later to reduce the marginal zones further by making R_1 more negative than -0.005 . However, it was found that this caused rapid deterioration of the lower zones ($\rho < 0.18$) for only a very small gain in the marginal zones.

So it seems that effectiveness of R_1 in controlling the higher order zonal aberration is limited to partial correction of the marginal zone. Therefore some additional property is required for controlling the intermediate zone.

2.5.6 The Effect of R_4 on the Marginal Zones.

Since R_1 is the only partly successful in reducing the marginal zones, our attention is turned to the parameter R_4 . In the surveys of the predicted LA' -curves of Figures 2.30 and 2.31, R_4 controls the magnitudes of all zones of the predicted curve below $\rho = 0.20$, mainly by reducing the effect of the 3rd and 7th order coefficients. However, we have found from the comparison made between the predicted LA' -curve and the ray-trace LA' -curve in Figure 2.32 that the coefficients beyond the 7th order, which we have ignored, are very large; it is the control of these higher orders that faces us here.

The effect of R_4 on the ray-trace LA' -curves for $R_1 = 0$ is shown in Figure 2.34. These results throw an

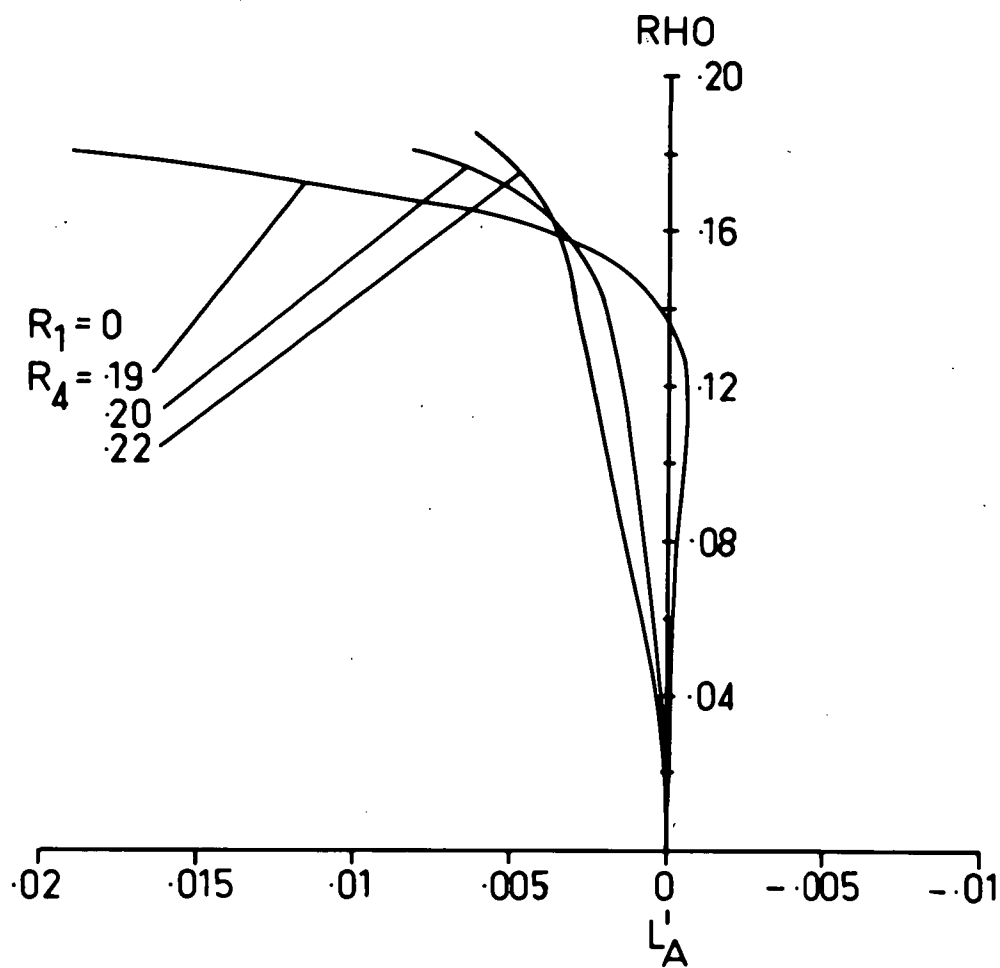


Fig. 2.34

entirely new light on the behaviour of the inner and outer zones of the aperture.

Between $\rho = 0.14$ and $\rho = 0.16$ the LA'-curves for $R_1 = 0.19, 0.20$ and 0.22 almost intersect in a common point and, therefore, in this intermediate region ($0.14 < \rho < 0.16$) the zonal aberration is nearly independent of R_4 . Below this intersection zone the zonal aberration is reduced as R_4 is decreased, just as it is with the predicted LA'-curves of Figures 2.30 and 2.31, but, above the intersection point the effect is reversed and the zonal aberration is increased as R_4 is reduced.

It is clear from the figure that the rate of change of the outer zones ($\rho > 0.16$) is very much greater than that of the lower zones ($\rho < 0.14$). Indeed, it is evident that the reduction of the marginal zones caused by R_4 is enormous in comparison with the increase in that of the lower zones. Thus R_4 seems to be the main parameter for controlling the aberration of the outer zones of the monochromatic type 121 system.

2.5.7 The Combined Effects of R_1 and R_4 on the Marginal Zones and the Intermediate Zones.

If we combine the results of the R_1 and R_4 studies we find that not one but both parameters play a significant part in controlling the zonal aberration of the monochromatic type 121.

One zone in particular, the intermediate zone, between $\rho = 0.14$ to $\rho = 0.16$, can only be zeroed by giving R_1 a small negative value because it has been shown to be independent of R_4 . From Figure 2.33, it is clear that this change in R_1 that zeroes the independent zone, will reduce most of the zones a little, but it will not be sufficient to make a significant reduction in the marginal zone ($\rho > 0.18$).

It seems that the thing to do in addition to decreasing R_1 is to increase R_4 because this will reduce the marginal zone effectively, (Figure 2.34), without changing the intermediate zone at all, and, at the same time, it will cause only a slight increase in the lower zones. Also the increase in the lower zones is opposed somewhat by the decrease in R_1 . Here then, is a very interesting combination of properties.

Now if we also consider how the accuracy or quality of the predicted LA' -curves varies with ρ and combine this result with the way LA' varies with R_1 , R_4 and ρ , then the possibility of two-zone correction becomes a certainty.

We see from Figure 2.33 that the predicted and ray-trace LA' -curves agree very well for $\rho = 0$ to $\rho = 0.14$. Therefore, combining this fact with those of R_1 and R_4 we can see that if the zone at $\rho = 0.14$ is made zero by a change in R_1 then we can expect the LA' -curves for $R_4 \gg 0.21$

to have positive zonal aberration below $\rho = 0.14$ and negative aberration above $\rho = 0.14$. We expect this pattern to be reversed at smaller values of R_4 , so that we will then have negative residuals in inner zones and positive residuals in the outer zones of the aperture. Thus, in between $R_4 = 0.19$ and $R_4 = 0.22$, we expect to obtain two-zone correction by careful choice of R_1 and R_4 (because we see that during the transition the lower zones lag behind the outer zones.)

2.5.8 Optimizing LA' with R_1 and R_4 .

Once the effects of R_1 and R_4 are understood it is apparent that a routine method is needed for finding the best system with correction at two zones. The obvious thing to do is to compare graphically surveys of the predicted LA'-curves versus R_4 with those of the corresponding ray-trace LA'-curves versus R_4 . Thus from the first survey of this kind we have the graphical pair, Figure 2.35(a) and Figure 2.35(b). In Figure 2.35(a) we have the predicted LA'-curves of the symmetrical systems, with $R_1 = 0$, plotted at intervals of $R_4 = 0.1$, and, in Figure 2.35(b), the corresponding LA'-curves calculated from zonal ray-traces.

The Figure 2.35(b) shows how the family of ray-trace LA'-curves have been spread out above $\rho = 0.16$, running from a large positive zonal aberration to a large negative zonal aberration. The aberrations of these outer zones

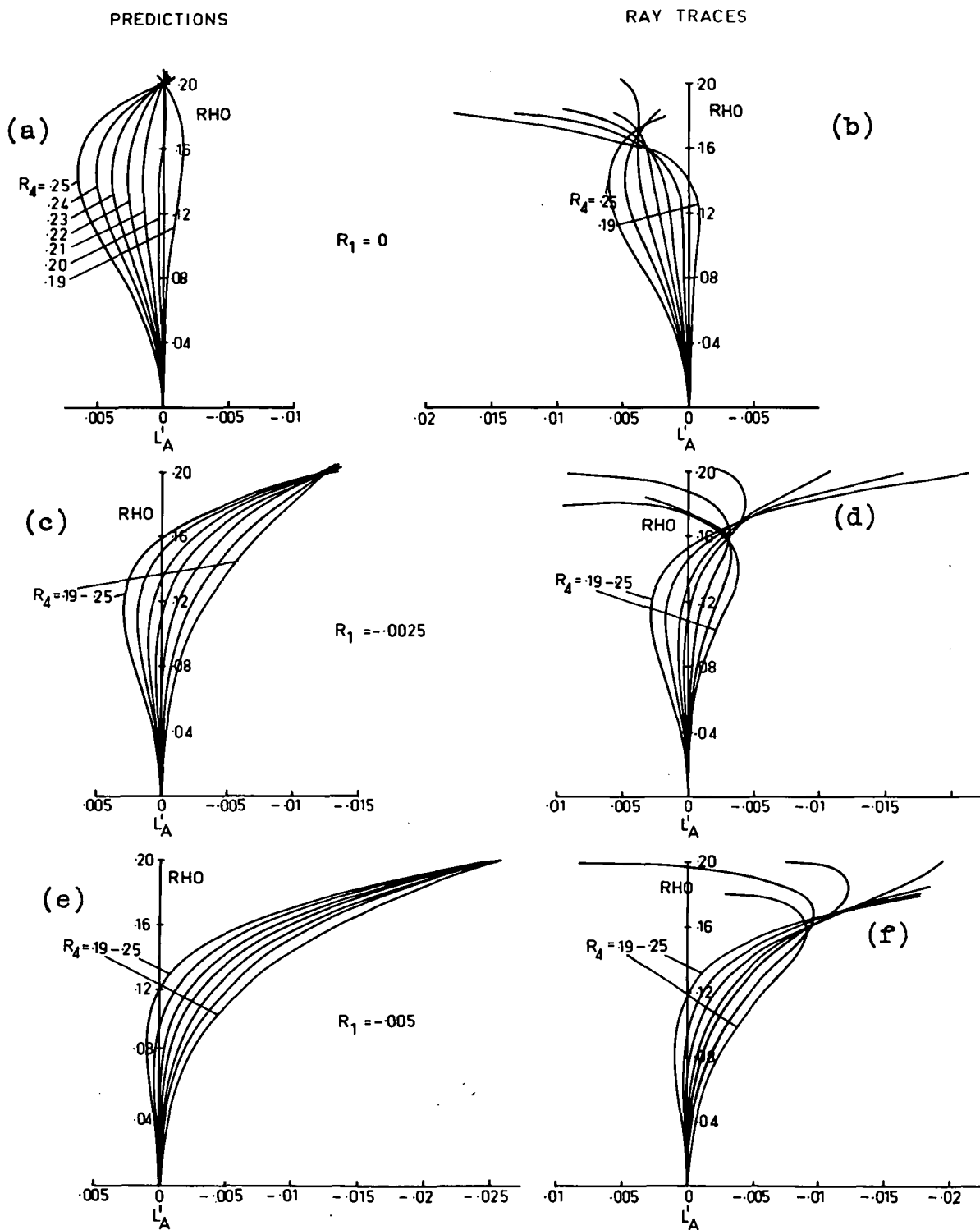
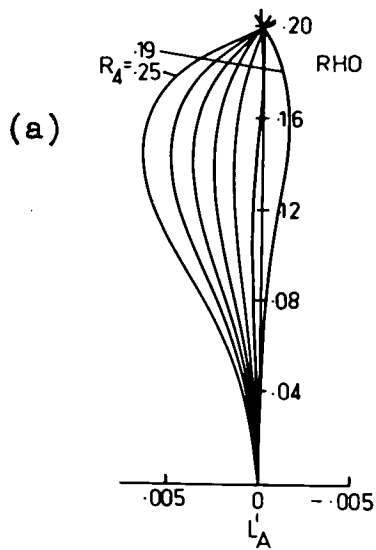


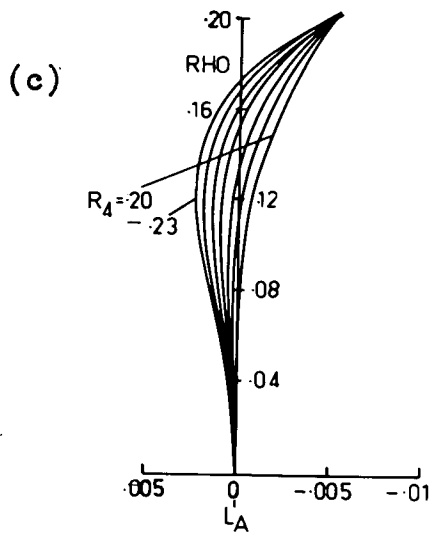
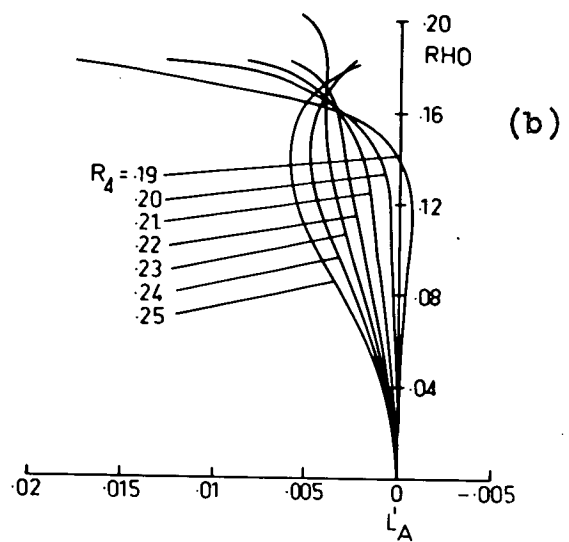
Fig. 2.35

PREDICTIONS

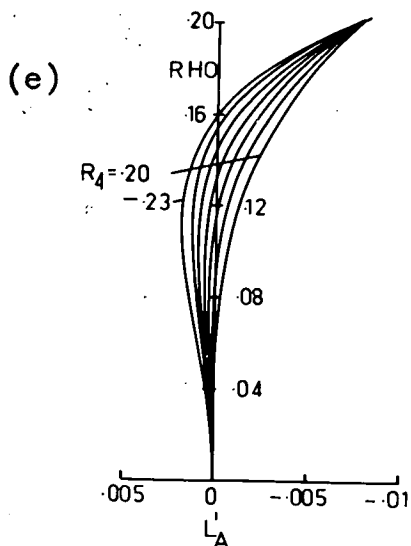
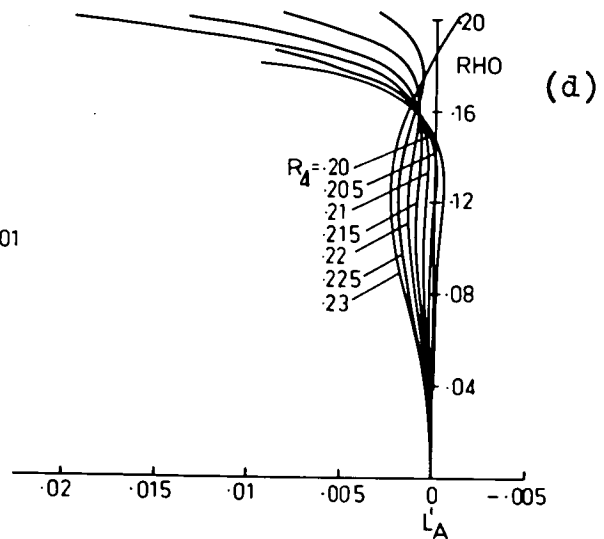
RAY TRACES



$R_1 = 0$



$R_1 = -.001$



$R_1 = -.0015$

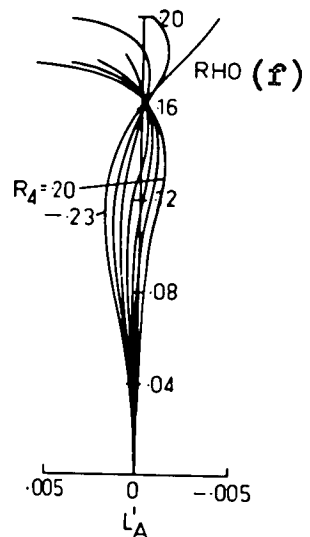


Fig. 2.36

cause them to be distributed in a fan-like spread about the system at $R_4 = 0.23$ which has the S-shaped curve but, unfortunately, it is tilted so that all zones have positive residuals.

In Figures 2.35(c) and 2.35(d) the surveys are repeated for the same range of R_4 , but this time with a negative spherical residual $R_1 = -0.0025$ instead of $R_1 = 0$. This confirms that the intersection point is at about $\rho = 0.16$ and it also shows that the curves retain their shape relative to each other fairly closely while they are being bent as a group from left to right as R_1 becomes more negative. The S-type core of the group of ray-trace curves is not far away from the optimum predicted system $R_4 = 0.20$ of Figure 2.35(a).

From this point on it is only a matter of repeating the surveys with smaller values of R_1 (see Figures 2.36 c,d,e,f) until the intersection point coincides with the vertical axis. In the final stages the parameter R_4 is stepped at the minimum effective interval ($\Delta R_4 = 0.005$, see section 2.5.3) in order to locate the two-zone correction with the maximum precision possible with this technique. Note the Figures 2.35(a) and (b) are reproduced again as Figures 2.36(a) and (b) for the sake of comparison.

The work with R_1 and R_4 is summarized in Figures 2.37 a, b and c. In these figures the predicted S-curve is shown with its corresponding ray-trace curve at the three

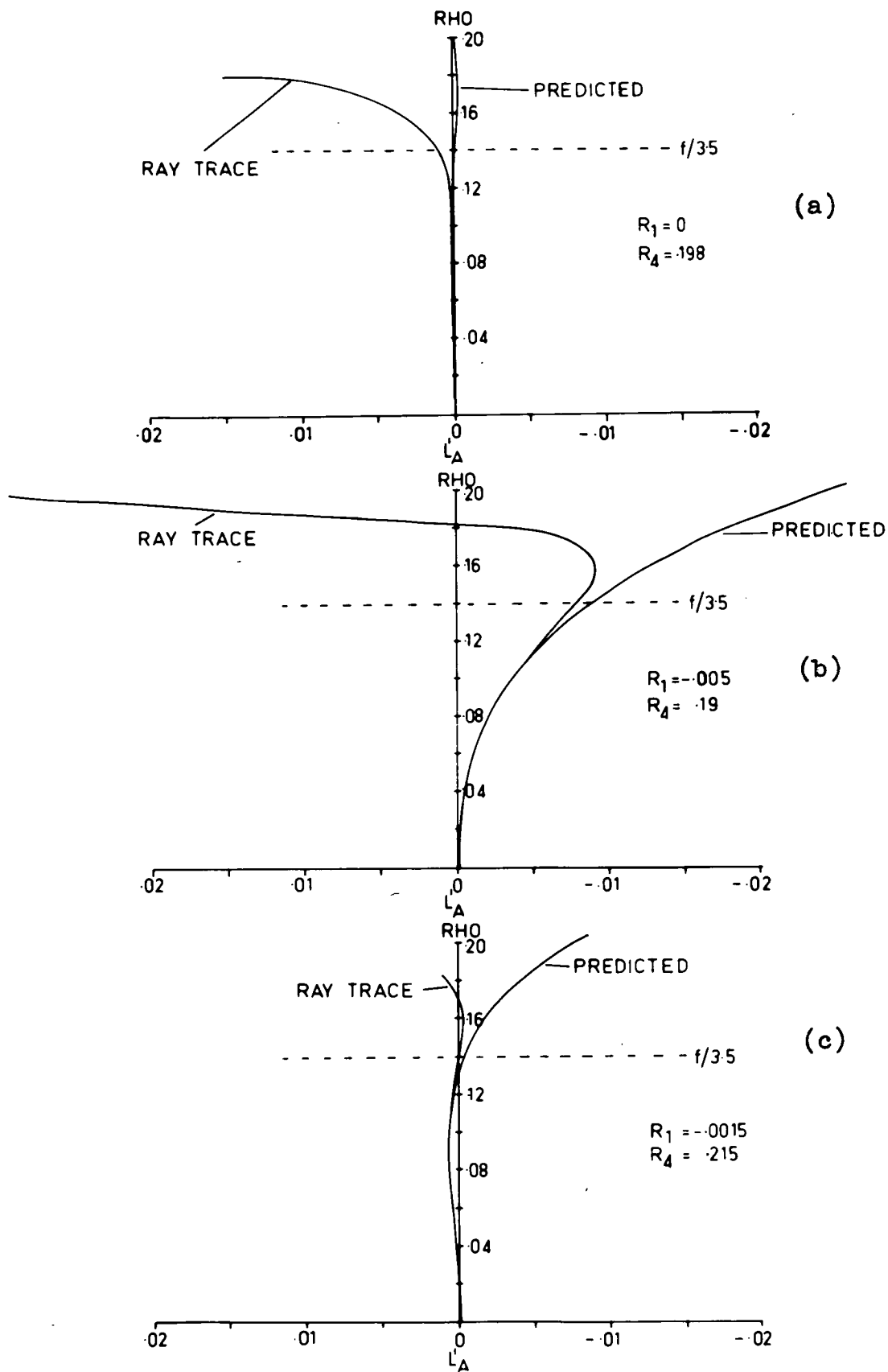


Fig. 2.37

principal stages of development in the application of R_1 and R_4 . The top Figure (2.37a) shows the predicted LA' -curve for $R_1 = 0$ and $R_4 = 0.198$. In the second Figure (2.37b) the effect of R_1 only is seen and in the final one (2.37c) the ray-trace LA' -curve with the two-zone correction is seen to appear when R_1 and R_4 are combined properly.

2.5.9 The Final Adjustment of the Monochromatic System.

2.5.9.1. Selecting the Optimum System. (The minimum effective interval of R_4 .)

From the surveys of groups of LA' -curves we have selected the symmetrical system at $R_1 = -0.0015$ and $R_4 = 0.215$ for further development. This system also has $R_2 = R_3 = R_5 = R_8 = 0$, $L = 0.2$ and $T = 0.05$; we will call this system SS(1). However, before proceeding with the development of SS(1) we will compare its spot-diagrams with those of systems either side of it so as to test our earlier hypothesis concerning the minimum effective interval R_4 (see section 2.5.3). For this purpose we have selected systems that occur at intervals of $\Delta R_4 = 0.005$ and for convenience called them SS(-1), SS(1) and SS(+1); thus they are at $R_4 = 0.210$, 0.215 and 0.220 respectively. Their spot-diagrams for a maximum aperture of $f/2.5$ ($\rho = 0.2$) and $V = 0^\circ$, 5° and 10° off-axis are shown in Figure 2.38.

The best axial-image appears to occur at $R_4 = 0.215$. This is confirmed by the zonal spot densities of Table 2.6 in which the percentage spots occurring inside a circle of

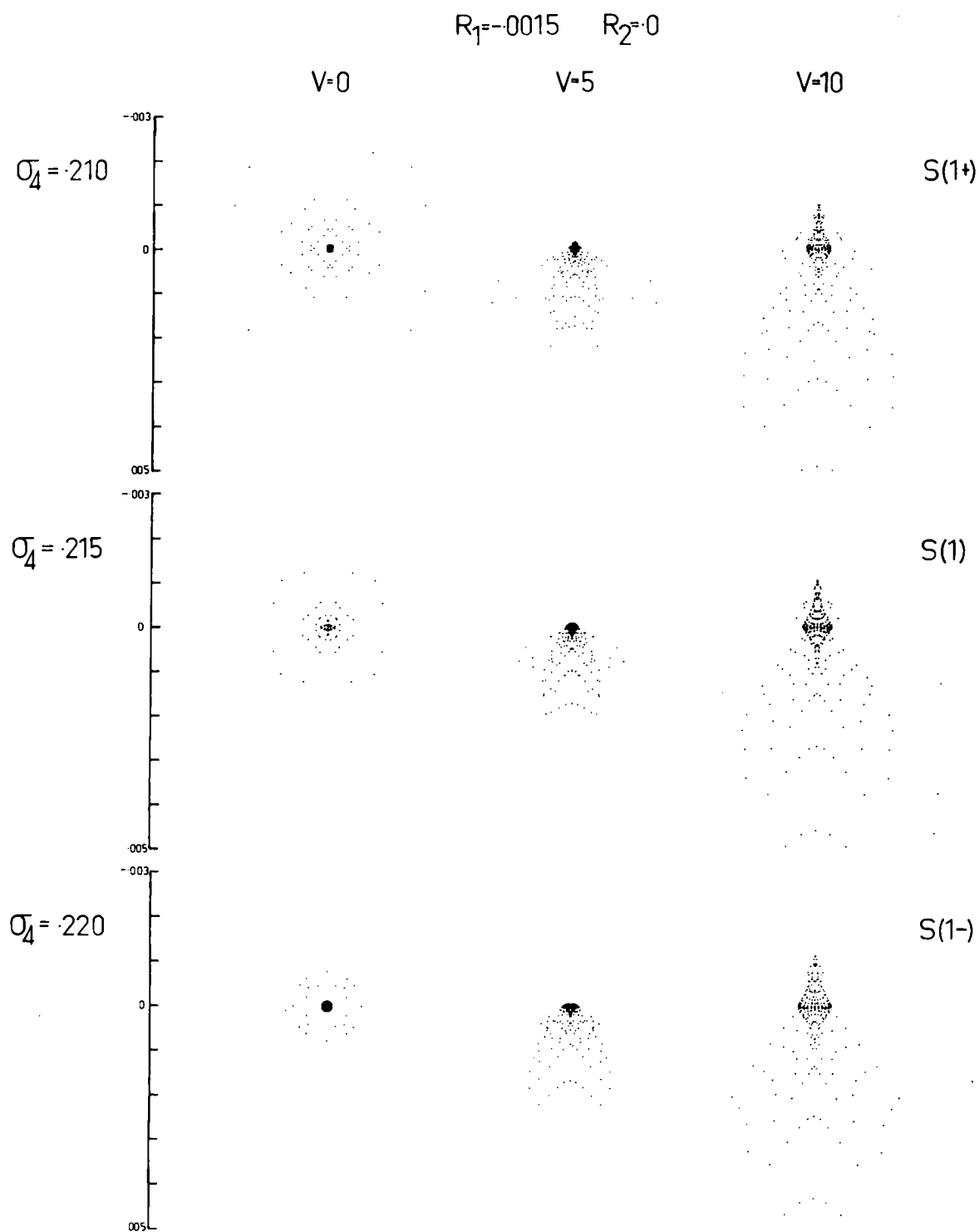


Fig. 2.38

given radius are shown against the radius in the left hand half of the table. The radius of the circle is measured in units of $f \times 10^{-4}$.

TABLE 2.6

| <u>Changing R_4</u> | | | | <u>Changing R_2</u> | | |
|------------------------------------|---|--------|--------|----------------------------------|-------|-------|
| Marginal Spherical $R_1 = -0.0015$ | | | | | | |
| System | SS(-1) | SS(1) | SS(+1) | SS(2) | SS(4) | SS(3) |
| Petzval R_4 | .210 | .215 | .220 | .215 | .215 | .215 |
| Coma R_2 | 0 | 0 | 0 | -.02 | -.06 | -.10 |
| Radius(\mathcal{U}) | Percentage Spots inside Circle of Radius (\mathcal{U}) at $V=0^\circ$. | | | | | |
| 1 | 80 | 82.5 | 73 | 77 | 78.5 | 67 |
| 2 | 80 | 87 | 92 | 83 | 80.5 | 78.5 |
| 3 | 80 | 92 | 92 | 83 | 85.5 | 83 |
| 4 | 85 | 92 | 92 | 88 | 92 | 85.5 |
| 5 | 87 | 92 | 94.5 | 88 | 92 | 85.5 |
| 6 | 87 | 97 | 95.5 | 90 | 92 | 90 |
| 7 | 92 | 97 | 95.5 | 92.5 | 92 | 90 |
| 8 | 92 | 97 | 100 | 92.5 | 92 | 90 |
| 9 | 92 | 97 | | 92.5 | 94.5 | 92 |
| 10 | 92 | 97 | | 92.5 | 94.5 | 94.5 |
| Spherical Coefficients | | | | | | |
| σ_1 | .092 | .135 | .178 | .124 | .101 | .078 |
| μ_1 | -6.99 | -7.24 | -7.50 | -7.13 | -6.91 | -6.69 |
| τ_1 | -0.506 | -21.08 | -40.5 | -16.76 | -7.75 | 1.40 |

We see that the process of choosing the LA'-curve with the minimum zonal aberrations in Figure 2.36(f) has enabled us to differentiate the spot densities of the axial image to within 3%. Such accuracy cannot be achieved with the

aberration coefficients. This evident from inspection of the spherical coefficients shown at the bottom of Table 2.6. These would lead us to select SS(-1).

2.5.9.2 Adjusting the Off-Axial Image of the Monochromatic System.

By inspection of Figure 2.38 it is clear that there is no significant difference in the appearance of the comatic flares of the off-axial images of the systems SS(-1), SS(1) and SS(+1). Therefore, the choice of SS(1) as the best system because of its superior axial image quality remains unchallenged when the field is taken into account.

The ray-coordinates ϵ_y^i and ϵ_z^i in the spot diagrams are plotted according to Buchdahl's convention in which, for example, a negative value of ϵ_y^i means that the ray intercepts the image plane above the ideal image point when the image is below the axis. Consequently, since the flare is directed downwards and is therefore positive then a negative residual of R_2 is required to balance it.

The balancing has been performed in three stages whose spot diagrams are shown in Figure 2.39. In order to achieve this the system SS(1) has been recomputed for $R_2 = -0.02$, $R_2 = 0.10$ and finally $R_2 = -0.06$. The resultant systems have been called SS(2), SS(3) and SS(4).

If we select the system with the most symmetrical off-axial spot-diagrams, then SS(3) is the obvious choice.

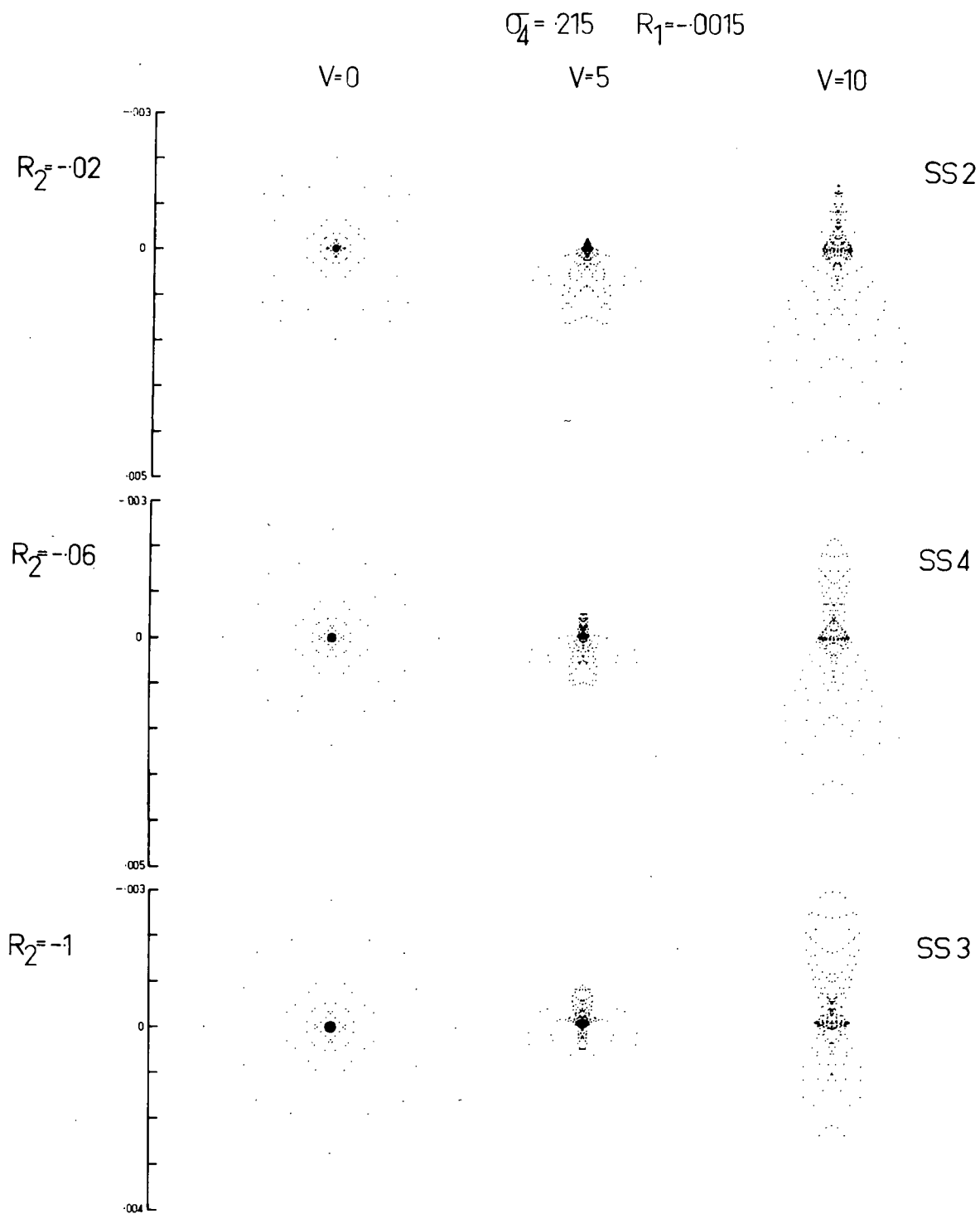


Fig. 2.39

TABLE 2.7

| System | | SS(2) | SS(4) | SS(3) |
|---------|-------|-------|-------|-------|
| Petzval | R_4 | 0.215 | 0.215 | 0.215 |
| Coma | R_2 | -0.02 | -0.06 | -0.10 |

| Radius (r) $f' \times 10^{-4}$ units | Percentage spots inside circle of radius(r) at $V = 5^\circ$. | | |
|---|---|-----|-----|
| 1 | 40% | 32% | 23% |
| 2 | 66 | 55 | 54 |
| 3 | 73 | 69 | 67 |
| 4 | 77 | 77 | 74 |
| 5 | 78 | 83 | 81 |
| 6 | 81.5 | 91 | 86 |
| 7 | 84 | 92 | 91 |
| 8 | 86 | 93 | 93 |
| 9 | 88 | 94 | 97 |
| 10 | 91 | 97 | 98 |

| Radius (r) $f' \times 10^{-4}$ units | Percentage spots inside circle of radius(r) at $V = 10^\circ$. | | |
|---|--|----|----|
| 1 | 9 | 10 | 7 |
| 2 | 19 | 18 | 18 |
| 3 | 40 | 35 | 34 |
| 4 | 49 | 49 | 51 |
| 5 | 54 | 54 | 54 |
| 6 | 59 | 57 | 59 |
| 7 | 65 | 62 | 63 |
| 8 | 67 | 65 | 67 |
| 9 | 72 | 69 | 69 |
| 10 | 72.5 | 72 | 72 |

If, on the other hand, we consider the spot density as well as the symmetry of the axial and off-axial point images, then we are inclined towards SS(4). We have already examined the spot densities of the axial pencils of SS(2), SS(3) and SS(4) in Table 2.6 and found SS(4) to be the most promising. Now we find nothing to alter this conclusion when we go off-axis.

The spot densities for 5° and 10° point-images of the systems SS(2), SS(3) and SS(4) are shown in Table 2.7 which complements the corresponding part of Table 2.6. There is little to choose between the densities of SS(2) and SS(4) but the flare at SS(2) seems less acceptable than that of SS(4). We will disregard SS(3) because it has only 23% of the spots in the first ring. In view of these and the above results we have developed SS(4) as the optimum system.

Before concluding the study of R_2 let us look at the effect the changes in R_2 have had on the group of LA'-curves that surround SS(1). Has this balancing of coma-flare disturbed the two-zone correction significantly? In other words, does R_2 interact with R_1 and R_4 appreciably? This question is examined in Figure 2.40 from which it is evident that there is a slight increase in the marginal zone near $R_4 = 0.215$. However, at this stage of the design, it is not worthwhile to alter R_4 . (We have showed since that the increase in R_4 of $\Delta R_4 = 0.005$ will restore the SS(4)

LA'-curve to the equivalent of that of SS(1) as it appears in Figure 2.36.)

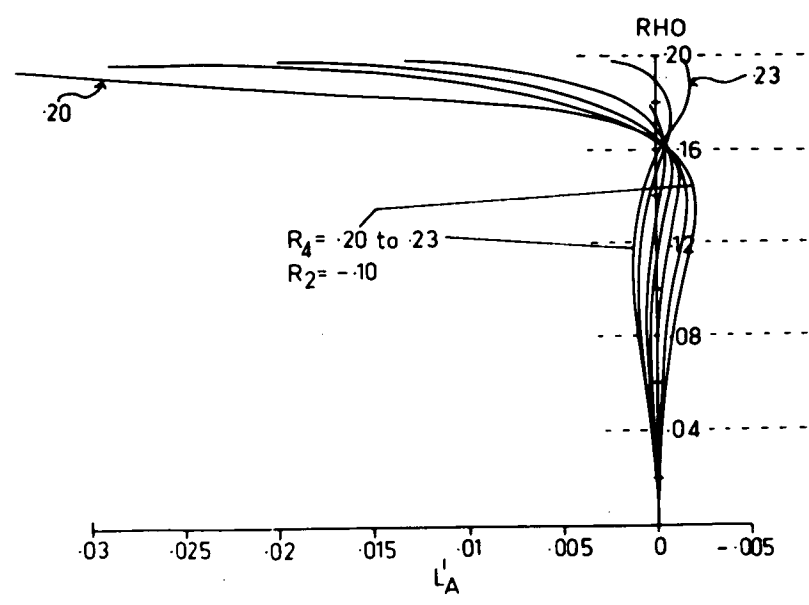
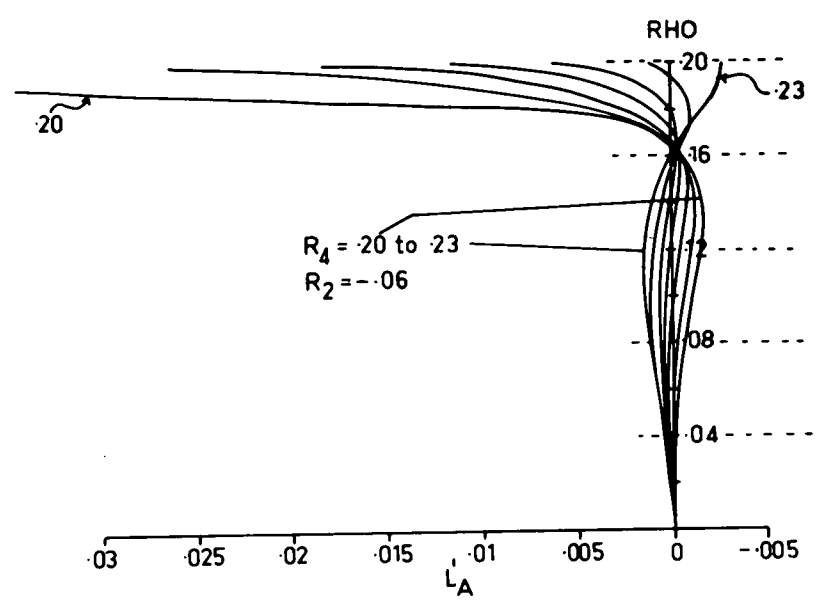
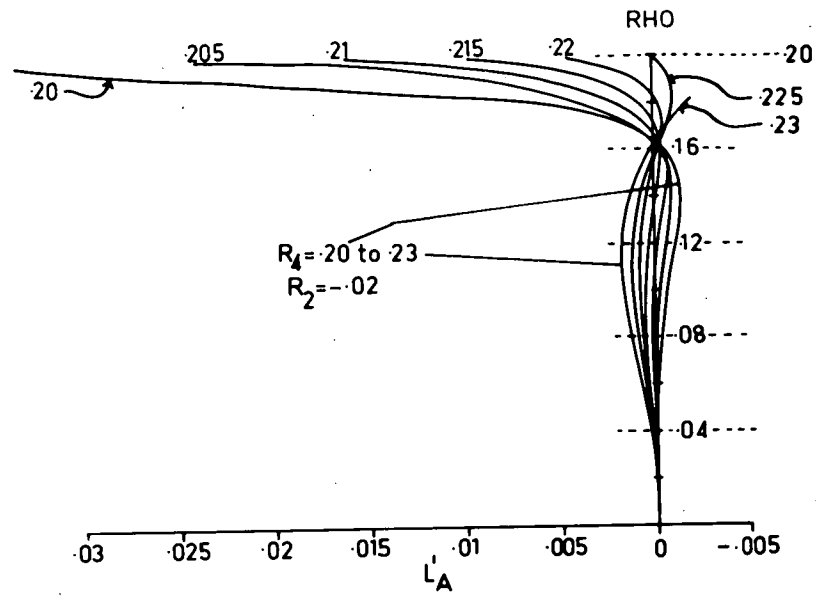


Fig. 2.40

CHAPTER 2.6 THE BASIC GLASS PARAMETERS AND THE OPTIMUM MONOCHROMATIC REGION.

2.6.0 Introduction.

In the preceding work we have examined the potential of the monochromatic-type 121 with respect to its basic parameters χ , k' , and P or their equivalent χ , k' and R_4 for a constant set of basic glass parameters (N_a, V_a) and (N_c, V_c) . So in order to conclude our study of the monochromatic design we must also consider the effects that changes in the basic glass parameters will have on the optimum region of (χ, k', P) -space. For instance, will some other combination of (N_a, V_a) and (N_c, V_c) cause an improvement in the convergence of the aberration coefficients with respect to χ , k' and P over what we have already achieved with glasses that were chosen on the basis of rules developed by other workers^(2.1, 3.2, 4.3) for the type 111 triplet?

The problem as we see it will not involve the basic glass parameters (N_b, V_b) which belong to the middle lens group b because, they have been studied implicitly through parameter k' . Through this earlier work we have shown V_b to be the more important parameter of this pair (N_b, V_b) . The conclusions made then agreed with similar observations arising from R.E. Hopkins' study of the type 111 triplet concerning the related quantity ΔV_b . (This

work^(4.3) supported our claim concerning the generality of the properties of the "basic parameters" of triplets.)

Therefore we must now consider the remaining basic glass parameters of lens group a and lens group b of the "basic triplet" of the type 121. Although in the type 121 these basic glasses of group a and group b are real glasses we will, for convenience, treat them as continuous variables. We lose nothing that is of value to us at this stage by doing this since our purpose is simply to determine whether or not the "optimum-monochromatic-region" which has been already established, is unique with respect to the basic glass parameters.

2.6.1 The Effect of Different Combinations of Basic Glasses.

2.6.1.1 Technique.

In order to provide an answer to the above question concerning the uniqueness of the optimum region, we have studied the trends in typical coefficients of the optimum-monochromatic-system (SS(4)) for comprehensive ranges of various combinations of the basic glass parameters. We recall that the system (SS(4)) is symmetrical and also has two-zone correction of spherical aberration, a flat tangential field and well corrected coma. In this study (SS(4)) has been recomputed at regular intervals of one or both of (N_a, V_a) and (N_c, V_c) . Therefore this work is a limited-interpolative-study of the basic glass paramet-

ers about the point SS(4) in our multi-variable space.

Three combinations have been studied, they are:

1. The system SS(4) with $N_a = N_c = 1.54$ to 1.70 in steps of $dN = 0.04$ and with $V_a = V_c = 56$ to 64 in steps of $dV = 4.0$.
2. The system SS(4) with $N_a = 1.54$ to 1.70 in steps of $dN = 0.04$, $V_a = 56$ to 64 in steps of $dV = 4.0$ and $N_c = 1.62101$, $V_c = 60.18$.
3. The system SS(4) with $N_c = 1.54$ to 1.70 in steps of $dN = 0.04$, $V_c = 56$ to 64 in steps of $dV = 4.0$ and $N_a = 1.62101$, $V_a = 60.18$.

The results are shown in Figures 2.41, 2.42 and 2.43.

In each figure the spherical coefficients of 3rd, 5th and 7th order (τ_1, μ_1, τ_1) and representative pairs of 5th order comatic coefficients (μ_2, μ_7) and 5th order astigmatic coefficients (μ_4, μ_{10}) are plotted against N for three values of V .

2.6.1.2 Discussion of Type 121 versus Basic Glass.

From a cursory inspection of Figures 2.41, 2.42 and 2.43 it is evident that we cannot improve on our initial set of glasses. Thus the selection of glass for the type 121 on the basis of Cruickshank's^(2.1) observations of the thin-lens parameters α and β of the type 121 is sound and, therefore, supports the fictitious-glass-theory. Indeed, with $N_a = N_c$ and $V_a = V_c$ (Figure 2.42) the only obvious improvement is made by increasing V to 64. This

reduces coma and astigmatism but it increases the primary spherical and, therefore, the field is improved at the expense of the aperture.

Figure 2.42 shows that there is a slight improvement in coma and astigmatism when $V_a = 64$ but this is not enough to make us pursue such a change.

In Figure 2.43 we see that an increase in N_c and V_c of the rear lens may produce a worthwhile improvement in both the coma and astigmatism. For example, if we make $N_c = 1.7$ and $V_c = 64$ then we get considerable reduction in \mathcal{M}_{10} , \mathcal{M}_2 and \mathcal{M}_7 . As for the spherical it appears that \mathcal{T}_1 , \mathcal{M}_1 and \mathcal{T}_1 are not significantly different from those of SS(4) and therefore zonal correction should be good. Consequently, in order to improve on the field of the type 121 already obtained, it would seem that an increase in the refractive index and V-number of the rear lens group c offers the most promise.

2.6.2 Proposing a Fictitious Glass for Lens Group c.

It is clear that none of the improvements suggested by the above results can be made with real glasses. The practical alternative is to construct a "fictitious basic glass" with the desired N and V for lens group c . This sort of thing, of course has been done with the Tessar which has resulted in an improvement on the field of the type 111 triplet.

A study of successful Tessar designs shows that their values of N_c and V_c are of about the same magnitude as those predicted in the above glass study of the type 121. This encourages us to proceed along these lines in an attempt to increase the field of the type 121 triplet without losing its zonal correction. Thus the study of the basic glasses (N_a, V_a) and (N_c, V_c) indicates that the type 122 may combine the best features of both the Hektor (type 121) and the Tessar (type 112).

We will leave the development of the type 122 until we have completed the design of the type 121. However, before returning to the type 121, let us select the fictitious-glass for lens group c.

2.6.3 Selecting the Fictitious Glass.

In pursuance of the combination of a Tessar with a Hektor, we have chosen the rear component of a Tessar (the 7A) that has been designed and constructed in this laboratory. The flint component of this cemented doublet is the Bausch and Lomb glass CF1(1.5282, 51.4) and the crown is the Chance glass DBC(1.6133, 57.5). The k' used in this Tessar is $k' = -1.8181$ and, therefore, this is a positive reversed doublet (PRD see section 1.1.3). A value of about $k' = -1.8$ is typical of the Tessars published in Von Rohr⁽¹⁹⁾.

The fictitious glass constants N_f and V_f corresponding to $k' = -1.8181 \dots$ are $N_F = 1.734$, $V_F = 67.5$. N_F and V_F are shown plotted against k' in Figure 2.44 in which the crossed-points are those quoted above for N_F and V_F .

$N_0 = N_c = 1.54$ to 1.70 $dN_0 = dN_c = 0.04$
 $V_0 = V_c = 56$ to 64 $dV_0 = dV_c = 4.0$

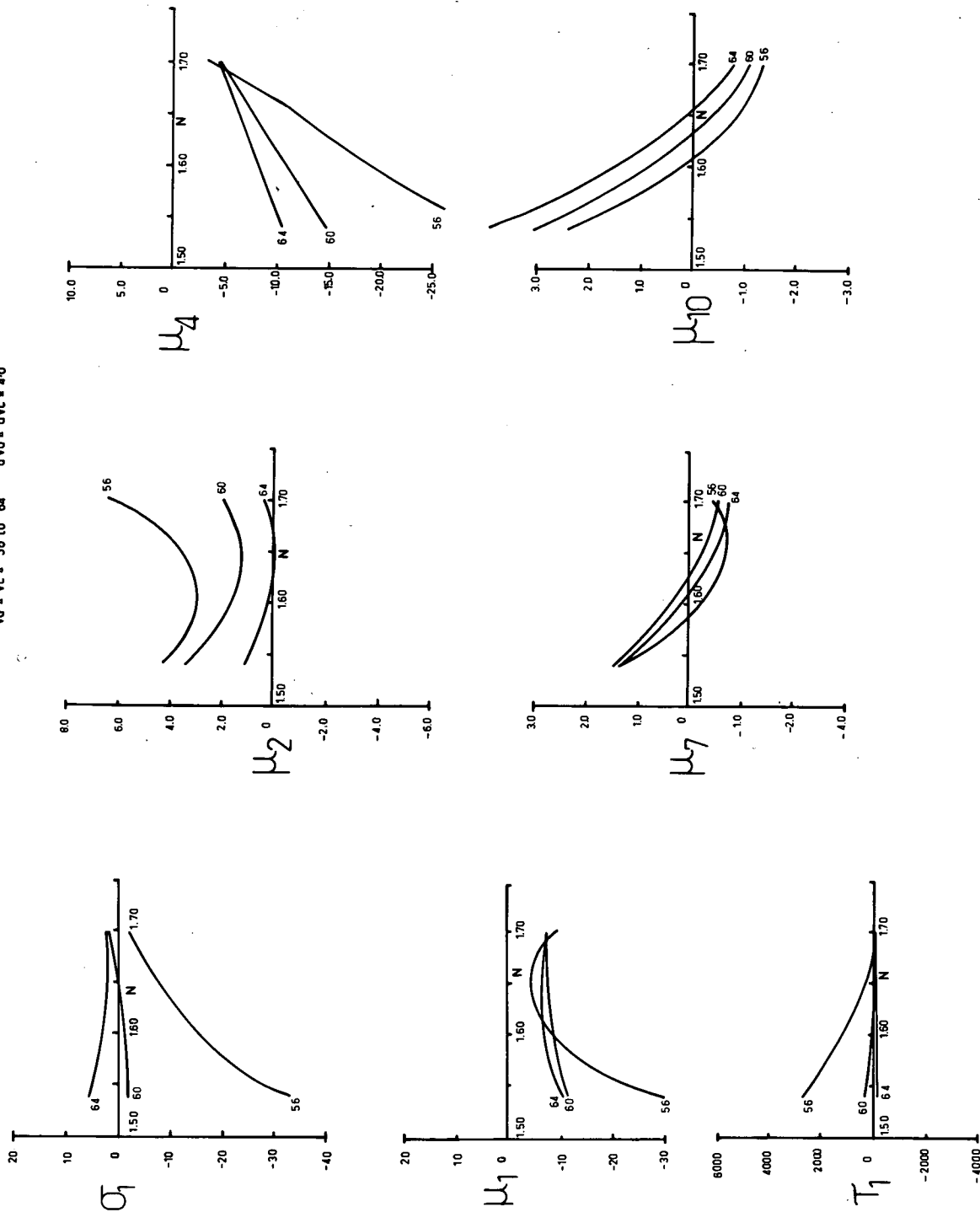


Fig. 2.41

$N_a = 154 \text{ to } 170$ $dN_a = 0.04$
 $V_a = 56 \text{ to } 64$ $dV_a = 4.0$

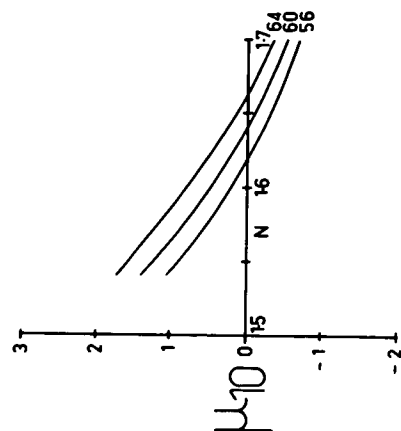
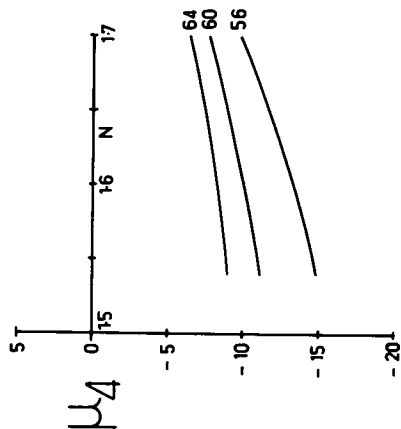
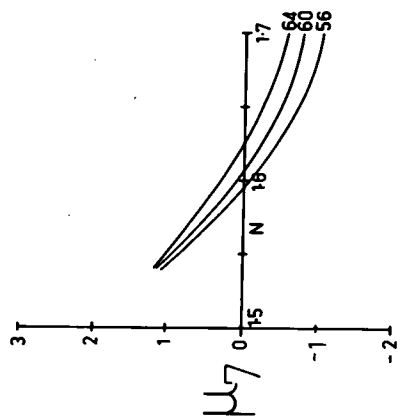
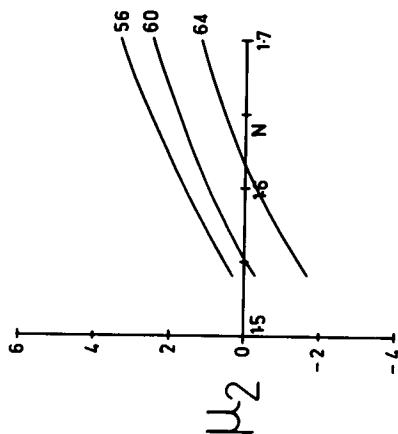
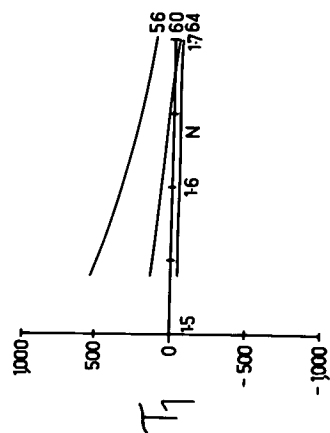
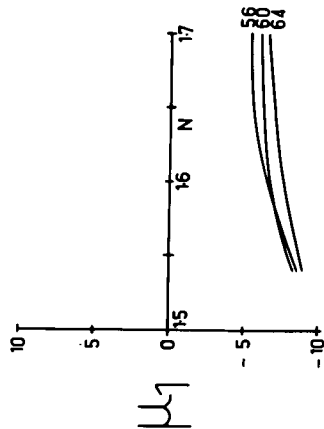
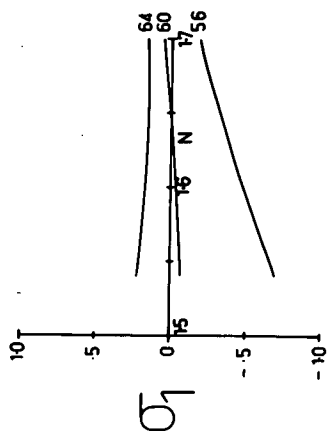
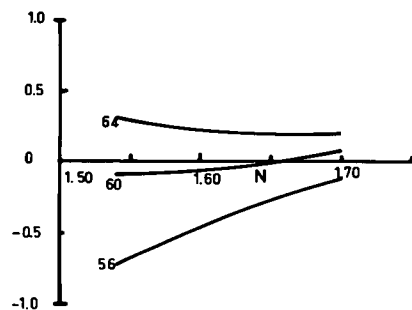


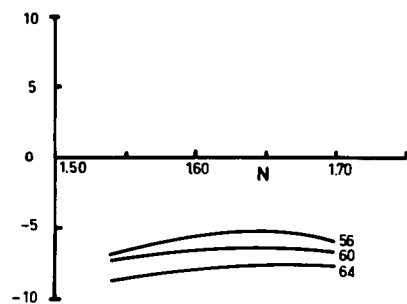
Fig. 2.42

Fig. 2.43

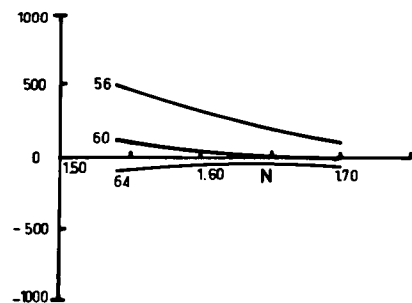
q



μ_1

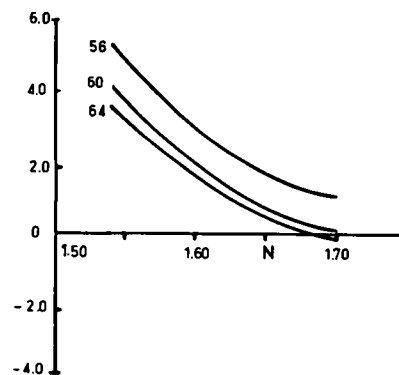


T_1

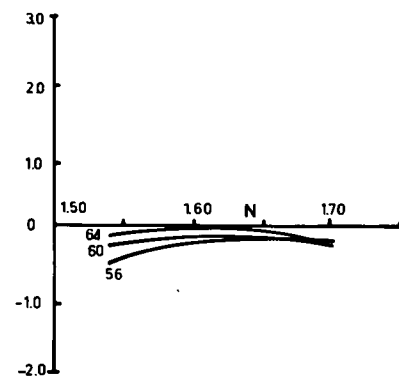


$N_c = 1.54$ to 1.70 $dN_c = 0.04$
 $V_c = 56$ to 64 $dV_c = 40$

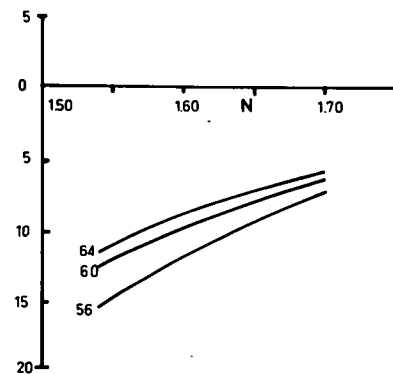
μ_2



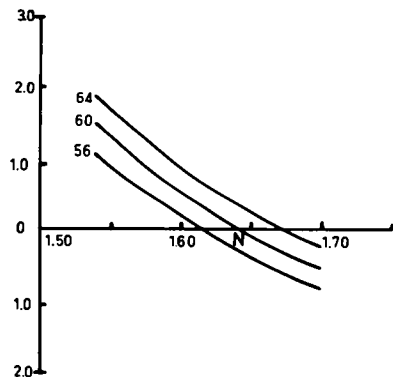
μ_7



μ_4



μ_{10}



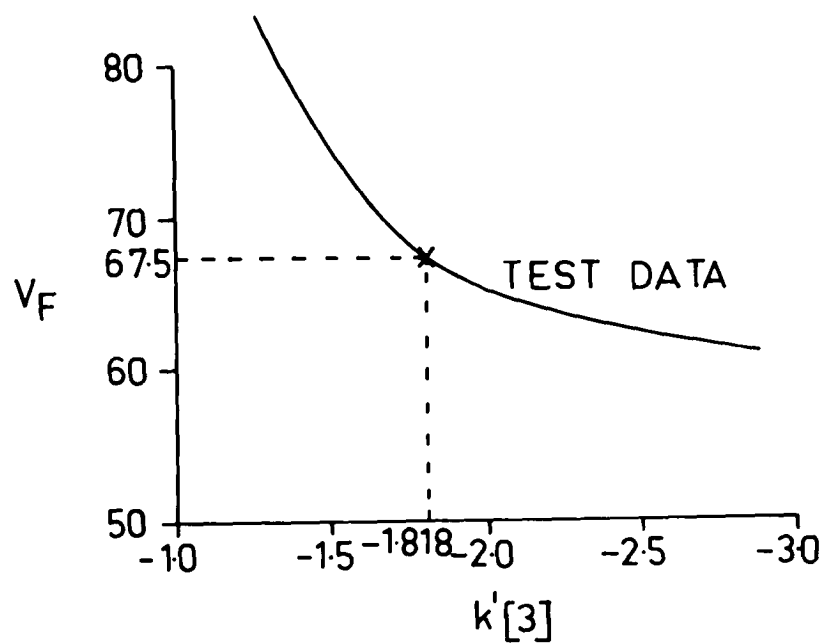
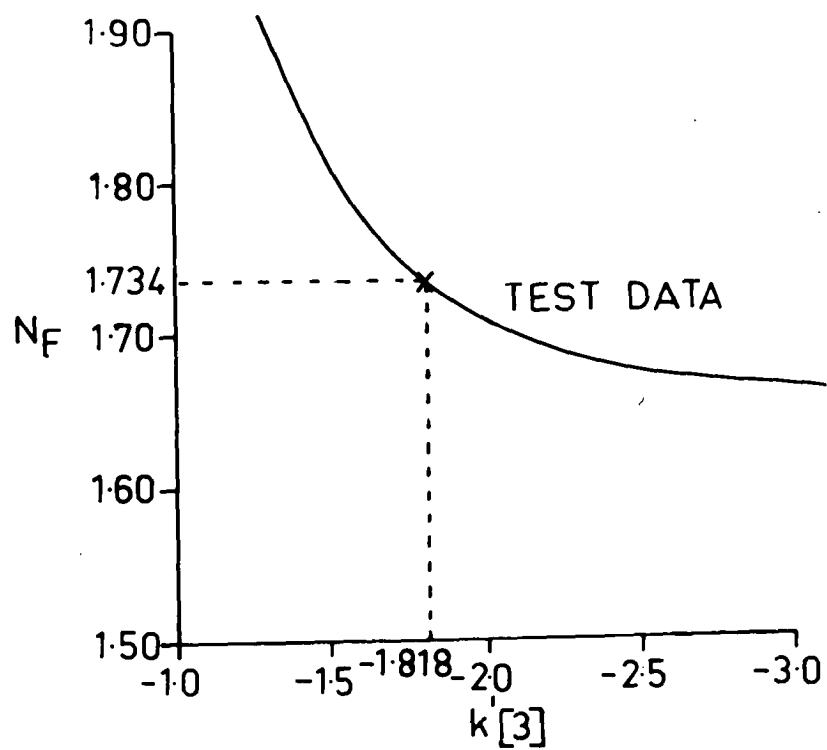


Fig. 2.44

SECTION 3.

CHROMATIC DESIGN

CHAPTER 3.1 DEVELOPING THE CHROMATIC TYPE 121.

3.1.0 Introduction.

In the sub-section 1.1.5 we discussed the degrees of freedom and concluded that they can be divided into two classes which simplify the design process. Thus we are able to pursue, for example, the design of the type 121 in two stages, a monochromatic stage and a chromatic stage.

The monochromatic stage was completed in Section 2 where the optimum monochromatic type 121 system SS(4) was developed from a particular set of real glasses. The set of glasses chosen was shown to be about the best that can be selected from the set of real glasses as far as the monochromatic system is concerned.

In Section 2 the type 121 system was optimized with respect to the "monochromatic-basic-construction parameters" λ , k' , P , S_1 , S_2 , S_4 , N_a , N_b , N_c , V_a , V_b and V_c . Thus the remaining construction parameters are the "chromatic-basic-construction parameters" L and T which, according to other workers, seem to have little effect on the monochromatic aberrations. Also, we recall that the initial values of L and T have been selected on the basis of the design experience of other workers with a view to minimizing the chromatic aberrations of the "monochromatic systems" of which SS(4) is the final one. Therefore, at this stage, we anticipate making only minor

changes in the L and T of this final monochromatic system SS(4) in order to develop an achromatic system from it, there being no need it seems to alter its monochromatic parameters.

We have already achieved an advanced stage of design in the form of a well corrected monochromatic system, therefore, from now on it seems futile to consider any quantity less than the exact chromatic aberration that is calculated from trigonometrical-ray-traces made in the final stage of the design process (see Figures 2.1, 2.2). Admittedly chromatic aberration coefficients have been developed, for example, by Buchdahl, but these only afford accurate predictions up to an aperture of $f/6.5^{(13.1)}$. Indeed, even from our own experience with LA' versus ρ of the monochromatic system, we can conclude that the chromatic predictions to 7th order are of little use beyond $f/3.5$. Consequently, in our approach to studying and optimizing the chromatic aberrations of the type 121, we will work between the first and last stage of the design process mapping, for example, LA' -curves for different wave-lengths against the basic parameters L and T .

We begin our attack on the chromatic aberration of the type 121 by studying the chromatic aberration of the axial pencil of rays because, this is a logical extension of our work with LA' in Section 2. After we have adjusted LA' we will consider the chromatic aberration of

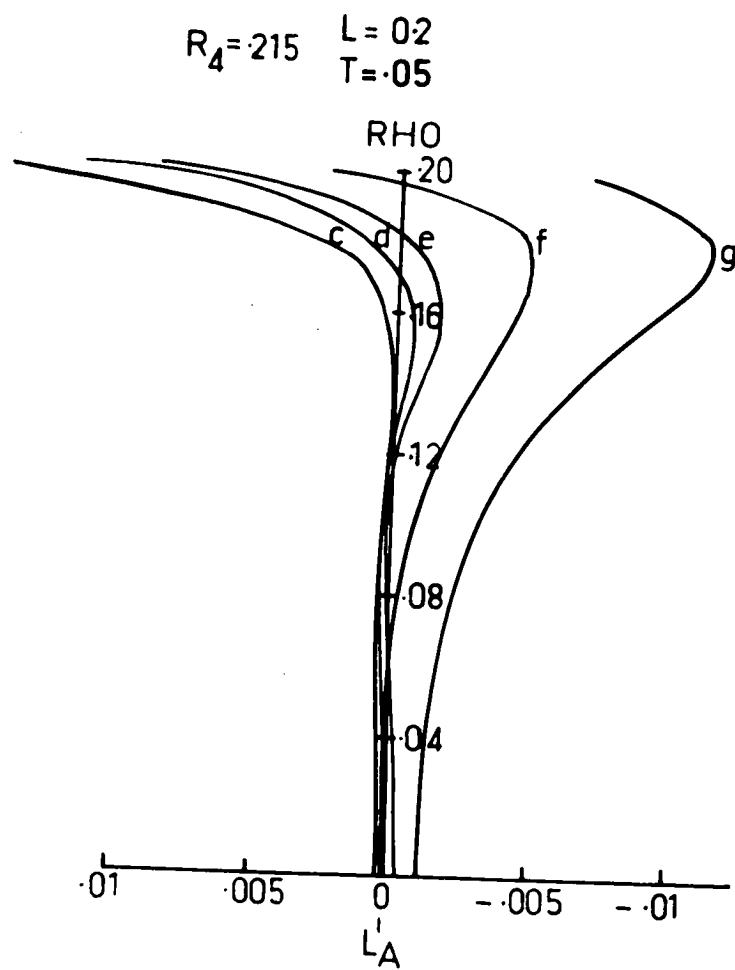


Fig. 3.1

the field by studying the transverse chromatic aberration versus field angle versus wave-length (λ). Thus we are assuming, initially, that not only do L and T act independently of the "basic-monochromatic-parameters" but also that they act independently of each other. This appears to be consistent with the opinion held by most workers in optical design.

3.1.1 The Chromatic Aberration of the Optimum Monochromatic System SS(4).

We begin our attack on the chromatic parameters by looking at the chromatic aberration of the optimum monochromatic system SS(4).

The zonal spherical aberration of SS(4) is plotted for the five standard wavelengths c, d, e, F, and g in Figure 3.1. This diagram shows implicitly the variation of the longitudinal chromatic aberration with respect to ρ from $\rho = 0$ to $\rho = 0.20$.

The parameters L and T have been selected in our initial design so as to make the paraxial quantities lch' and tch' zero for the c and F wavelengths, or nearly so, in the final system SS(4). However, we find for these initial values ($L = 0.2$ and $T = 0.05$) that SS(4) has $lch' = 0.0006$ and $tch' = 0.00026$. They are not zero but it is evident from Table 3.1.1 that they are well within tolerance for $f' = 4.00$ inches. (Note the computed values in

Table 3.1

| | Computed Values for SS(4) | | | | Theoretical Values | |
|--------------------------|---------------------------|---------|---------|-----------|--------------------|-------------|
| Zonal Radius | LA' versus Focal Range | | | | Tolerances | |
| | LA'd | LA'c | LA'F | LA'c-LA'F | LZA' | Focal Range |
| .02 | .00005 | -.00005 | .00005 | -.0001 | .6 | .1 |
| .04 | .0001 | -.00032 | .00005 | | | |
| .06 | .00027 | -.0001 | -.00002 | | | |
| .08 | .00036 | .00009 | -.00024 | | | |
| .10 | .00033 | .00023 | -.00071 | .00094 | .01 | .0016 f/5 |
| Focal Range fails .12 | .000099 | .00025 | -.00156 | .004 | .008 | .0013 f/4 |
| .14 | -.00031 | .00018 | -.00285 | .00303 | .005 | .0008 |
| LZA' fails .16 | -.00052 | .00048 | -.00432 | .00480 | .0047 | .0008 |
| .18 | .00116 | .00295 | -.00459 | .00754 | .0037 | .0006 |
| .20 | .01146 | .01450 | .00258 | .012 | .003 | .0005 |

$$LZA' = 6 \text{ wavelengths} / N' \sin^2 U' m$$

$$\text{Focal Range} = 1 \text{ wavelength} / N' \sin^2 U' m$$

(Conrady^(17.1) P138 and P199)

the table are for $f' = 1.0$, therefore they must be multiplied by 4.)

Actually, it is the zone at about $\rho = 0.07$ and not the paraxial zone, that has a common image plane for the c and F wavelengths. They are focussed at $x = -0.0005$ from the ideal image plane. Beyond $\rho = 0.07$ both the spherical and longitudinal chromatic aberrations continue to increase but the tolerances are not exceeded until ρ lies in the range $0.12 < \rho < 0.16$. The focal range fails after $\rho = 0.12$ and the zonal aberration fails after $\rho = 0.16$.

In Figure 3.2 we have the axial-spot-diagrams of the system SS(4) at an aperture of $f/2.5$ for the five standard colours c, d, e, F and g and also the off-axial spot diagrams at 5° and 10° in d-light. (The off-axial diagrams are included in d-light only, in this and all later arrays of spot diagrams, with the exception of Figure 3.2, for the sole purpose of detecting any unusual variation in the monochromatic correction-state of the field while we are correcting the axial colour.)

The Figure 3.2 shows very clearly by the size of the halo around c and F spots that the blue end of the spectrum is well out of adjustment. However, it is evident from the Figures 3.1 and 3.2 that the system SS(4) would be almost satisfactory for a maximum aperture somewhere between $\rho = 0.12$ and $\rho = 0.14$ ($f/4$ to $f/3/5$). In view of this evidence the problem of controlling the chromatic

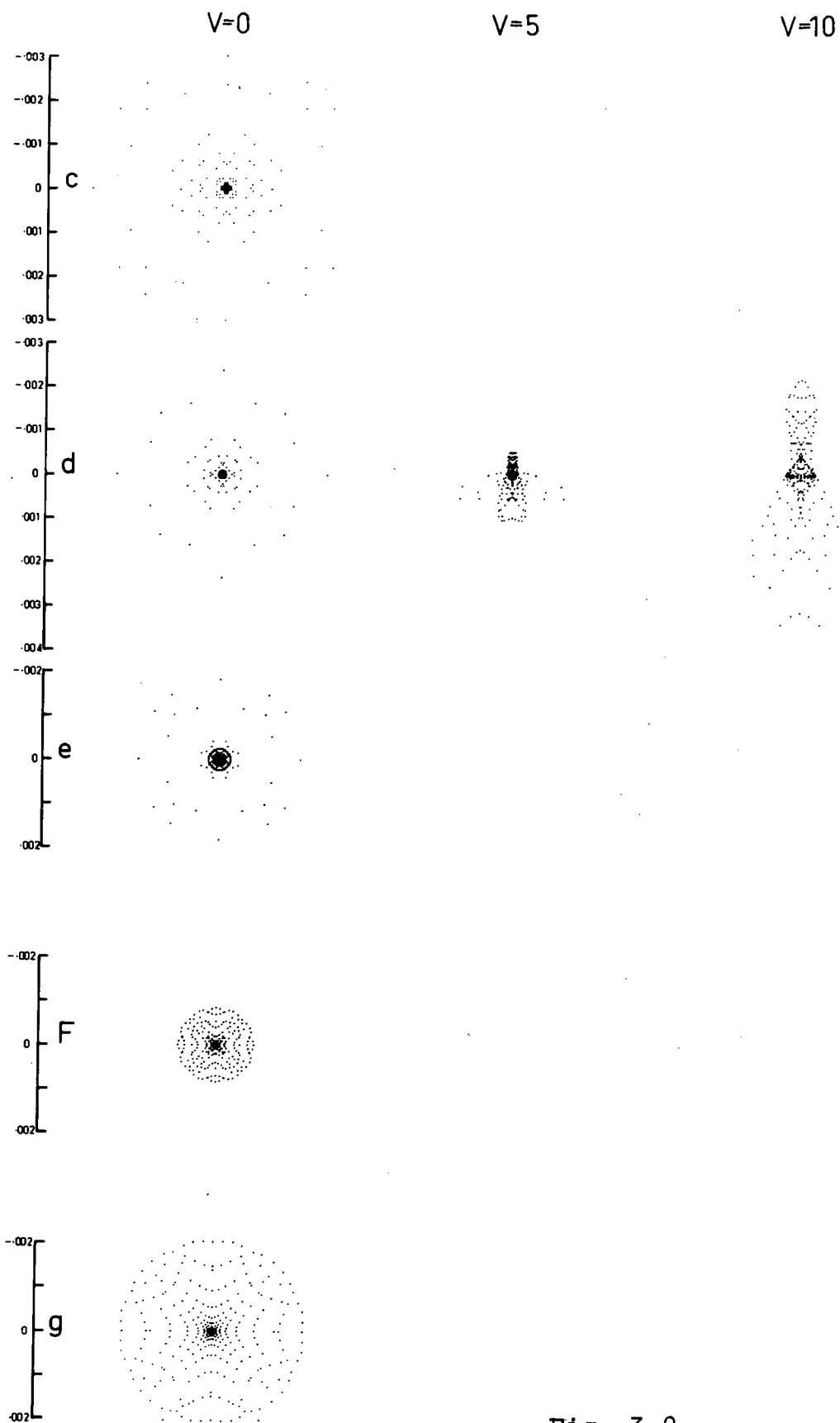


Fig. 3.2

aberrations is similar to the monochromatic design problem already treated in that it is once again mainly one of controlling the zones beyond $f/3.5$.

3.1.2 The Effect of Changing L.

In the first attempt to improve the longitudinal chromatic aberration of SS(4) we decided to make lch' and tch' zero. This was achieved by iterating the 3rd order triplet with respect to L and T until lch' and tch' were within $\pm (10^{-5})$ of zero. Although this iterative process was discarded after adjusting lch' and tch' in favour of the more logical design process of relating L and T to quantities computed from trigonometrical-ray-traces, nevertheless, the changes that occurred in this instance form an interesting step in colour control.

After automatically adjusting lch' and tch' to zero by iteration, L has become $L = 0.165$, T has become $T = 0.025$ and the focal plane of the c and F wavelengths from the axial zone has changed from $LA' = -0.0005$ to $LA' = -0.00037$. We see in Figure 3.3 that the inner zones have improved slightly but unfortunately at the same time the marginal and intermediate zones have deteriorated compared with those in Figure 3.1. The intermediate zones, however, have greater longitudinal chromatic aberration and the marginal zones have greater spherical aberration than system SS(4). In view of our initial assumptions we do not ascribe any of these zonal changes to T. Thus a small

$R_A = .215$ $L = .165$
 $T = .023$

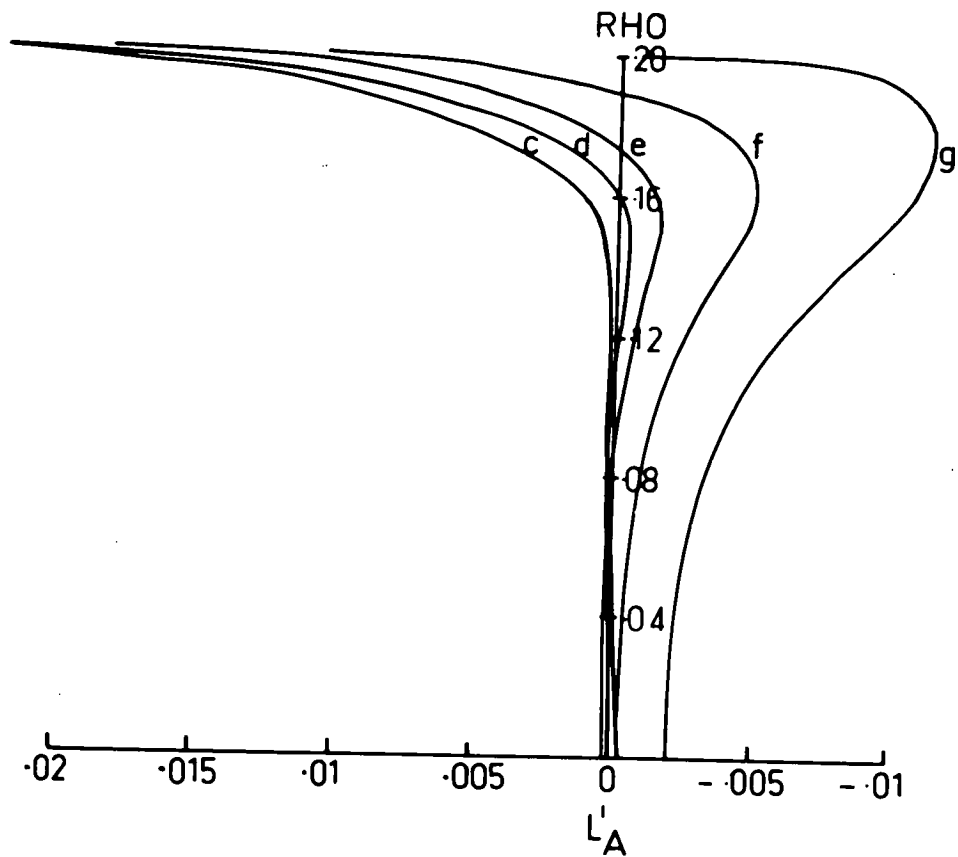


Fig. 3.3

change in L of $L = -0.035$ has had little effect on the zones below $\rho = 0.15$ but, it has on the other hand, produced significant changes in the intermediate and marginal zones even though they are unsatisfactory changes. This attempt to improve the chromatic aberration of the lower zones by iteration has caused a substantial increase in the chromatic aberration of the outer zones, but this is not serious as the increase produced in the spherical aberration of these marginal zones. Clearly, improvement of both the longitudinal chromatic and the marginal spherical aberration must lie in the direction of increasing L .

Let us now examine the effect of L alone. We will make this new chromatic study of the type 121 at $T = 0.025$ so that the systems from now on will satisfy our original condition that tch' be zero. However, since it is expected that changing T from 0.05 to 0.025 has no significant influence on the axial image then we can assume that the continuity between these later systems at $T = 0.025$ and SS(4) at $T = 0.05$ will be preserved as far as L and the LA' -curves are concerned.

The first change in L is shown in Figure 3.4 where L has been increased to $L = 0.25$ and, therefore, except for T and L this system is the same as SS(4) in all other respects. This increase in L has reduced the longitudinal-chromatic-aberration of all zones substantially and also completely reversed the spherical aberration of the

$$R_4 = .215 \quad L = .25 \\ T = .025$$

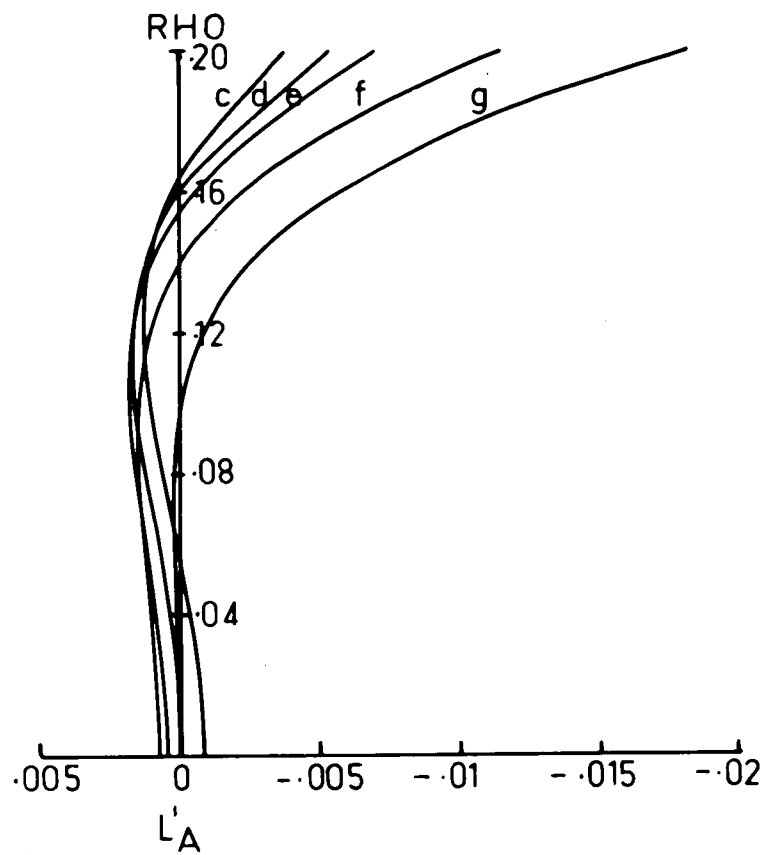


Fig. 3.4

marginal zones. A further increase in L to $L = 0.3$ is seen in Figure 3.5 to have produced a very even balance of chromatic aberration of all zones while, at the same time, it has caused only a slight increase in the marginal spherical in excess of that at $L = 0.25$.

Indeed, the system shown in Figure 3.5 is well corrected for both zonal chromatic and spherical aberration up to an aperture of $f/3.1$ ($\rho = 0.16$). The set of curves is of similar shape to those of Pentacs (see Figure 3.27, chapter 3.3) designed by Argentieri and Cruickshank. (These systems are similar in that they have over-corrected marginal spherical combined with well-corrected longitudinal chromatic aberration.)

3.1.3 Zonal Achromatism and Reduced Petzval. (The effects on the zonal aberration of combining R_4 and L .)

We have found by increasing L that we have achieved reasonable achromatism for all zones up to an aperture of $f/3.1$ but in doing so we have lost two-zone correction. However, in the following we see that a comparison of the broad behaviour of the LA' -curves of this chromatic study with that of the LA' -curves of the R_4 study leads us to a unique solution of the type 121 triplet, and, in addition initiates a fresh understanding it seems of the general problem of convergence of triplet solutions.

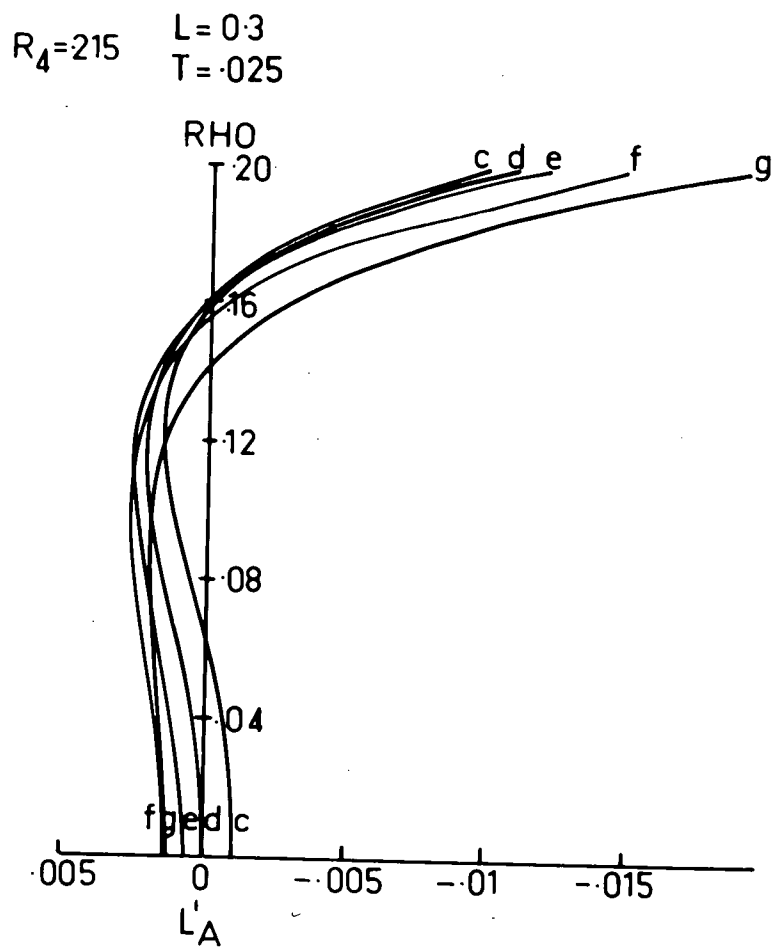


Fig. 3.5

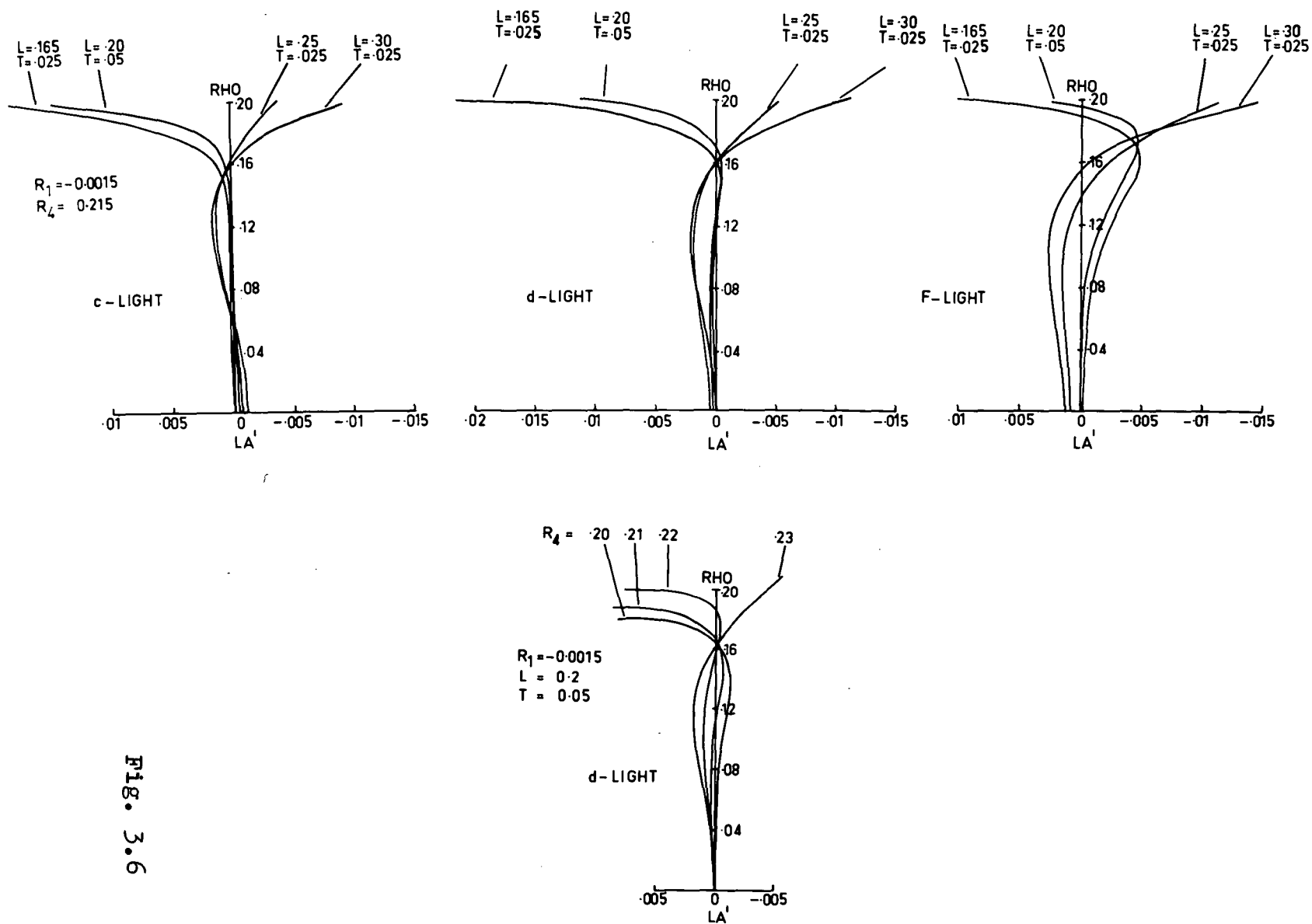


Fig. 3.6

If we consider the shape of the LA' -curve of a particular colour as we progress through the Figures 3.3, 3.4 and 3.5 then we get a group of curves that is similar to a group of LA' -curves versus R_4 which were plotted in Figures 2.35 and 2.36. It is evident that LA' versus ρ versus L is similar to LA' versus ρ versus R_4 . Following this idea further, we see that the LA' -curves of Figures 3.4 and 3.5 are reminiscent of those with R_4 greater than the optimum R_4 -value of the monochromatic systems. Therefore, it is evident that the spherical aberration of the intermediate and marginal zones (the zones above the stationary zone at $f/3.5$) may be changed from positive to negative by increasing either L or R_4 . This property offers the very interesting possibility of correcting the colour whilst at the same time reducing the Petzval curvature. Thus by applying this property we propose to recover the spherical balance of the marginal zones without, we hope, losing the chromatic correction.

The effect of L on LA' versus ρ with λ constant is shown in the top row of Figure 3.6 for c-light, d-light and F-light. Directly beneath the d-light graph we have the effect of R_4 on LA' versus ρ in d-light. Comparing the d-light diagrams confirms that there is a remarkable similarity between the effects of R_4 and L on the monochromatic system.

$$R_4 = .20 \quad L = .25$$

$$T = .025$$

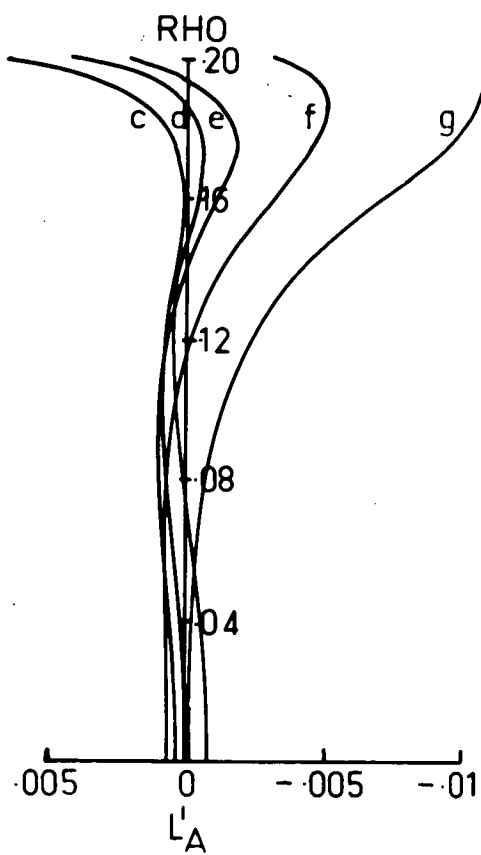


Fig. 3.7

It is clear from the top row of graphs of Figure 3.6 that the effect of L on the marginal zones remains largely unaltered as the wavelength changes. Therefore, the possibility of controlling the marginal spherical of the chromatic system with R_4 is seen to be very probable at this stage.

The reduction of R_4 was first performed for the system with $L = 0.25$. We chose this system first, because R_4 was more likely to reverse a modest aberration of the marginal zone than the larger aberration associated with a larger value of L . (This decision was made as a result of our earlier experience with marginal zones and R_4 .)

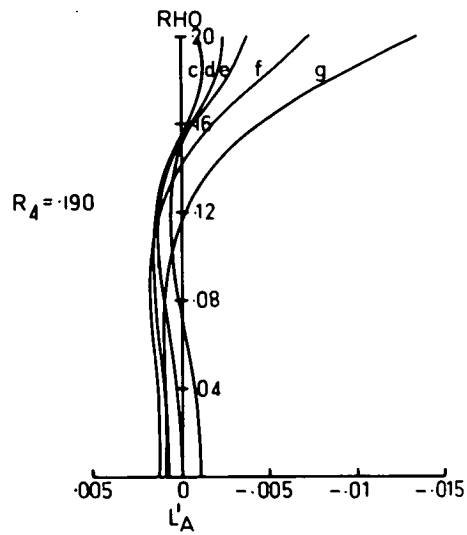
This system at $L = 0.25$, $T = 0.025$ with R_4 reduced by $\Delta R_4 = 0.015$ to $R_4 = 0.20$ is shown in Figure 3.7. As we had anticipated, the marginal zones are reversed and also, as we hoped, much of the chromatic correction is retained.

After the successful balancing with the smaller value of L we sought the reduction of the marginal zones of the system with $L = 0.30$. This was pursued in three steps, the results of which appear in Figure 3.8 where we have LA' versus the five standard wavelengths for $R_4 = 0.19$, 0.185 and 0.180 . From these it is evident that the reduction of R_4 below $R_4 = 0.185$ begins to introduce serious under-correction of the marginal zones. Thus $R_4 = 0.185$ appears to be the optimum system at $L = 0.30$ and $T = 0.025$. We have called this system SS(15).

The spot diagrams of SS(15) are shown in Figure 3.9. An obvious improvement has occurred in the axial colour of SS(15) over that of SS(4) (see Figure 3.2) but further improvement is required. Also, the comatic flare is still rather large at 5° off-axis. However, we notice that the off-axial spot diagrams follow the trend of the axial spot diagrams. Consequently, the effect of L on the off-axial spot diagrams can be inferred from the axial spot diagrams. Therefore, a plot of the field in d-light seems sufficient when the axial spot diagrams are available for all colours.

Before continuing with the correction of colour, it was considered worthwhile to readjust the coma of SS(15) by further increasing the negative 3rd order coma residual (R_2). This was completed in two stages, the sequence commencing at SS(15) with $R_2 = -0.06$ and passing through $R_2 = -0.08$ to $R_2 = -0.2$. The spot diagrams used to assess this adjustment are not reproduced here because the effect has been seen in other systems, for example, those in Figure 2.39. However, we have reproduced the groups of LA'-curves versus ρ versus wavelength for the two stages in Figure 3.10 so as to show that R_2 has a small yet significant effect on the zonal spherical aberration beyond $f/3.5$. It is evident that the reduction of R_2 has induced small increments in both the zonal spherical and longitudinal chromatic aberration.

L = .30
T = .025



System SS15

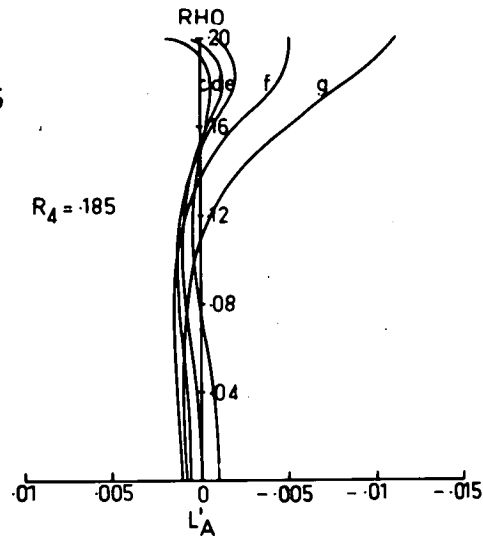
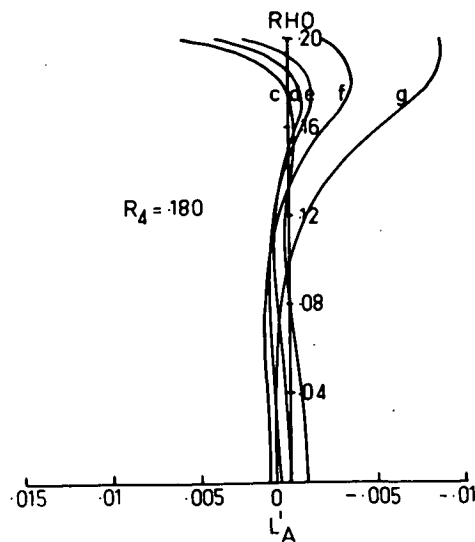


Fig. 3.8



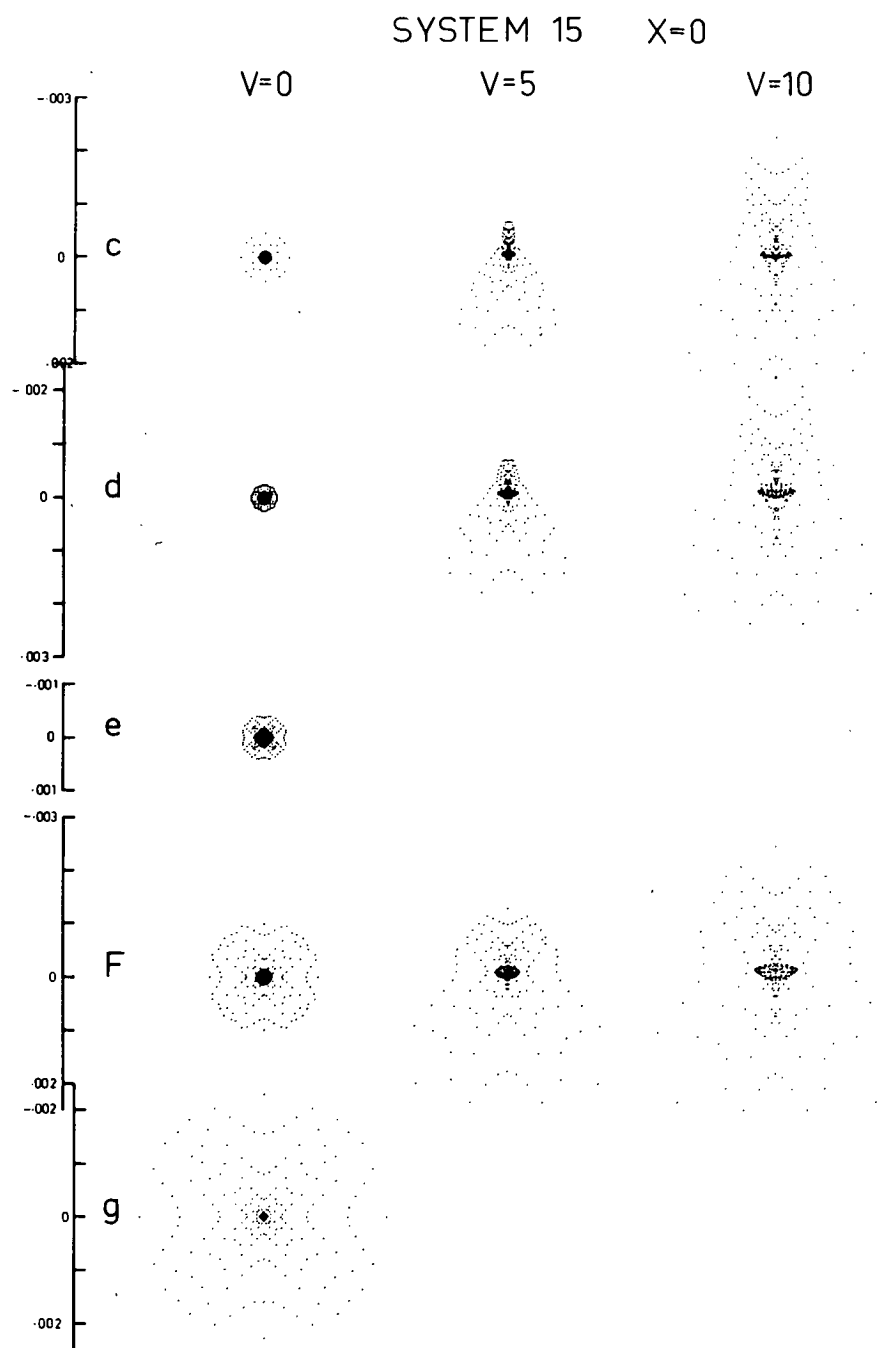


Fig. 3.9

L=30 T=.025 R₄=.185

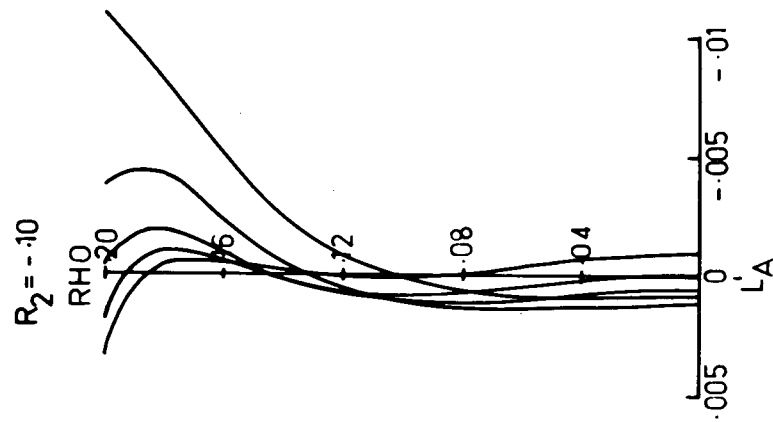
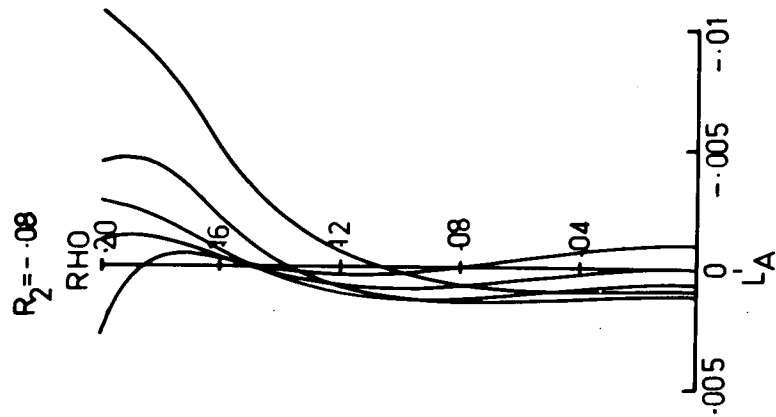
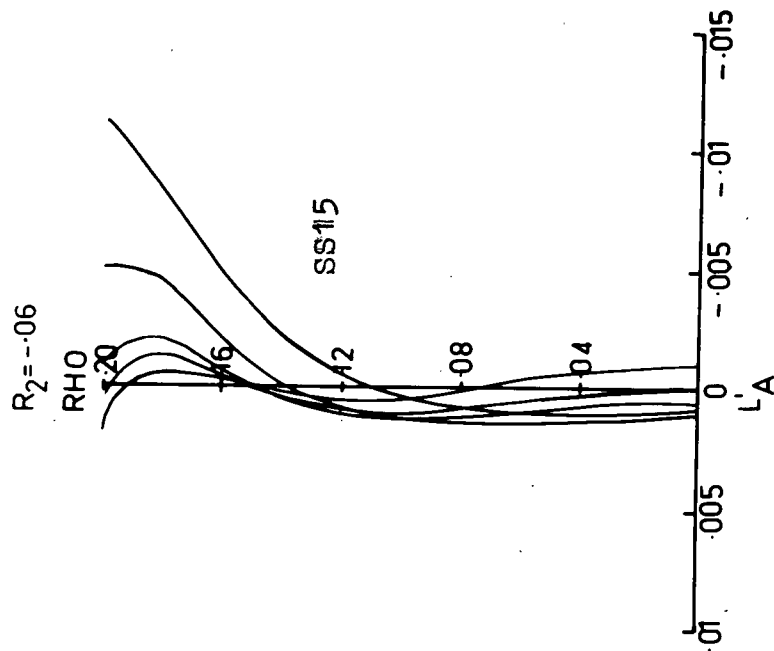


Fig. 3.10

Conclusions.

We can summarize the results of the study of L and R_4 with the following two rules:

1. The spherical aberration of the marginal zones ($> f/3.5$) is decreased by increasing either L or R_4 .
2. As the chromatic aberration of the marginal zones is reduced the optimum system occurs at smaller values of the Petzval sum.

Clearly an earlier assertion of the independence of L and R_4 (or P) does not apply to the marginal zones.

3.1.4 Adjusting the Transverse Chromatic Aberration with T and its Effect on the Longitudinal Chromatic Aberration and the Petzval Curvature.

3.1.4.1 Final Adjustment of L and R_4 .

After discovering how to control the zonal aberrations with L and R_4 three closely related systems were developed. The first of these was generated with the aim of having the smallest possible Petzval associated with the smallest possible chromatic and monochromatic zonal aberrations, especially in the marginal zones. In view of the work of the preceding section, this type of correction-state was sought by simultaneously increasing L and reducing R_4 as far as practicable. The optimum system satisfying these conditions was obtained with $L = 0.4$ at the surprisingly low value of $R_4 = 0.130$ (c.f. SS(4))

with $R_4 = 0.215$, see section 2.5.9.2). The LA' versus ρ versus wavelength curves of this system which we will call SS(20) are plotted in the left hand position of the middle row of Figure 3.11.

Beyond $L = 0.4$ it was found that little improvement occurred in the longitudinal chromatic aberration of the marginal zones. Moreover, the ability of R_4 to control the marginal zones deteriorates near $L = 0.5$ to such an extent, that it cannot recover the correction-state once it is disturbed by these extremely large values of L .

It is evident from Figure 3.11 that the marginal spherical of SS(20) is larger than we would wish (that is, $LA' > 0.005$ for $\rho > 0.18$). This, however, has been reduced to our normal value of $LA' = 0.005$ in system SS(21) by increasing the Petzval residual by $\Delta R_4 = 0.005$ to $R_4 = 0.135$, giving the more compact group of LA' -curves shown in the middle diagram of Figure 3.11.

The spot diagrams of SS(20) and SS(21) are shown in Figures 3.12 and 3.13. It is evident that the axial spot diagrams of SS(20) are much more compact than those of SS(21), but SS(21) has less halo. However, we notice that in spite of the last adjustment of R_2 , which was made initially to system SS(15), that both systems SS(20) and SS(21) still show a considerable amount of coma-like flare at 5° and a lesser, but still significant, amount at 10° . This extra coma has been balanced in system SS(24), which is SS(21) with R_2 now equal to -0.14 instead of -0.10 . The

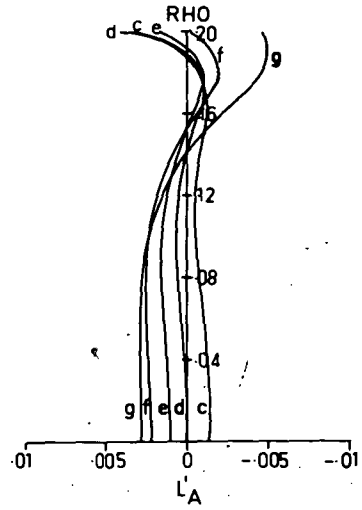
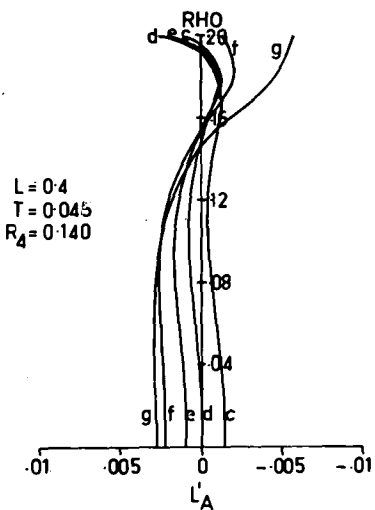
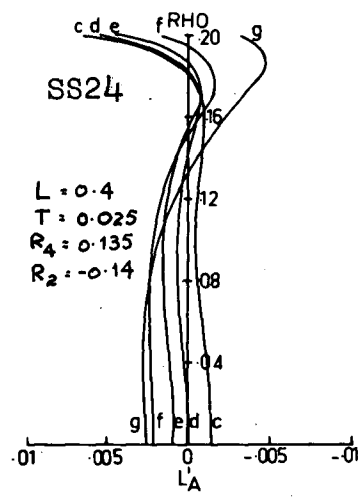
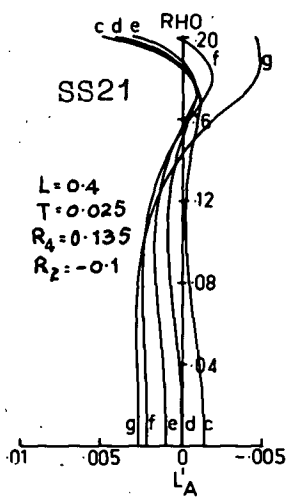
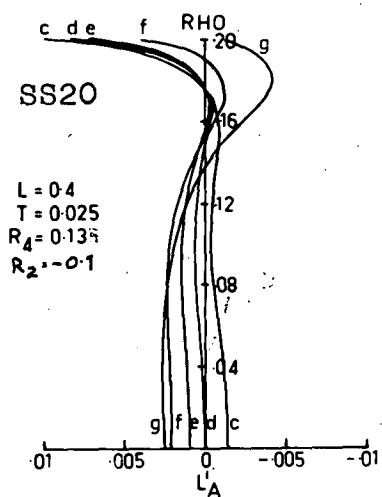
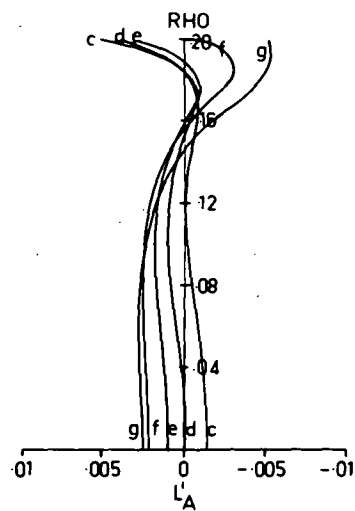
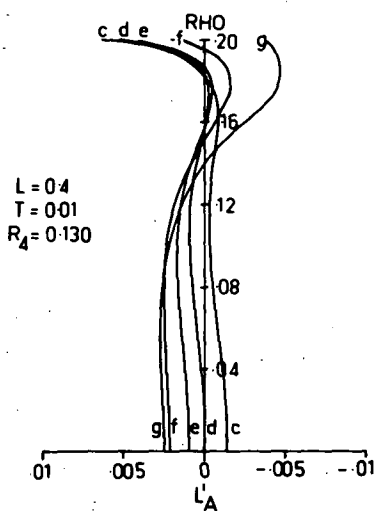


Fig. 3.11

SYSTEM SS20 $X=0$

V=0

V=5

V=10

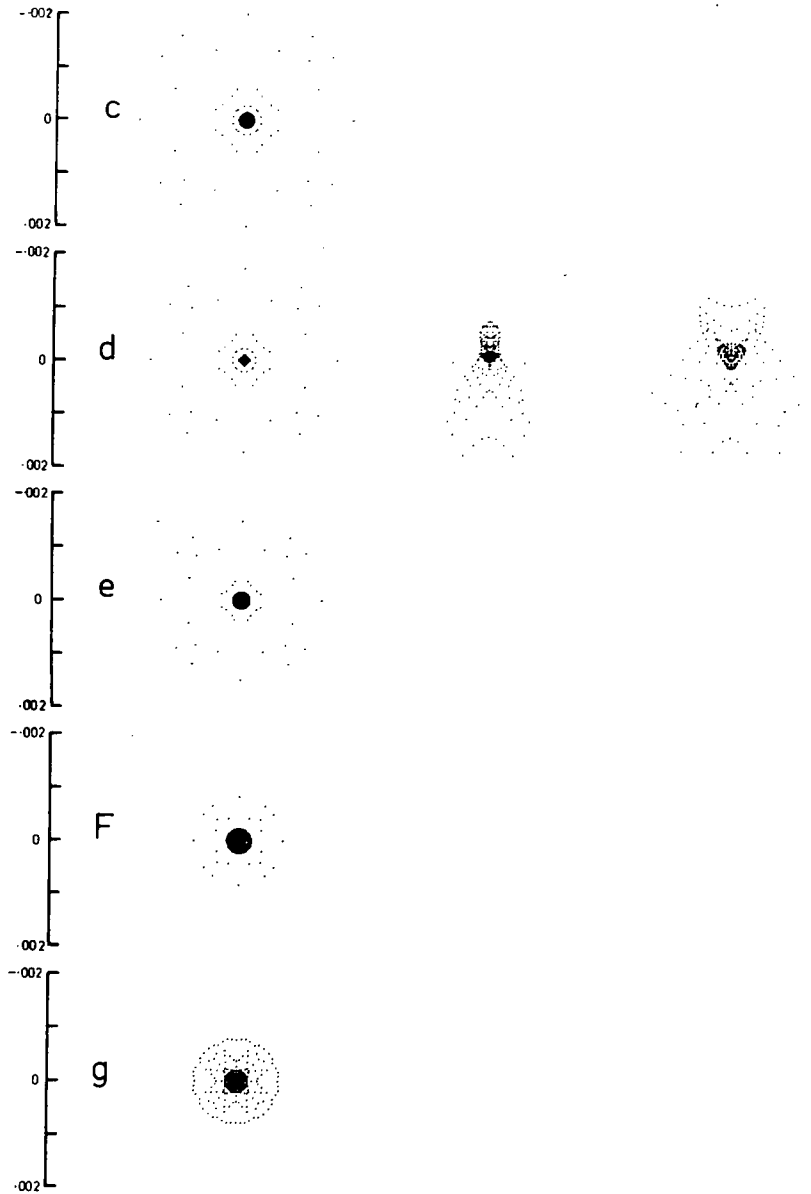


Fig. 3.12

SYSTEM SS21 X=0

V=0

V=5

V=10

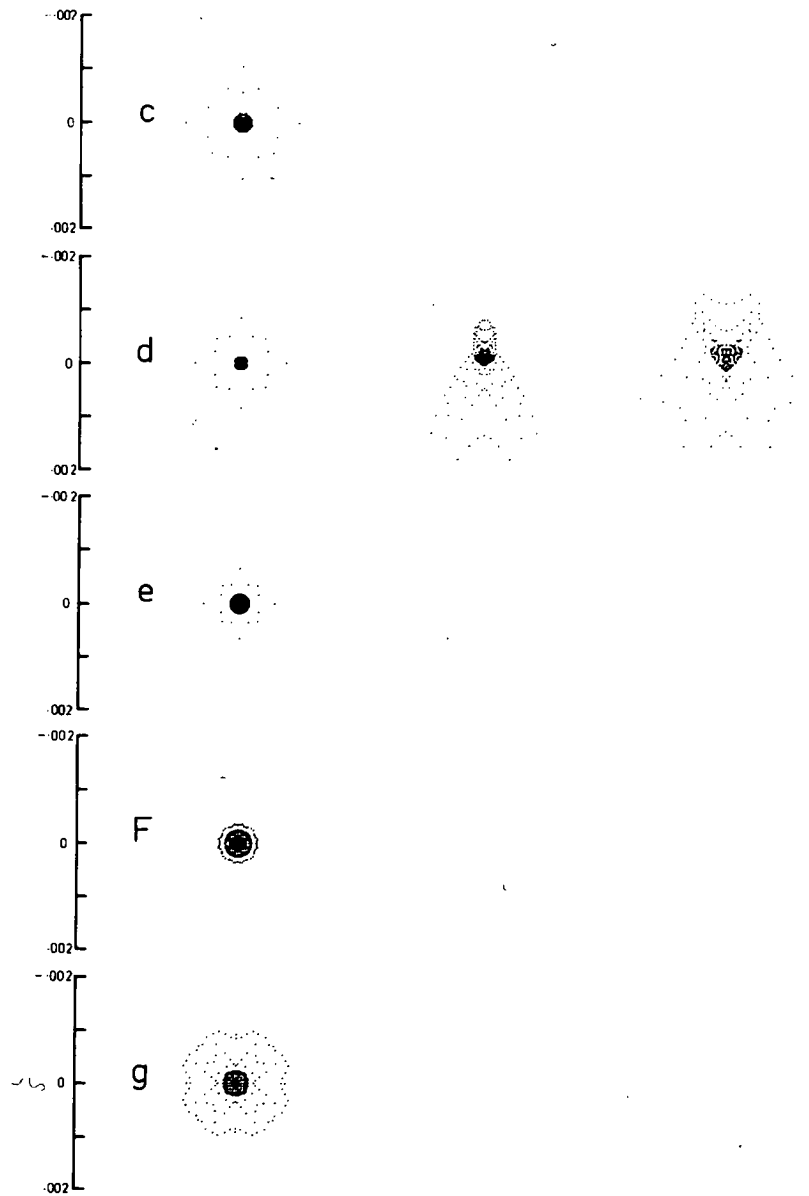


Fig. 3.13

SYSTEM **SS24** $X=0$

$V=0$

$V=5$

$V=10$

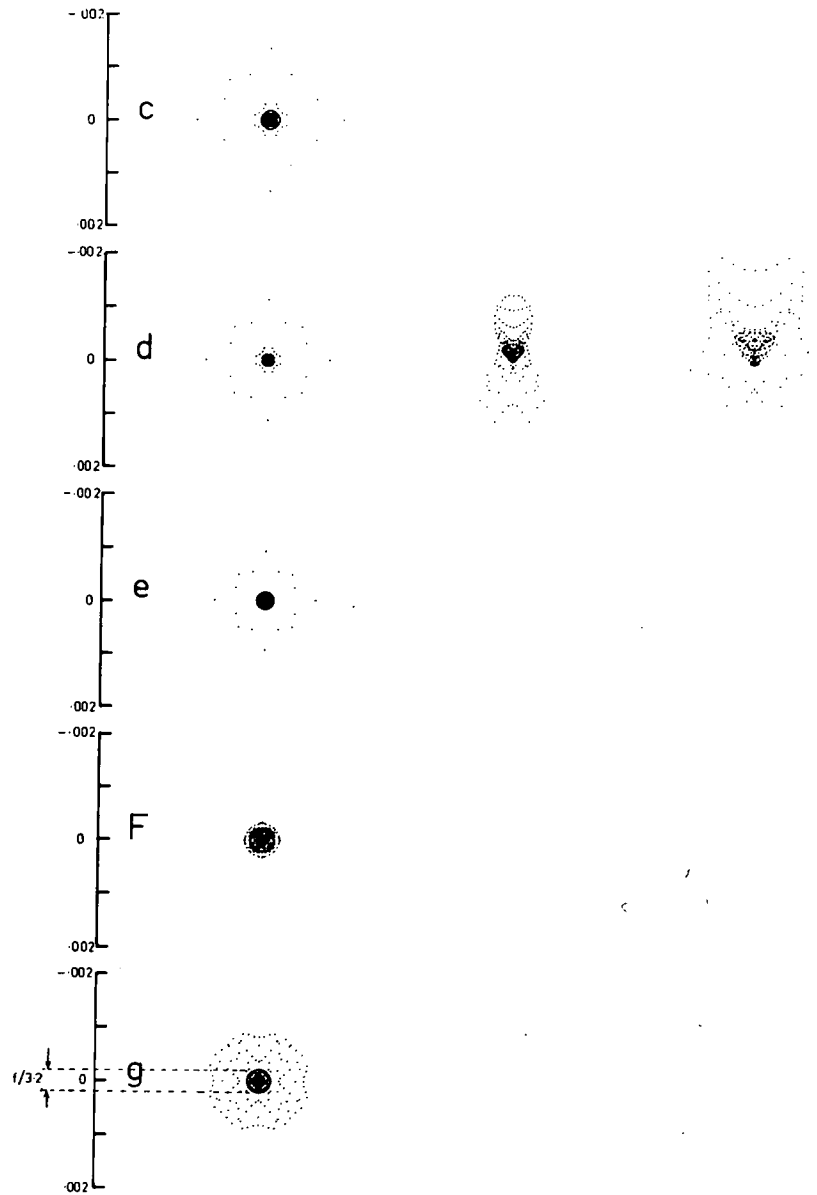


Fig. 3.14

LA'-curves of SS(24) are shown in the extreme right hand of the middle row of Figure 3.11 and its spot-diagrams are shown in Figure 3.14.

When we consider the information we have obtained about the performance of the systems SS(20), SS(21) and SS(24) both on-axis and off-axis up to this stage, we find that we cannot separate them conclusively. Each system is superior to the others in one or more aspects of LA'-curves or spot diagrams. Consequently, in the concluding stages of the design of the type 121 we will study the effect of the remaining parameter (T) on these three systems which have good axial correction.

3.1.4.2 The Effect of T on the Axial and Off-Axial Pencils of the Type 121.

The "principal-performance-parameters" used in the study of T are LA' and ϵ_y' , both of which are calculated directly from trigonometrical ray-traces of the systems which are generated by the SS-programme; predictions are not used for the reasons given above (see 3.1.0). The parameter ϵ_y' is the displacement of the principal-ray of specified colour relative to the image point of the same principal-ray of the base colour (d-light), in the paraxial image plane. It has been computed for the maximum aperture ($f = 0.2$, $f/2.5$) at field angles of $V = 2.5^\circ$, 5° , 7.5° and 10° for the five standard colours.

The effect of T on the axial and off-axial pencils of the type 121 is portrayed in Figures 3.11 and 3.15 which

are complementary diagrams. They show the effect of T in the region surrounding the optimum systems SS(20), SS(21) and SS(24) which occupy the middle row in each figure.

In Figure 3.11 we observe the change in LA' versus ρ versus λ caused by T and similarly in Figure 3.15 the change it causes in ζ_y' versus \bar{H} versus λ ($\bar{H} = \tan v$).

We have varied T over a considerable range that spans $T = 0.025$. Starting from the top of Figure 3.15, T increases from $T = 0.01$ to $T = 0.04$ in steps of $\Delta T = 0.015$ and in the process the order of the ζ_y' curves versus \bar{H} versus λ is reversed. At the top of the page we have the colour sequence c, d, e, F and g which becomes g, F, e, d and c at the bottom. Clearly a minimum exists for ζ_y' versus T and for all practical purposes it occurs at $T = 0.025$ which is the value arrived at previously after the automatic adjustment of the tch' to zero, (see section 3.1.2).

Turning our attention back to the Figure 3.11 we observe, contrary to our earlier supposition, that T has a significant effect on the axial image. Once again, as we found with R_2 , R_4 and L , it is the marginal zones ($\rho > 0.16$) that are affected; the zones below $\rho = 0.16$ are not. When T is increased the marginal zones become more positive. This is seen when we go from the top row of Figure 3.11 to the middle row; during this process the marginal aberration is doubled.

Again, as with L and R_2 , the marginal zones are adjusted by changing R_4 . For example, in passing from the

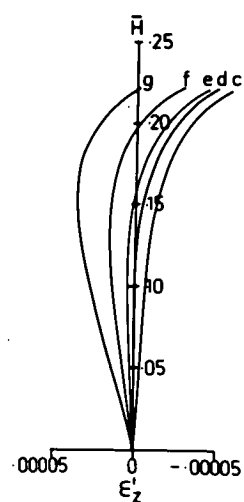
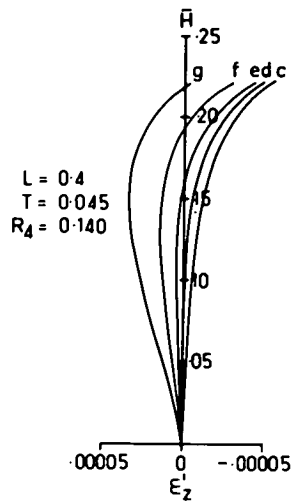
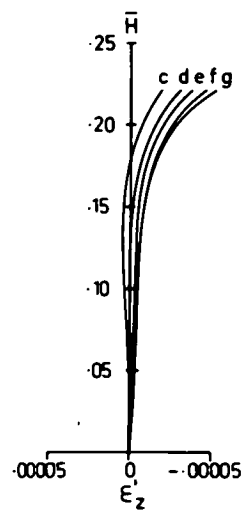
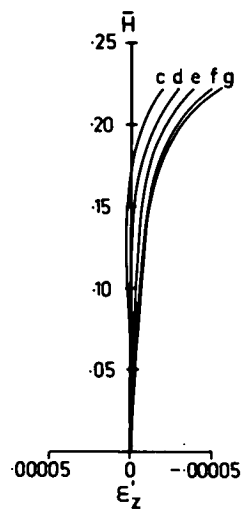
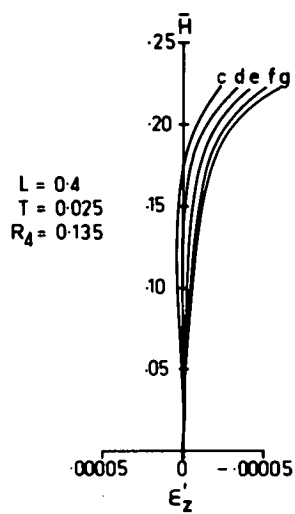
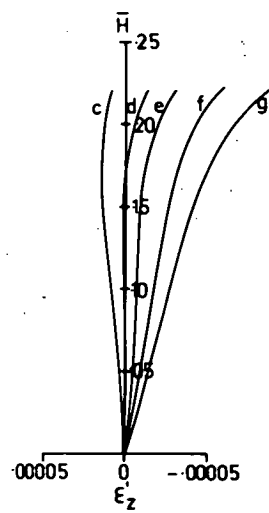
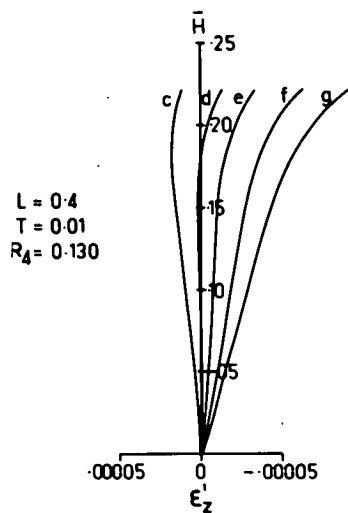


Fig. 3.15

top left hand diagram of Figure 3.11 where $T = 0.01$ to SS(20) in the middle row where $T = 0.025$, the marginal zone is increased from about 0.005 to 0.01. This marginal increase is reduced to the initial value that the system had at $T = 0.01$ in going from SS(20) to SS(21). The reduction, of course, is caused by the change $\Delta R_4 = 0.005$. Similarly, in going from SS(20) to the bottom left hand system, T changes to $T = 0.045$ and in this case, the marginal correction is preserved by increasing R_4 to $R_4 = 0.140$. Thus $\Delta T = 0.015$ is balanced by $\Delta R_4 = 0.005$.

It is evident from Figure 3.15 that although T changes the separations of the ϵ_y^1 -curves it has no significant effect on their curvature which, of course, is the distortion. This can only be modified by changing the residual R_5 . The systems depicted in Figure 3.11 and 3.15 have $R_5 = 0$ which we have not bothered to alter in view of the small amount of distortion present. We have left changing R_5 until the stop is shifted out of the middle lens into one of the air-spaces, in which case, we expect that we will have to balance significant additional distortion caused by the disturbance of the symmetry.

Conclusions.

Contrary to earlier expectations T does affect the axial pencil. However, like L , it only influences the marginal zones significantly although in this respect it is not as severe as L .

We can summarize the effects of T in two rules:

1. As T increases the spherical aberration of the marginal zones ($\rho > 0.16$ or $> f/3.5$) increases. (Thus when T is changed R_4 must be changed in the same sense in order to preserve marginal correction.)
2. The transverse aberration ϵ_y' has an optimum minimum with respect to χ , k' , P , L , T . (If ϵ_y' is positive then it will be reduced by increasing T .)

3.1.5 Discussion of some Important Properties Observed during the Adjustment of the Chromatic Aberrations.

In Table 3.2 we have assembled some important parameters of the systems with two-zone correction which have been computed at the main stages of the adjustment of L and T . We recall that these systems are SS(4) (the optimum monochromatic system), SS(15) (the first major balance of R_4 and L) and the three final systems SS(20), SS(21) and SS(24) which we cannot as yet separate satisfactorily. All of these systems are similar at apertures less than $f/3.5$, however, they differ significantly beyond $f/3.5$.

The most important thing of immediate practical use coming out of this table is that the spherical coefficients of these systems are almost unchanged during the adjustment of L and T . Their sign-pattern remains $+-$ and their order of magnitudes do not vary significantly. Thus we have found that two-zone correction is associated with a characteristic set of spherical coefficients of which the

TABLE 3.2

BLOCK 1. BASIC PARAMETERS

| System | χ | k' | P | L | T | Na | Va | Nb | Vb | Nc | Vc | $\Delta V = V_a - V_b$ |
|--------|---------|--------|--------|-----|-------|---------|-------|--------|--------|---------|-------|------------------------|
| SS4 | -0.4772 | -2.859 | 0.5567 | 0.2 | 0.05 | 1.62101 | 60.18 | 1.5585 | 35.800 | 1.62101 | 60.18 | 24.28 |
| SS15 | -0.5501 | -3.108 | 0.4377 | 0.3 | 0.025 | " | " | 1.5628 | 36.164 | " | " | 24.02 |
| SS20 | -0.6298 | -3.105 | 0.2210 | 0.4 | 0.025 | " | " | 1.5628 | 36.160 | " | " | 24.02 |
| SS21 | -0.6197 | -3.147 | 0.2414 | 0.4 | 0.025 | " | " | 1.5634 | 36.213 | " | " | 23.97 |
| SS24 | -0.6159 | -3.134 | 0.2420 | 0.4 | 0.025 | " | " | 1.5632 | 36.197 | " | " | 23.98 |

BLOCK 2. PERFORMANCE PARAMETERS

| System | Residuals | | | | | | | |
|--------|-----------|-------|----|-------|----|----------|-----------|----|
| | R1 | R2 | R3 | R4 | R5 | R6 | R7 | R8 |
| SS4 | -0.0015 | -0.06 | 0 | 0.215 | 0 | 0.0006 | 0.00027 | 0 |
| SS15 | " | " | " | 0.185 | " | 0.00219 | -0.000042 | " |
| SS20 | " | -0.10 | " | 0.130 | " | -0.00007 | 0 | " |
| SS21 | " | -0.10 | " | 0.135 | " | -0.00007 | 0 | " |
| SS24 | " | -0.14 | " | 0.135 | " | -0.00006 | 0 | " |

BLOCK 3.

| System | Spherical Coefficients | | | Power Ratio | d3 |
|---------|------------------------|---------|----------|----------------------|--------|
| | σ_i | μ_i | τ_i | ϕ_c / ϕ_a | |
| SS4 | 0.1010 | -6.906 | -7.752 | 1.7997/1.5338 = 1.17 | 0.0832 |
| SS15 | 0.1729 | -7.298 | -46.57 | 1.908 / 1.530 = 1.25 | 0.1094 |
| SS20 | 0.1399 | -7.144 | -25.99 | 2.058 / 1.587 = 1.30 | 0.1319 |
| SS21 | 0.1634 | -7.251 | -37.98 | 2.044 / 1.578 = 1.30 | 0.1316 |
| SS24 | 0.1416 | -7.034 | -29.80 | 2.041 / 1.578 = 1.30 | 0.1320 |
| Average | 0.1449 | -7.090 | -29.57 | | |

average values are about $\overline{G}_1 = 0.15$, $\overline{\mu}_1 = -7$, $\overline{T}_1 = -30$.

This property has been used in the later stages of this design to locate the system with two-zone correction whenever the basic parameters have been altered. Thus all we need do when, for example, we alter L , is first to generate systems with the new L over a range of R_4 in steps of $\Delta R_4 = 0.005$. Then it is only a matter of plotting the spherical coefficients versus R_4 and from this graph locating the system with the characteristic set of spherical coefficients. The system selected in this way has two-zone correction. (Note this method is also used with 122 system.)

The existence of the stable set of characteristic spherical coefficients for two-zone systems has an important implication. Since we are able to find the optimum $f/2.5$ system by the pattern of the 3rd, 5th and 7th order coefficients, then it follows that the higher order spherical coefficients (greater than 7th) are very stable over a wide range of the basic parameters. This seems remarkable in view of our earlier work on optimizing LA' with respect to the basic parameters, when it was found that the marginal zones were extremely sensitive to R_4 and L , and to a lesser extent to R_2 and T . Therefore, this stability of the higher aberrations requires further investigation but we will leave this until section 3.2.2.2.

Let us now compare the basic-parameters and the residuals generated from them. The basic-parameters are

shown in Block 1 and the residuals of the systems generated from them are shown in Block 2. We have already found in our treatment of the LA' -curves that P, L and T interact strongly as far as the marginal zones are concerned, and now we find on comparing Blocks 1 and 2 of Table 3.2 that χ and k' are disturbed significantly as well. Thus all the basic parameters interact strongly at large apertures. Therefore, attempts to design on the basis of associating each parameter with a single aberration residual, can be expected to have little chance of success in view of this complex relationship.

When we recall the comparison of ray-trace and predicted LA' versus ρ versus λ -curves we see that designing for apertures of less than $f/3.5$ is fairly simple (at most, tedious). Designing at less than $f/3.5$ is easy for two reasons; firstly, the obvious one, that 7th order predictions are reasonably accurate up to $f/3.5$ and secondly, for the less obvious reason which we have discovered, that seemingly satisfactory low-aperture performance is generated over a wide range of the basic-parameters. This latter benefit results from the apparent stability that the lower zones have with respect to chromatic-basic-parameters L and T.

Past workers have noticed that certain quantities assume particular values when a type 111 triplet is well corrected. The most notable ones seem to be the length of the system and the power ratio of the two positive lenses

(ϕ_c / ϕ_a) . The length of the type 121 system that we have developed is proportional to either one of its separations, therefore, in order to observe changes associated with the overall length, we need only look at either d_3 or d_6 . We have tabled d_3 . The other quantity, the power ratio, can be identified with R.E. Hopkins basic parameter $K (= \frac{\Delta u_a}{\Delta u_c})$ which is the inverse of the power ratio (ϕ_c / ϕ_a) . It is evident that the over-all length is a performance parameter which, according to our nomenclature, is a "fundamental-performance-parameter" and, in particular, it is equivalent to our fundamental-performance-parameter d_3 . On the other hand, the power ratio is a "basic-parameter" equivalent to our χ (see chapter 2.2).

It has been remarked by many workers that the longer the system the smaller the longitudinal chromatic aberration. This is demonstrated very clearly in Block 3 where the separation d_3 is seen to increase in going from SS(4) to SS(24). Thus the optimum system is associated with the greatest overall length. However, the small magnitude of the change in length, occurring for L changing from 0.2 to 0.4, suggests that perhaps it is not the most suitable parameter for controlling the optimization of a wide aperture triplet. This conclusion is supported by the graphs of d_3 and d_6 versus (χ, k', P) shown in Figure 2.4 from which it is evident that the variation in length is not as suitable as the spherical coefficients for locating the optimum region. The location of the

simultaneous minima of the spherical coefficients shown in Figure 2.29 would appear to provide a more precise method for finding the optimum system.

We also note that the basic parameter ΔV is about 24 for all the systems SS(4) to SS(24). This is like the average value 25 which is quoted by R.E. Hopkins as being about the optimum for the type 111.

The distribution of power between the first and the last lenses is used as a basic-parameter by several workers including R.E. Hopkins. It is evident from the table that $\phi_c/\phi_a = 1/K$ is approximately 1.3 (Block 3, Table 3.2) for the optimum-chromatic-type 121 systems SS(20), SS(21) and SS(24). We know that we have contrived to generate these systems with minimum zonal aberration for all zones up to $f/2.5$. Therefore, zonal correction is associated with a basic parameter $\phi_c/\phi_a = 1.3$ which agrees with an observation made by H.D. Taylor. His remarks are reported recently by Lessing as follows - "In an astrographic triplet designed by Taylor⁽¹⁰⁾ it was found that it was impossible to remove zonal aberration by figuring when the third power was equal to the first. However, when the third power was made one-and-a-half times the first, the zonal aberration decreased to such an extent that figuring could remove it entirely."

The above evidence further supports our claim for the general behaviour of triplets being like that shown in our study of coefficients versus (χ, k', P) . Thus yet

another facet of published work supports our view that
the picture of convergence of the coefficients and the
residuals which we have constructed for the type 121 applies
generally to systems of triplet structure at least.

CHAPTER 3.2 THE SIMULTANEOUS CONVERGENCE OF ALL AVAILABLE
ORDERS OF SPHERICAL ABERRATION COEFFICIENTS
WITH RESPECT TO THE BASIC PARAMETERS

\mathcal{X} , k' , P , L , T .

3.2.0 Introduction.

After a lengthy and at times involved investigation of the type 121 triplet we have developed three very well optimized systems in Chapter 3.1. During this development we have encountered many aspects at apertures less than $f/3.5$, which are similar to those observed by other workers for other triplet-types. Consequently, we have concluded that these aspects are facets of the more complete picture which we observed when we mapped the coefficients with respect to the monochromatic parameters (\mathcal{X} , k' , P). However, although our low aperture work is easily interpreted we find, on the other hand, that our work on the marginal zones has apparently taken us beyond our earlier picture of convergence of the 3rd, 5th and 7th order aberration coefficients versus (\mathcal{X} , k' , P) which was discovered in Section 2. Nevertheless, in spite of this, agreement has been found with the few published results concerning optimization of wide aperture triplet systems. But, these points of agreement only give us, mainly, a goal for two of the construction parameters, the power ratio ϕ_c/ϕ_a and the length of the system. What we would like to do now is to find a simple model for the

"wide-aperture-chromatic-system" similar to the one we have constructed for the monochromatic-system of aperture less than $f/3.5$, in Section 2.

3.2.1 Review of Indirect Evidence of the Convergence of Coefficients with Respect to all the Basic Parameters (\mathcal{X} , k' , P , L , T).

Let us begin the search for a new model by reviewing the entire optimization process of the type 121 as we have experienced it. We recall that we showed at the beginning of Section 2 that the type 121 could be studied interpolatively in two stages. First of all monochromatically, by mapping all the coefficients of 3rd, 5th and 7th order with respect to all the "basic-monochromatic-parameters" (\mathcal{X} , k' , P). As a result of this, we were able to isolate a unique monochromatic region in which almost all the coefficients tended to zero. In particular, all of the spherical coefficients approached zero and in doing so systems with spherical coefficients having alternating signs occurred. Such systems were predicted to give two-zone correction.

Attempts to produce a real $f/2.5$ system with two-zone correction, from a predicted one, failed because the higher orders of spherical aberration (beyond the 7th) were significant. These higher orders were not predicted by the coefficient maps of 3rd, 5th and 7th order and so we discarded "interpolative-coefficient-mapping" in the advanced

stages of design. Thus we proceeded to adjust the marginal zones (greater than $f/3.5$) with the aid of LA' -curves that were calculated directly from ray-traces. This method was successful in achieving two-zone correction.

In passing, we note that since two-zone correction has been achieved then it follows that some of the spherical coefficients of greater order than the 7th have been reduced to values near zero. This is easily visualized when we recall the behaviour of the spherical aberration of the marginal zones in Figures 2.35 and 2.36, where it seems, that some of the spherical coefficients of order greater than the 7th must be minimized, because, the marginal zones run from positive to negative as R_4 increases. Thus, from this very abstract picture of the system given by the LA' -curves, we observe indirectly the behaviour of higher order coefficients (> 7 th order) with respect to the basic parameters. (These coefficients are of higher order than those already obtained analytically and shown in the (χ, k', P) -maps of Section 2.)

Finally, in the chromatic stage because it seemed that we were faced with controlling only the marginal zones with L and T , we did not bother to map the 3rd, 5th and 7th order coefficients but proceeded, instead, with the mapping of the LA' -curves versus L and T . Our decision to omit the coefficient maps was also supported by the attitude of other workers who implied that L and T would only have trivial effects on our monochromatic system, at least, at less

than $f/3.5$. They said little about higher apertures.

Our first results with L showed that it had a critical influence on zones beyond $f/3.5$. However, we showed that the zones could be controlled with R_4 during correction of the longitudinal chromatic aberration with L . Thus we found that the chromatic aberration was adjusted at a smaller value of R_4 than that which occurred in our monochromatic design. The opposite happened when T was adjusted, but it had less effect on the outer zones than L , consequently, the adjustment of the axial and off-axial colour produced considerable improvement in the Petzval coefficient (R_4). The net result of the interaction of L , T and R_4 has been to produce, not only, an optimum achromatized $f/2.5$ system, but also, it has improved the lower aperture system as well. The latter point is the one we have tended to take for granted while we have been primarily concerned with the higher aperture performance. But clearly, the lower aperture system has the benefit of the smaller Petzval as well.

Thus, stopping down the optimum $f/2.5$ chromatic system to $f/3.5$ produces a system superior to the optimum monochromatic $f/3.5$ system SS(4) of Section 2. Therefore, it is evident that both the optimum chromatic and monochromatic systems of high and low aperture coincide in (χ, k', P, L, T) -space. Clearly the optimum values of L and T apply to both the chromatic and monochromatic

systems of both high and low aperture.

What we have found is that there is an optimum set of (λ, k', P) for the monochromatic stage and an optimum set of (P, L, T) for the chromatic stage; therefore P belongs to both stages of the design process. Moreover, we have found P to be more strongly associated with L and T than with λ and k' and, therefore, the optimum monochromatic set depends on the chromatic set. Consequently, we must revise our approach to the design process. Clearly it is not good enough to optimize a monochromatic system and then adjust the chromatic system without considering the interaction between the two stages (especially between the parameters P, L, T.) Obviously, this applies even when we want the system to work monochromatically, although it is not what we expect from the approach adopted by designers in general. Indeed, it appears that a very casual attitude is adopted towards the chromatic parameters when designing low aperture systems (less than $f/3.5$). The tendency seems to be, to select L so that the low aperture residuals are a minimum, whereas, we see that we should minimize all zones on-axis and off-axis with the correct combination of (λ, k', P, L, T) .

It is well known that maximum zonal correction is achieved if the marginal spherical is zero and the 0.707 zone is a minimum, preferably zero. We have observed that LA' is a minimum for all λ near the 0.707 zone when the type 121 is optimized. However, this does not guarantee that

the system is the optimum one. We have shown in this work that R_4 or P must be as small as possible also. It is evident from the work with LA' versus R_4 versus L that we can find systems with optimum zonal correction for all λ over a considerable range of R_4 simply by minimizing the 0.707 zone with L . Of these systems the optimum one seems to be the one with the smallest R_4 and the largest permissible L .

3.2.2 Direct Evidence Confirming the Simultaneous Convergence of the Spherical Coefficients of all Available Orders Versus (χ , k' , P , L , T)!

3.2.2.0 Discussion.

We are now aware of the interaction between the basic parameters (χ , k' , P , L , T) at high as well as low apertures. Consequently, we have had to modify our approach to the design process and consider the connection between the monochromatic and chromatic stages. During the elucidation of this interaction several properties involving spherical coefficients have been found, which cannot be explained by our simple model of coefficient convergence in (χ , k' , P)-space, (Chapter 2.2). Therefore, we will examine these unexplained properties and propose a new model which will account for them.

The properties we must consider may be divided into two groups, those concerning the 3rd, 5th and 7th order coefficients, and those involving orders greater than the

7th order. This grouping divides the coefficients according to the portion of the aperture that they seem to influence most. Thus the 3rd, 5th and 7th orders, which we have partly mapped already, affect the zones below $f/3.5$ and the orders greater than 7th affect the zones beyond $f/3.5$. Of course, as yet, we have only seen the effect of the higher orders indirectly through LA' -curves or spot diagrams. However, we will consider the 3rd, 5th and 7th orders first, and defer looking at the higher orders until these lower orders are pictured clearly in (χ, k', P, L, T) -space.

3.2.2.1 Convergence of 3rd, 5th and 7th Order Spherical Coefficients Versus (χ, k', P, L, T) Demonstrated.

We have found that the 3rd, 5th and 7th order spherical coefficients of the two-zone symmetrical system retain a characteristic-pattern while L and T are optimized. Not only are they constant during this process but they are also nearly simultaneously zero. As well as this, an important change occurs in R_4 , it becomes smaller, which means, of course, that the basic-parameter P becomes smaller similarly because, it is virtually a linear function of R_4 (see Chapter 2.2).

After considering the above properties we propose that even when L and T are changed the coefficients and the predicted marginal spherical will still converge with respect to (χ, k', P) in the same simple way as before, except for the difference that the rate of convergence of the spherical parabolas with respect to P will vary with L and T . In the

original monochromatic-survey the coefficients were mapped with respect to (χ, k', P) with $L = 0.2$ and $T = 0.05$. Such a map is a " (χ, k', P) -section" of (χ, k', P, L, T) -space at $L = 0.2, T = 0.05$. Consequently, if we change L and T we select a new " (χ, k', P) -section" in which we have to relocate the "optimum-monochromatic-region".

In view of the evidence which we have about L and T we expect the optimum region to occur at a smaller value of P when either L is increased or T is decreased. On the other hand we do not expect the χ and k' values of the "optimum region" to change appreciably (see Table 3.2) during the adjustment of L and T ; the "optimum region" should remain near $k' = -3.0$ and $\chi = -0.5$. Thus we anticipate that σ_1, μ_1, τ_1 and ϵ'_{Sph} will approach zero simultaneously at smaller values of P when either L is increased and/or T is decreased.

The behaviour of the σ_1, μ_1, τ_1 and ϵ'_{Sph} versus (χ, k', R_4, L, T) is shown in Figures 3.16 to 3.21. Each figure maps the spherical coefficients and the marginal spherical of the 3rd order type 121 triplets with respect to the three basic parameters χ, R_4 and L .

We have used R_4 instead of P because we have become accustomed to it in the advanced stages of our design process. However, we have already shown that (χ, k', P) -maps are not very different from (χ, k', R_4) -maps and, therefore, conclusions about one will do for the other as far as the general behaviour is concerned.

If we assume that R_4 and P are equivalent for our present purpose, then Figures 3.16 and 3.21 map the region of (χ, k', P, L, T) -space which surrounds the point ($L = 0.2$, $T = 0.05$) of our original monochromatic survey in uniform steps of L and T . Looking at this group of figures is very like looking at a set of (χ, k', P) -sections which occur at different L and T . (We have, however, plotted (χ, R_4, L) -sections in each of these figures which will seem strange at first, so in order to orient ourselves with respect to our earlier (χ, k', P) -survey we will locate the original survey in this (χ, R_4, L, T) -grid.)

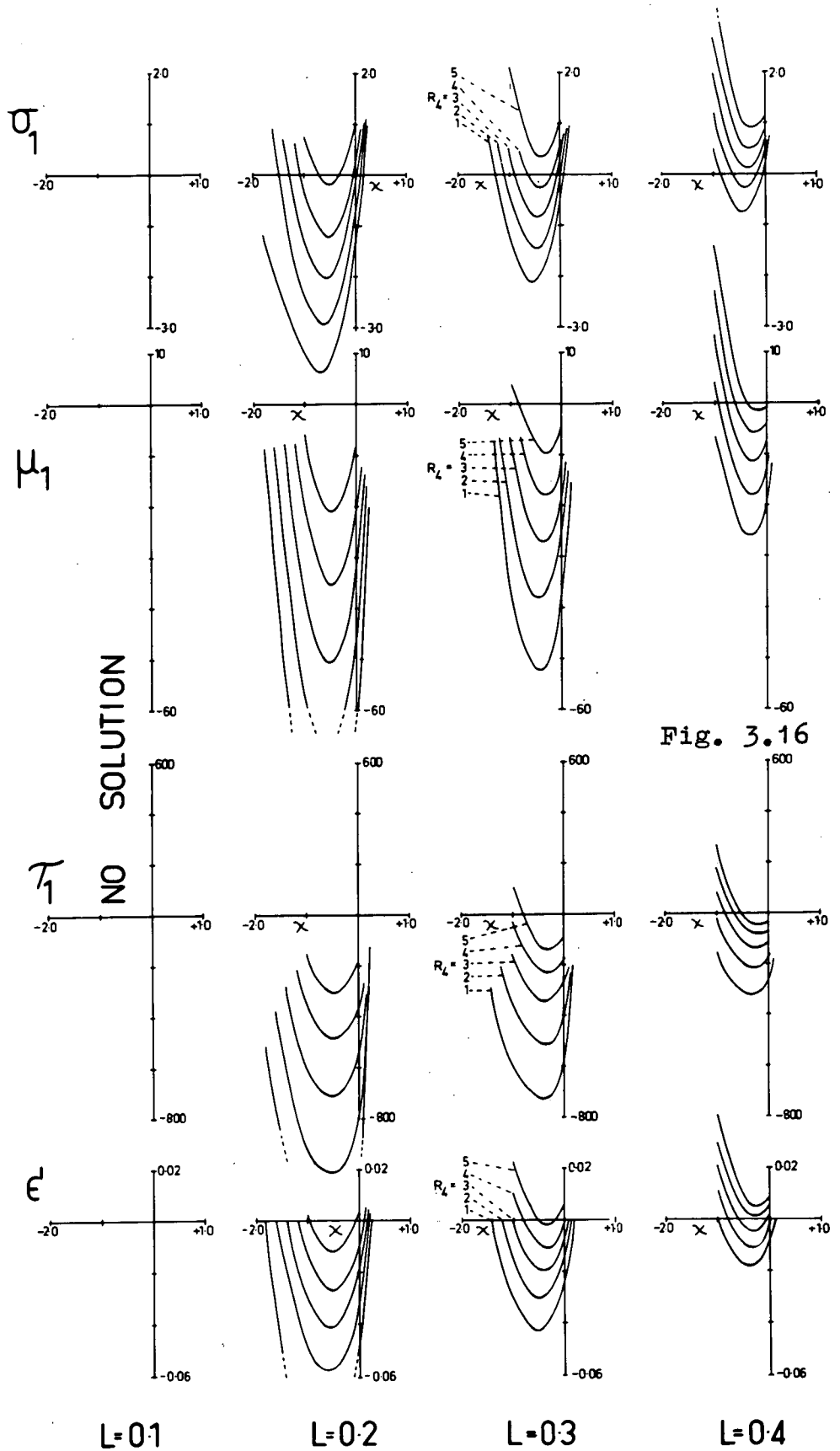
To assist us in visualizing the results and in locating our original monochromatic survey, we have constructed a schematic diagram of the arrangement of the (χ, R_4, L) -sections in (χ, R_4, L, T) -space at $k' = -4.0$ (see Figure 3.22). Each row of this schematic diagram represents one of the Figures 3.16 to 3.18 which, therefore, are (χ, R_4, L) -sections at $k' = -4$ that occur at different T .

Each of the Figures 3.16 to 3.17 are at $k' = -4$ but the T of each becomes progressively smaller in steps of $\Delta T = 0.04$ starting at $T = 0.09$ in Figure 3.16 and decreasing to $T = 0.01$ in Figure 3.18. Therefore, these figures map the spherical coefficients and ϵ_{Sph}' with respect to (χ, P, L, T) at $k' = -4$ and Figures 3.19 to 3.21 repeat this map at $k' = -3$.

Portion of the original (χ, k', P) -map (at $L = 0.2$, $T = 0.05$) is compressed into a single column of diagrams in Figure 3.17. It is evident that the column at $L = 0.2$ in

$$T=0.09$$

$$k=-4.0$$



$T_1 = 0.5$
 $k = -4.0$

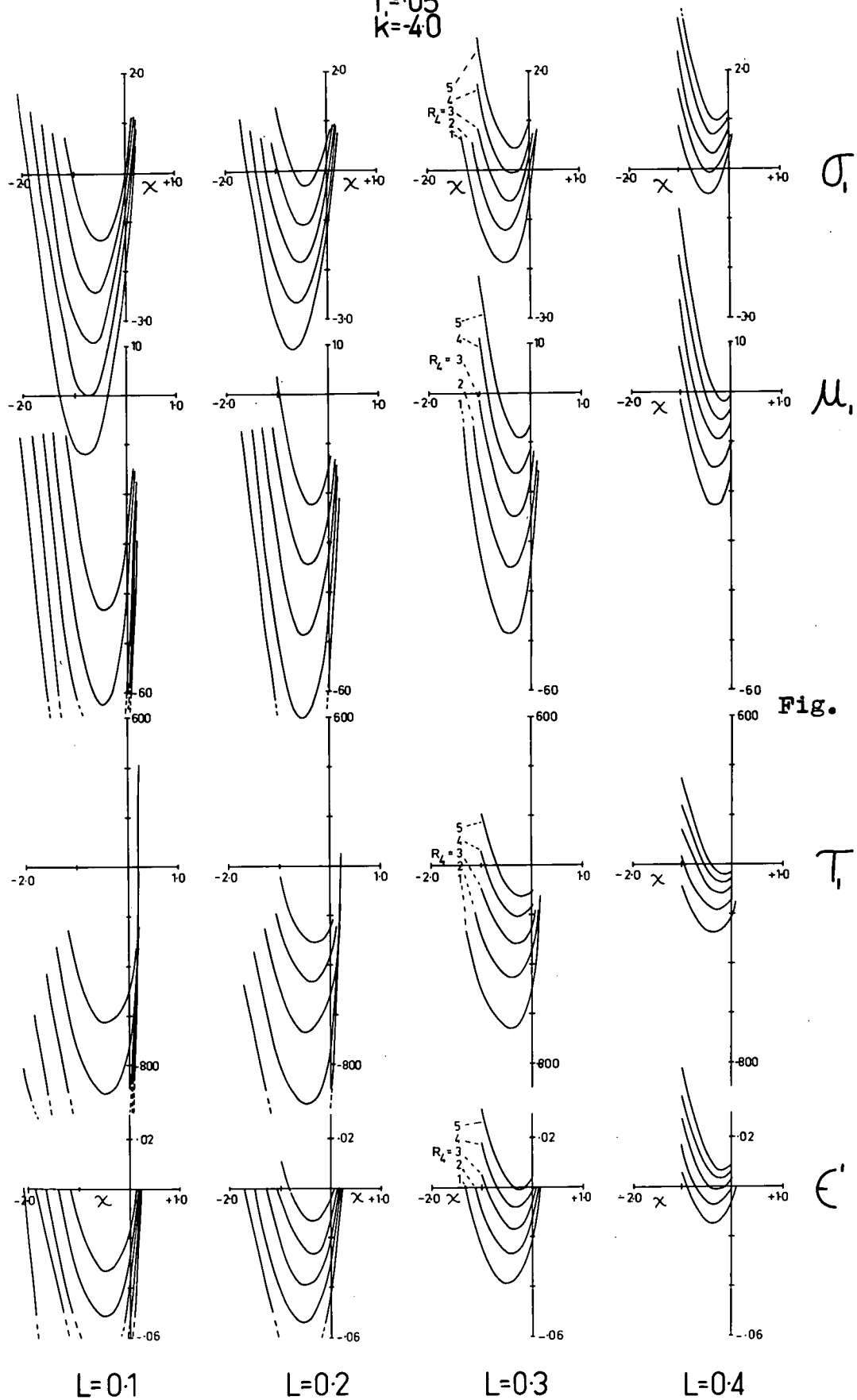


Fig. 3.17

$T = 0.1$
 $k = -4.0$

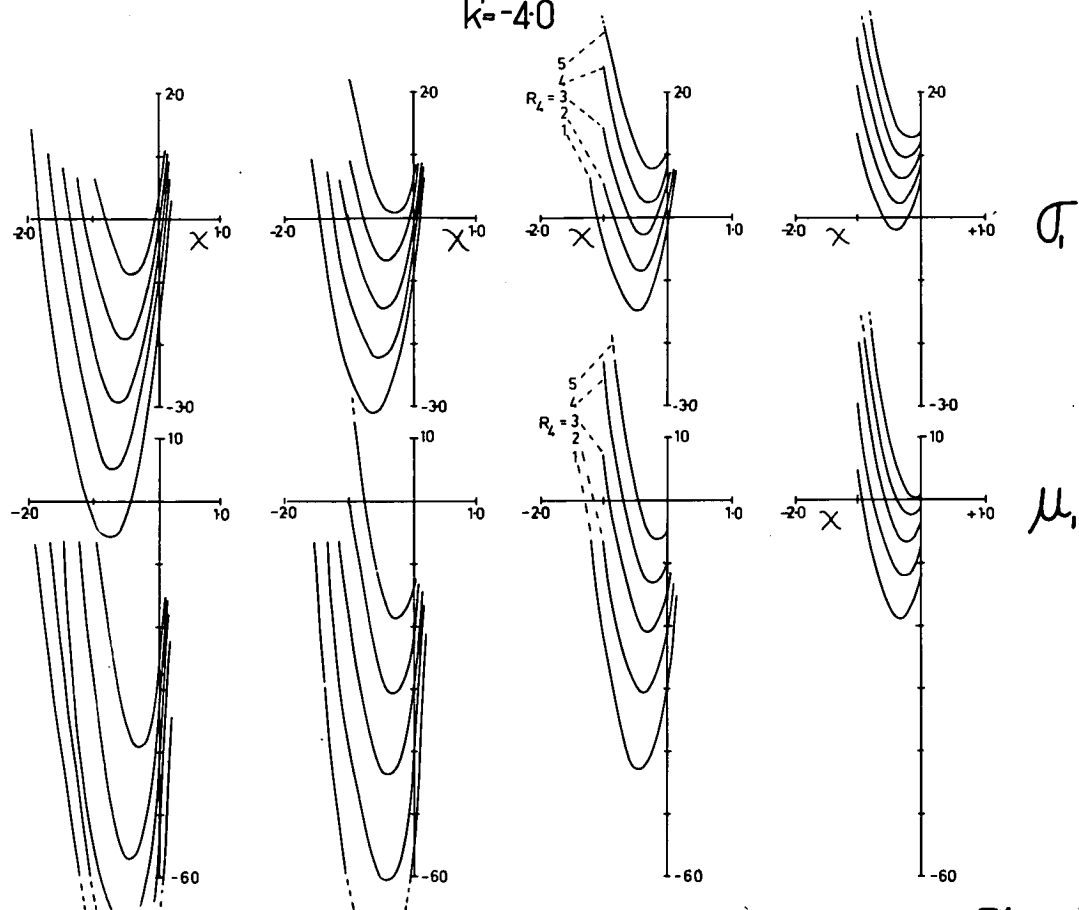
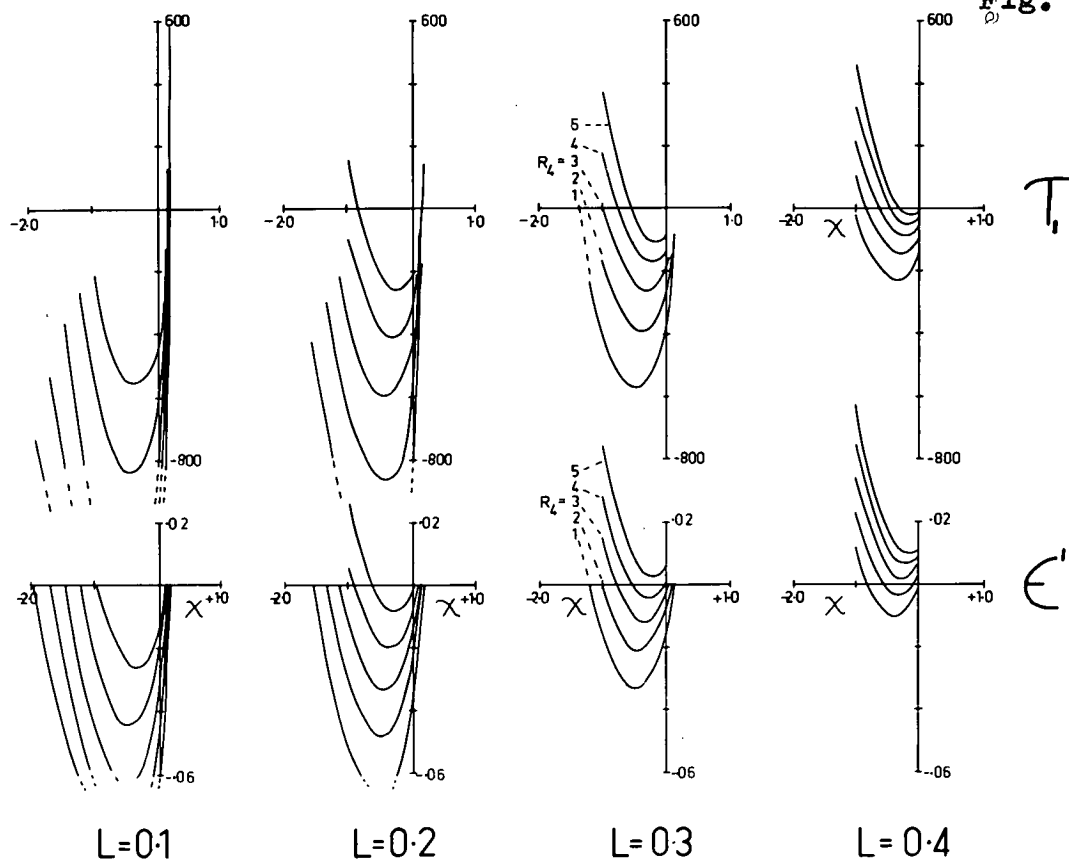


Fig. 3.18



$T=0.09$
 $k=-3.0$

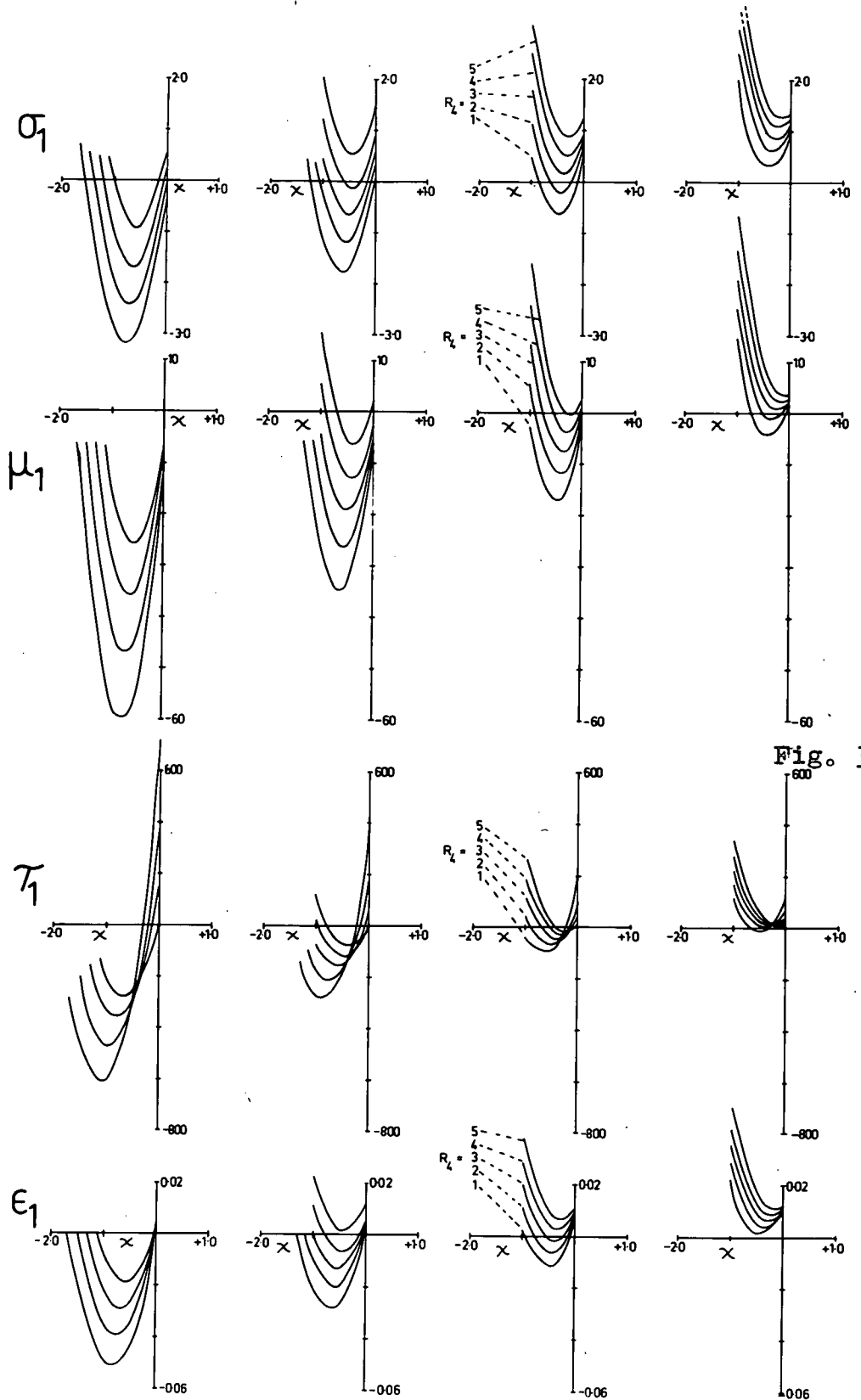


Fig. 3.19

$L=0.1$

$L=0.2$

$L=0.3$

$L=0.4$

$T = 0.5$
 $k = 30$

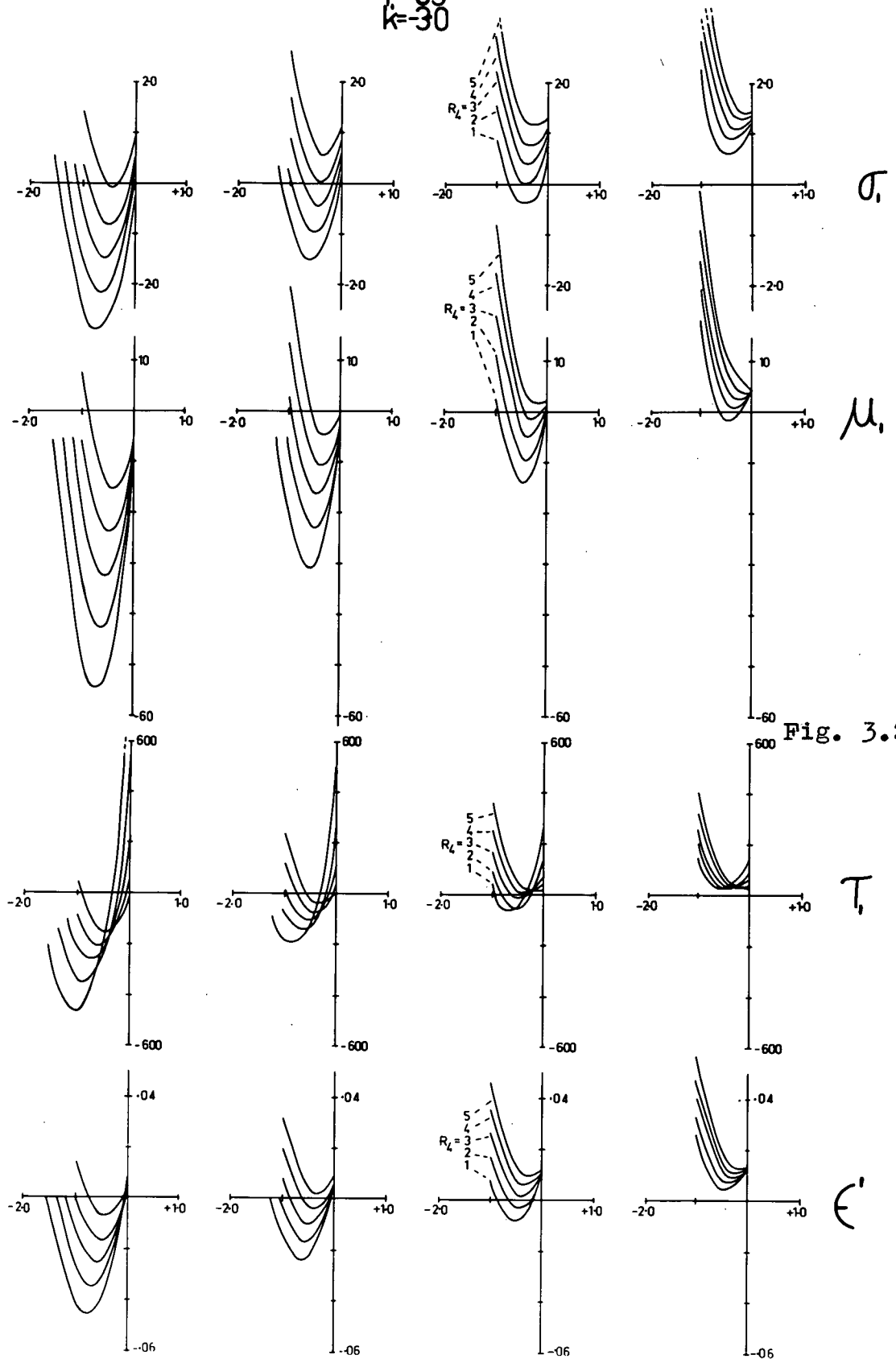


Fig. 3.20

$T = 0.01$
 $k = -30$

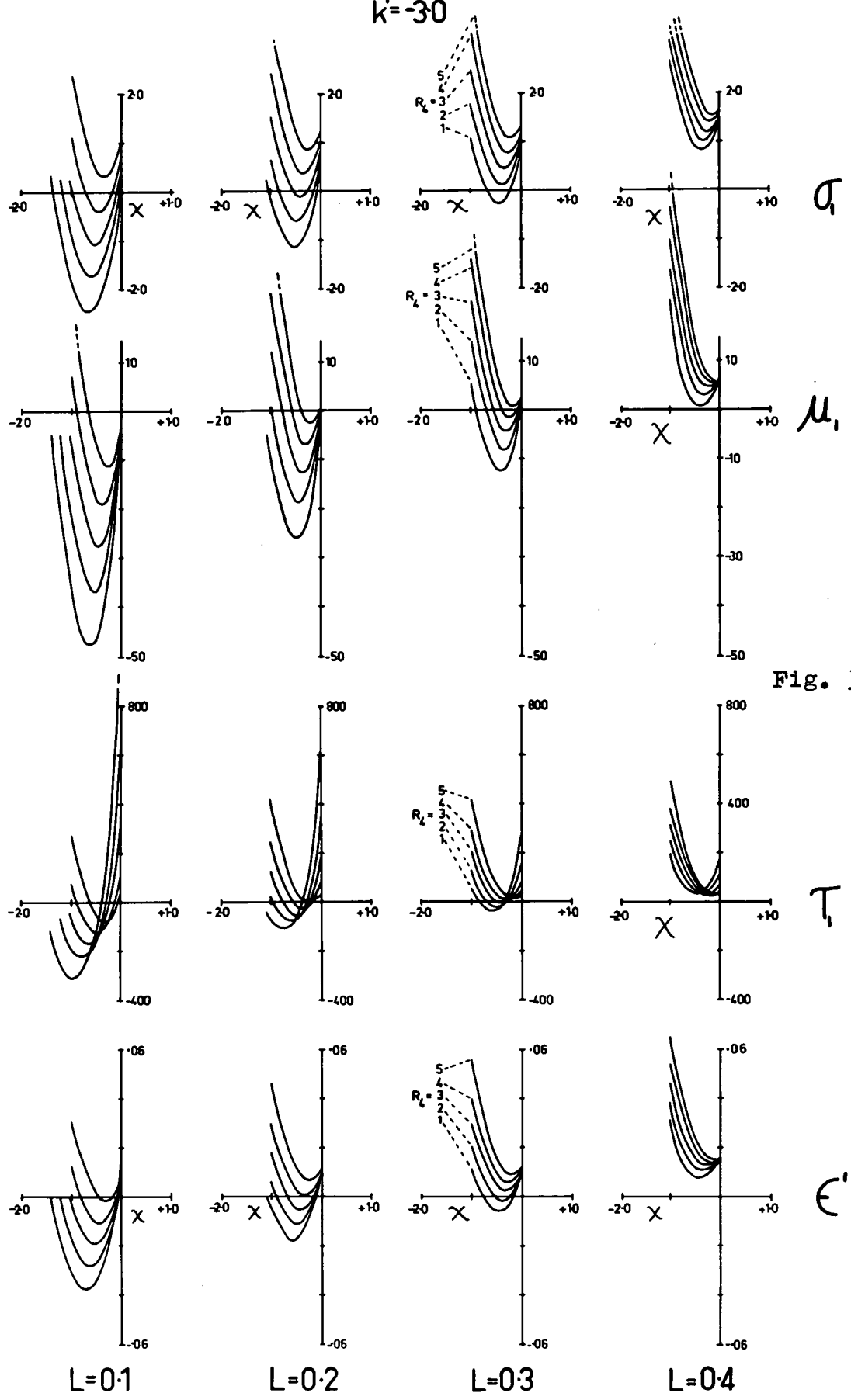


Fig. 3.21

This row is
Fig. 3-15

This row is
Fig. 3-16

This row is
Fig. 3-17

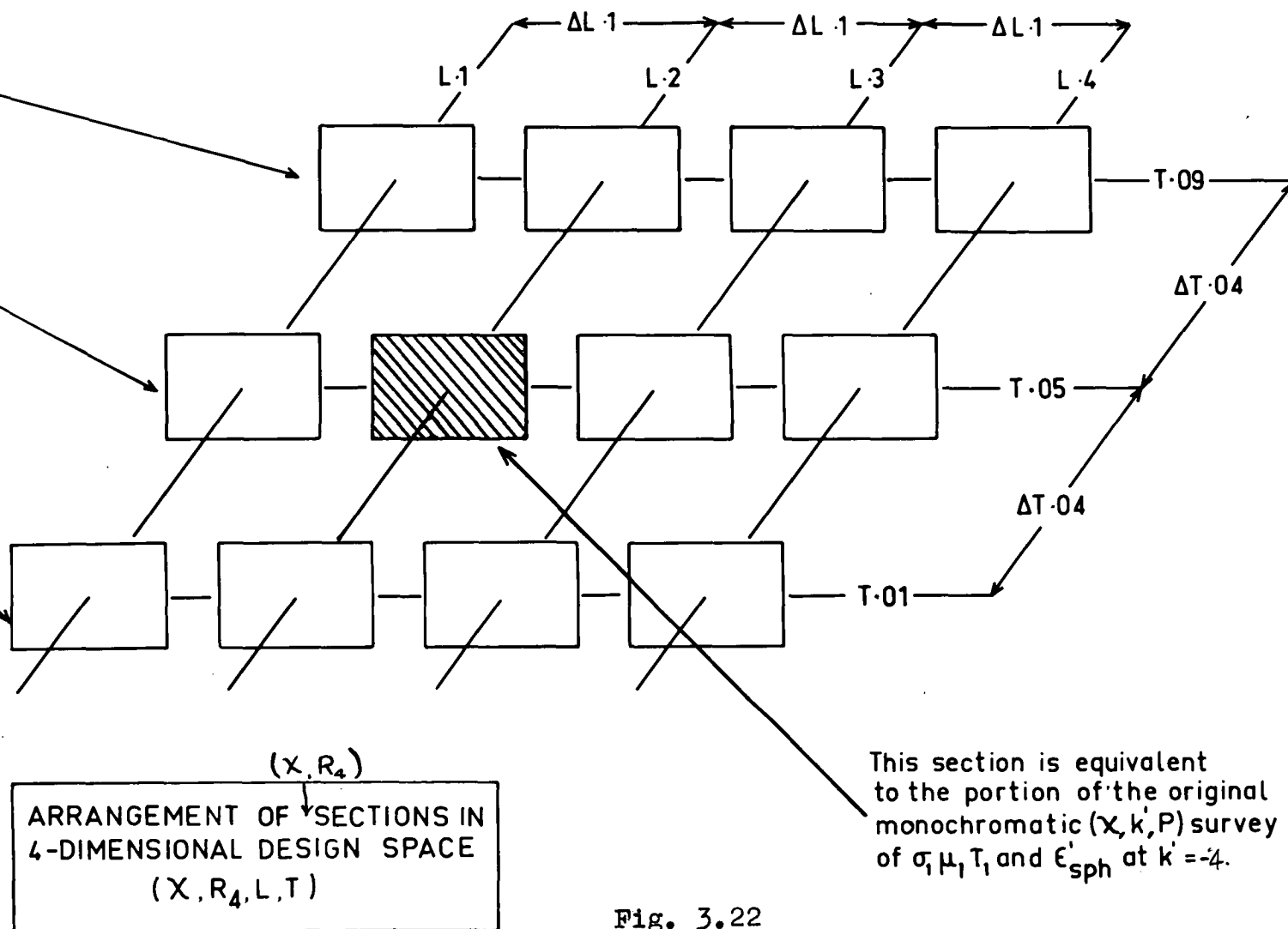


Fig. 3.22

Figure 3.17 contains the equivalent of all the P-curves at $k' = -4$. Or, in other words, it is as though we have erased all except the $k' = -4$ curves in the original $(\sigma_1, \mu_1, \tau_1, c'_{\text{Sph}})$ versus (χ, k', P) diagram of Figure 2.3, and then superimposed the P-axes of this original survey column by column. It follows, also that the column $L = 0.2$ in Figure 3.20 contains all the equivalent curves of the original survey at $k' = -3$.

In each of the Figures 3.16 to 3.21 the curves of the $L = 0.3$ column are identified by numbers 1 to 5 (these numbers have been omitted in the other columns for the sake of clarity.) The bottom curve has a Petzval coefficient of $R_4 = 0.16$ and the ones above it increase in steps of $\Delta R_4 = 0.02$ running from number 1 at $R_4 = 0.16$ to curve number 5 at $R_4 = 0.24$.

In view of our past experience with the coefficients mapping only the two values of k' -4 and -3 is sufficient for observing the broad behaviour.

The comprehensive maps of the spherical coefficients (Figures 3.16 to 3.21) confirm that their general behaviour remains similar to that of the original monochromatic survey. It is evident that as L increases and T decreases groups of curves are compressed and raised above the -axis.

Moreover, inspection of the corresponding comatic and astigmatic 5th and 7th order coefficients (not shown)

shows that all of these still follow the trend of the spherical coefficients when L and T are changed. Thus most of the coefficient-parabolas converge towards zero at smaller Petzval as L and T are optimized.

Clearly the region of maximum compression and elevation of the groups of curves is where we would like to generate a real system. This, of course, is where we have found the optimum type 121 SS(20) to occur ($L = 0.4$, $T = 0.025$, $R_4 = 0.130$, $\chi = -0.6298$, $k' = 3.105$), see Table 3.2. Therefore, the concept of a single optimum region in (χ, k', P, L, T) -space and the supposition that this region is conveniently located by finding the position of the simultaneous minima of the marginal spherical aberration and the spherical coefficients of at least the first three orders, at the smallest, P , is supported.

3.2.3 The Study of the Spherical Coefficients Extended to the 9th and 11th Order.

3.2.3.0 Introduction.

We have noticed, indirectly, in several instances in the course of developing the type 121 to work at $f/2.5$, evidence which suggests that the spherical coefficients of order greater than the 7th behave very much like the lower orders. Indeed, our design problem has been found to be concerned more with the higher orders than with the lower ones. Thus any direct evidence which shows how these

coefficients are controlled by the basic parameters will assist in confirming the design principles at apertures greater than $f/3.5$.

Buchdahl recently has developed the 9th order (quaternary)^(13.4) and 11th order (quinary)^(13.8) spherical aberration coefficients. He has also published computing schemes which extend his earlier scheme for the 3rd, 5th and 7th orders to provide these 9th and 11th order spherical coefficients. Thus we have the means for computing two of the higher orders analytically.

3.2.3.1 Computing Techniques using 9th and 11th Order Spherical Coefficients.

Following the programming technique established in Section 1, we have programmed the scheme for the 3rd, 5th, 7th, 9th and 11th spherical coefficients as a sub-routine Sph(357911). It is like the earlier sub-routine Sph(357) in that it computes spherical coefficients from a given set of lens specifications (fundamental parameters). This sub-routine has been incorporated in a simple programme called "Sphco" which computes the coefficients and predicted zonal spherical for each order up to the 11th. Thus one can look at the spherical coefficients and their effect on ϵ'_{Sph} at various orders if desired. (ϵ'_{Sph} to 11th order is given by $\epsilon'_{\text{Sph}} = \sigma_1 \rho^3 + u_1 \rho^5 + \tau_1 \rho^7 + q_1 \rho^9 + u_1 \rho^{11}$). The programmer may terminate ϵ'_{Sph} at any order thus he can analyse the contributions of the individual orders at various ρ .

Table 3.3

| d-light | Spherical Coefficients | | | | | Coma | Petzval | Basic Parameters | | | | |
|---------------|------------------------|---------|----------|--------|--------|------------|------------|------------------|--------|------|-----|------|
| | σ_1 | μ_1 | τ_1 | Q_1 | U_1 | σ_2 | σ_4 | χ | k' | P | L | T |
| System | | | | | | | | | | | | |
| SS(-1) | .0074 | -6.5272 | 44.753 | 3083.9 | 80,473 | 0 | .200 | -.521 | -2.784 | .491 | .2 | .05 |
| SS(1) | .1350 | -7.2431 | -21.080 | 1176.4 | 36,805 | 0 | .215 | -.485 | -2.882 | .555 | .2 | .05 |
| SS(+1) | .2616 | -8.140 | -77.202 | 226.1 | 7,894 | 0 | .230 | -.453 | -3.047 | .620 | .2 | .05 |
| SS(4) | .1010 | -5.906 | -7.752 | 1,462 | 41,923 | -.06 | .215 | -.477 | -2.859 | .556 | .2 | .05 |
| SS(6) | .2452 | -7.812 | -75.158 | -3,383 | 4,284 | -.06 | .215 | .495 | -3.200 | .559 | .25 | .025 |
| SS(12) | .3051 | -8.207 | -102.4 | -1,006 | -8,691 | -.06 | .215 | -.487 | -3.571 | .560 | .30 | .025 |
| SS(20) | .1398 | -7.144 | -25.99 | 951.3 | 32.301 | -.1 | .130 | -.629 | -3.105 | .220 | .40 | .025 |
| SS(21) | .1633 | -7.251 | -37.981 | 596.52 | 24.083 | -.1 | .135 | -.619 | -3.147 | .241 | .40 | .025 |
| SS(24) | .1415 | -7.034 | -29.80 | 760.3 | 27.000 | -.14 | .135 | -.615 | -3.134 | .241 | .40 | .025 |

The sub-routine Sph(357911) has also been used in place of Sph(357) in the RL-programme and in the SS-programme. The size of these 9th and 11th order versions of the programmes exceeds the main store of the Elliott 503 computer. However, a backing store which was installed during this work, allows the programme to be run in segmented form. (The compiler for operating the segmented programmes is not yet fool-proof and, so far, we have only had consistent results with the RL-programme. The extra complication of the SS-programme has caused intermittent failure, thus preventing serious surveys with it.)

3.2.3.2 Behaviour of 9th and 11th order Buchdahl

Coefficients in the Optimum-Monochromatic-Region.

In Figure 2.35 and 2.36 we observed the variation of LA' versus ρ versus R_4 . These figures showed that the region beyond about $\rho = 0.15$ was minimized by R_4 . We now ask, is this due to some freak balancing of all the higher orders or, does it mean that the higher orders pass through zero in the same way that σ_1 , μ_1 and τ_1 do in the region of $R_4 = 0.215$.

The above question is examined in Table 3.3 (top three entries) in which the spherical coefficients of 3rd, 5th, 7th, 9th and 11th order are shown for the three systems SS(-1), SS(1) and SS(+1) which straddle the optimum monochromatic-region (see Section 2.5.9.1). It is evident that all these orders of spherical coefficients pass through zero in the optimum region as R_4 goes from 0.20 to 0.23.

2/

Table 3.4

System SS(-1)

Surface Contributions

| Surface | σ_1 | μ_1 | τ_1 | Q_1 | U_1 |
|---------|------------|---------|----------|-----------|------------|
| 1 | 1.145 | 2.980 | 9.157 | 30.746 | 109.178 |
| 2 | 1.905 | 12.302 | 73.537 | 428.684 | 2486.830 |
| 3 | -6.238 | -45.173 | -325.830 | -2459.562 | -19402.733 |
| 4 | 1.728 | 24.498 | 371.403 | 5860.312 | 94366.133 |
| 5 | -1.803 | -17.418 | -171.125 | -1104.364 | 5033.510 |
| 6 | .341 | 4.389 | 48.853 | 321.943 | -2226.172 |
| 7 | 2.912 | 11.875 | 38.757 | 6.147 | 106.729 |
| Total | .0007 | -6.527 | 44.753 | 3083.907 | 80473.476 |

System SS(1)

| | | | | | |
|-------|--------|---------|----------|-----------|------------|
| 1 | 1.135 | 2.938 | 8.975 | 29.963 | 105.790 |
| 2 | 1.660 | 10.457 | 60.404 | 339.711 | 1897.146 |
| 3 | -5.691 | -39.807 | -276.457 | -1999.043 | -15056.681 |
| 4 | 1.475 | 18.840 | 258.129 | 3681.867 | 53592.664 |
| 5 | -1.610 | -15.121 | -150.939 | -1175.087 | -3348.418 |
| 6 | .285 | 3.594 | 41.267 | 343.509 | 878.570 |
| 7 | 2.880 | 11.854 | 37.540 | -44.559 | -1563.555 |
| Total | .135 | -7.243 | -21.080 | 1176.362 | 36505.518 |

System SS(+1)

| | | | | | |
|-------|--------|---------|----------|-----------|------------|
| 1 | 1.156 | 3.030 | 9.370 | 31.668 | 113.193 |
| 2 | 1.398 | 8.708 | 49.200 | 269.498 | 1461.800 |
| 3 | -5.174 | -35.279 | -237.861 | -1659.097 | -12002.435 |
| 4 | 1.208 | 13.789 | 168.305 | 2139.733 | 27766.099 |
| 5 | -1.460 | -13.520 | -138.676 | -1244.213 | -8655.876 |
| 6 | .236 | 2.968 | 35.608 | 350.901 | 2610.609 |
| 7 | 2.896 | 12.162 | 36.850 | -114.635 | -3399.031 |
| Total | .261 | -8.140 | -77.202 | -226.144 | 7894.359 |

Clearly these coefficients lag one behind the other as the order increases, with the exception of μ_1 , which appears to precede the rest slightly in approaching zero in this (χ, k', R_4) -section at $L = 0.2$, $T = 0.05$.

In Table 3.4 we have the surface contributions of the systems SS(-1), SS(1) and SS(+1). The columns depict the surface contributions of $\sigma_1, \mu_1, \tau_1, Q_1$ and U_1 from right to left and the rows represent the surfaces from 1 to 7. The bottom row of each system contains the sum of of the surface contributions, that is, the coefficients of the system.

The reason for reproducing the surface contributions is to allow us to examine them in the light of a comment made by Buchdahl. At the conclusion of his paper^(13.4) in which he deals with the 9th order spherical he says, "Qualitatively speaking in the design of a system which is intended to perform satisfactorily at a maximum of $f/2$, say, one will in general aim at individual contributions which (with $f' = 1$) are at most of the order of 1000." It is clear that this has been achieved with the optimum-monochromatic type 121. Thus two-zone correction is associated with a Q_1 of the order of 1000.

3.2.3.3 Behaviour of the 9th and 11th Order Spherical Coefficients in the Optimum-Chromatic-Region.

The spherical coefficients of the systems appearing at different stages of the chromatic design of the type

121 are shown in the lower part of Table 3.3. This sequence of systems begins with SS(4) (the optimum-monochromatic-system) then runs through SS(6) and SS(12) to the final systems SS(20), SS(21), SS(24) that occur close together in the optimum-chromatic-region of (λ, k', P, L, T) .

The systems SS(4), SS(6) and SS(12) are three of the four systems which were used to demonstrate the effect of L on LA' at different wavelengths in Figure 3.6. Now considering these systems in Table 3.3 it is evident that the spherical coefficients of all available orders pass successively through zero as L is increased. We also note on comparing SS(4), SS(6) and SS(12) with SS(-1) and SS(+1) that

$$\Delta Q_1 / \Delta R_4 \approx 2 \Delta Q_1 / \Delta L$$

and

$$\Delta U_1 / \Delta R_4 \approx 2 \Delta U_1 / \Delta L$$

This confirms the conclusion arrived at earlier during the study of LA' versus P versus λ that R_4 and L have similar effects on the spherical coefficients which are associated with the marginal zones.

Comparing the optimum systems SS(20), SS(21) and SS(24) with SS(1) shows that colour correction has not caused any significant change in the magnitude of the spherical coefficients of the first five orders. Thus the characteristic pattern of the spherical coefficients associated with two-zone correction extends to include the 11th order at least. Of course the "optimum-chromatic-system" occurs at about $R_4 = 0.13$ as compared with SS(1) or SS(4)

Table 3.5.1

| | | Spherical Coefficients | | | | | | | |
|--------|---|------------------------|---------|----------|--------|---------|-------|-----|------|
| | | σ_1 | μ_1 | τ_1 | Q_1 | U_1 | R_4 | L | T |
| SS(4) | c | .138 | -6.31 | .707 | 1,582 | 43,671 | | | |
| | d | .101 | -6.90 | -7.75 | 1,461 | 41,923 | .215 | .2 | .05 |
| | e | .071 | -7.37 | -14.4 | 1,366 | 40,547 | | | |
| | F | .007 | -8.36 | 28.5 | 1,166 | 37,678 | | | |
| | g | -.077 | -9.64 | -46.6 | 909 | 33,993 | | | |
| SS(6) | c | .274 | -7.36 | -69.1 | -253 | 5,342 | | | |
| | d | .245 | -7.81 | -75.1 | -338 | 4,284 | .215 | .25 | .025 |
| | e | .221 | -8.16 | -79.9 | -401 | 3,447 | | | |
| | F | .170 | -8.91 | -89.9 | -534 | 1,709 | | | |
| | g | .102 | -9.89 | -102.9 | -704 | -523 | | | |
| SS(12) | c | .328 | -7.86 | -98 | -953 | -8,040 | | | |
| | d | .305 | -8.20 | -102 | -1,006 | -8,691 | .215 | .30 | .025 |
| | e | .286 | -8.47 | -105 | -1,049 | -9,210 | | | |
| | F | .245 | -9.04 | -112 | -1,137 | -10,285 | | | |
| | g | .190 | -9.79 | -122 | -1,251 | -11,669 | | | |
| SS(20) | c | .160 | -6.77 | -19.8 | 1,061 | 34,237 | | | |
| | d | .139 | -7.14 | -26.0 | 951 | 32,302 | .130 | .4 | .025 |
| | e | .123 | -7.43 | -30.8 | 866 | 30,809 | | | |
| | F | .087 | -8.05 | -41.0 | 692 | 27,799 | | | |
| | g | .037 | -8.86 | -54.0 | 474 | 24,098 | | | |

Table 3.5.2

Change in Spherical Coefficients of SS(4) and SS(20) due to change in λ .

| $\Delta\lambda$ | $\Delta\sigma_1$ | | $\Delta\mu_1$ | | $\Delta\tau_1$ | | ΔQ_1 | | ΔU_1 | |
|-----------------|------------------|--------|---------------|--------|----------------|--------|--------------|--------|--------------|--------|
| | SS(4) | SS(20) | SS(4) | SS(20) | SS(4) | SS(20) | SS(4) | SS(20) | SS(4) | SS(20) |
| c - d | .037 | .020 | .61 | .37 | 8.4 | 6.2 | 121 | 110 | 1750 | 1935 |
| d - c | .030 | .016 | .47 | .29 | 7.6 | 4.8 | 95 | 85 | 1376 | 1493 |
| e - F | .064 | .046 | 1.00 | .62 | 14.1 | 10.2 | 200 | 174 | 2870 | 3000 |
| F - g | .084 | .050 | 1.28 | .81 | 18.7 | 13.0 | 257 | 218 | 85 | 3700 |

at $R_4 = 0.215$. Thus the correction of the colour has reduced P from 0.55 to 0.24.

The question comes to mind as to how the spherical coefficients vary with wavelength? In answer to this we have shown the spherical coefficients of SS(4), SS(6), SS(12) and SS(20) for five wavelengths in Table 3.5.1.

It is evident from the Table 3.5.1 that except for σ_1 all the spherical coefficients of all orders for all the wavelengths shown are reduced together as L is increased from 0.2 in SS(4) to 0.3 in SS(12) while R_4 is constant. However on going to SS(20) R_4 is reduced to 0.13 and this causes a dramatic change in the spherical coefficients. The "optimum-chromatic-system" SS(20) shows less variation of the coefficients with wavelength than the "optimum-mono-chromatic-system" SS(4), however, the pattern of the spherical coefficients with regard to both sign and their order of magnitude remains unchanged from λ_c to λ_g in both these systems. Thus the optimization with respect to R_4 , L and T has mainly produced less variation of the spherical coefficients with wavelength. (See Table 3.5.2 in which SS(4) and SS(20) are compared in this respect.) Indeed the characteristic pattern associated with two-zone correction holds fairly well from c to F. (See Table 3.5.1) but it deteriorates rapidly as λ_g is approached and obviously σ_1 is the spherical coefficient most sensitive to change in wavelength.

The above computation of the spherical coefficients to 11th order has been repeated for the other optimum-chromatic-systems SS(21) and SS(24); they are found to behave in a similar way to SS(20). The surface contributions of the spherical coefficients of these three systems SS(20), SS(21) and SS(24) have been computed also. This has shown that the 9th order surface contributions are of the order of 1000 for all wavelengths for these optimum systems.

3.2.3.4 The Convergence of the 9th and 11th Order Spherical Coefficients versus (χ , R_4 , L, T) Demonstrated.

The segmented form of the RL-programme has been used to repeat the "limited-interpolative-survey" of the spherical coefficients versus all the "basic parameters" (χ , k' , P, L, T). This programme as mentioned above uses the procedure Sph(357911) to compute the first five orders of spherical coefficients of the 3rd order triplet.

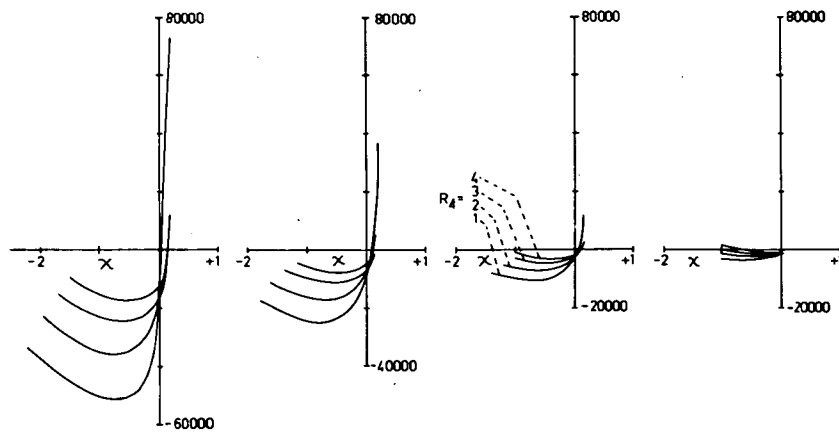
Some results have been obtained and are plotted in Figures 3.23 and 3.24. They are the (χ , R_4 , L)-sections at $k' = -4$ for $T = 0.05$ and $T = 0.01$ for Q_1 , U_1 and ϵ'_{Sph} . In this work R_4 takes the values 0.14 to 0.20 in steps of $\Delta R_4 = 0.02$. The bottom curve which is denoted by $R_4 = 1$ is actually $R_4 = 0.14$ and the top curve $R_4 = 4$ is $R_4 = 0.20$.

It is evident that Q_1 and U_1 follow the trend of σ_1 , μ_1 and τ_1 , however, they lag behind them. The groups of curves are compressed and raised as L increases and T decreases. So it seems that the optimum region occurs

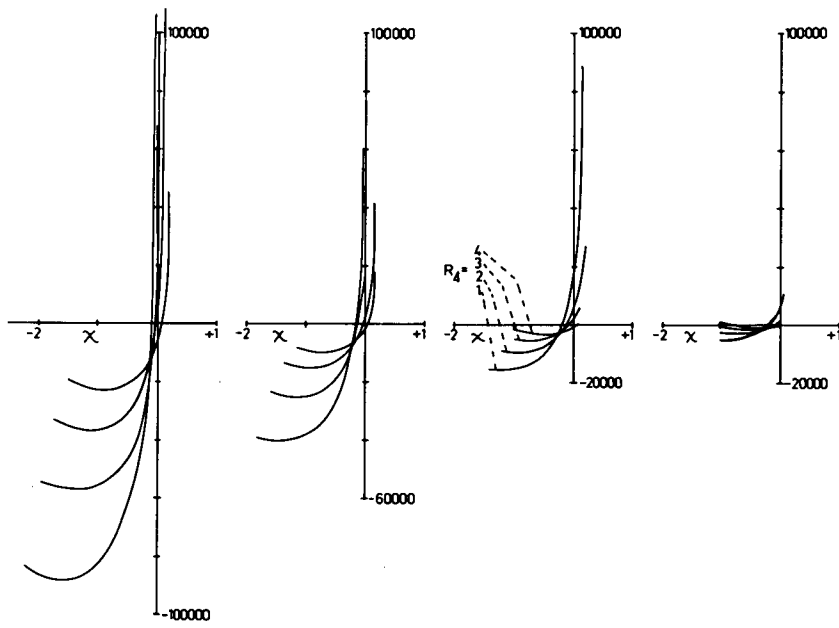
when at least the first five orders of spherical coefficients are near zero in (χ, k', P, L, T) -space. The survey shown in Figure 3.23 and 3.24 is all that could be computed in time available. However the trend is so obvious that further work along these lines at say $k' = -3$ cannot be expected to show anything other than the elevation of all the groups for an increase in k' .

$T=0.01 \quad k'=-4.0$

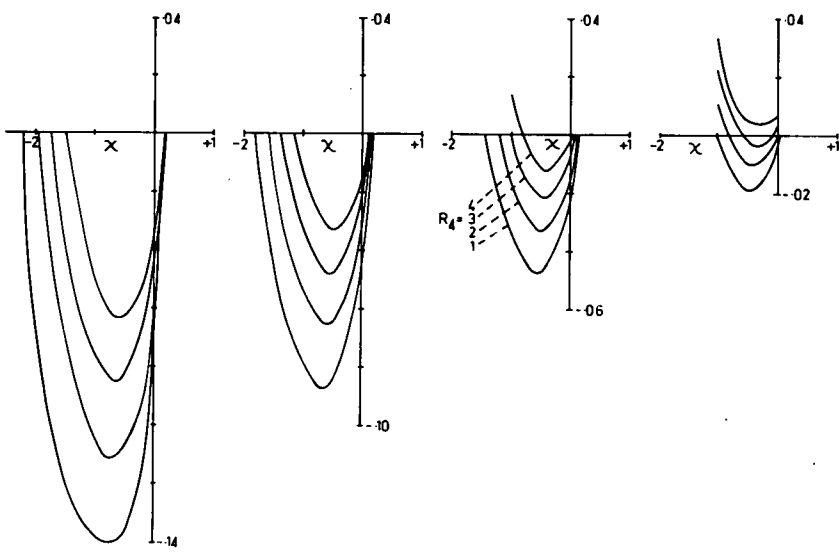
Q_1



U_1



ϵ'



$L=0.1$

$L=0.2$

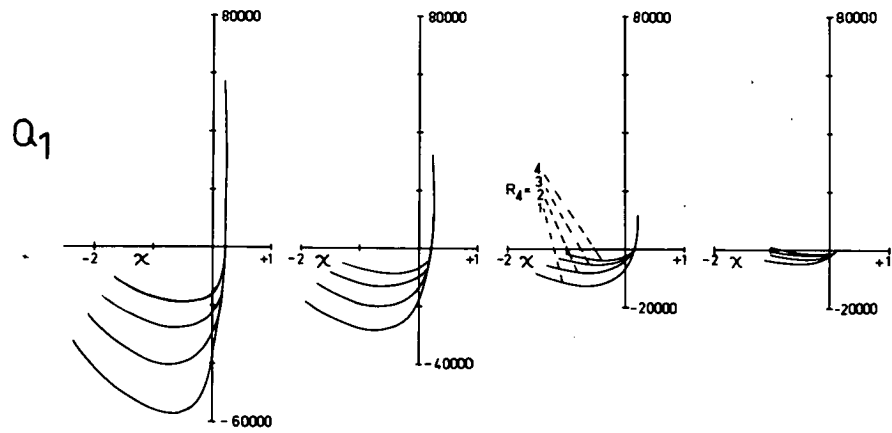
$L=0.3$

$L=0.4$

Fig. 3.23

$T=0.05$ $k'=-4.0$

Q_1



U_1

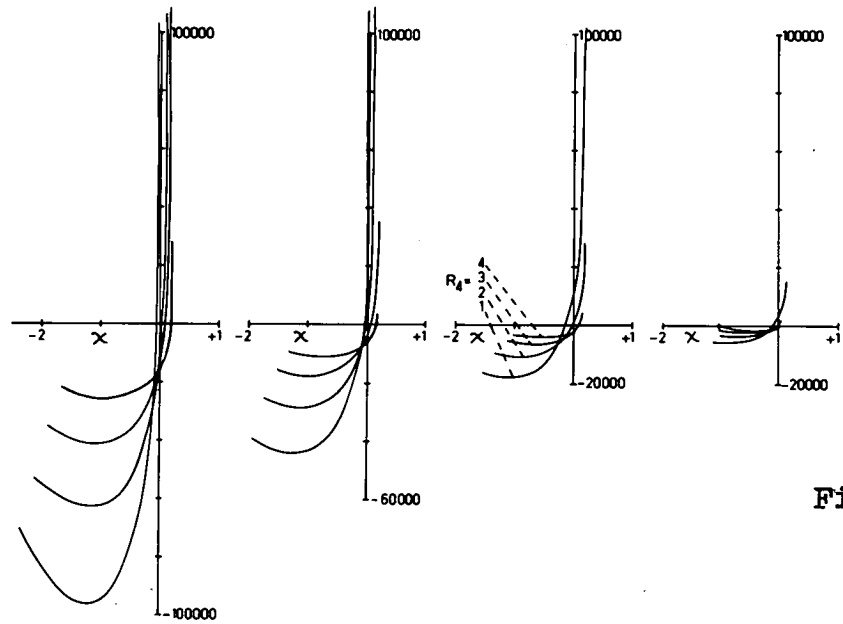
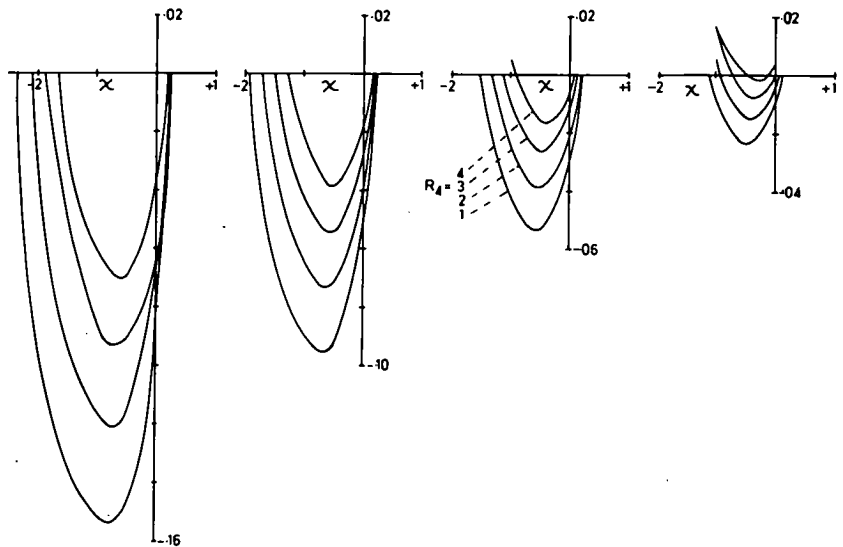


Fig. 3.24

ϵ'



$L=0.1$

$L=0.2$

$L=0.3$

$L=0.4$

CHAPTER 3.3 THE OPTIMUM TYPE 121 WITH THE STOP IN AIR.

3.3.0 Introduction.

The optimum chromatic type 121 systems (SS(20), SS(21) and SS(24)) have been generated with the stop at the front principal point of the cemented doublet which is lens group b. In this chapter the effect that shifting the stop outside the middle lens group has on the aberration-residuals of the type 121 is examined and the system is re-designed so as to restore the correction state.

3.3.1 Computing Technique for Shifting the Stop.

Shifting the stop alters the paths of the off-axial paraxial-rays and therefore changes the aberrations of the off-axial images. Thus, shifting the stop modifies the system prior to iteration of 3rd order residuals with respect to the shapes. This modification has been taken care of in the basic-programme by introducing a sub-routine that computes the coordinates of the principal ray of any selected off-axial pencil for a given position of the aperture stop. This sub-routine occurs immediately after thickening in the sub-routine AC(x).

3.3.2 Optimizing the System after Shifting the Stop.

In Figure 3.25 three stages in the control of the aberrations induced by shifting the stop are depicted. Once again we have the aberrations of the axial-pencil

shown by LA' versus ρ versus λ and those of the off-axial pencil by the transverse aberrations ϵ'_y versus \bar{H} versus λ .

At the top of Figure 3.25 we have the aberrations of the system SS(20) with its stop in air at the front-surface of the lens group b. Indeed this is the only real stop-position we have considered in this work because the time available was insufficient for making a thorough study of changes in the stop-position with the existing computing facilities.

Comparing the ϵ'_y -curves of SS(20) of the Figure 3.25 with the corresponding curves of the original SS(20) in Figure 3.15 it is evident that considerable distortion and some transverse-chromatic-aberration have been introduced by simply moving the stop into the front air-space just outside the lens group b. Re-adjustment of these aberrations involves modification of the parameters L , T , R_4 and R_5 . Using the principles established earlier they are reduced as follows:

1. ϵ'_y for all \bar{H} by increasing T .
2. the distortion (curvature of ϵ'_y -curves) for all λ , by changing R_5 .
3. the increase in the marginal LA' , which has been induced by increasing T , by increasing R_4 .

Thus in the middle pair of graphs in Figure 3.25 we see the bunching of the ϵ'_y -curves (reduction of transverse-chromatic aberration) produced by $\Delta T = +0.025$ and

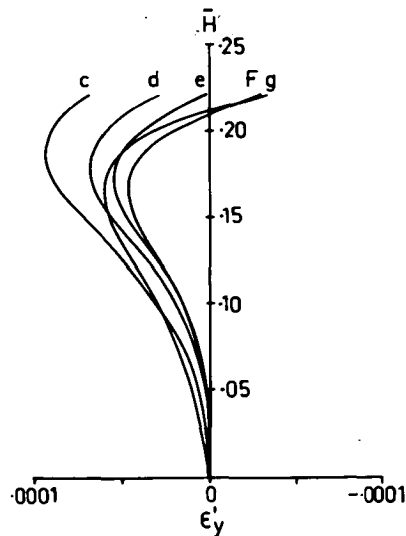
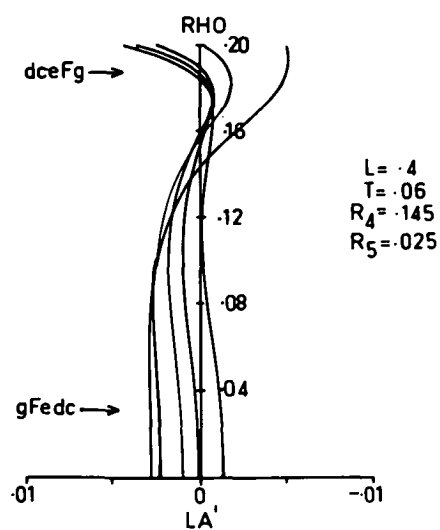
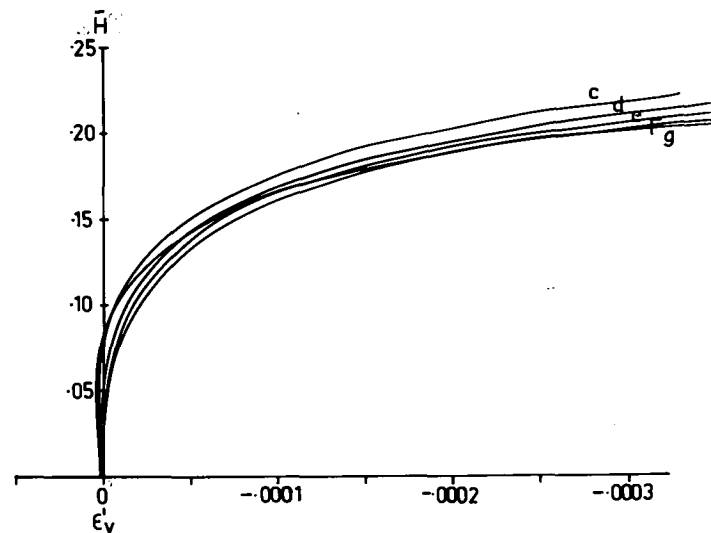
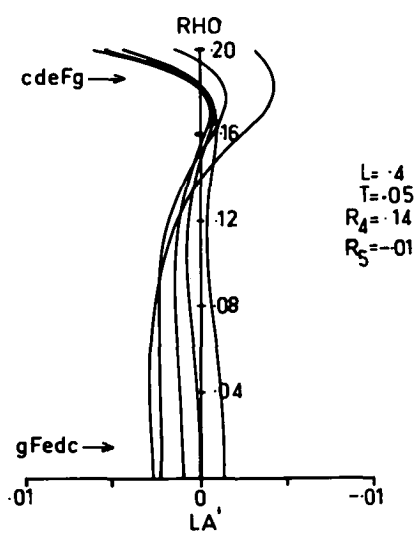
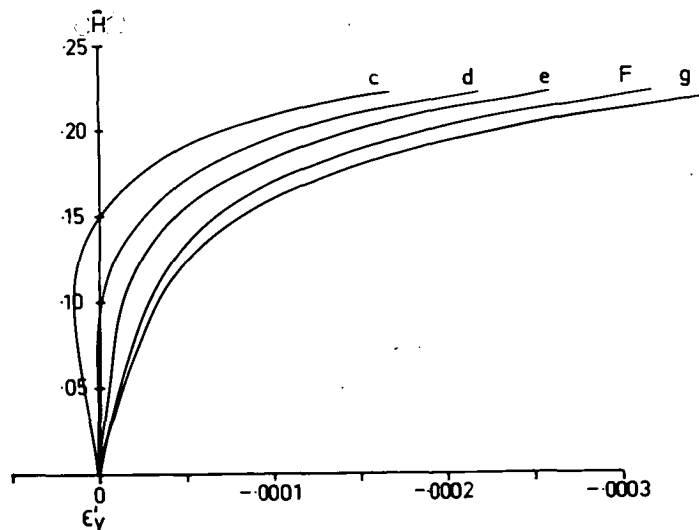
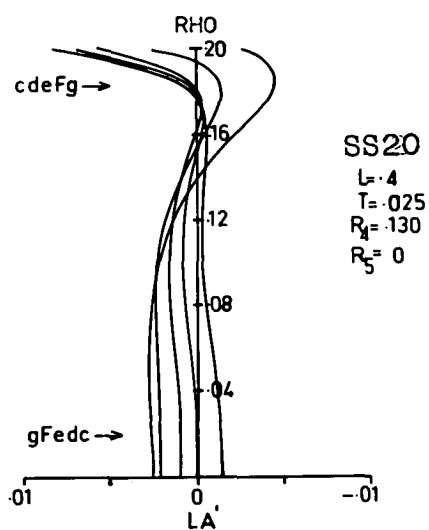


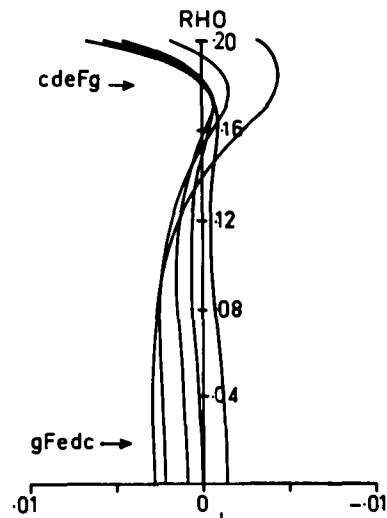
Fig. 3.25

the increased distortion caused by an incorrect change in R_5 of $\Delta R_5 = -0.01$. Also the marginal zones of the ~~curves~~ corresponding LA' -curves have been controlled by $\Delta R_4 = 0.001$ which has been more than sufficient to off-set the effect of $\Delta T = 0.025$. In the bottom pair of Figures we see mainly the effect of the correct use of R_5 . A positive 3rd order residual of $R_5 = 0.025$ has reduced the maximum aberration to $\epsilon_y' < 0.0001$ for all λ .

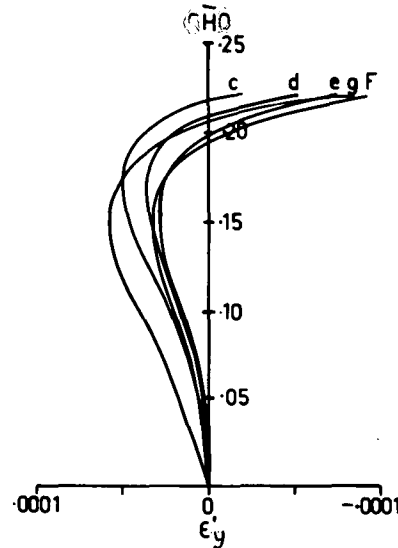
Finally in Figure 3.26 we have two systems with almost identical families of LA' and ϵ_y' -curves but they differ in their coma residual R_2 . Thus we have FS11 which is considered to be derived from SS(20) and FS12 which is considered to be derived from SS(24). Their spot diagrams are shown in Figures 3.28 and 3.29 where it is evident that the small difference in R_2 between the systems produces a more symmetrical flare in the case of FS12. However this is at the expense of the sharpness of the point image.

In Figures 3.30 and 3.31 the effect on the spot diagrams of stopping down the system FS12 to $f/2.8$ and $f/3.1$ is shown. It is evident that the flare in the axial image is caused by the outer zone between $0.18 < \rho < 0.20$. It seems that nothing of value is contributed by the outer zone and therefore it would appear that $f/2.8$ is about the maximum useful aperture of the type 121.

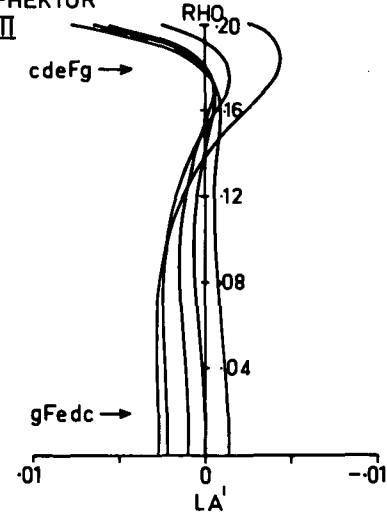
ALHA-HEKTOR Mk I



FS 11
 $L = .4$
 $T = .07$
 $R_2 = -.1$
 $R_4 = .145$
 $R_5 = .02$



ALHA-HEKTOR Mk II



FS 12
 $L = .4$
 $T = .07$
 $R_2 = -.14$
 $R_4 = .145$
 $R_5 = .02$

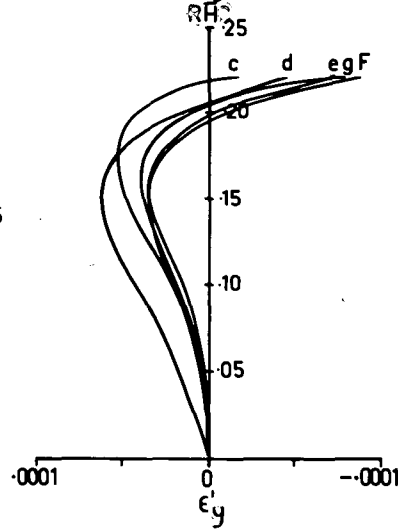


Fig. 3.26

ARGENTIERI PENTAC $f/2.5$

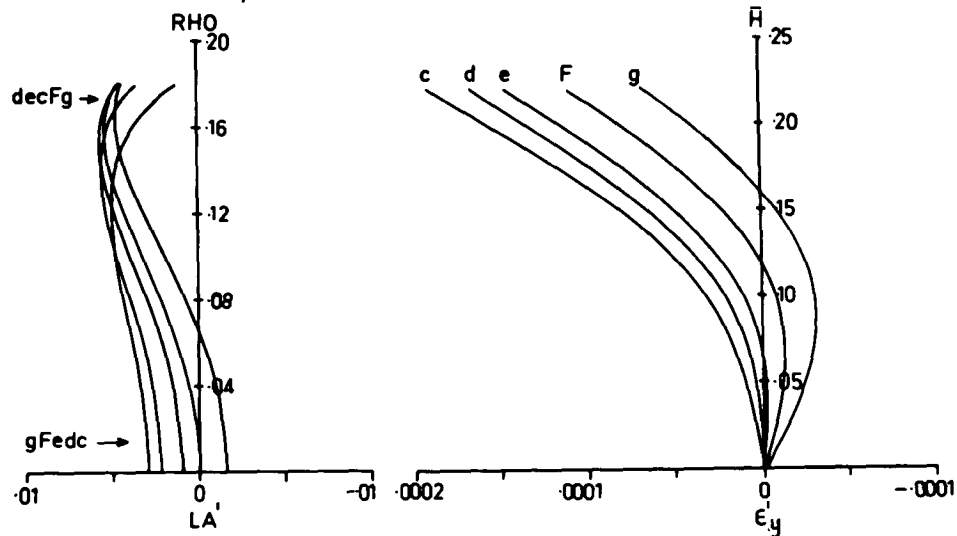
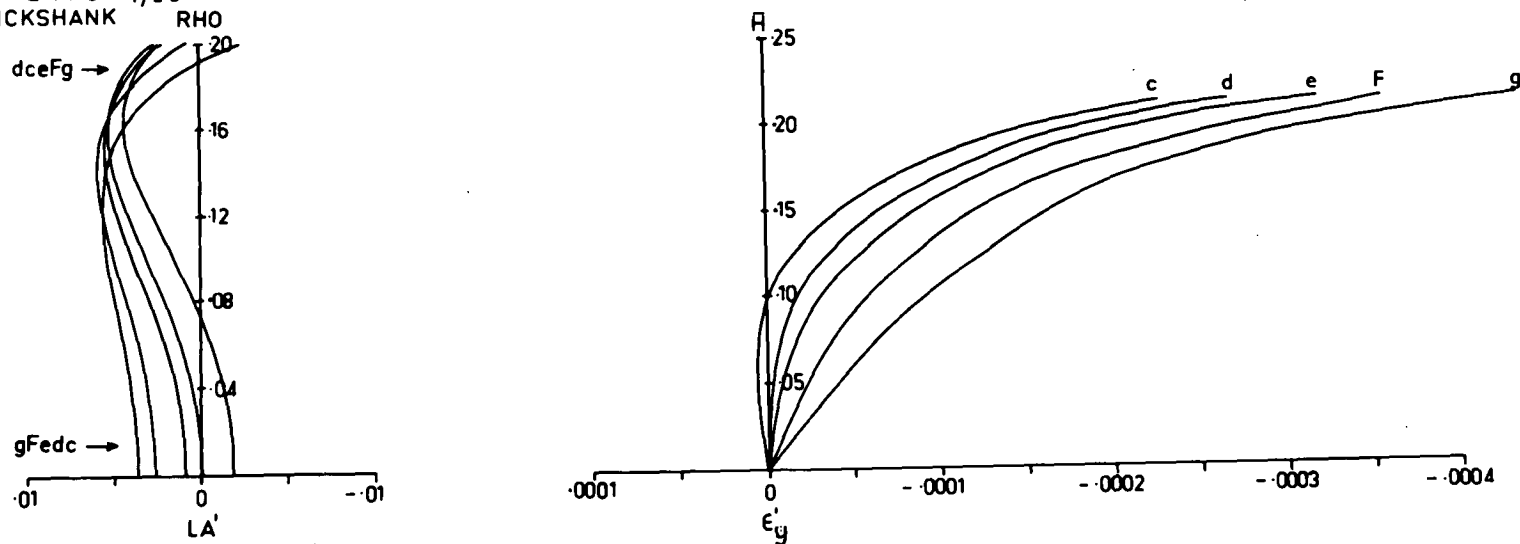


Fig. 3.27

H4 PENTAC $f/2.5$
CRUICKSHANK



3.3.3 Comparing the Hektor with the Pentac.

Two Pentac systems which have been described in the literature are now examined for the sake of comparing the potential of the type 121 with some aspects of the performance of equivalent systems which have been proved. These have been designed by Cruickshank and Argentieri to work at a maximum aperture of $f/2.5$ which is the same as the Hektor (type 121). (The Cruickshank triplet has been produced commercially and proved to be a very successful projection lens.)

Considering LA^0 and ϵ_y^1 only, the Hektor compares favourably with these Pentacs (compare Figures 3.26 and 3.27). It has superior correction of ϵ_y^1 and it has slightly smaller chromatic variation of LA^1 up to $\rho = 0.16$ ($f/3.1$). However the Pentacs seem to have better correction of the extreme marginal zone; they appear to make more use of the light between $\rho = 0.18$ and $\rho = 0.20$. This seems to be due to over-correcting the marginal zones. We can do the same by increasing R_4 and L so as to swing the LA^1 -curves across to the right. Indeed this type of correction of LA^1 versus ρ versus λ was referred to in the discussion of Figure 3.5, see section 3.1.2. However the relative merits of these different types of correction is outside the scope of this work.

The spot diagrams of the Pentacs are shown in Figures 3.32 to 3.35. The point of interest here is the evidence of the dramatic improvement that an image plane

Table 3.6

FS12 - Type 121 ALHA HEKTOR

$f/2.5$ ($\ell = 0.2$) $x = 0$

At $V = 0^\circ$

| Radius | c | d | e | F | g |
|--------|-----|-----|-----|-----|-----|
| 1 | 56% | 85% | 58% | 22% | 17% |
| 2 | 90 | 90 | 92 | 59 | 44 |
| 3 | 90 | 92 | 94 | 97 | 61 |
| 4 | 92 | 94 | 94 | 98 | 66 |
| 5 | 94 | 94 | 94 | 98 | 73 |
| 6 | 94 | 94 | 94 | 100 | 76 |
| 7 | 94 | 94 | 94 | | 84 |
| 8 | 94 | 94 | 97 | | 89 |
| 9 | 94 | 94 | 98 | | 100 |
| 10 | 94 | 97 | 98 | | |
| 11 | 6 | 3 | 2 | | |

At $V = 5^\circ$

| | | | | | |
|----|--|----|--|--|--|
| 1 | | 16 | | | |
| 2 | | 43 | | | |
| 3 | | 58 | | | |
| 4 | | 66 | | | |
| 5 | | 72 | | | |
| 6 | | 77 | | | |
| 7 | | 81 | | | |
| 8 | | 83 | | | |
| 9 | | 87 | | | |
| 10 | | 92 | | | |
| 11 | | 8 | | | |

At $V = 10^\circ$

| | | | | | |
|----|--|----|--|--|--|
| 1 | | 13 | | | |
| 2 | | 32 | | | |
| 3 | | 48 | | | |
| 4 | | 50 | | | |
| 5 | | 54 | | | |
| 6 | | 60 | | | |
| 7 | | 63 | | | |
| 8 | | 67 | | | |
| 9 | | 69 | | | |
| 10 | | 72 | | | |
| 11 | | 28 | | | |

Table 3.7

H4-Pentac CRUICKSHANK

$f/2.5$ ($\rho = 0.2$) $x = -0.004$

At $V = 0^\circ$

| Radius | c | d | e | F | g |
|--------|-----|-----|-----|-----|-----|
| 1 | 49% | 34% | 41% | 36% | 35% |
| 2 | 65 | 82 | 65 | 57 | 59 |
| 3 | 98 | 100 | 97 | 94 | 81 |
| 4 | 100 | | 100 | 94 | 85 |
| 5 | | | | 94 | 90 |
| 6 | | | | 98 | 90 |
| 7 | | | | 100 | 92 |
| 8 | | | | | 94 |
| 9 | | | | | 94 |
| 10 | | | | | 94 |
| 11 | | | | | 4 |

At $V = 5^\circ$

| | | | | | |
|----|--|----|--|--|--|
| 1 | | 25 | | | |
| 2 | | 70 | | | |
| 3 | | 87 | | | |
| 4 | | 92 | | | |
| 5 | | 93 | | | |
| 6 | | 93 | | | |
| 7 | | 95 | | | |
| 8 | | 95 | | | |
| 9 | | 96 | | | |
| 10 | | 96 | | | |
| 11 | | 4 | | | |

At $V = 10^\circ$

| | | | | | |
|----|--|----|--|--|--|
| 1 | | 16 | | | |
| 2 | | 29 | | | |
| 3 | | 43 | | | |
| 4 | | 55 | | | |
| 5 | | 71 | | | |
| 6 | | 84 | | | |
| 7 | | 86 | | | |
| 8 | | 87 | | | |
| 9 | | 88 | | | |
| 10 | | 88 | | | |
| 11 | | 12 | | | |

Table 3.8

FS12 Stopped down to $f/2.8$

$(\rho = 0.18) \quad x = 0$

At $V = 0^\circ$

| Radius | c | d | e | F | g |
|--------|-----|------|-----|-----|-----|
| 1 | 64% | 100% | 57% | 27% | 22% |
| 2 | 100 | | 100 | 70 | 59 |
| 3 | | | | 100 | 80 |
| 4 | | | | | 83 |
| 5 | | | | | 87 |
| 6 | | | | | 94 |
| 7 | | | | | 97 |
| 8 | | | | | 100 |
| 9 | | | | | |
| 10 | | | | | |
| 11 | | | | | |

At $V = 5^\circ$

| | | | | | |
|----|--|----|--|--|--|
| 1 | | 21 | | | |
| 2 | | 50 | | | |
| 3 | | 65 | | | |
| 4 | | 71 | | | |
| 5 | | 77 | | | |
| 6 | | 81 | | | |
| 7 | | 86 | | | |
| 8 | | 90 | | | |
| 9 | | 91 | | | |
| 10 | | 95 | | | |
| 11 | | 5 | | | |

At $V = 10^\circ$

| | | | | | |
|----|--|----|--|--|--|
| 1 | | 14 | | | |
| 2 | | 37 | | | |
| 3 | | 54 | | | |
| 4 | | 58 | | | |
| 5 | | 63 | | | |
| 6 | | 68 | | | |
| 7 | | 71 | | | |
| 8 | | 76 | | | |
| 9 | | 79 | | | |
| 10 | | 83 | | | |
| 11 | | 17 | | | |

shift produces in a system that has significant but fairly constant zonal spherical aberration. Figures 3.32 and 3.33 show the spot diagrams of the Pentacs in their paraxial image planes (at $X = 0$) in which it is evident that all the spot diagrams are extremely de-focussed. The dramatic improvement evident in Figures 3.34 and 3.35 has been achieved by shifts of $X = -0.004$ for the H4 and $X = -0.003$ for the Argentieri Pentac. (X measured in units of f' .) However an image plane shift is not required with the present correction state of the Hektor, its zonal spherical is so small that the paraxial image plane is its best focal plane.

It is evident from the configuration of the spot diagrams that the Hektor possibly has better axial performance than the Pentacs and very similar off-axial behaviour. However these qualitative conclusions are only partly supported by the analysis of the spot diagrams which are presented in Tables 3.6 and 3.7. (We have only reproduced the H4-Pentac densities because the performance of both Pentacs is very similar.)

In each table we have the distribution of light in the spot diagrams for the five wavelengths at 0° and for d-light only at 5° and 10° . Each row gives the percentage of the light of the incident pencil that lies inside a circle centred on the principal-ray in an image plane distant X from the paraxial image plane. Starting with a radius of 0.0001 of the focal length the radius of the circle

increases in steps of 0.0001 to 0.001. Thus we have distribution of light inside ten concentric circles in a selected image plane.

If we set 0.0004 as the maximum radius of the circle for comparing the systems (this corresponds to an image patch of 0.0012 inches radius for $f' = 4$ inches) then with such a criterion the Pentac has the superior spot diagrams. However, if we use a smaller scanning-circle then clearly the Hektor has the better axial image. It is evident that the Pentac has better balance of colour towards the blue end of the spectrum which is obviously due to better control of the marginal zone with respect to the wavelength, which has been produced by over-correcting it with L and R_4 .

The Pentac has 91% of the incident light inside a circle of 0.0004 radius at 5° off-axis and 50% at 10° , whereas the Hektor has 67% at 5° and 41% at 10° . Thus the assessment of the spot diagrams shows the Pentac to be the better system at $f/2.5$. However, the performance of the Hektor seems creditable when we recall that it is only a 4-component system being compared with the Pentac a 5-component system.

In Table 3.8 the densities of the spot diagrams of the Hektor are analysed with the aperture reduced to $f/2.8$. It is evident that removal of the extreme marginal zone creates a very much better system. The $f/2.8$ system

FS 11 $P=0.2$ $f/25$
 $V=0$ $V=5$ $V=10$

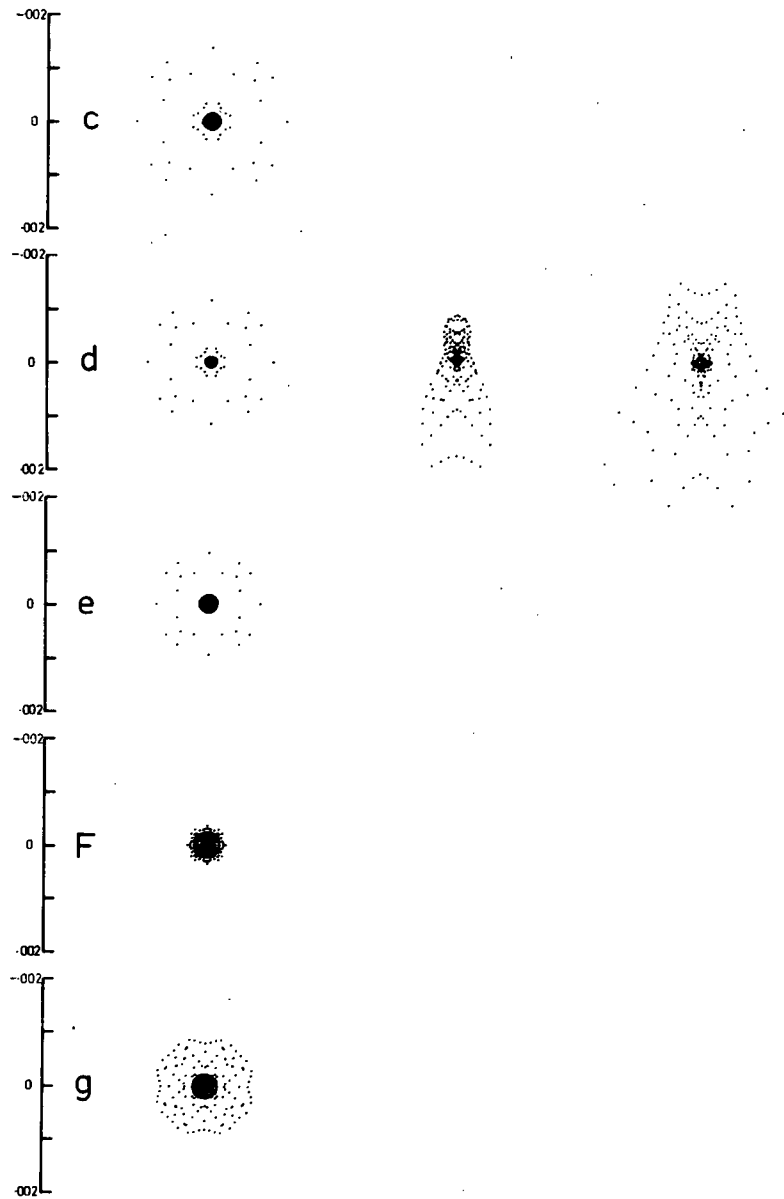


Fig. 3.28

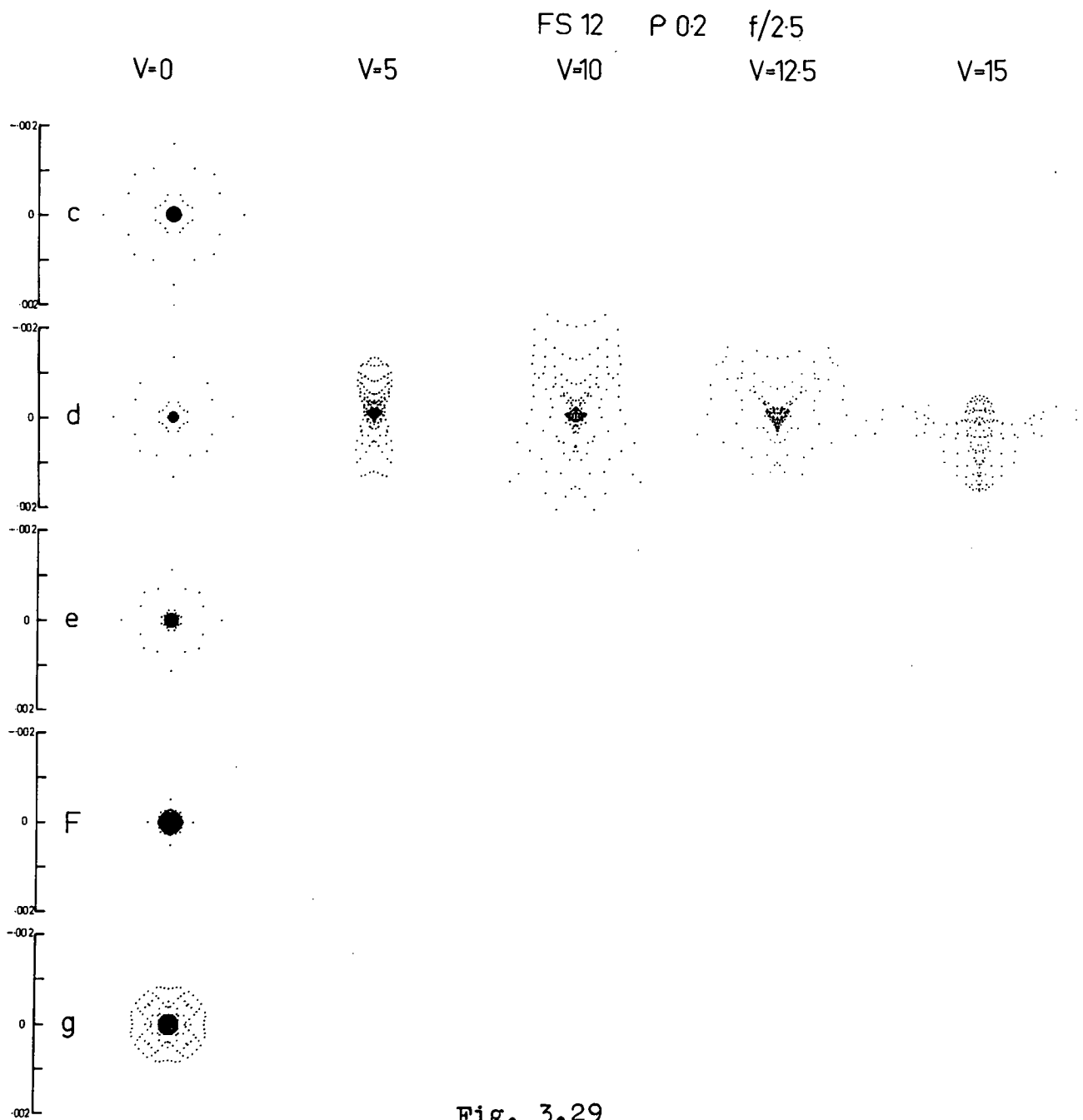


Fig. 3.29

FS12 P=0.18 f/2.8

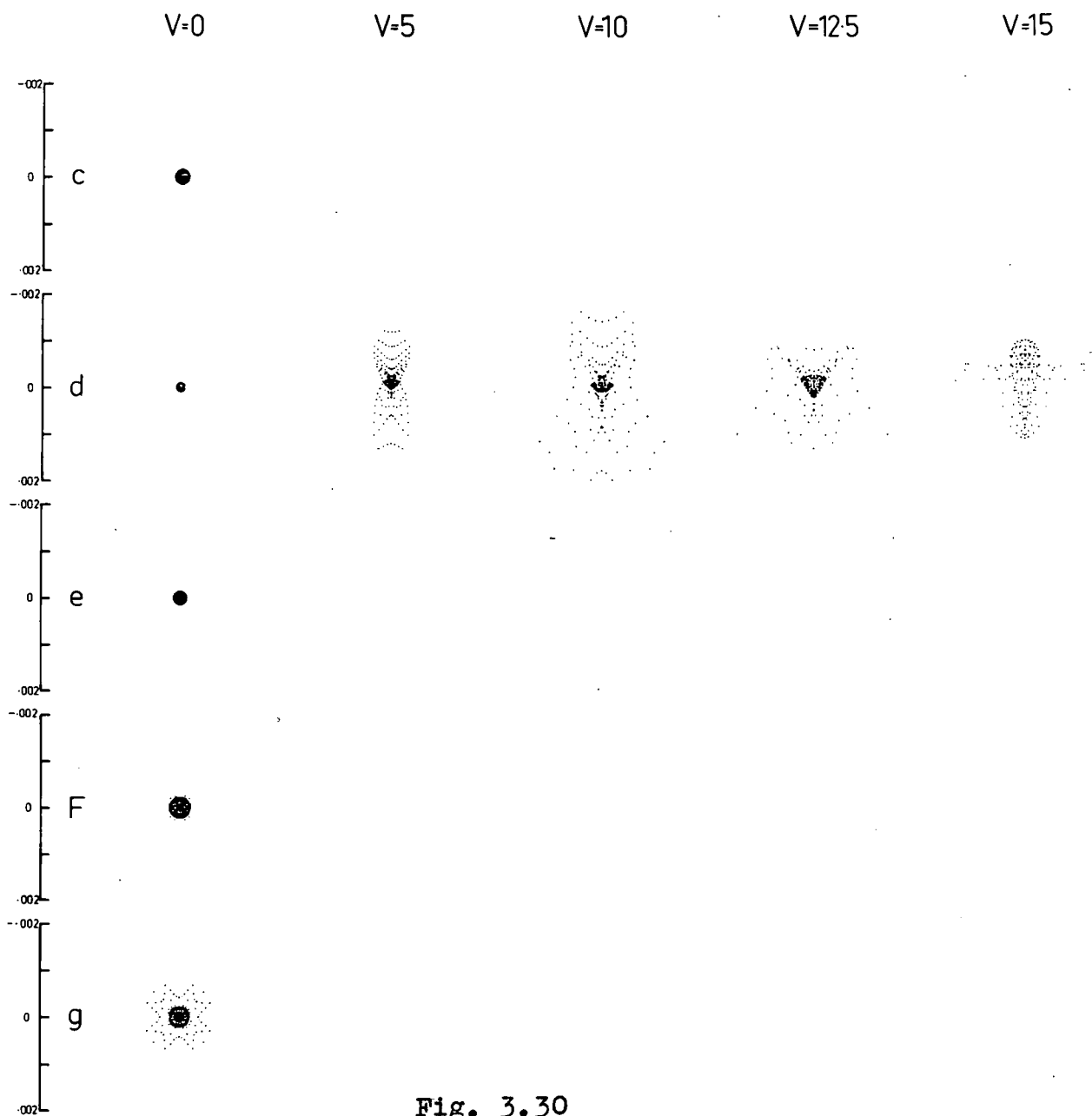
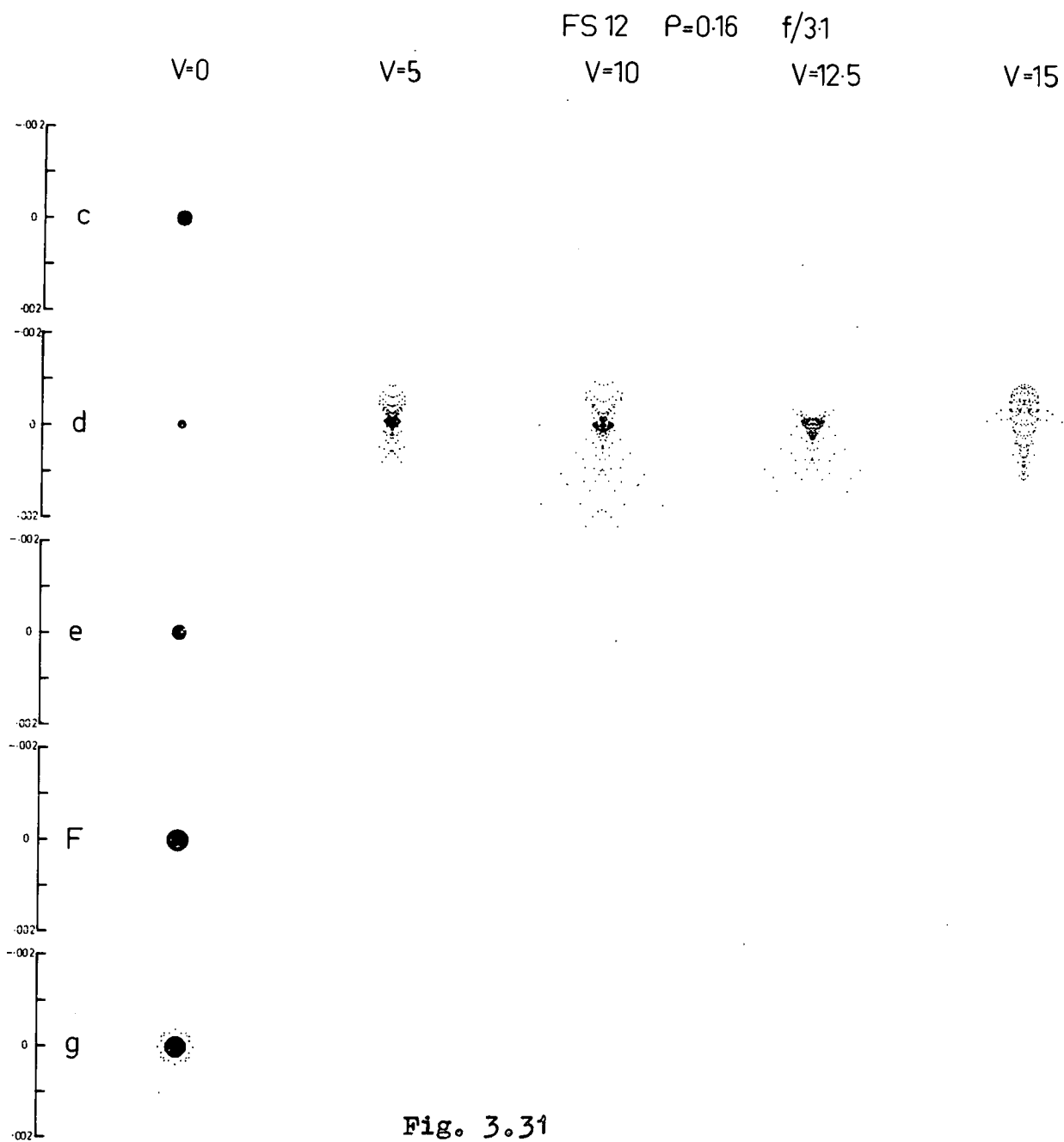


Fig. 3.30



PENTAC H4 X=0

V=0

V=5

V=10

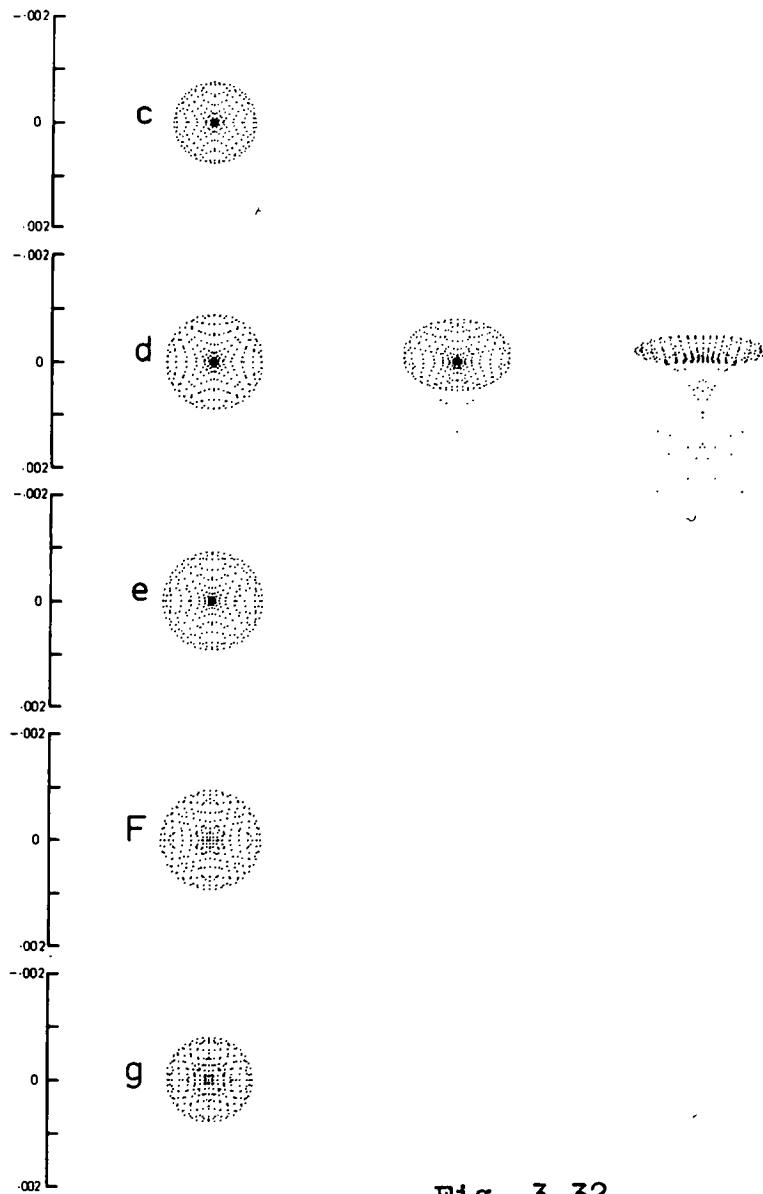


Fig. 3.32

ARGENTIERI $X=0$

$V=0$

$V=5$

$V=10$

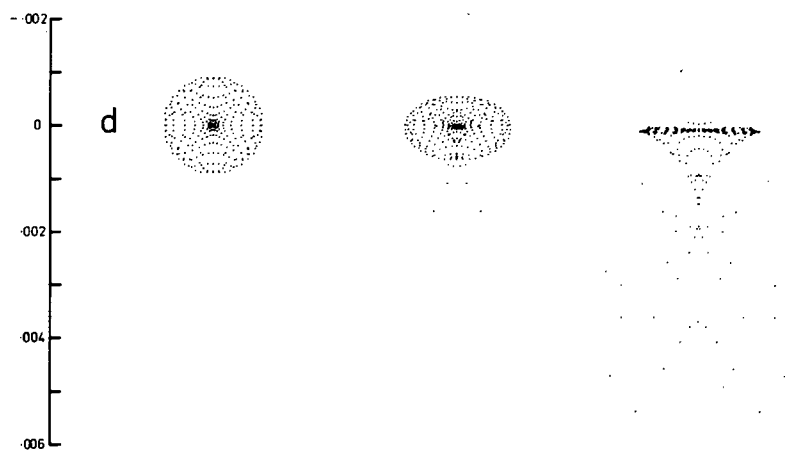


Fig. 3.33

PENTAC H4

$X = -.004$

V=0

V=5

V=10

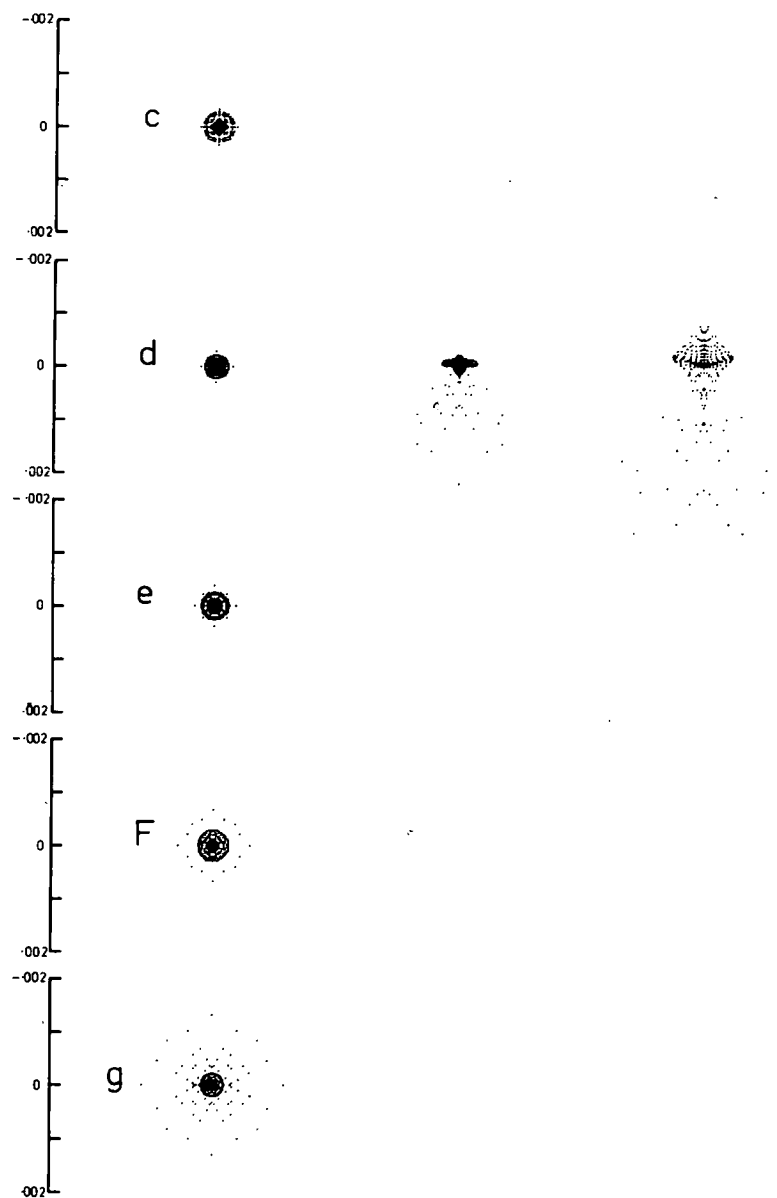


Fig. 3.34

ARGENTIERI $X = -0.003$

V=0

V=5

V=10

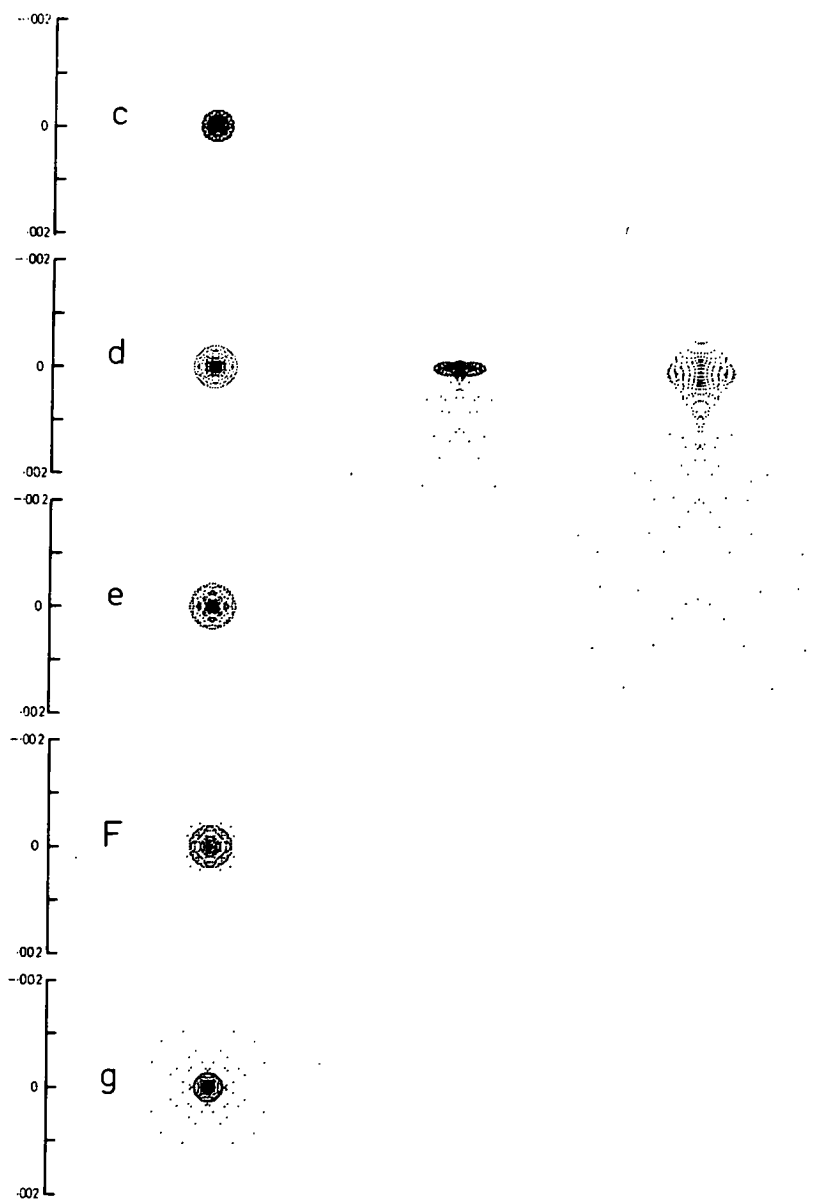


Fig. 3.35

has 71% at 5° and 58% at 10° inside a radius of 0.0004 and on axis most of the light is inside a radius of 0.0002.

3.3.4 Comparing the Parameters of the Type 121 with the Pentac at Various Design Stages.

In Table 3.9 the construction parameters which occur at the three main stages of development of the type 121 are compared with the H4-Pentac. The systems are SS(4), "the optimum-monochromatic-system", SS(24) the "optimum-chromatic-system" with the stop in the lens group b, FS12 the optimum type 121 with the stop at the front surface of lens group b and the H4-Pentac.

It is evident that the basic parameters (\mathcal{X} , k' , P , L , T) are more sensitive to design changes than either ΔV_b or ϕ_c/ϕ_a and therefore would seem to be preferable. Again we note the characteristic pattern of the spherical coefficients associated with two-zone correction. Moreover, it is evident that the critical design parameters during chromatic correction are P and L .

The greatest difference between the basic parameters of the type 121 and the Pentac occurs for ΔV . It was noted earlier that the type 121 had a ΔV very near that quoted by R.E. Hopkins for the type 111; however, the Pentac has the extraordinary value of $\Delta V = 61.12$. The basic parameters (N_a , N_b , N_c) of the Pentac are near enough to be considered normal values for triplets but the basic parameters (V_a , V_b , V_c) are abnormal.

Let us consider the effect of a large ΔV on the type 121. This, we know, would raise all the aberration curves in (χ, k', P) -space well above the χ -axis at moderate P , L and T . Consequently, in order to have any prospect of a solution the curves would have to be lowered and converged by increasing P and L and then reducing T . Thus it would seem that such a solution would have a fairly large σ_1 , P and L associated with reduced astigmatic coefficients μ_4 , μ_5 and μ_6 . This prediction fits the Pentac fairly well, since it has $\sigma_1 = 0.366$ compared with the 0.136 of the type 121. $P = 0.566$ compared with $P = 0.28$ and $L = 0.58$ compared with $L = 0.4$. Indeed, even T is reduced to $T = 0.0024$ as compared with $T = 0.07$ of the type 121.

Except for σ_1 the spherical aberration coefficients (up to the 11th order) of the Pentac are of the same order of magnitude as those of the type 121 but they are all negative. This gives the overcorrection of the marginal zone which seems to benefit the axial performance at maximum aperture. Thus on axis the Pentac and the type 121 solutions differ primarily in σ_1 and $\sigma_4 (= R_4)$.

In Table 3.10 all the 3rd, 5th and 7th order coefficients are compared. Clearly the Pentac has significantly smaller coefficients in every case except for the primary spherical (σ_1), the tertiary spherical (τ_1) and the Petzval coefficient (σ_4). In particular, the Pentac,

as predicted above, has small values for μ_4 , μ_5 and μ_6 which, therefore, means small oblique spherical aberration and, consequently, enhances the prospect of a good field. This is confirmed by the values of \bar{H}_n (see section 2.3.1) and the corresponding values of the semi-field angle V shown at the bottom of Table 3.10. These examples support the conclusion of section 2.3.1 that the 7th order \bar{H}_n predicts the maximum possible semi-field far more accurately than the 5th order \bar{H}_n when the semi-field approaches 20° . It is also evident that the 5th order \bar{H}_n is good enough for semi-fields of about 10° .

The 7th order \bar{H}_n is 0.196 for the system FS12 and the large value of 0.402 for the Pentac. Therefore, the predicted semi-field of the final type 121 is about 11° which agrees very well with our spot diagrams and their analysis. The Pentac on the other hand is predicted to have a semi-field of 22° . Thus the Pentac is predicted to have the better off-axial performance. This has been borne out by the spot diagram analysis.

We also note that the value of ϕ_c/ϕ_a of the Pentac is very near 1.5 which is the ratio recommended by Taylor for getting small zonal spherical.

The optimum Pentac solution as we saw above has a fairly large σ_1 when the spherical coefficients are optimized. Thus, of necessity, the axial correction of the Pentac consists of reducing a 3rd-order-residual with a set of negative higher-order-residuals of opposite sign.

On the other hand the type 1121 allows the designer to minimize all spherical coefficients (including \tilde{G}_1) up to the 11th order at least. Thus in this work we have adopted the technique of minimizing all spherical coefficients and then combined this with sign variation of the orders so as to produce a minimum total residual. However, after looking at the Pentac it may be better for the marginal zone of the type 121 if all the outer zones were overcorrected slightly rather than undercorrected.

Table 3.9

| | Type 121 | | | Type 212 | Type 122 |
|-------------------------------|------------------------------|--------------------------|--------------------------|------------|--------------------------|
| | Optimum Monochromatic System | Optimum Chromatic System | Optimum Chromatic System | | Optimum Chromatic System |
| System | SS(4) | SS(24) | FS12 | H4-Pentac | SS(25.1) |
| Basic Parameters | | | | | |
| k_1' | -.477 | -.615 | -.528 | -.346 | -.294 |
| k_2' | --- | --- | --- | -.540 | --- |
| k_3' | -2.859 | -3.133 | -3.056 | --- | -3.334 |
| P | --- | --- | --- | -2.255 | -2.200 |
| L | .556 | .241 | .282 | .566 | .147 |
| T | .2 | .4 | .4 | .58 | .3 |
| | .05 | .25 | .07 | .0024 | .075 |
| Fundamental Parameters | | | | | |
| c_1 | 2.130 | 2.088 | 2.216 | 2.050 | 2.628 |
| c_2 | -.369 | -.491 | -.410 | -2.026 | -.827 |
| c_3 | -2.163 | -2.629 | -2.512 | -.336 | -2.370 |
| c_4 | -4.291 | -4.878 | -4.821 | -1.516 | -4.653 |
| c_5 | 2.433 | 2.898 | 2.933 | 2.608 | 3.503 |
| c_6 | .909 | .946 | .979 | 1.144 | .399 |
| c_7 | -2.037 | -2.401 | -2.290 | 3.373 | 3.177 |
| c_8 | | | | -1.652 | -2.098 |
| p | .222 | .318 | .187 | .273 | .232 |
| d_1 | 0 | 0 | 0 | 0 | .10 |
| d_2 | .1 | .1 | .1 | .135 | .10 |
| d_3 | .083 | .131 | .128 | .03 | .073 |
| d_4 | .07 | .07 | .07 | .118 | .07 |
| d_5 | .02 | .02 | .02 | .03 | .02 |
| d_6 | .083 | .132 | .128 | .075 | .133 |
| d_7 | .07 | .07 | .07 | .03 | .02 |
| d_8 | | | | .14 | .10 |
| Performance Parameters | | | | | |
| σ_1 | .101 | .141 | .136 | .366 | .305 |
| μ_1 | -6.206 | -7.033 | -7.102 | -4.315 | -12.336 |
| τ_1 | -7.751 | -29.802 | -24.652 | -52.395 | -77.853 |
| Q_1 | 1461.8 | 760.2 | 935.9 | -466.14 | 1236.1 |
| U_1 | 41923 | 26996 | 30381 | -3806 | 59259 |
| Na/Va | 1.62/60.18 | 1.62/60.18 | 1.62/60.18 | 1.66/125.5 | 1.62/60.18 |
| Nb/Vb | 1.55/35.8 | 1.56/36.2 | 1.56/36.09 | 1.50/64.4 | 1.56/36.43 |
| Nc/Vc | 1.62/60.18 | 1.62/60.18 | 1.62/60.18 | 1.65/84.99 | 1.69/63.81 |
| ΔV | 24.38 | 23.98 | 24.09 | 61.12 | 23.75 |
| ϕ_c/ϕ_a | 1.17 | 1.30 | 1.26 | 1.49 | .84 |

Table 3.10

| System | SS(4) | SS(24) | PS12 | H4-Pentac | SS(25.1) |
|---|---------|---------|---------|-----------|----------|
| Performance Parameters - Buchdahl Aberration Coefficients | | | | | |
| σ 1 | 1.010 | .141 | .136 | .366 | .305 |
| 2 | -.060 | -.14 | -.14 | -.037 | 0 |
| 3 | -.071 | -.045 | -.048 | -.049 | -.04 |
| 4 | .215 | .135 | .145 | .232 | .12 |
| 5 | 0 | 0 | .02 | -.016 | 0 |
| μ 1 | -6.907 | -7.033 | -7.102 | -4.315 | -12.34 |
| 2 | -.127 | -.839 | 1.363 | .882 | -4.194 |
| 3 | -.070 | -.535 | .932 | .625 | -2.775 |
| 4 | -8.247 | -10.543 | -10.338 | -4.415 | -5.093 |
| 5 | -4.012 | -4.428 | -4.402 | -1.911 | -2.839 |
| 6 | -4.379 | -6.320 | -6.145 | -2.885 | -2.560 |
| 7 | -.506 | .862 | 4.778 | .331 | 2.778 |
| 8 | -.179 | 1.01 | 3.480 | .237 | 1.929 |
| 9 | -.257 | -.002 | 1.448 | .146 | .852 |
| 10 | -.144 | 3.760 | 1.719 | -.295 | 3.734 |
| 11 | -.450 | -.007 | -.353 | -.471 | .028 |
| 12 | -.296 | -.007 | -.345 | -.161 | -.107 |
| τ 1 | -7.751 | -29.80 | -24.652 | -52.395 | -77.85 |
| 2 | 62.141 | 76.51 | 69.804 | 9.367 | -2.414 |
| 3 | 45.805 | 57.08 | 51.782 | 6.740 | -2.633 |
| 4 | -67.090 | -87.76 | -120.14 | -27.208 | -24.68 |
| 5 | -50.757 | -50.06 | -62.064 | -18.525 | -31.56 |
| 6 | -17.229 | -57.42 | -97.391 | -8.050 | 34.92 |
| 7 | -27.523 | -19.92 | 46.656 | 2.051 | 37.44 |
| 8 | -23.774 | -14.58 | 39.320 | -.121 | 34.68 |
| 9 | -14.416 | -13.21 | 19.910 | 1.165 | 15.98 |
| 10 | -1.289 | -.251 | 2.117 | -.328 | 2.503 |
| 11 | -15.170 | 22.74 | 7.021 | -9.686 | 58.28 |
| 12 | -1.210 | 59.54 | 37.523 | -1.659 | 98.62 |
| 13 | -3.367 | 3.07 | .473 | -2.365 | 9.551 |
| 14 | -3.352 | 32.16 | 19.964 | -2.168 | 54.77 |
| 15 | -4.144 | 19.02 | 5.959 | 1.510 | 11.12 |
| 16 | 3.385 | 14.77 | 3.350 | .723 | 8.397 |
| 17 | .934 | 4.418 | .963 | .495 | 2.024 |
| 18 | 3.480 | 17.91 | 11.159 | 2.566 | 18.61 |
| 19 | .059 | 1.489 | .412 | -.091 | 1.5 |
| 20 | -.036 | -.884 | -2.496 | -.353 | -1.044 |
| 5th Order H_n | 1.72 | .4214 | .592 | 2.05 | .404 |
| 5th Order V | 32° | 8.8° | 12.2° | 37° | 8.4° |
| 7th Order H_n | .404 | .147 | .196 | .402 | .141 |
| 7th Order V | 22° | 8.4° | 11.1° | 21.9° | 8.0° |

CHAPTER 3.4 THE DEVELOPMENT OF A TYPE 122 TRIPLET WITH TWO-ZONE CORRECTION.

3.4.0 Introduction.

In this chapter the design principles established for the basic parameters during the development of the type 121 are used to develop a type 122 with two-zone correction of its spherical aberration. The type 122 was proposed as the next stage in the systematic development of triplets after the type 121. We recall that it arose out of the study of the basic-glass-parameters at the end of section 2.

3.4.1 A Limited Interpolative Study of the Monochromatic Type 122.

The type 122 has been derived from the type 121 by replacing the back component with a cemented doublet constructed from the Bausch and Lomb flint CF1(1.5282, 51.4) and the Chance crown DBC(1.6133, 57.5). The negative component leads the positive component, therefore the k -prime of this positive doublet is less than -1 (see chapter 1.1 and chapter 2.6).

All the programmes which were developed for the type 121 have been converted in the manner described in

Section 1 to generate the type 122. The main differences have been caused by the introduction of the additional "monochromatic-basic-parameter" $k'[3]$ which is the k -prime of the positive doublet. With the introduction of $k'[3]$ it is necessary for the k -prime of the negative doublet to be denoted by $k'[2]$. (Note in the graphs of this chapter it is due to an oversight still shown as k').

A "limited-interpolative-study" has been made of the monochromatic 3rd order type 122 triplets with respect to the monochromatic parameters χ , $k'[2]$, R_4 and $k'[3]$ at $L = 0.2$ and $T = 0.05$. This survey is similar to the (χ, k', P) -survey which initiated the study of the type 121 in Section 2. Thus this survey has been performed with an equivalent R and L programme which has computed the 3rd order type 122 triplets at regular intervals throughout $(\chi, k'[2], R_4, k'[3])$ -space. (We recall that the 3rd order triplet has $R_2 = R_3 = R_5 = 0$). The systems have been computed for the grid with

1. $\chi = 0, -0.5, -1, \chi_L, \chi_R$ and χ_{TP} .
2. $k'[2] = -3, -3.5, -4$.
3. $R_4 = 0.12, 0.14, 0.16$.
4. $k'[3] = -1.8, -2.0, -2.2$.

In addition to computing the usual σ_1 , μ_1 , τ_1 and ϵ'_{Sph} to 7th order, the new version of the R and L programme gives all the other 3rd and 5th order coefficients as well. However, in view of the experience with the type 121, it has been necessary to consider only the 3rd, 5th and 7th order spherical coefficients in conjunction with a few representative 5th order coefficients in order to locate the optimum monochromatic region. Consequently, only σ_1 , μ_1 , τ_1 , ϵ'_{Sph} , μ_2 , μ_7 , μ_4 and μ_{10} have been plotted.

The "limited interpolative study" is depicted as (χ , $k'[2]$, R_4)-sections at three values of $k'[3]$ (-1.8, -2.0 and -2.2). In Figures 3.36, 3.37 and 3.38 σ_1 , μ_1 , τ_1 and ϵ'_{Sph} are shown in these section. Similarly in Figures 3.39, 3.40 and 3.41 the coma coefficients μ_2 and μ_7 are shown, and in 3.42, 3.43 and 3.44 the astigmatic coefficients μ_4 and μ_{10} are shown.

Considering ϵ'_{Sph} it is evident that the minima lie to the right of $\mathcal{X} = -0.5$. Indeed, in nearly all cases both right and left hand solutions are to the right of $\mathcal{X} = -0.5$. Furthermore, it has been found that this means that both the left and right hand solutions have the same asymmetry; the back separation of the components is greater than the front separation. Consequently, in the rare instance when it occurs, the symmetrical solution of the type 122 is an extreme left hand solution at something like $k'[2] = -12$. Therefore symmetry is no longer associated with a tangential or turning point solution.

The condition that σ_1, μ_1, τ_1 and ϵ'_{Sph} shall pass through zero almost simultaneously is only satisfied near $k'[2] = -3$ in Figure 3.38 where $k'[3] = -2.2$. In particular the optimum region seems to be near $k'[2] = -3$ and $R_4 = 0.14$ in this section of $k'[3]$. Thus the introduction of the positive doublet has reduced R_4 of the type 122 to 0.14 as compared with the $R_4 = 0.20$ of the equivalent monochromatic type 121. However, this occurs with a very much larger σ_1 of about 0.5 as against about 0.2 which was predicted in the monochromatic survey of the type 121.

It is evident from Figures 3.41 that the type 122 generated in the optimum region of Figure 3.38 will have 5th order coma not unlike the type 121. On the other hand it is evident from Figure 3.44 that it will have

at least half that of the optimum type 121. This represents a substantial improvement in μ_4 which brings the triplet partly into line with the Pentac. The effect of $k'[3]$ on μ_4 is quite powerful, it reduces μ_4 to zero in the interval $k'[3] = -1.8$ to -2.0 for all R_4 and $k'[2]$ shown.

In this work we decided to develop the type 122 system in the optimum region occurring at $k'[3] = -2.2$. The decision was based on the monochromatic survey described above, which, with regard to $k'[3]$, is rather crude. However, the main purpose at this stage was considered to be the need to find support for the design principles which were established for the basic parameters P, L and T during the development of the type 121. As far as finding the best type 122 is concerned, it is felt now that the optimum region could be better optimized with respect to $k'[3]$. Indeed it would seem to be nearer $k'[3] = -2.0$ rather than -2.2 . A lot more work could be spent on this point alone.

It is interesting to find that the optimum region has not moved significantly away from the $k'[2] = -3$ of the optimum type 121. Moreover, at or near this value of -3 , the coefficients μ_1 and τ_1 are almost independent of $k'[3]$ and R_4 . The 3rd order spherical coefficient σ_1 , however, is susceptible to changes in $k'[3]$ although like μ_1 and τ_1 it is nearly independent of R_4 . This sensitivity of σ_1 to $k'[3]$ may not allow a reasonable system to be generated near $k'[3] = -2.0$ as proposed above.

$$L=0.2$$

$$T=0.05$$

$$k'_{[3]}=-1.8$$

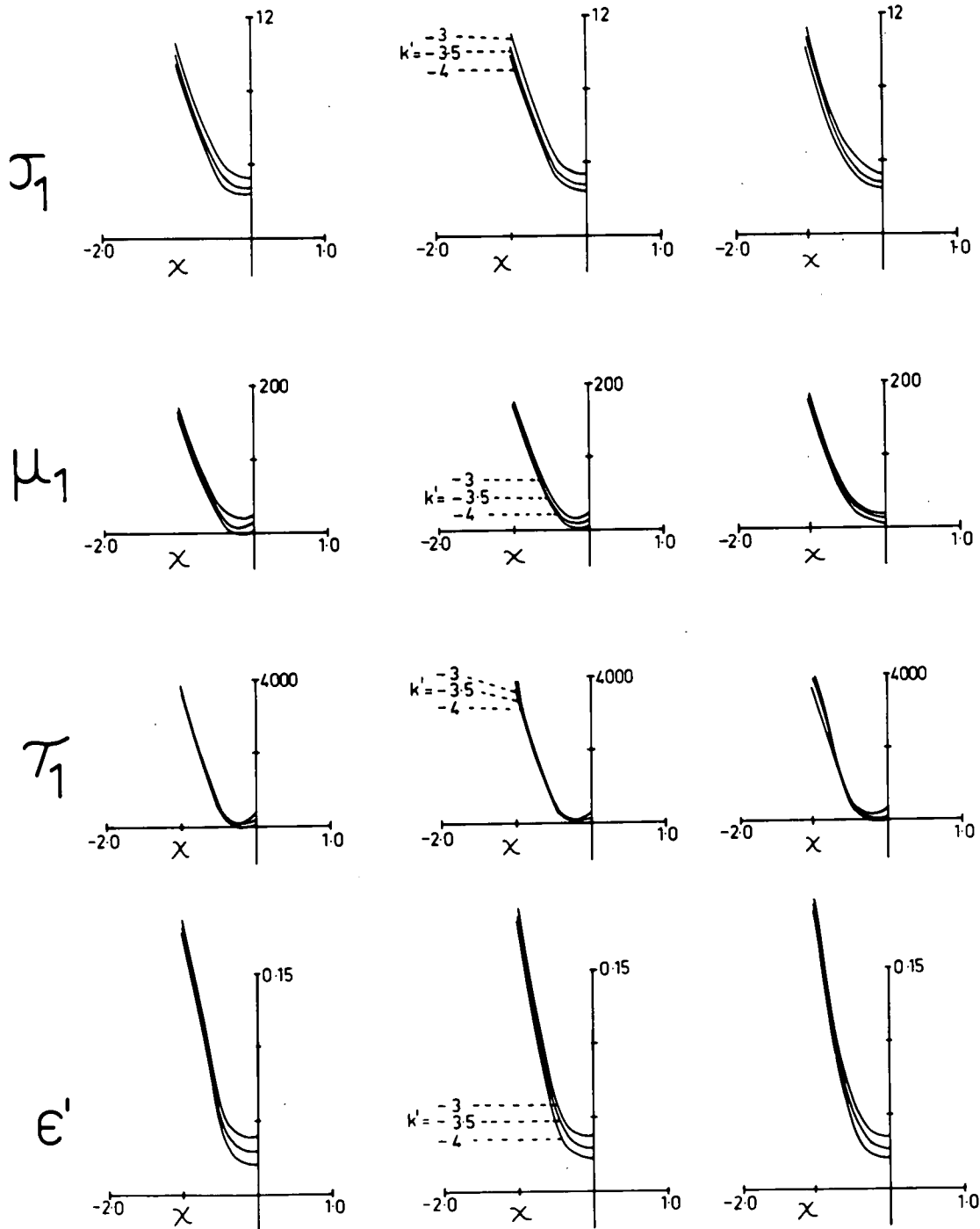
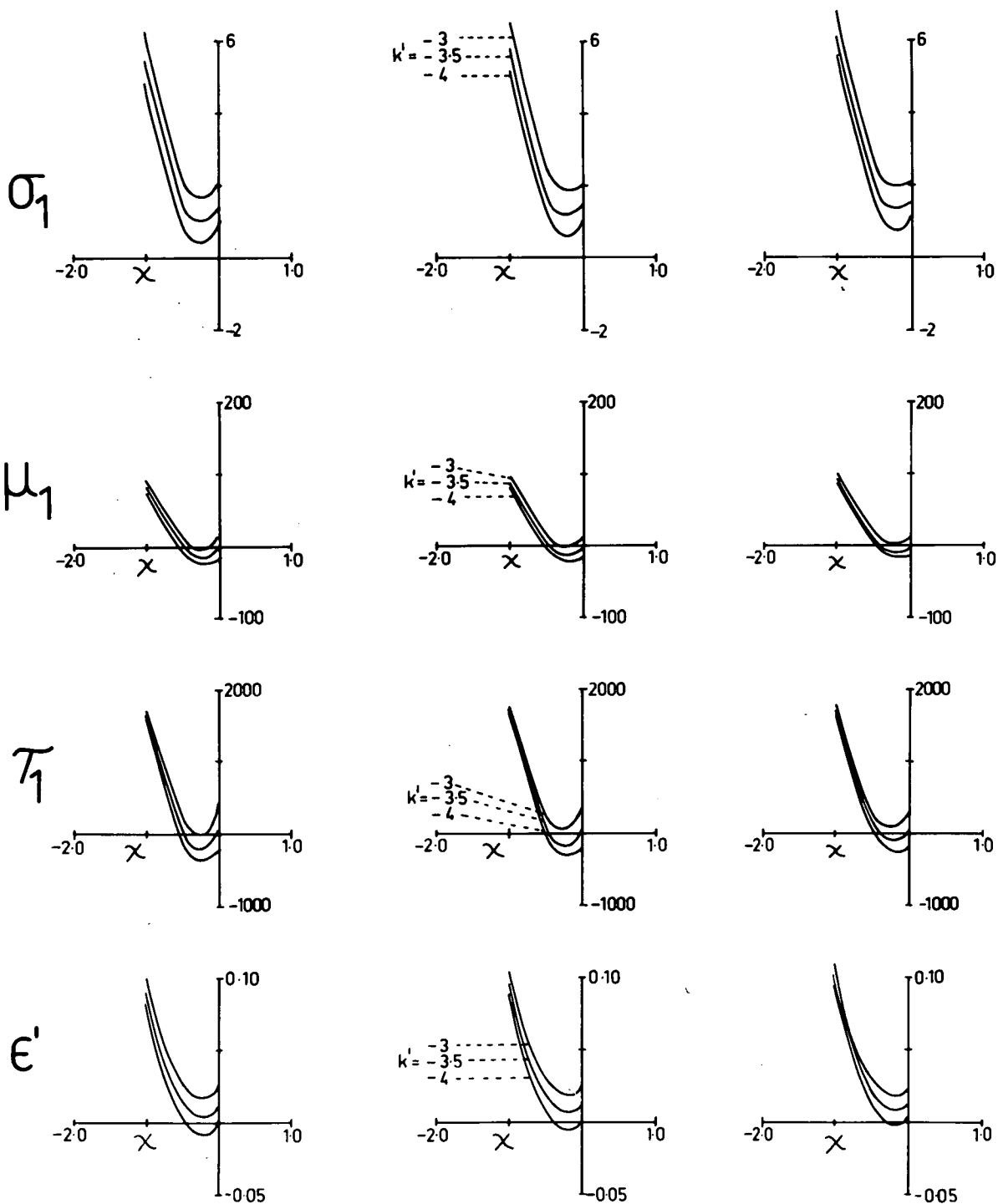


Fig. 3.36

$$L = 0.2$$

$$T = 0.05$$

$$k'_1[3] = -2.0$$



$$R_4 = 0.14$$

$$R_4 = 0.15$$

$$R_4 = 0.16$$

Fig. 3.37

$$L=0.2$$

$$T=0.05$$

$$k'_{[3]}=-2.2$$

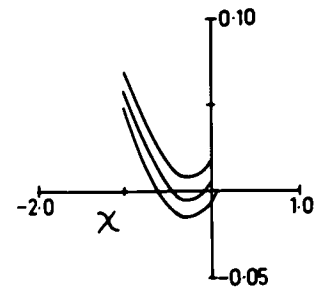
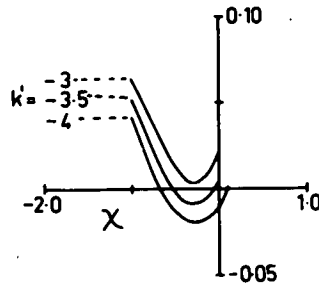
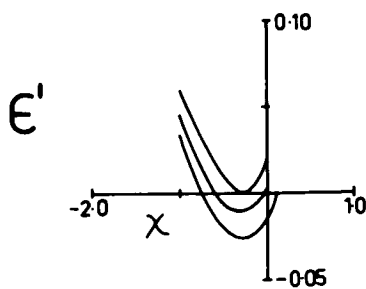
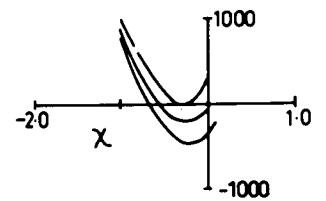
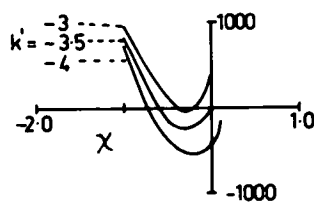
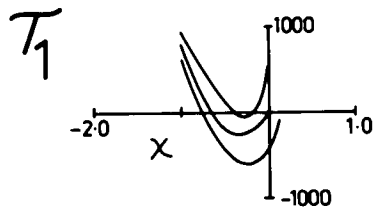
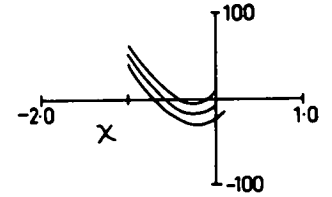
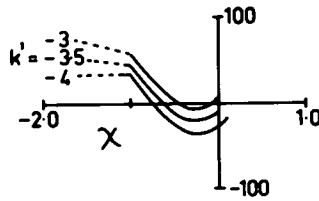
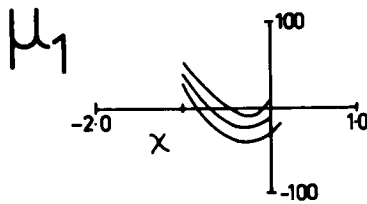
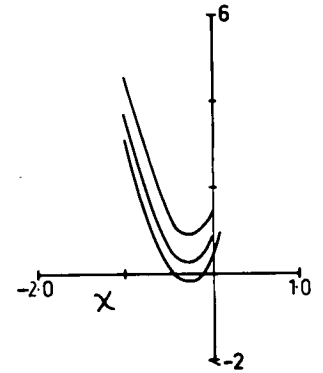
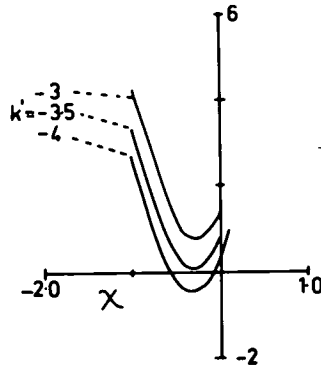
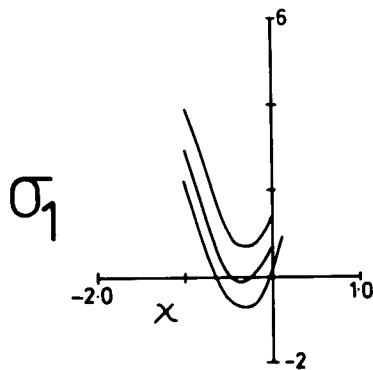


Fig. 3.38

$$R_4=0.14$$

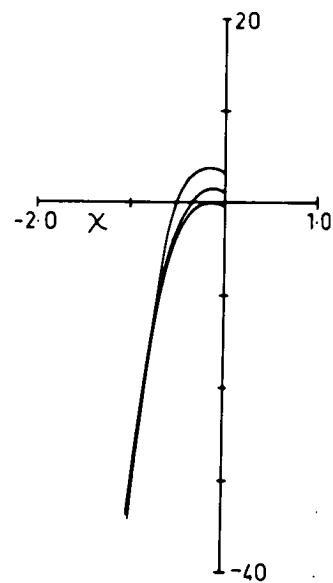
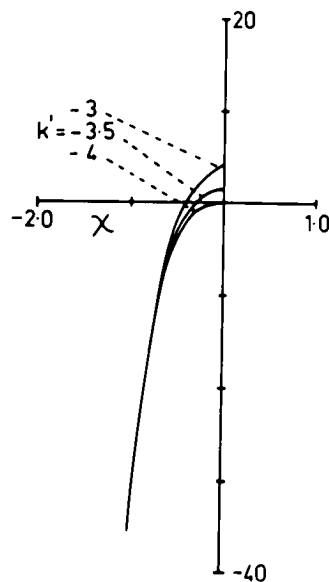
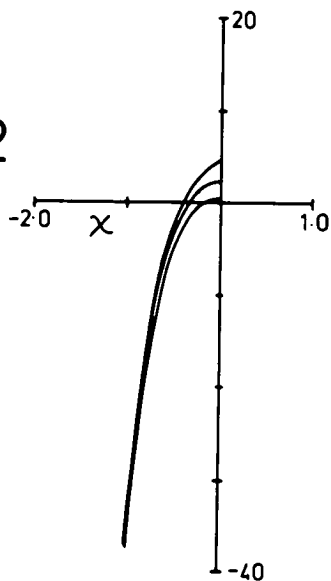
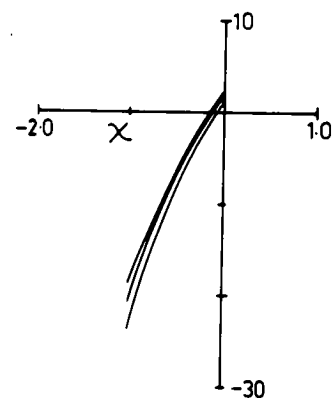
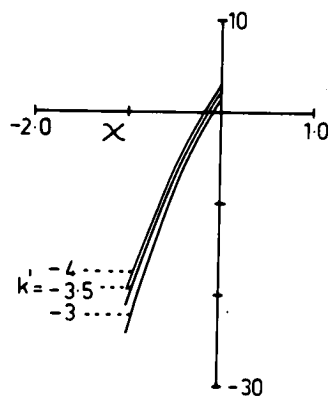
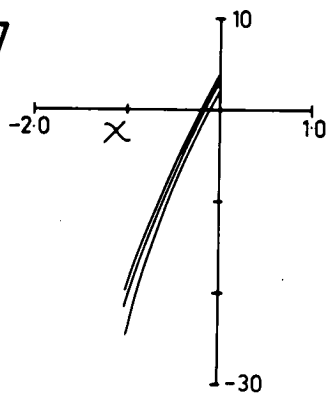
$$R_4=0.15$$

$$R_4=0.16$$

$$L=0.2$$

$$T=0.05$$

$$k'_{[3]}=-1.8$$

 μ_2

 μ_7


$$R_4=0.14$$

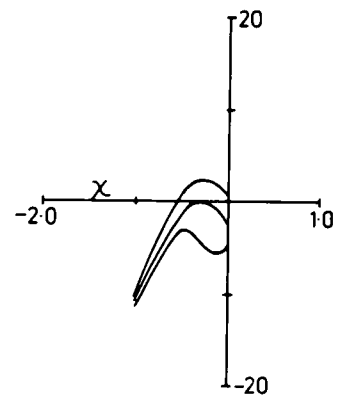
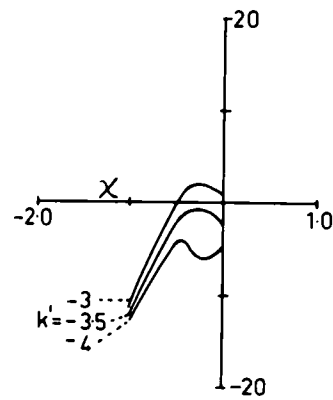
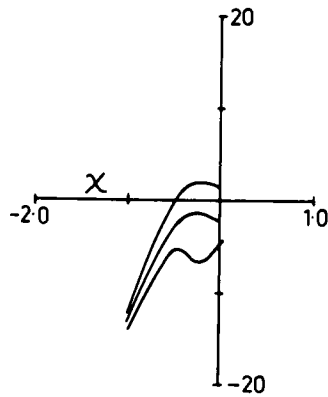
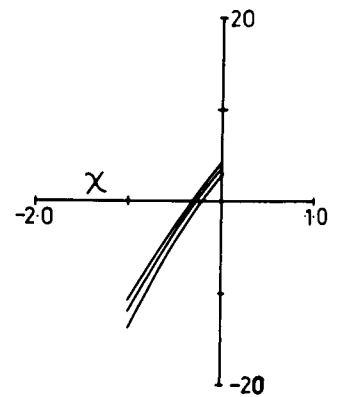
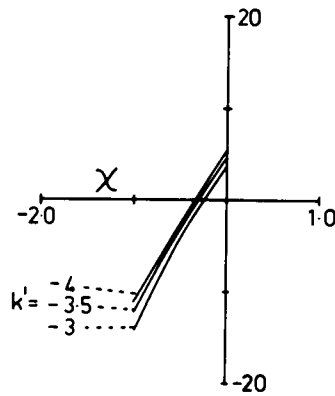
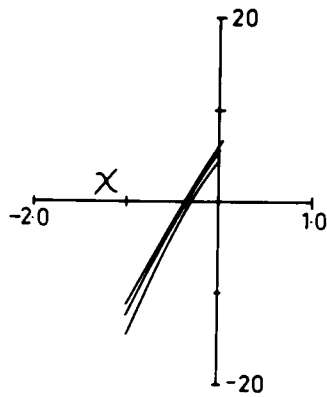
$$R_4=0.15$$

$$R_4=0.16$$

Fig. 3.39

$$\begin{aligned} L &= 0.2 \\ T &= 0.05 \end{aligned}$$

$$k'_{[3]} = -2.0$$

 μ_2

 μ_7


$$R_4 = 0.14$$

$$R_4 = 0.15$$

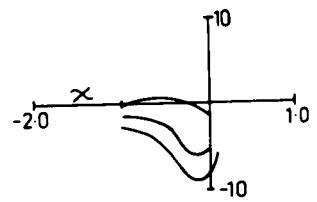
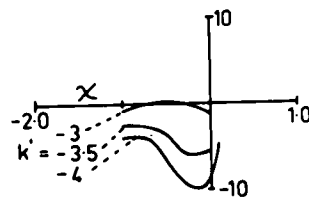
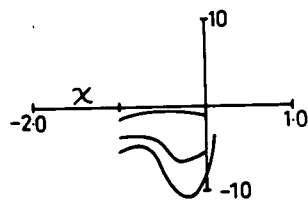
$$R_4 = 0.16$$

Fig. 3.40

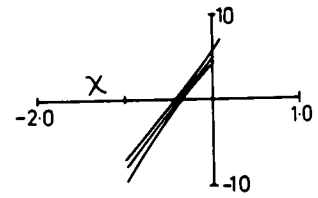
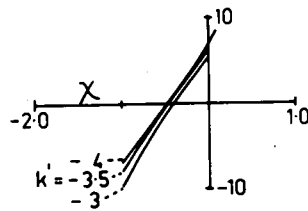
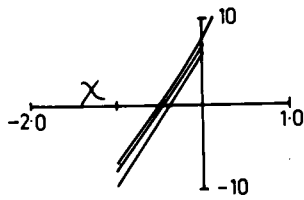
$$\begin{aligned} L &= 0.2 \\ T &= 0.05 \end{aligned}$$

$$k'_{[3]} = -2.2$$

μ_2



μ_7



$$R_4 = 0.14$$

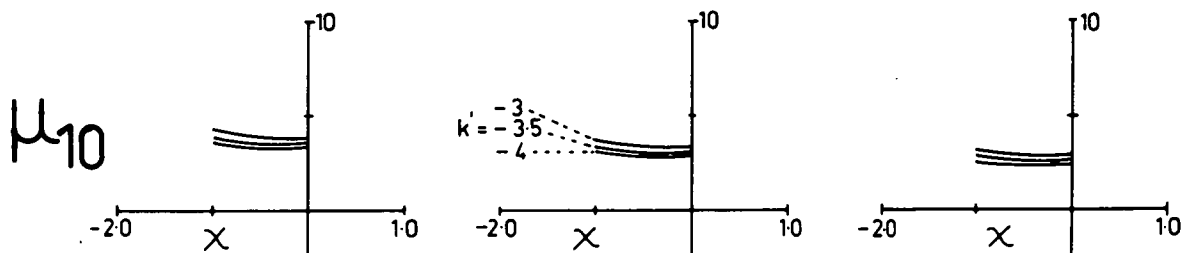
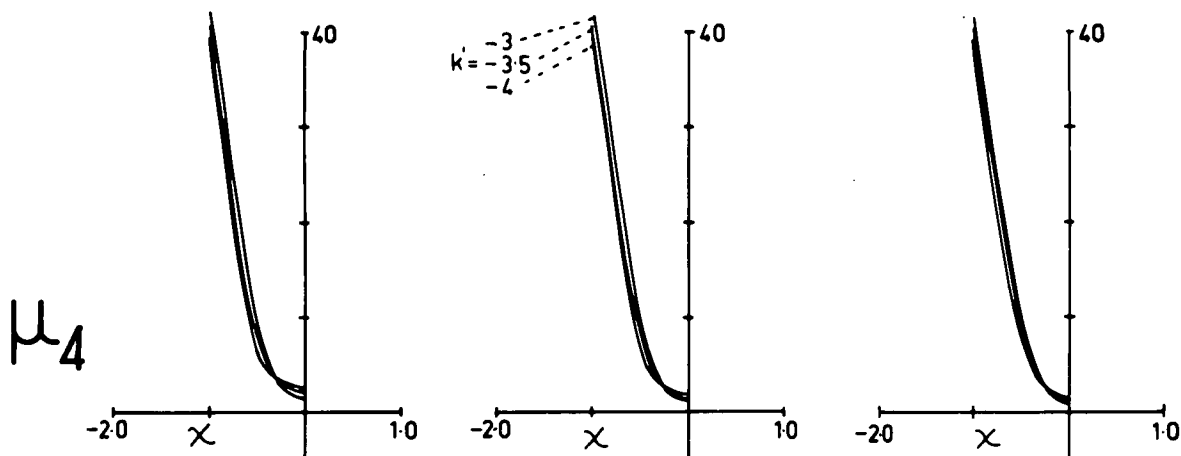
$$R_4 = 0.15$$

$$R_4 = 0.16$$

Fig. 3.41

$$\begin{aligned} L &= 0.2 \\ T &= 0.05 \end{aligned}$$

$$k'_3 = -1.8$$



$$R_4 = 0.14$$

$$R_4 = 0.15$$

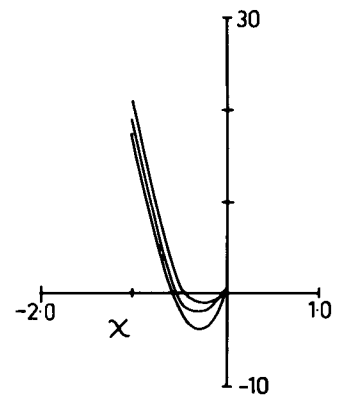
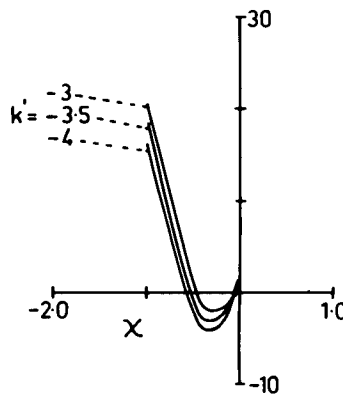
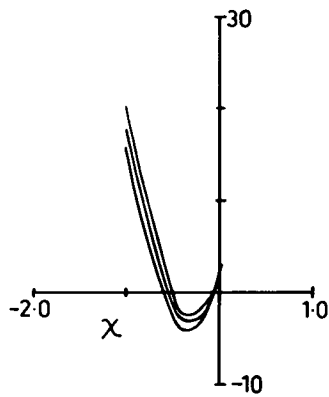
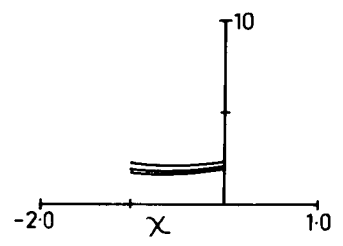
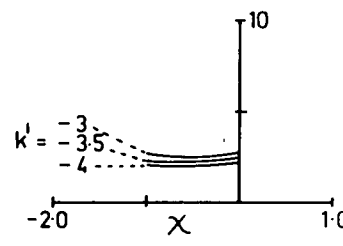
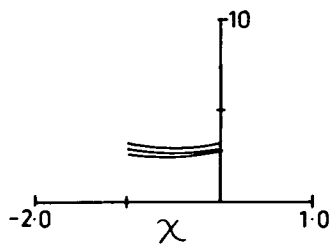
$$R_4 = 0.16$$

Fig. 3.42

$$L=0.2$$

$$T=0.05$$

$$k'_3 = -2.0$$

 μ_4

 μ_{10}


$$R_4 = 0.14$$

$$R_4 = 0.15$$

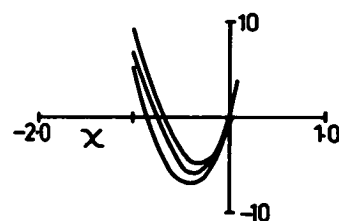
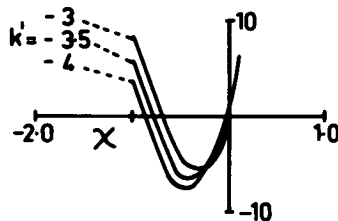
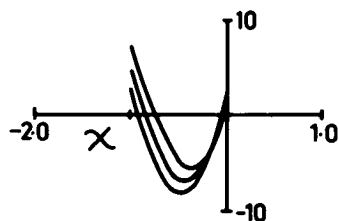
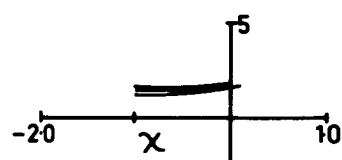
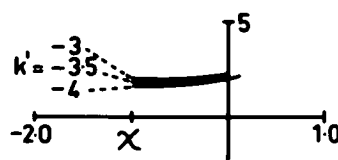
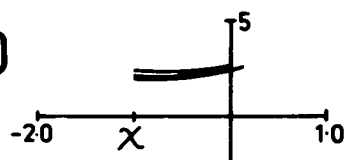
$$R_4 = 0.16$$

Fig. 3.43

$$L=0.2$$

$$T=0.05$$

$$k'_{[3]} = -2.2$$

 μ_4

 μ_{10}


$$R_4 = 0.14$$

$$R_4 = 0.15$$

$$R_4 = 0.16$$

Fig. 3.44

For the present we assume that the optimum monochromatic region at $L = 0.2$, $T = 0.05$ is near the following $k'[2] = -3$, $k'[3] = -2.2$, $R_4 = 0.14$ and $\chi = -0.25$.

Summary.

The introduction of a new monochromatic ^{basic} parameter $k'[3]$ has a very strong influence on μ_4 , μ_5 and μ_6 and σ_1 . The main effect has been to reduce the oblique spherical aberration at the expense of the primary spherical aberration.

3.4.2 Optimizing the Chromatic Type 122 Triplet.

The σ_1 , μ_1 , τ_1 and ϵ'_{Sph} -curves versus χ of the type 122 (see Figure 3.38) for the $(\chi, k'[2], R_4)$ -section at $k'[3] = -2.2$, $L = 0.2$ and $T = 0.05$ lies close to the χ -axis near $R_4 = 0.14$. This state of affairs is similar to that which occurred with the type 121 in the (χ, k', P) -section at $L = 0.2$, $T = 0.05$. Therefore the optimum monochromatic solution is expected to be close to the turning point solution which is tangential to the χ -axis.

Experience has shown that solutions in the tangential region cannot be generated with the R and L programme, they can only be found with the SS-programme which iterates the spherical residual with respect to the symmetry parameter, R_8 , (see section 2). A study of the symmetry of the type 122 has shown that its turning point solutions are obtained with $R_8 = 0.6$; whereas, we recall, that the turning point solutions of the type 121 are symmetrical and therefore are

located with $R_8 = 0$.

Using the technique developed for finding the optimum solution of the type 121 we have mapped the spherical coefficients σ_1 , μ_1 and τ_1 of the 3rd order type 122 triplets which have $R_8 = 0.6$. This survey has been made for the following ranges of the parameters R_4 , L and T :

$R_4 = 0.08$ to 0.16 in steps of $\Delta R_4 = 0.02$.

$L = 0.2, 0.3, 0.35, 0.4$.

$T = 0.05, 0.075, 0.10$.

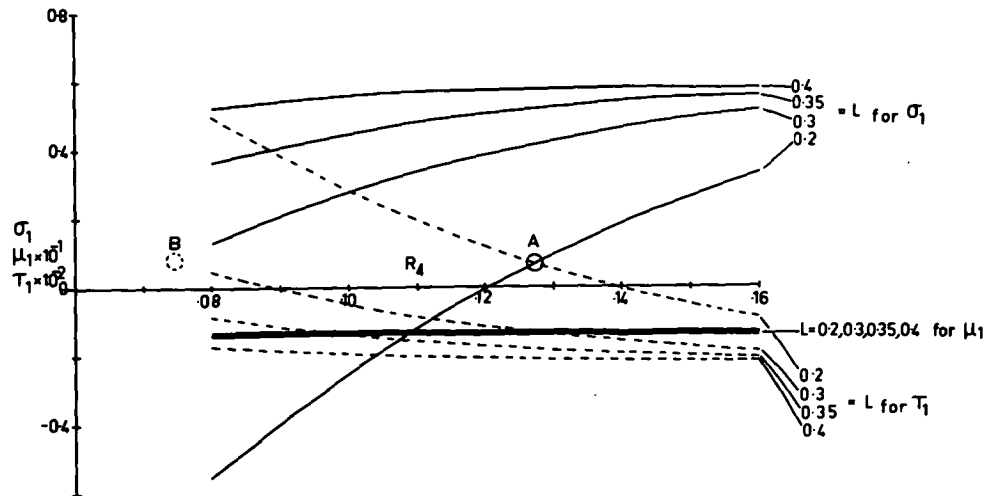
The coefficients obtained in this study are shown versus R_4 and L in the three sections of T in Figure 3.45.

It is evident from the figure that the position of the simultaneous minima of the spherical coefficients at given L and T is determined by the intersection of σ_1 and τ_1 (μ_1 is almost constant for all L , T and R_4). Thus in this figure the path of the optimum region is traced through $(\chi, k'[2], R_4, L, T)$ -space at $k'[3] = -2.2$. Clearly the behaviour is similar to the type 121: the pattern of the spherical coefficients associated with the optimum region occurs at reduced R_4 as L is increased and as T is decreased.

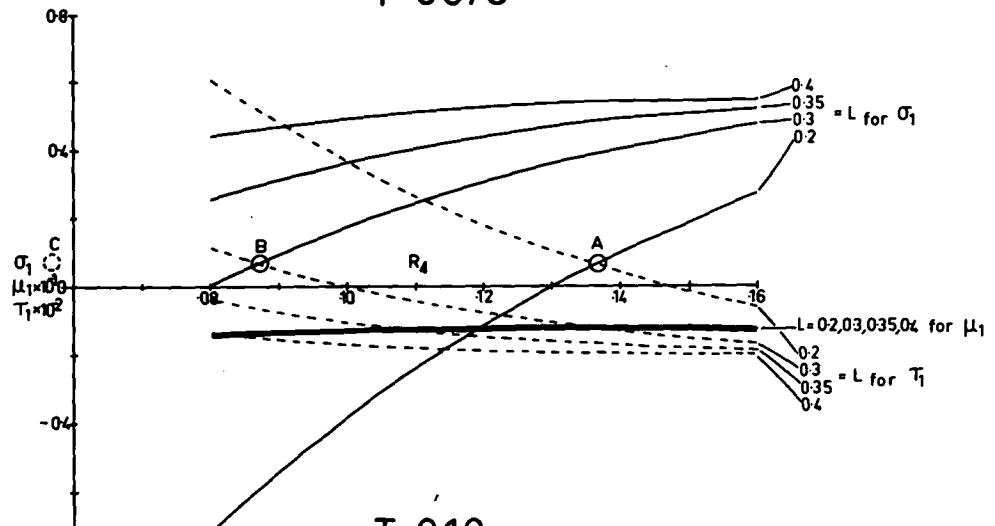
The "optimum monochromatic region" of the initial R and L survey of the type 122, which was described in the previous section, is located near the point A in the graph at the top of Figure 3.45. The systems in this region surrounding A have been developed and examined in the usual

$$k[3] = -2.2$$

$$T = 0.05$$



$$T = 0.075$$



$$T = 0.10$$

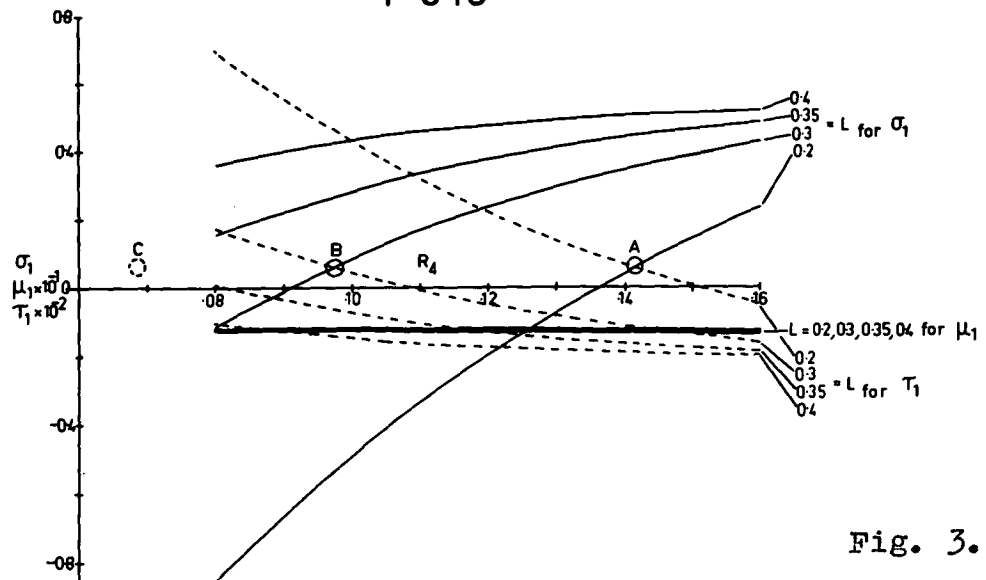


Fig. 3.45

way with ray-traces. From these ray-trace-surveys the optimum system with two-zone correction for this section at $L = 0.2$, $T = 0.05$ and $k' [3] = -2.2$ was found at $R_4 = 0.14$. Its LA' versus ρ versus λ -curves and ϵ'_y versus \bar{H} versus λ -curves are shown in Figures 3.46 and 3.47.

Drawing on our experience with the type 121 we predicted that L should be increased and R_4 reduced in order to correct the LA' -curves of Figure 3.46. Similarly we predicted that T should be increased so as to correct the transverse chromatic aberration evident in Figure 3.47.

The correction of LA' is shown in Figures 3.48, 3.49 and 3.50 and the correction of ϵ'_y is shown in the complementary set of Figures 3.51, 3.52 and 3.53. The first stage in the correction of the longitudinal chromatic aberration is shown at the top of Figure 3.48 where the effect of increasing L in steps of 0.1 is seen to have progressively corrected the longitudinal chromatic aberration of all the zones. However, as expected, the marginal zones have been considerably overcorrected. This overcorrection has been restored, by the reduction of R_4 , at $L = 0.3$ only; clearly R_4 has little effect on the marginal zones in the region of $L = 0.4$. Moreover the corresponding sets of ϵ'_y which are seen in Figure 3.51, show little variation during the optimization of R_4 and L .

It is evident from Figures 3.51, 3.52 and 3.53 that the optimum system occurs very near $T = 0.075$ (Figure 3.52), as far as ϵ'_y is concerned. This is also seen to be

the case with LA'. Clearly it is evident from Figures 3.49 and 3.52 that the optimum system with two-zone correction lies near $L = 0.3$, $T = 0.075$ and $R_4 = 0.12$ (this system is called SS(25.1)). (However, considering these results in the light of more recent experience it is felt that L could be increased and $k'[3]$ reduced.)

3.4.3 The Parameters of the Type 122 Compared with those of the Type 121 and the Pentac.

The construction parameters and the performance parameters of the final type 122 (system SS(25.1)) are presented in the last columns of Tables 3.9 and 3.10. This system is developed to a stage that lies somewhere between SS(4) and SS(24) since it still has $R_2 = 0$ and its stop is at the first principal point of the lens group b. However, since the variation in the parameters of the type 121 from SS(4) to FS12 is small, then it seems that the main properties can be observed at an early stage of the design.

The basic parameters are at the most elementary level of the design process. At this level the type 122 is only similar to the Pentac in the order of magnitude of χ . The remaining basic parameters $k'[2]$, P , L , and T are like those of the type 121. As far as the other types of basic parameters are concerned we find, for example,

ΔV unchanged but ϕ_c/ϕ_a is very much less than that of either the type 121 or the Pentac.

When we examine the spherical coefficients we find that the type 122 is again only similar in one case to the Pentac, its order of magnitude of σ_1 , the others have remained much the same as those of the type 121.

It is evident that the main changes in the coefficients have occurred with σ_1 and (μ_4, μ_5, μ_6) as was predicted in the limited interpolative study of the type 122. These changes in performance parameters are associated with a change in the basic parameter χ . This change in χ has also noticeably affected the performance parameter R_8 .

It seems that the stage of development reached with the type 122 is sufficient for testing the design principles and for noting the main differences between it, the type 121, and the Pentac. It is difficult at this stage, however, to say whether it is potentially better than the type 121 with regard to field. Looking at its spot diagrams (for d-light) shown in Figure 3.54 one feels that there has been some gain at 5° but the 10° image is comatic. The first thing to do here would be to adjust R_2 and to shift the stop before attempting further comparison of its potential with the type 121.

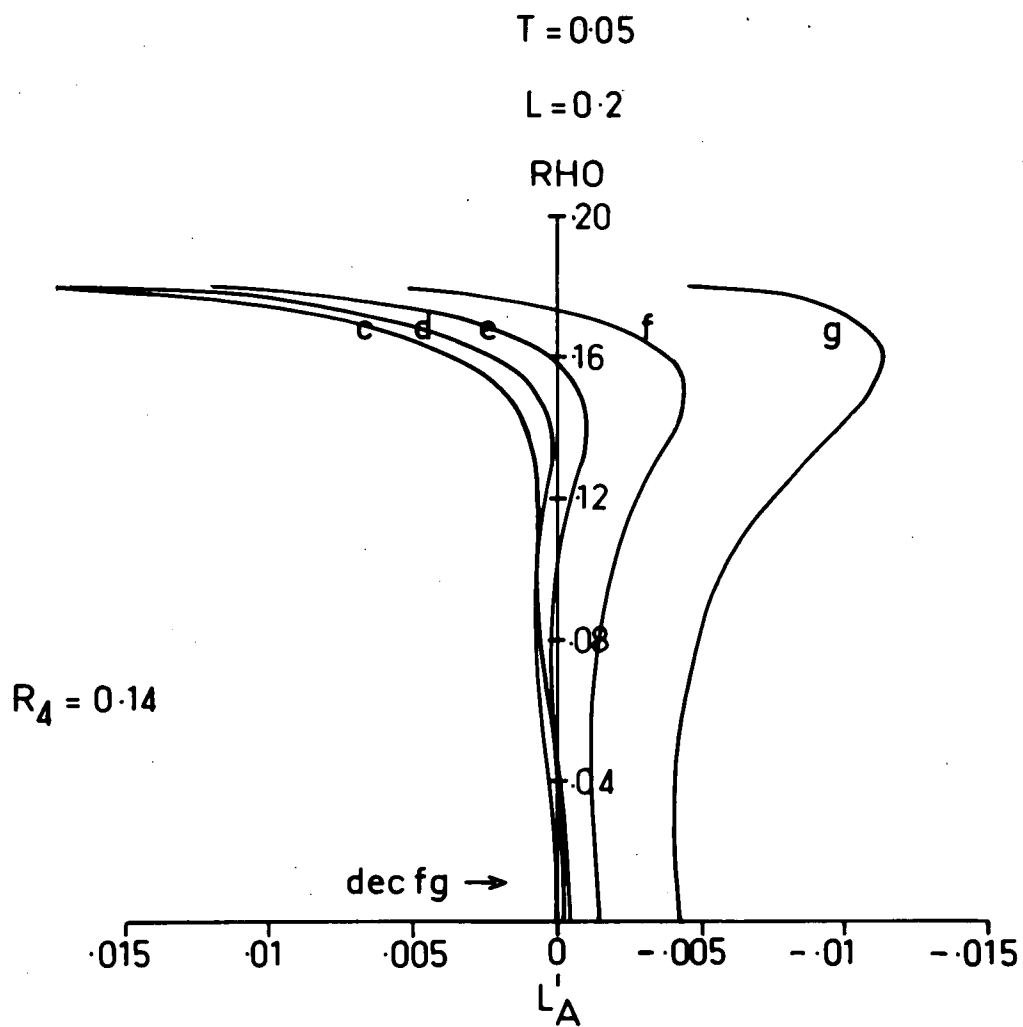


Fig. 3.46

$$T = 0.05$$

$$L = 0.2$$

$$R_4 = 0.14$$

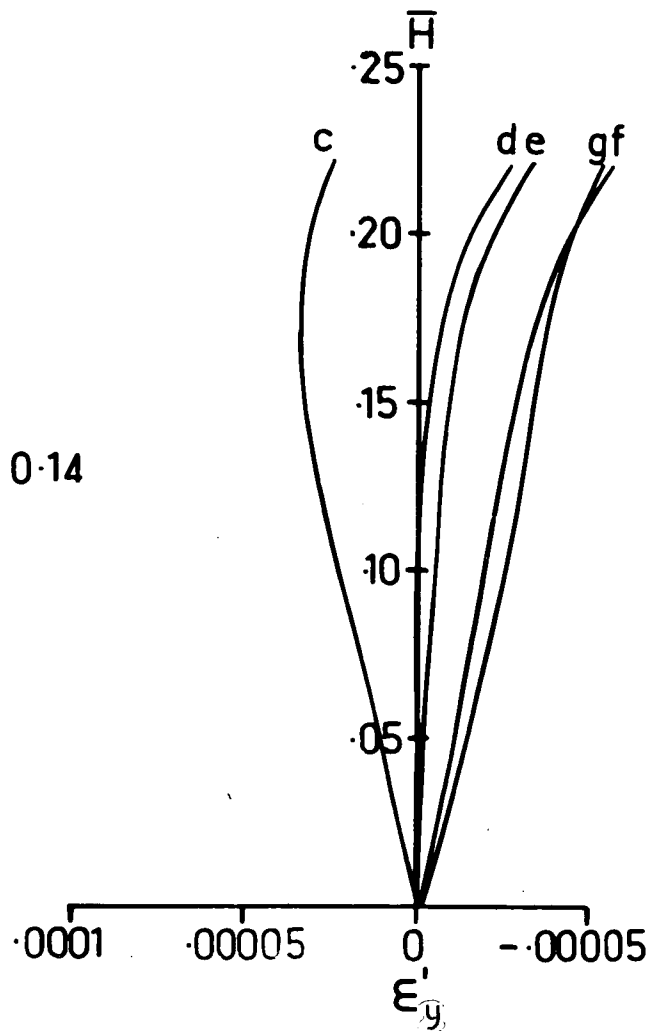


Fig. 3.47

$T = 0.05$

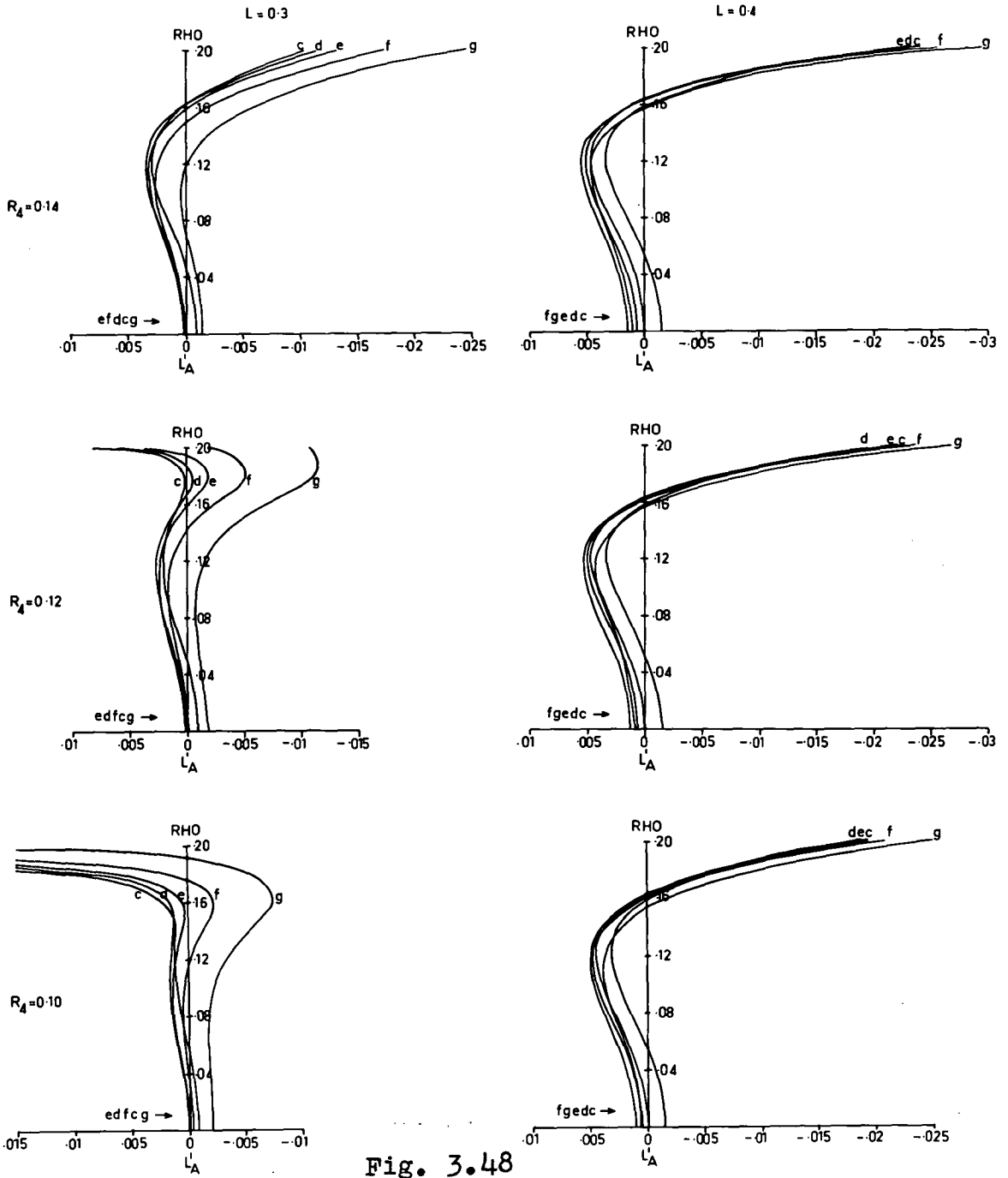


Fig. 3.48

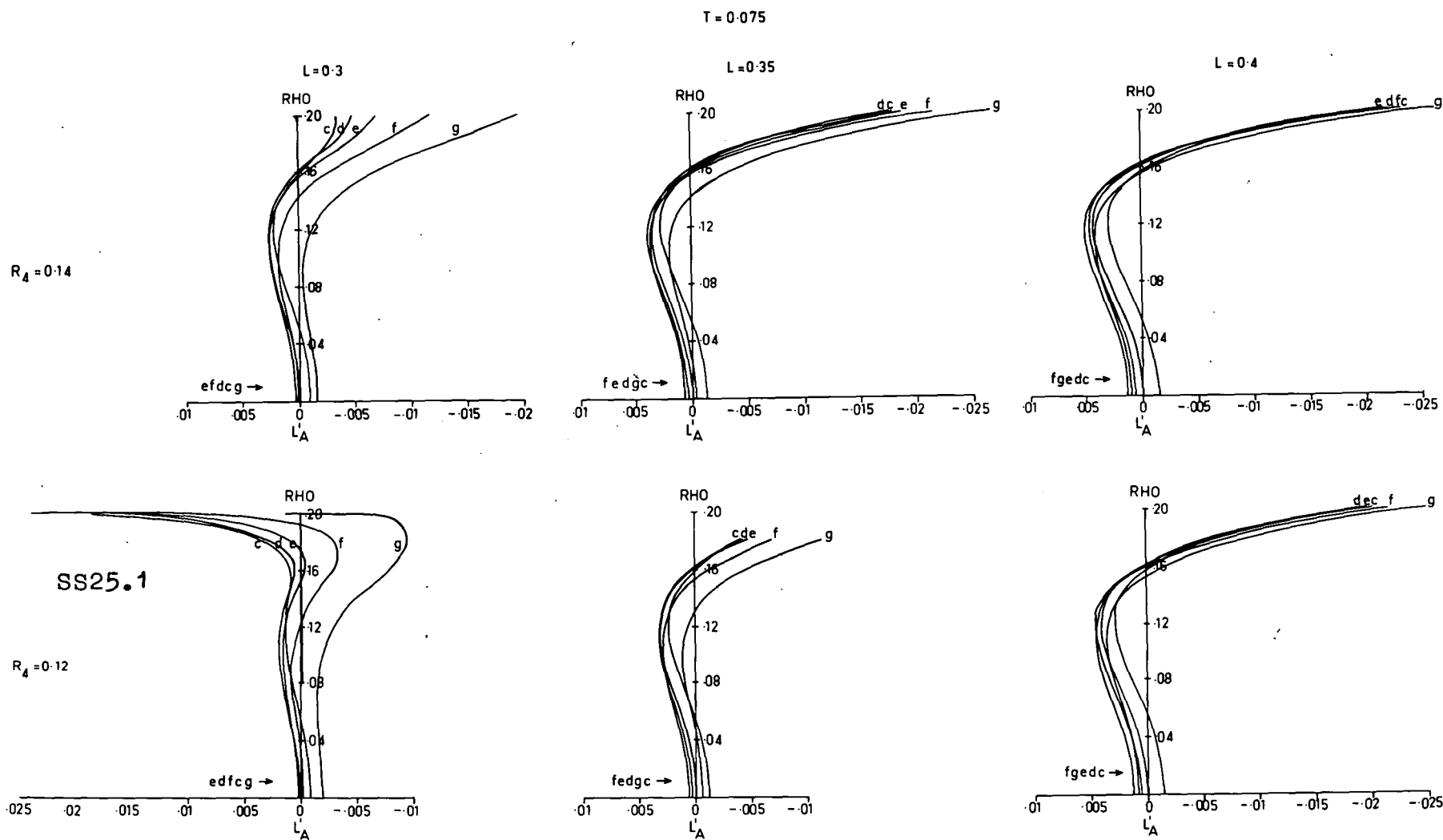


Fig. 3.49

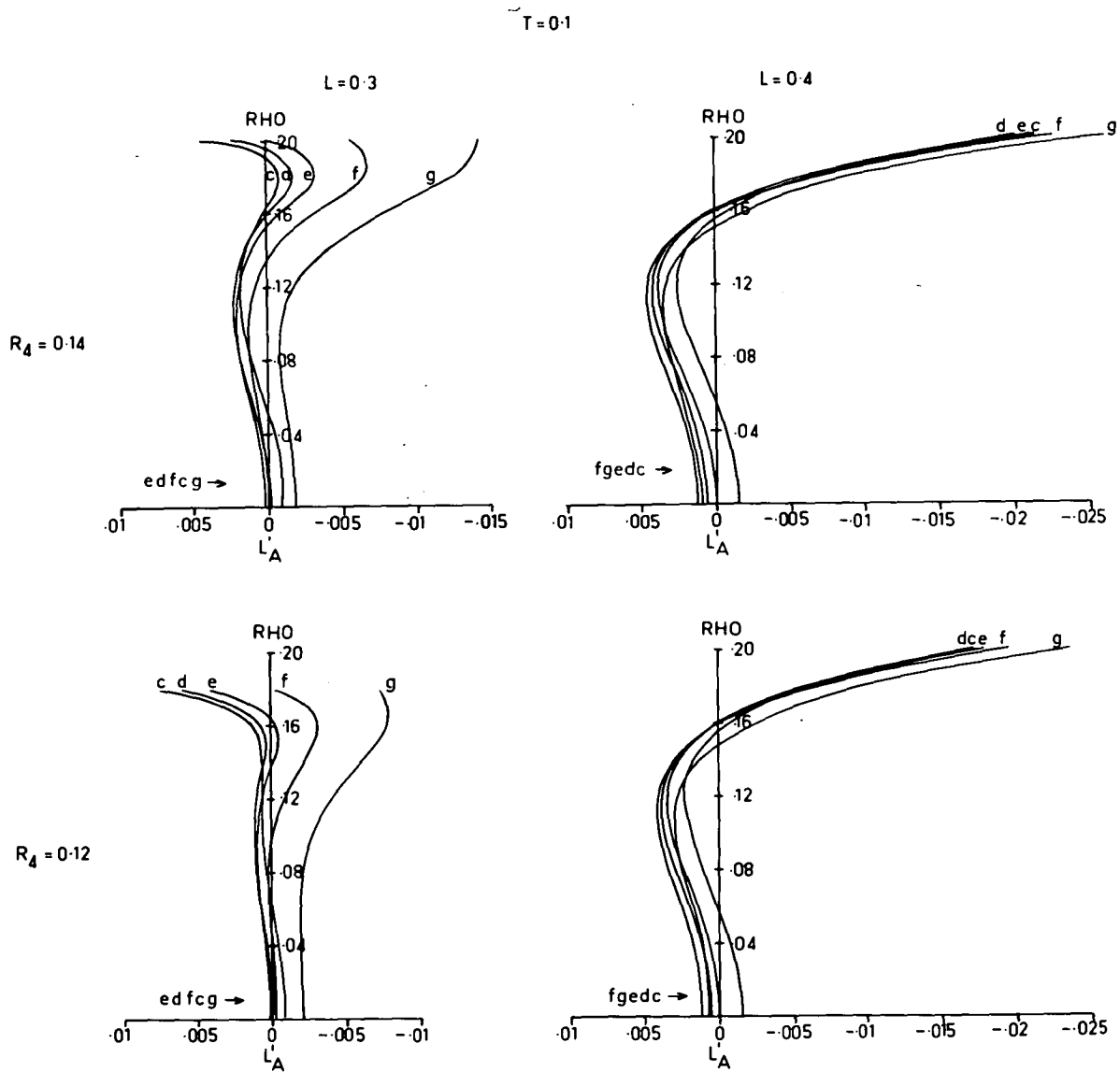


Fig. 3.50

$T = 0.05$

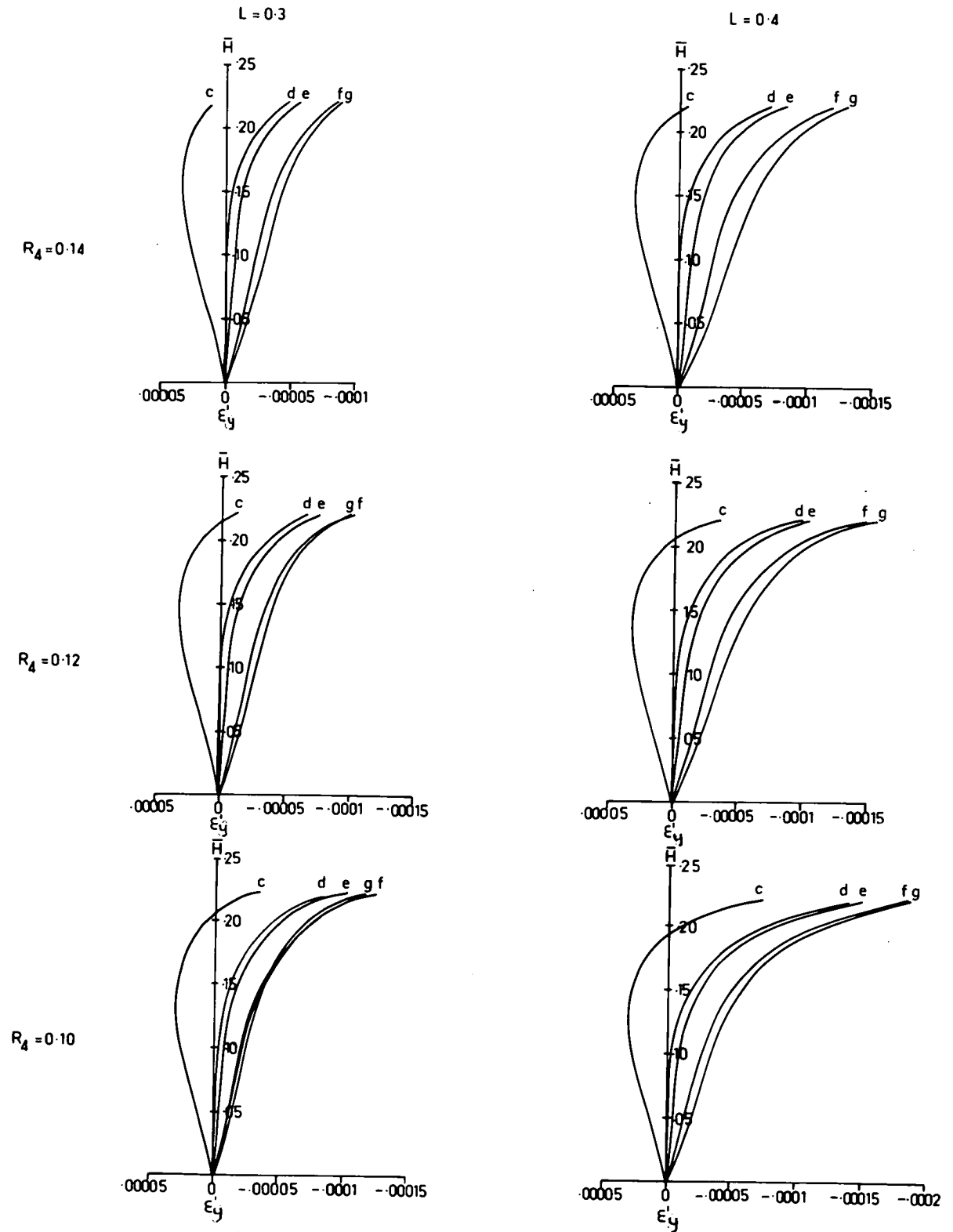


Fig. 3.51

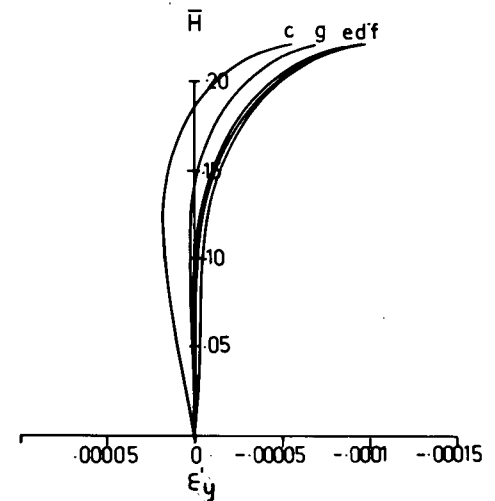
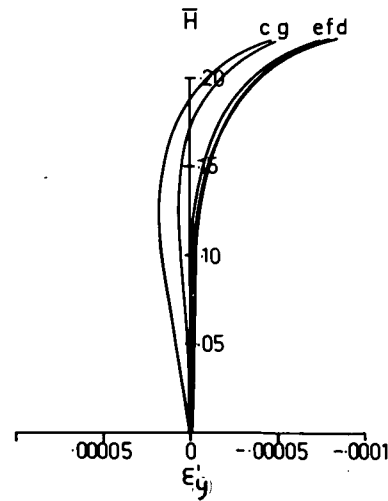
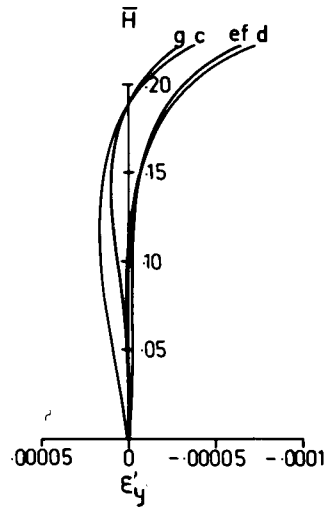
$T = 0.075$

$L = 0.3$

$L = 0.35$

$L = 0.4$

$R_4 = 0.14$



$R_4 = 0.12$

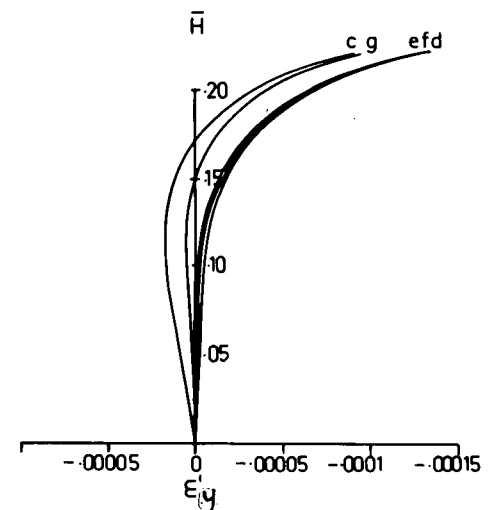
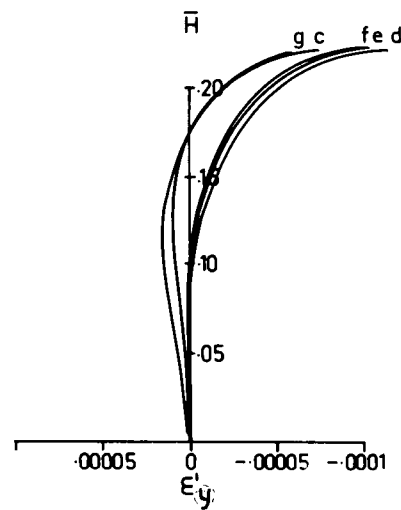
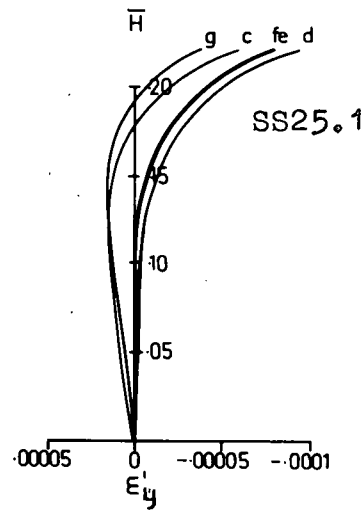


Fig. 3.52

$T = 0.1$

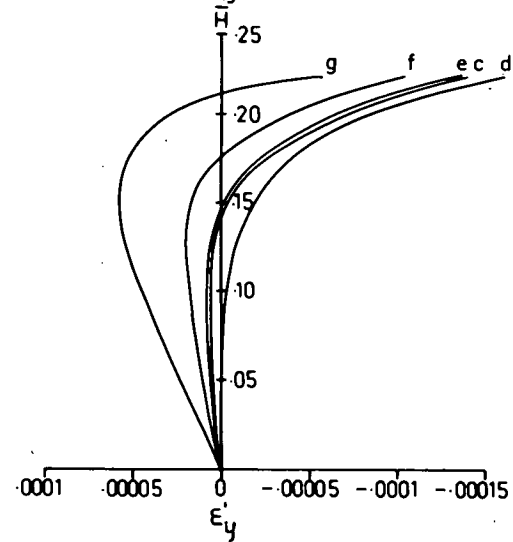
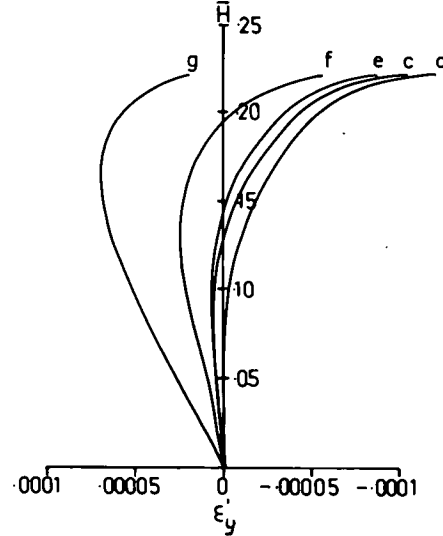
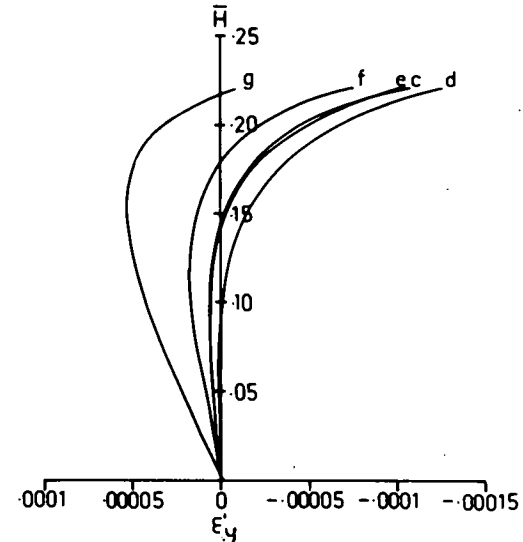
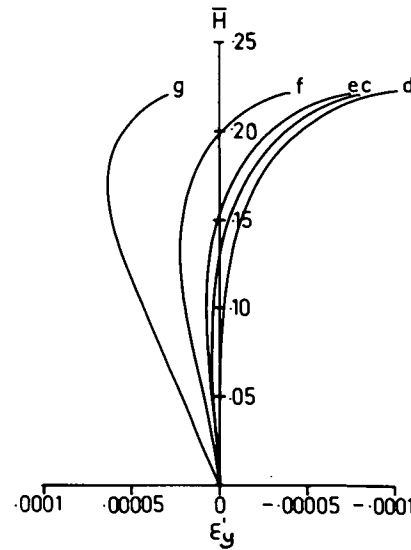
$L = 0.3$

$L = 0.4$

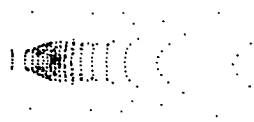
$R_4 = 0.14$

Fig. 3.53

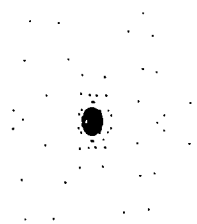
$R_4 = 0.12$



V=10



TYPE 122
V=5



V=0

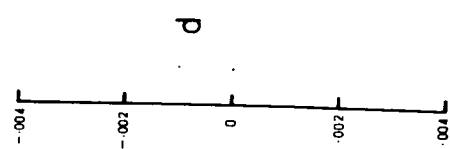
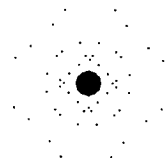


Fig. 3.54

CHAPTER 3.5 CONCLUDING REMARKS.

3.5.1 General

The dilemma encountered in the design of a type 121 triplet when the aperture exceeds $f/3.5$, which was demonstrated in Chapter 1.4, has been overcome in sections 2 and 3 by the limited interpolative design technique. This has led to finding that the marginal spherical aberration is controlled mainly by the joint effects of the design parameters R_4 (the Petzval sum) and L (the longitudinal chromatic aberration). A similar interaction of design parameters has been found to occur with the off-axial-image: it is controlled principally by the combination of design parameters T (the transverse chromatic aberration residual) and R_5 (the 3rd order distortion residual). However in the final stages of optimization the interaction of the four parameters R_4 , L , T and R_5 must be considered. (R_1 remains very stable during the advanced stages of design.)

The above behaviour has been explained by the concept of all the coefficients converging simultaneously towards zero or some value near zero in the multi-dimensional design space which is defined by $(\bar{\Phi}, \chi, k', P, L, T)$. This concept has also led to a simple method for locating the "optimum region" rapidly and accurately: the optimum region occurs when the Petzval sum is as small as practicable

and the spherical aberration coefficients of at least the first three orders (σ_1, μ_1, τ_1) are near zero or have their lowest set of values with respect to $(\Phi, \chi, k', P, L, T)$. Thus mapping all the coefficients is not required when locating the optimum region.

As a result of this concept, the optimum monochromatic system is found to coincide with the optimum chromatic system. Thus in designing for apertures smaller than $f/3.5$ the design should also be optimized with respect to all the basic parameters of both the monochromatic and chromatic types; the monochromatic parameters and basic parameters cannot be treated separately if the Petzval sum is to be minimized. This also applies to a monochromatic system of large aperture.

The method of locating the optimum region using the "principle" of simultaneous convergence of the spherical aberration coefficients applies to the type 122 and also there is evidence in the literature indicating that it applies to the type 111 triplet as well. Finally since it has been shown in Section 2 that published results suggest that the "principle" applies to a telephoto system then it may well be a principle with wide application. Thus it seems that the "limited interpolative design technique" may lead to systematic automatic design.

3.5.2 New Work.

The interpolative mapping of the aberration coefficients of the type 111 seems to be the problem requiring immediate attention. If this interpolative study is carried out and it is found to support the principle of simultaneous convergence of the spherical coefficients, then the way is clear for extending the process to other triplet types and other systems. Indeed, at this stage, there would be justification for the construction of an automatic design programme based on this convergence of the spherical coefficients.

Finally, the design method, which has been developed in this work, should be extended so as to produce maps of the "optical transfer function" versus the "basic parameters".

ACKNOWLEDGEMENTS

I wish to thank Dr. F.D. Cruickshank for suggesting the investigation of the type 121 triplet and for his many helpful comments and useful discussions.

I thank Professor G.R.A. Ellis and Professor H.A. Buchdahl for their interest and stimulating comments.

I wish to express very sincere thanks to my wife Cecile for the illustrations and typing of the thesis, to Mrs. B.J. Brown for plotting many of the original graphs and spot diagrams and to Miss C. Lewis for operating the computer.

In conclusion I thank the Minister of Supply Senator Denham Henty and his department for the generous support which made this work possible.

REFERENCES.

1. R.E. Stephens, "The Design of Triplet Anastigmat Lenses of the Taylor Type", J.O.S.A, Vol.38, No.12, 1032-1039, (1948).
- 2.1 F.D. Cruickshank, "The Design of Photographic Objectives of the Triplet Family", Australian J. Phys., Vol.11, No.1, 41-54, (1958).
- 2.2 F.D. Cruickshank, "The Design of Photographic Objectives of the Triplet Family", Australian J. Phys., Vol.13, No.1, 27-42, (1960).
- 2.3 F.D. Cruickshank, "Rev. Opt. (Theor. Instrum.) 35: 292. (1956).
- 2.4 F.D. Cruickshank and G.A. Hills, "Use of Optical Aberration Coefficients in Optical Design", J.O.S.A, Vol.50, No.3, 379-387, March (1960).
- 2.5 F.D. Cruickshank, "Tracts in Geometrical and Optical Design", University of Tasmania, No.1, "The Paraxial Properties of a Refracting Optical System", (1962).
- 2.6 F.D. Cruickshank, "Tracts in Geometrical and Optical Design", University of Tasmania, No.2, "The Third Order Aberration Coefficients of a Refracting Optical System", (1960).
- 2.7 F.D. Cruickshank, "Tracts in Geometrical and Optical Design", University of Tasmania, No.3, "The Thin Lens and Systems of Thin Lenses", (1961).
- 2.8 F.D. Cruickshank, Private Communication.
- 3.1 N.v.d.W. Lessing, "Considerations on the Selection of Optical Glasses in Apochromats", J.O.S.A., Vol.48, No.4, 269-273, (1958).
- 3.2 N.v.d.W. Lessing, "Selection of Optical Glasses in Taylor Triplets (Special Method)", J.O.S.A., Vol.48, No.8, 558-562, (1958).
- 3.3 N.v.d.W. Lessing, "Selection of Optical Glasses in Taylor Triplets (General Method)", J.O.S.A., Vol.49, No.1, 31-34, (1959).

- 3.4 N.v.d.W. Lessing, "Selection of Optical Glasses in Taylor Triplets with Residual Longitudinal Chromatic Aberration", J.O.S.A., Vol.49, No.9, 872-874, (1959).
- 4.1 R.E. Hopkins, "Optical Design on Large Computers", Inst. of Optics, University of Rochester, Rochester, N.Y., U.S.A. (1961).
- 4.2 R.E. Hopkins and G. Spencer, "Creative Thinking and Computing Machines in Optical Design", J.O.S.A., Vol.52, No.2, 172-176, (1961).
- 4.3 R.E. Hopkins, "Third-Order and Fifth-Order Analysis of the Triplet", J.O.S.A., Vol.52, No.4, 389-394, (1962).
- 5.1 R. Kingslake, "Automatic Predesign of the Cooke Triplet Lens", Proc. of Conf. on Optical Instruments, London, (1961).
- 5.2 R. Kingslake, "Lens Design", Chap.1, Vol.3, Applied Optics and Optical Engineering, Academic Press, New York, London, (1965).
- 6.1 C.G. Wynne, "Lens Designing by Electronic Digital Computer: 1", Proceedings of Physical Society, LXXIII, 5, (1959).
- 6.2 C.G. Wynne, "The Relevance of Aberration Theory to Computing Machine Methods", Proc. of Conf. on Optical Instruments, London, (1961).
7. Kazuo Sayanagi, "The Role of Optical Transfer Function in Optical Design Techniques", Proc. of Conf. on Optical Instruments, London, (1961).
8. D.P. Feder, "Automatic Lens Design with a High-Speed Computer", J.O.S.A., Vol.52, No.2, 177-183, (1961).
9. R.R. Shannon and B. Tatian, "A Study of Optical Glasses for Large Aperture Systems", Conf. on Physics of Optical Glass, Physical Society, Latham, Lancashire, England, (1963).
10. W.J. Smith, "Control of Residual Aberrations in the Design of Anastigmat Objectives", J.O.S.A., Vol.48, No.2, 98-105, (1957).

- 11.1 R. Wooldridge and J.F. Ractliffe, "An Introduction to Algol Programming", English Universities Press, London, (1963).
- 11.2 H. Bottenbruch, "Structure and Use of Algol 60", Oak Ridge, National Lab., Oak Ridge, Tennessee.
- 11.3 Elliott Computing Division, "503 Technical Manual", Vol.2, Part 1, Sect.3, March (1964).
- 12.1 P.W. Ford, Journal Opt. Soc. America, 49, 875. (1959).
"Use of a Digital Computer for the Calculation of Aberration Coefficients".
- 12.2 P.W. Ford, "New Ray Tracing Scheme", J.O.S.A., Vol.50, No.6, 528-533, (1960).
- 13.1 H.A. Buchdahl, "Optical Aberration Coefficients", Monograph, Oxford University Press, (1954).
- 13.2 H.A. Buchdahl, "Optical Aberration Coefficients II. The Tertiary Intrinsic Coefficients", J.O.S.A., Vol.48, No.8, 563-567, (1958).
- 13.3 H.A. Buchdahl, "Optical Aberration Coefficients III. The Computation of the Tertiary Coefficients", J.O.S.A., Vol.48, No.10, 747-756, (1958).
- 13.4 H.A. Buchdahl, "Optical Aberration Coefficients IV. The Coefficient of Quaternary Spherical Aberration", J.O.S.A., Vol.48, No.10, 757-759, (1958).
- 13.5 H.A. Buchdahl, "Optical Aberration Coefficients V. On the Quality of Predicted Displacements", J.O.S.A., Vol.49, No.11, 1113-1121, (1959).
- 13.6 H.A. Buchdahl, "Optical Aberration Coefficients VI. On Computations Involving Coordinates Lying Partly in the Image Space", J.O.S.A., Vol.50, No.6, 534-539, (1960).
- 13.7 H.A. Buchdahl, "Optical Aberration Coefficients VII. The Primary, Secondary and Tertiary Deformation and Retardation of the Wave Front", J.O.S.A., Vol.50, No.6, 539-544, (1960).
- 13.8 H.A. Buchdahl, "Optical Aberration Coefficients VIII. Coefficient of Spherical Aberration of Order Eleven", J.O.S.A., Vol.50, No.7, 678-683, (1960).

14. R.J. Heimer, "Examples of Asymmetrical Unity Magnification Lenses", Optical Soc. of America, Colombia, Ohio, U.S.A., (1967).
15. W.J. Smith, "Control of Residual Aberrations in the Design of Anastigmat Objectives", J.O.S.A., Vol.48, No.2, 98-105, (1957).
16. L.C. Martin, "Technical Optics", Vol.II, Pitman & Sons Ltd, London, (1950).
- 17.1 A.E. Conrady, "Applied Optics and Optical Design", Vol.I, Dover Publications, (1957).
- 17.2 A.E. Conrady, "Applied Optics and Optical Design", Vol.II, Dover Publications, (1960).
18. L.B. Benny, "Mathematics for Students of Engineering and Science", Oxford University Press, (1954).
19. W. Merté, R. Richter and M.von Rohr, "Das photographische Objektiv", Springer, Vienna, (1932); Edwards, Ann Arbor, Michigan, (1944).
20. Encyclopaedic Dictionary of Physics, Pergamon Press, Vol.2, p249, (1961).
21. E. Wolf, "Progress in Optics", Vol.I, 63, (1966).
- 22.1 H.D. Taylor, British Patent No. 22607/93, (1893).
- 22.2 H.D. Taylor, "Description of Lenses", Roy.Astronomical Soc., Monthly Notices, Vol.64, 613-624, May (1904).
- 22.3 H.D. Taylor, "Optical Designing as an Art", Trans. of Opt. Society, Vol.22, 143-167, (1923).
- 23 "A Discussion on the Future of Geometrical Optics", Trans. of Opt. Soc., Vol.22, 201-224, (1921).